

Microdous amblyrhynchos sp. nov., a new member of the small-toothed sleepers (Teleostei, Gobiiformes, Odontobutidae) from Guangxi, southern China

Jiantao Hu^{1,2}, Chun Lan³, Chenhong Li^{1,2}

1 Shanghai Universities Key Laboratory of Marine Animal Taxonomy and Evolution, Shanghai Ocean University, Shanghai 201306, China **2** Engineering Research Center of Environmental DNA and Ecological Water Health Assessment, Shanghai Ocean University, Shanghai 201306, China **3** Guangxi Duan Yao Autonomous County Aquatic Technology Station, Duan 530700, China

Corresponding author: Chenhong Li (chli@shou.edu.cn)

Academic editor: Nina Bogutskaya | Received 4 November 2022 | Accepted 20 February 2023 | Published 10 March 2023

<https://zoobank.org/3CA1ADD3-91AF-4169-B656-66F02CE797D2>

Citation: Hu J, Lan C, Li C (2023) *Microdous amblyrhynchos* sp. nov., a new member of the small-toothed sleepers (Teleostei, Gobiiformes, Odontobutidae) from Guangxi, southern China. ZooKeys 1153: 1–13. <https://doi.org/10.3897/zookeys.1153.97139>

Abstract

Microdous amblyrhynchos, a new species, the second one in the genus, from the family Odontobutidae, is described from the Hongshui River, in the upper reaches of the Xijiang River of the Pearl River drainage, Baise City, Guangxi Zhuang Autonomous Region, southern China. This species is distinguished from its only congener, *M. chalmersi*, by the blunt snout (vs. pointed); mean snout length/head length ratio 0.27 (vs. 0.3); eye not extending outward (vs. protruding); mean interorbital width/head length ratio 0.25 (vs. 0.11). Additionally, the results of molecular phylogenetic analysis confirmed that *M. amblyrhynchos* sp. nov. is distinct from its sister species, *M. chalmersi*.

Keywords

Freshwater sleepers, morphology, phylogeny, taxonomy, Xijiang River

Introduction

The family Odontobutidae comprises about 15–22 species in seven genera (Iwata 2011; Li et al. 2018). They are typically small, benthic, ambush predators that are endemic to freshwater ponds and creeks of eastern and southern Asia. This family can be distinguished

from other gobiiforms by the following combination of characters: (1) six branchiostegal rays; (2) separated pelvic fins; (3) well-developed scapula excluding the cleithrum and proximal radials; and (4) longitudinally distributed lines of cephalic sensory papillae (Hose and Gill 1993; Iwata 2011; Li et al. 2018). Li et al. (2018) revealed two clades within Odontobutidae using nuclear gene capture data, one of which includes three monophyletic genera: *Microdous* Li, 2018 (southern China and northern Vietnam) as sister to a clade consisting of *Micropercops* Fowler & Bean, 1920 (China, Japan and the Korean Peninsula) and *Sineleotris* Herre, 1940 (southern China and the Indo-China Peninsula).

Microdous Li, He, Jang, Liu & Li, 2018 was established for *Phylipnus chalmersi* Nichols & Pope, 1927 and distinguished from other genera of Odontobutidae by a unique combination of the following character states: (1) presence of suborbital bone; (2) presence of complete cephalic sensory canals; (3) small and cuspidal gill rakers; (4) gill openings extending to under the front part of the eyes; (5) absence of vertical bands on the sides; (6) absence of a dark band under the eye; and (7) presence of an irregular black fleck on the upper part of the base of the pectoral fin in preserved specimens (Li et al. 2018). In the present study, a new species in the previously monotypic *Microdous* is described from Guangxi, southern China. The new species is also supported by a molecular phylogenetic analysis of mitochondrial cytochrome c oxidase subunit I (COI) implemented to evaluate the position of the new species among closely related taxa.

Materials and methods

In total, eight specimens were collected from Lihong Village (24°26.21'N, 106°26.72'E; c. 870 m a.s.l.), Yuhong Town, Lingyun County, Baise City, Guangxi Zhuang Autonomous Region using fish traps (Fig. 1). Specimens were preserved in 95% ethanol in the field then transferred to 75% ethanol. The right pectoral fins of six specimens were

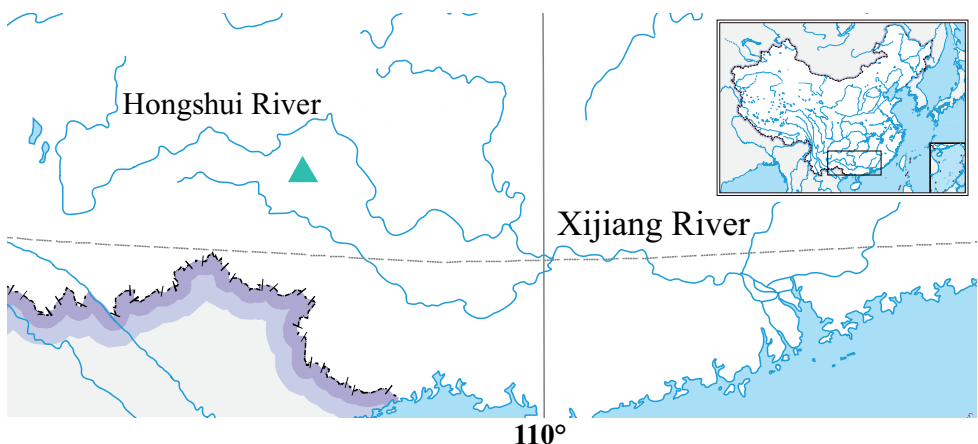


Figure 1. The sampling location of *Microdous amblyrhynchos* sp. nov. in China (inset) indicated by the green triangle.

clipped for molecular analysis, and then the specimens were fixed in 10% formalin and transferred into 75% ethanol for morphological examination. All specimens were assigned with a collection number (CL) to facilitate sample tracking. Five specimens (holotype and four paratypes) were used to collect morphological measurements and most counts except for the number of gill rakers and vertebrae (Table 1). Three paratypes were used in the molecular analysis. Seven specimens were used to calculate snout length/ head length ratios in order to examine whether the snout was blunter in the new species than in that of *M. chalmersi*.

Type specimens were deposited at the Fish Collection of the Shanghai Ocean University (SOU), China. Collection numbers and voucher numbers (in parentheses) of specimens of the new species are as follows: CL3084-1 (= SOU1801010-1), CL3084-2 (= SOU1801010-2), CL3084-3 (= SOU1801010-3), CL3084-4 (= SOU1801010-4),

Table 1. Morphological characters for the type specimens of *Microdous amblyrhynchos* sp. nov.

Characters	SOU1801010-7	SOU1801010-8	SOU1801010-1	SOU1801010-2	SOU1801010-3
Counts					
Dorsal fins	VIII;I/9	VII;I/9	VII;I/9	VII;I/9	VIII;I/10
Pectoral fins	15	15	15	15	15
Pelvic fins	I/5	I/5	I/5	I/5	I/5
Anal fin	I/8	I/8	I/8	I/8	I/8
Caudal fin	15	15	15	15	15
Lateral scales	41	40	40	40	41
Transverse scales	13	13	13	13	13
Predorsal scales	24	23	21	21	23
Gill rakers	4+9 (counted on a non-type specimen)				
Vertebrae	16+18 (counted on a non-type specimen)				
Measurements					
Total length (TL), mm	89.9	81.6	83.6	75.4	90.2
Standard length (SL), mm	74.9	66.9	69.8	63.2	76.2
Percentage of SL (%)					
Head length	30.1	27.9	30.3	31.3	29.2
Predorsal length	35.8	36.1	37.4	39.4	37.2
Snout to second dorsal fin	54.8	55.1	57.6	55.7	54.9
Snout to anus	56.5	55.5	55.5	57.0	56.1
Snout to pelvic fins	31.0	30.3	31.2	32.1	29.5
Length of caudal peduncle	26.9	26.3	26.1	25.6	24.9
Depth of caudal peduncle	11.7	10.4	10.8	10.6	10.2
Body depth at first dorsal fin origin	19.0	17.0	19.4	18.6	18.2
Body width at anal fin origin	12.9	9.1	12.0	9.5	10.0
Length of first dorsal fin base	12.5	13.6	14.3	11.3	14.7
Length of second dorsal fin base	20.1	19.5	20.0	18.9	19.3
Length of anal fin base	12.6	13.1	15.3	12.8	13.0
Length of pectoral fin	22.0	20.6	22.6	23.8	22.0
Length of pelvic fin	15.9	17.7	18.4	19.9	18.5
Percentage of head length (%)					
Snout length	26.4	27.3	27.3	27.8	27.0
Maximum head depth	59.3	60.0	64.0	55.3	61.9
Maximum head width	61.0	62.7	64.9	58.0	62.2
Interorbital width	26.8	26.2	27.2	26.9	26.1
Eye diameter	21.0	21.6	19.2	20.4	22.1
Lower jaw length	31.6	36.5	33.3	28.4	33.4

CL3084-5 (= SOU1801010-5), CL3084-6 (= SOU1801010-6), CL3084-7 (= SOU1801010-7), CL3084-8 (= SOU1801010-8).

Morphological measurements, counts and observations followed Wu et al. (2008). Nomenclature of cephalic sensory pores followed Akihito (1986). Each specimen was sexed by morphology of the urogenital papilla (Miller 1992). Two non-type specimens were dissected for counts of the number of gill rakers and vertebrae, and for examination of the vomerine region.

Genomic DNA was extracted using an Ezup Column Animal Genomic DNA Purification Kit (Sangon, Shanghai, China). Partial sequences (~ 1500 bp) of cytochrome c oxidase subunit I (COI), covering whole barcoding region was amplified from three paratype specimens (SOU1801010-1, SOU1801010-2, SOU1801010-3) as well as from comparative specimens (Table 2) using Vazyme 2× Taq Plus Master Mix II (Sangon, Shanghai) with a forward primer, CCATTTTACCTGTGRCAATCACACG, and a reverse primer CAGAGCGTTATGTRTCTGGCTTGAA according to Zhou et al. (2022). The following thermal cycles was followed: an initial denaturation at 94 °C for 5 min, 30 cycles of denaturation at 94 °C for 30 sec, primer annealing at 55 °C for 30 sec, extension at 72 °C for 1 min, and the final extension was 7 min at 72 °C (Zhou et al. 2022). The amplified products were checked on 1% agarose gels before sending to Azenta (Suzhou, Jiangsu, China) for sequencing. The sequence of three paratype specimens were lodged in GenBank with accession numbers OP536373, OP536374 and OP536375.

Sequences of additional material were retrieved from the National Center for Biotechnology Information database (Table 2). All sequences were aligned and analyzed using MEGA11 (Tamura et al. 2021). A maximum-likelihood tree including all genera of Odontobutidae except for *Terateleotris* was reconstructed under the HKY+G model with 1000 bootstrap replications. The resulting tree was visualized in FigTree v. 1.4.4 (Rambaut 2018).

Table 2. Localities, voucher information and GenBank accession numbers for the samples used in this study.

Species	Collection number	Locality	GenBank numbers
<i>Microdous amblyrhynchos</i>	SOU1801010-1	Baise, Guangxi, China	OP536373,
	SOU1801010-2		OP536374,
	SOU1801010-3		OP536375
<i>Microdous chalmersi</i>	CL2076-3	Wuzhishan, Hainan, China	OQ319987,
	CL2076-5		OQ319988
<i>Sineleotris saccharae</i>	25012	Fangchenggang, Guangxi, China	OQ382855
<i>Neodontobutis hainanensis</i>	20272	Hainan, China	OQ330750
<i>N. lani</i>	25911	Longzhou, Guangxi, China	OQ330749
<i>Micropercops swinbonis</i>	–	–	NC_021763.1
<i>Odontobutis sinensis</i>	–	–	NC_022818.1
<i>O. haifengensis</i>	–	–	NC_036056.1
<i>O. interruptus</i>	–	–	NC_027583.1
<i>O. potamophilus</i>	–	–	NC_022706.1
<i>O. platycephala</i>	–	–	NC_010199.1
<i>O. yaluensis</i>	–	–	NC_027160.1
<i>Percottus glenii</i>	–	–	NC_020350.1
<i>Rhyacichthys aspro</i>	–	–	NC_004414.1

Taxonomic account

Microdous amblyrhynchos sp. nov.

<https://zoobank.org/2C35228B-6C4A-4D19-B8EC-C0E03CB2D67E>

Figs 2, 3

Blunt-snout small-toothed sleeper, Dùn Wěnxì Chǐ Yòu, 钝吻细齿鲮 (Chinese)

Type material. Holotype. SOU1801010-7 (CL3084-7) (Fig. 2), male, 74.9 mm standard length (SL), obtained from an unnamed stream of a tributary of the Hongshui River, upper reaches of the Xijiang River of the Pearl River basin; Lihong Village (24°26.21'N, 106°26.72'E; c. 870 m a.s.l.), Yuhong Town, Lingyun County, Baise City, Guangxi, China (Fig. 1); collected using fish trap by J.H. Lan, May 2020.

Paratypes. SOU1801010-8 (CL3084-8), female, 66.9 mm SL; SOU1801010-1 (CL3084-1), male, 69.8 mm SL; SOU1801010-2 (CL3084-2), male, 63.2 mm standard length; SOU1801010-3 (CL3084-3), male, 76.2 mm SL. Sampling data same as for the holotype.

Diagnosis. *Microdous amblyrhynchos* sp. nov. can be distinguished from the only congener *M. chalmersi* by the following character states: snout blunt, snout length/head length ratio 0.26–0.28, mean 0.27 (vs. pointed, snout length/head length ratio 0.28–0.32); eye large, but not protruding outward, interorbital width larger than eye diameter, interorbital width/head length ratio 0.22–0.27, mean = 0.25 (vs. large and protruding eye, interorbital width equal to or smaller than eye diameter, interorbital width/head length ratio 0.11–0.12) (Fig. 4).

Description. Morphometric and meristic data for the holotype and paratypes are presented in Table 1. The maximum standard length (SL) was 76.2 mm.

First dorsal fin rays VII or VIII; second dorsal fin rays I/9–10; anal fin rays I/8–9; pectoral fin rays 15; pelvic fin rays I/5; caudal fin rays 15; longitudinal scale rows 40–41; transverse scale rows 13; predorsal scales 21–24; gill rakers 4+9; vertebrae 34 (16+18).

Body stout, slightly compressed posteriorly. Head large, slightly depressed. Eye large, located in anterior half of head, not protruding outward. Several rows of tiny conical teeth on both jaws. Tiny, slender, teeth-like dermal projections in vomerine region (Fig. 5A). Gill opening extending to under anterior part of eye. Cephalic sensory canals complete (Fig. 6). Urogenital papilla distinct, rest behind the anus opening (Fig. 7).

Posterior tip of dorsal fin reaching origin of second dorsal fin when depressed. Second dorsal fin ends distinctly anterior of origin of caudal fin. Caudal fin and pectoral fin large, elliptical. Pelvic fins well separated, rear tip not reaching anus. Interopercle and subopercle naked. Ctenoid scales on dorsal and lateral side of body, ventral side of body posterior to anus and opercle, transforming ctenii present. Small cycloid scales on predorsal area, cheek, nape, preopercle, base of the pectoral fin, breast and abdomen.

Coloration in life. Head black and dark brown with black dots on cheek. Body side yellowish, several irregular dark patches and orange dots on the side. Back dark



Figure 2. *Microdous amblyrhynchos* sp. nov., SOU1801010-7, holotype, 74.9 mm standard length, Baise City, Guangxi **A** dorsal **B** lateral **C** ventral.

brown. Unpaired fins possessing several inconspicuous stripes of dark spots and white edge. Pectoral fins and pelvic fins transparent and dusky. An irregular black fleck on upper part of base of pectoral fin. Ventral side of abdomen pale, with dull and inconspicuous dark patches. Urogenital papilla dark brown (Fig. 3A).

Coloration preserved. Head dark brown with black dots on the cheek. Body side brown, orange dots absent. Back brown. Irregular black fleck on upper part of base of pectoral fin dull and inconspicuous. Ventral side of abdomen light brown. Urogenital papilla whitish (Fig. 3B).

Sexual dimorphism. Urogenital papilla elongate with a wide base, tapering and with a narrow tip in male; truncated in female (Fig. 7).

Cephalic sensory canals system. Anterior extension in front of interorbital with three pairs of pores A, B and C, and a single interorbital pore D. A pair of pores E lateral to pore D. Lateral section of oculoscapular canal with a series of seven pairs of pores: F to L (terminal). Preopercular canal extending to ventral side of preopercle, with five pairs of pores: M (dorsal) to Q (ventral) (Fig. 6).



Figure 3. *Microdous amblyrhynchos* sp. nov. **A** live male individual with spawning coloration from a local market in Yuhong Town, Lingyun County, Baise City, Guangxi, China; photo taken in summer, 2019 **B** fresh non-type specimen, male, deposited at collection of Duan Yao Autonomous County Aquatic Technology Station, Guangxi; preserved in 10% formalin.

Cephalic sensory papillae. Neuromast numerous, small and densely set in mostly longitudinally arranged rows (Fig. 6).

Biology. *Microdous amblyrhynchos* can be found in small creeks or rivers with slow moving, clear water and rocky bottom. Some remains of chitin exoskeleton of crustaceans were found in the anus opening of the holotype, suggesting that *M. amblyrhynchos* is carnivorous. The male's head would turn black with several orange dots on the body sides during their spawning seasons.

Etymology. This species is named for its blunt snout distinguishing it from *M. chalmersi*. The species name derives from Greek *ambly* meaning dull or blunt and *rhynchos* meaning snout.

Phylogenetic analysis. The COI tree with three individuals of *M. amblyrhynchos* and representative species of all available Odontobutidae genera except for *Terateleotris* is shown in Fig. 8. *Rhyacichthys aspro* Valenciennes, 1837 was used as the outgroup following Li et al. (2018). All genera of Odontobutidae were monophyletic in the tree.

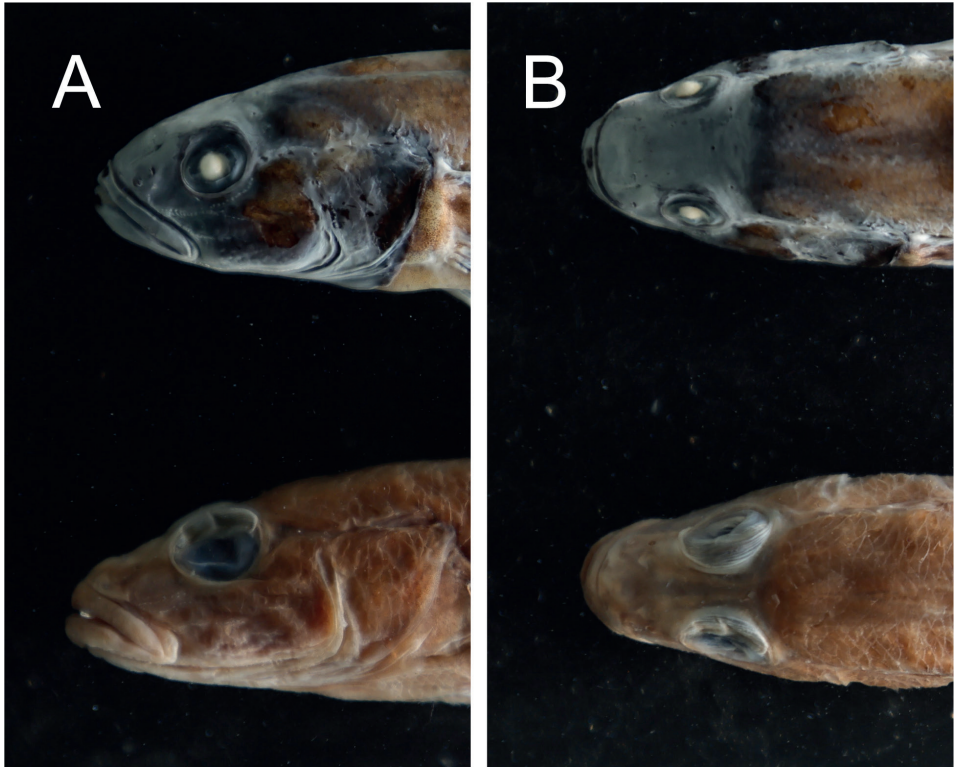


Figure 4. Head lateral (A) and dorsal (B) view of *Microdous amblyrhynchos* sp. nov. (upper, SL 74.9 mm, SOU1801010-7) and *M. chalmersi* (lower, SL 83.0 mm, SOU070504).

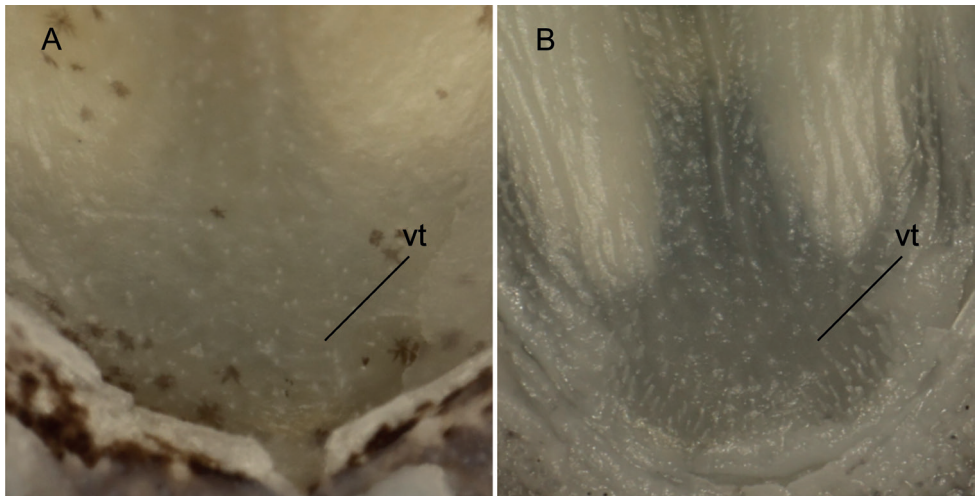


Figure 5. Vomer region **A** *Microdous amblyrhynchos* sp. nov. SOU1801010-5 **B** *M. chalmersi* CL2076-1. Abbreviation: vt, vomerine teeth-like dermal projections.

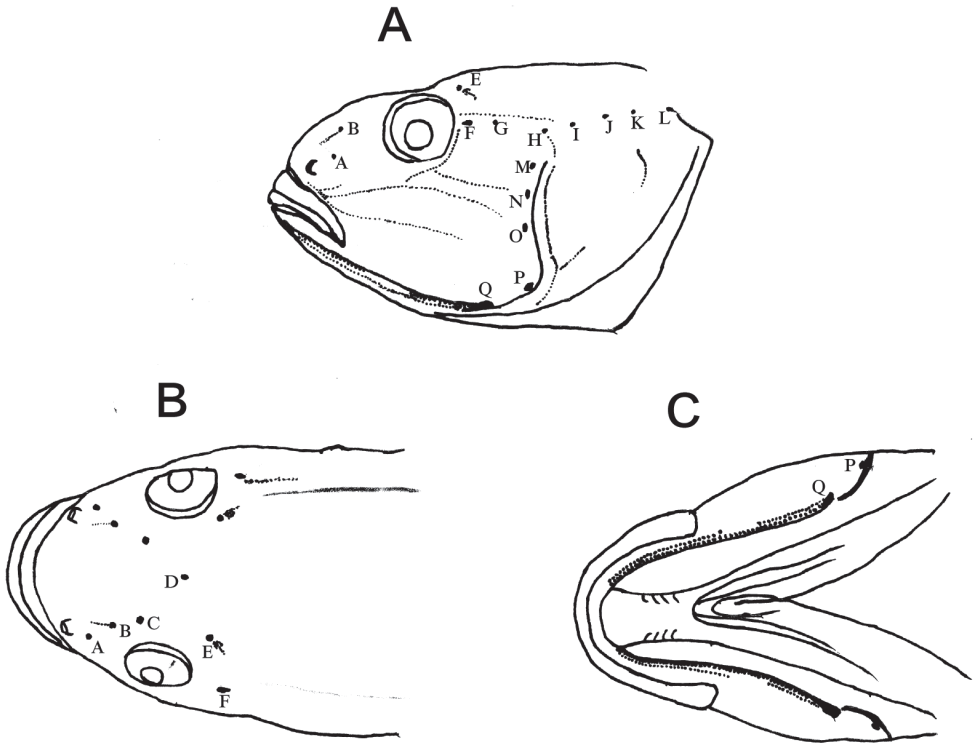


Figure 6. Patterns of main cephalic sensory papilla lines (rows of dots) and cephalic sensory canal system (red spots, A–Q) of *Microdous amblyrhynchos* sp. nov. (SOU1801010-7, holotype) in lateral (A), dorsal (B) and ventral (C) view.

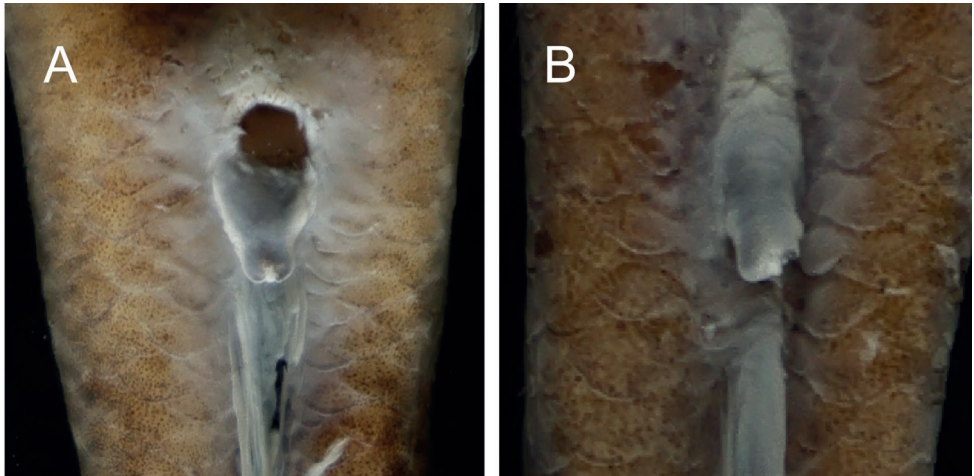


Figure 7. Urogenital papilla of *Microdous amblyrhynchos* sp. nov. SOU1801010-7 (A male) and SOU1801010-8 (B female).

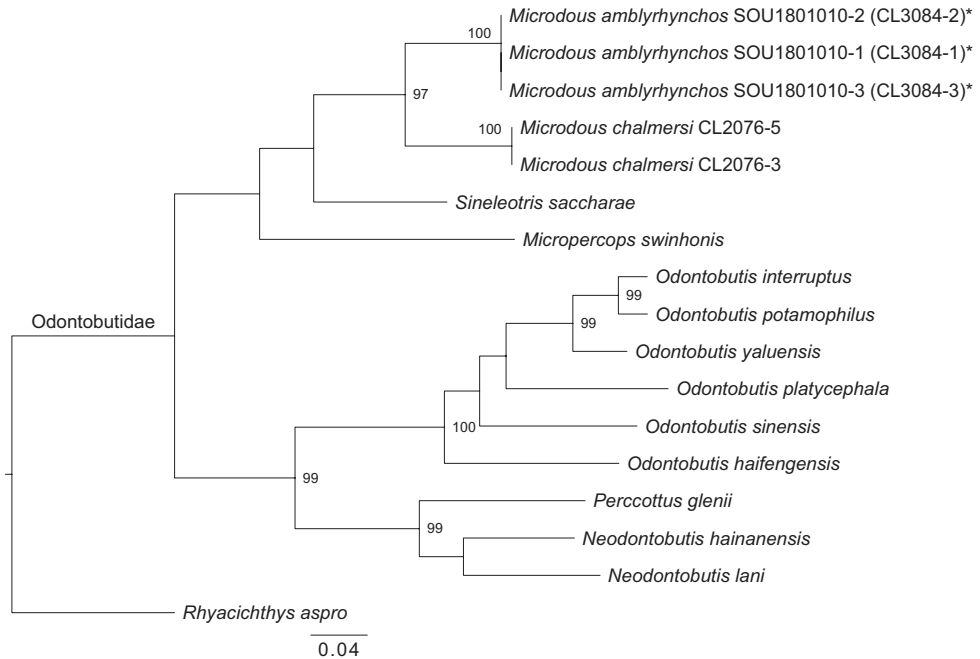


Figure 8. Maximum-likelihood (ML) tree of *Microdous amblyrhynchos* sp. nov., and other species of the Odontobutidae, based on sequences (~ 1500 bp) covering the whole barcoding region of cytochrome c oxidase subunit I (COI) gene. Numbers at nodes indicate the bootstrap support (BS). BS < 95 are not shown. SOU1801010-1, SOU1801010-2, and SOU1801010-3 are the voucher numbers of the paratypes. CL2076-3 and CL2076-5 are the collection numbers of *M. chalmersi*.

All *M. amblyrhynchos* specimens formed a clade distinct from *M. chalmersi*. The p-distance between *M. amblyrhynchos* and *M. chalmersi* was 10.7% (Suppl. material 1), suggesting that *M. amblyrhynchos* is a distinct species of the genus *Microdous*.

Discussion

Microdous differs from other genera of the Odontobutidae by the following characters: lateral line absent (present in *Terateleotris*); barbel-like projection on sensory papilla absent (present in *Neodontobutis*); prevomerine teeth absent (present in *Perccottus*); cephalic sensory canals complete (moderate in *Micropercops*, absent or reduced in *Odontobutis*); maximum head width/maximum head depth ratio slightly greater or equal to 1 (vs. maximum head depth/maximum head width far less than 1 in *Sineleotris*); and dark band under eye (vs. present in *Sineleotris*).

Our analyses using both morphological and molecular data clearly suggest that the specimens collected from Yuhong Town, Lingyun County, Baise City, Guangxi, southern China should be recognized as a new species belonging to the genus *Microdous*.

This new species can be morphologically distinguished from its only congener by its wider interorbital width, blunt snout, and non-extending eyes. A single specimen (as *Perccottus chalmersi*) from Xiajia village, Lingyun town was described by Zheng (1981) that had a blunt snout and dark fins with several inconspicuous stripes formed of dark spots. This specimen might in fact be a record of *M. amblyrhynchos*; however, it was inaccessible for comparison due to its unknown whereabouts.

The genus *Microdous* was established by Li et al. (2018) for *P. chalmersi* and the etymology of the generic name is “small + teeth” in Greek, referring to “a curved band of fine teeth on the vomer” (Nichols and Pope 1927) or “slender and tiny teeth on the vomer region of the fish” (Li et al. 2018), which were also mentioned as “vomerine teeth” in other studies (Zheng 1981; Wu et al. 2008). This character state is present in both *M. amblyrhynchos* and *M. chalmersi* (Fig. 5). However, our stereomicroscopic observation of the vomerine region showed that these projections growing directly from skin are different from the prevomerine teeth in other species such as *Perccottus glenii* Dybowski, 1877. Similar “skin teeth” were also found in *Neodontobutis hainanensis* Chen, 2002 and *Sineleotris saccharae* Herre, 1940 (Chen and Zheng 1985; Pan 1991). These vomerine teeth-like dermal projections are weak and tiny compared to the size of the fish, leaving their function as unclear.

Our phylogenetic analysis (Fig. 8) showed that *Microdous* is monophyletic, and the specimens of *M. amblyrhynchos* formed a clade distinct from *M. chalmersi*. *Microdous* was dated to the Miocene (17.9 Ma) and its origin was estimated as from southern China (Li et al. 2018). Biogeographical (Li 1981; Zhu 2016), palaeobotanical (Yao et al. 2009) and geological (Liang 2018) studies indicated that the Hainan Island was adjacent to the mainland several times due to plate movement, volcanic activity or sea level change since the Eocene epoch (30 Ma) (Liang 2018). Thus, the repeated connections and separations between Hainan Island and mainland could account for the divergence between *M. chalmersi* and *M. amblyrhynchos*.

The present-day distribution of genus *Microdous* includes southern China and northern Vietnam (Kottelat 2001 as *Perccottus chalmersi*). However, the Laotian species *Sineleotris namxamensis* (Chen & Kottelat, 2004) shares closest morphological similarities with the genus *Microdous* rather than the genus *Sineleotris*, such as the absence of a dark band under the eye and the arrangement of the cephalic sensory canal system. Thus, *S. namxamensis* would be better placed in the genus *Microdous*; the taxonomy of this species requires further research and molecular evidence.

Due to the rarity of the species, we know nothing about the reproduction, life cycle, and behavior of *M. amblyrhynchos*. Currently, the new species is only known from its type locality despite frequent surveys in Guangxi, suggesting that it is probably a species with a restricted distribution range. Habitat degradation at the type locality due to invasive species and illegal electric fishing may threaten the survival of this species. Therefore, we recommend that *M. amblyrhynchos* should be listed as a Vulnerable (VU) species [IUCN Red List criteria A1cde+B1b(iii)+D2].

According to Li et al. (2018), southern China maybe the region where the family Odontobutidae originated. This region has high Odontobutidae species diversity,

including eight species of five genera. A new member of the genus *Neodontobutis*, *N. lani* (Zhou et al. 2022) was described recently from Longzhou Town, Guangxi, Zuojiang River basin, suggesting that more new species from these places may be uncovered.

Comparative material

All *M. chalmersi* specimens examined for morphological comparison were deposited in the Fish Collection of the Shanghai Ocean University, China with the registration tags 76V8791, 76V8792, 76V9228, from Qiongzong, Hainan, May 1976; HN832384 from Changjiang, Hainan, May 1983, and 070504 from Wuzhishan, Hainan, May 1983; CL2076-1 from Wuzhishan, Hainan, August 2018.

Ethical approval

All animal procedures performed in this research were done so in accordance with the “Ethical Standards of the Shanghai Ocean University (2020)”.

Acknowledgements

We thank Mr Jiahu Lan for collecting the samples, Mr. Mingwei Zhou and Miss Fangxin Wang for assisting with molecular lab work. This work was supported by “Science and Technology Commission of Shanghai Municipality (19410740500)” to C. Li.

References

- Akihito P (1986) Some morphological characters considered to be important in gobiid phylogeny. In: Uyeno T, Arai R, Taniuchi T, Matsuura K (Eds) Indo-Pacific Fish Biology Proceedings of the Second International Conference on Indo-Pacific Fishes. The Ichthyological Society of Japan, Tokyo, 629–639. <https://www.kunaicho.go.jp/joko/pdf/file0.pdf>
- Chen I-S, Kottelat M (2004) *Sineleotris namxamensis*, a new species of sleeper from northern Laos (Teleostei: Odontobutididae). *Platax* 1: 43–49.
- Chen W, Zheng CY (1985) On three new species of the family Eleotridae from Guangdong province, China. *Journal of Jinan University* 1: 73–80. [Natural Science and Medicine Edition]
- Hoesel D, Gill A (1993) Phylogenetic Relationships of Eleotridid Fishes (Perciformes: Gobioidae). *Bulletin of Marine Science* 52: 415–440.
- Iwata A (2011) Systematics of Odontobutidae. *The Biology of Gobies*. Science Publishers, Enfield, 61–77.
- Kottelat M (2001) Freshwater fishes of Northern Vietnam. World Bank, Washington, 123 pp.

- Li S (1981) Studies on Zoogeographical Divisions for Fresh Water Fishes of China. Science Press, Beijing, 292 pp. [In Chinese]
- Li HJ, He Y, Jiang JJ, Liu ZZ, Li CH (2018) Molecular systematics and phylogenetic analysis of the Asian endemic freshwater sleepers (Gobiiformes: Odontobutidae). *Molecular Phylogenetics and Evolution* 121: 1–11. <https://doi.org/10.1016/j.ympev.2017.12.026>
- Liang G (2018) A study of the genesis of Hainan Island. *Geology in China* 45: 693–705. [In Chinese]
- Miller PJ (1992) The sperm duct gland: A visceral synapomorphy for gobioid fishes. *Copeia* 1992(1): 253–256. <https://doi.org/10.2307/1446565>
- Nichols J, Pope CH (1927) The fishes of Hainan. *Bulletin of the American Museum of Natural History* 54: 321–394. <https://digitallibrary.amnh.org/handle/2246/1840>
- Pan JH (1991) The Freshwater Fishes of Guangdong Province. Guangdong Science and Technology Press, Guangzhou, 578 pp. [In Chinese]
- Rambaut A (2018) FigTree v 1.4.4. <http://tree.bio.ed.ac.uk/software/figtree/> [accessed 15 Aug 2022]
- Tamura K, Stecher G, Kumar S (2021) MEGA11: Molecular Evolutionary Genetics Analysis Version 11. *Molecular Biology and Evolution* 38(6): 3022–3027. <https://doi.org/10.1093/molbev/msab120>
- Wu HL, Zhong JS, Chen I-S, Chong DH, Ni Y, Shen GY, Zhao SL, Shao KT (2008) Fauna Sinica, Ostichthyes, Perciformes (V), Gobioidae. Science Press, Beijing, 951 pp. [In Chinese]
- Yao YF, Bera S, Ferguson D, Mosbrugger V, Paudyal K, Jin JH, Li CS (2009) Reconstruction of paleovegetation and paleoclimate in the Early and Middle Eocene, Hainan Island, China. *Climatic Change* 92(1–2): 169–189. <https://doi.org/10.1007/s10584-008-9457-2>
- Zheng BS (1981) Freshwater Fishes of Guangxi. Guangxi People's Press, Nanning, 257 pp. [In Chinese]
- Zhou MW, He AY, Wang FX, Li YS, Li CH (2022) *Neodontobutis lani*, a new sleeper fish of the family Odontobutidae (Teleostei: Gobiiformes) from Guangxi, southern China. *Zootaxa* 5134(1): 113–124. <https://doi.org/10.11646/zootaxa.5134.1.5>
- Zhu H (2016) Biogeographical Evidence Help Revealing the Origin of Hainan Island. *PLoS ONE* 11(4): e0151941. <https://doi.org/10.1371/journal.pone.0151941>

Supplementary material I

Pairwise distances based on COI gene among all species used in this study

Authors: Jiantao Hu, Chun Lan, Chenhong Li

Data type: table (excel file)

Copyright notice: This dataset is made available under the Open Database License (<http://opendatacommons.org/licenses/odbl/1.0/>). The Open Database License (ODbL) is a license agreement intended to allow users to freely share, modify, and use this Dataset while maintaining this same freedom for others, provided that the original source and author(s) are credited.

Link: <https://doi.org/10.3897/zookeys.1153.97139.suppl1>

A new species of *Gracixalus* (Anura, Rhacophoridae) from northwestern Vietnam

Tung Thanh Tran¹, Anh Van Pham^{2,3}, Minh Duc Le^{2,4,5},
Nam Hai Nguyen¹, Thomas Ziegler^{6,7}, Cuong The Pham^{8,9}

1 Vinh Phuc College, Phuc Yen District, Vinh Phuc Province, Vietnam **2** Faculty of Environmental Sciences, University of Science, Vietnam National University, Hanoi, 334 Nguyen Trai Road, 11416 Hanoi, Vietnam **3** Center for Biodiversity & Environment Research, Tay Bac University, Son La City, Son La Province, Vietnam **4** Central Institute for Natural Resources and Environmental Studies, Vietnam National University, Hanoi, 19 Le Thanh Tong, 11021 Hanoi, Vietnam **5** Department of Herpetology, American Museum of Natural History, Central Park West at 79th Street, New York, New York 10024, USA **6** Cologne Zoo, Riehler Straße 173, 50735, Cologne, Germany **7** Institute of Zoology, University of Cologne, Zùlpicher Straße 47b, 50674, Cologne, Germany **8** Institute of Ecology and Biological Resources, Vietnam Academy of Science and Technology, 18 Hoang Quoc Viet Road, Hanoi, Vietnam **9** Graduate University of Science and Technology, Vietnam Academy of Science and Technology, 18 Hoang Quoc Viet Road, Cau Giay, Hanoi, Vietnam

Corresponding author: Cuong The Pham (cuongiebr@gmail.com)

Academic editor: Angelica Crottini | Received 17 August 2022 | Accepted 19 February 2023 | Published 10 March 2023

<https://zoobank.org/A0129BDE-8689-4259-B9EC-7F462641DD0C>

Citation: Tran TT, Pham AV, Le MD, Nguyen NH, Ziegler T, Pham CT (2023) A new species of *Gracixalus* (Anura, Rhacophoridae) from northwestern Vietnam. ZooKeys 1153: 15–35. <https://doi.org/10.3897/zookeys.1153.93566>

Abstract

A new species of small tree frog is described from northwestern Vietnam based on morphological differences and molecular divergence. *Gracixalus truongi* **sp. nov.** is distinguishable from its congeners and other small rhacophorid species on the basis of a combination of the following characters: size relatively small, SVL 32.2–33.1 mm in males, 37.6–39.3 mm in females; head slightly wider than long; vomerine teeth absent; snout round and long RL/SVL 0.17–0.19 in males, 0.16–0.17 in females; spines on upper eyelid absent; supratympanic fold distinct; tympanum distinct; dorsal skin smooth; throat smooth and venter granular; tibiotarsal projection absent; webbing of fingers rudimentary, toes with moderately developed webbing; dorsum moss-green, with an inverse Y-shaped dark green marking extended from interorbital region to posterior region of dorsum; external vocal sac absent in males; males with a nuptial pad on finger I. In the molecular analyses, the new species has no clear sister taxon and is at least 4.5% divergent from other congeners based on a fragment of the mitochondrial 16S rRNA gene.

Keywords

16S rRNA, Dien Bien Province, *Gracixalus truongi* sp. nov., morphology, Rag1, Son La Province, taxonomy

Introduction

The genus *Gracixalus* Delorme, Dubois, Grosjean & Ohler, 2005 is known from southern China through mainland Indochina, i.e., Cambodia, Laos, Vietnam, and southwards to Thailand. This genus consists of 18 recognized species, ten of which have been described in the last ten years (Frost 2022). In Vietnam, five species were recently discovered, namely *G. lumarius* Rowley, Le, Dau, Hoang & Cao, 2014; *G. sapaensis* Matsui, Ohler, Eto & Nguyen, 2017; *G. trieng* Rowley, Le, Hoang, Cao & Dau, 2020; *G. ziegleri* Le, Do, Tran, Nguyen, Orlov, Ninh & Nguyen, 2021; and *G. yunnanensis* Yu, Li, Wang, Rao, Wu & Yang, 2019. Recent phylogenetic analyses showed that there are still several unnamed distinct lineages in the *G. jinxiuensis* species group, indicating that species richness of *Gracixalus* remains underestimated (e.g., Matsui et al. 2017; Chen et al. 2018).

During our recent field work in northwestern Vietnam, specimens of a small treefrog species were collected in the karst forest of Dien Bien and Son La provinces. This treefrog taxon appears to be a member of the genus *Gracixalus* due to its small size (SVL < 40 mm), the presence of intercalary cartilage between terminal and penultimate phalanges of digits, tips of digits expanded into large discs bearing circum-marginal grooves, the vomerine teeth being absent, horizontal pupil, tibia ~ 4–5× longer than wide, translucent skin, inner (first and second) and outer (third and fourth) fingers not opposable, and dorsum with an inversed Y-shaped dark brown marking on dorsum (Fei et al. 2009; Rowley et al. 2011, 2020; Chen et al. 2018; Yu et al. 2019; Le et al. 2021). Closer examination showed that this taxon could be clearly distinguished from other known members of the genus by a combination of several morphological features in adults. In the phylogenetic analyses, this taxon forms a lineage independent from its congeners and clusters within the *Gracixalus jinxiuensis* species group with a high support level. Owing to these distinctions, we describe it herein as a new species.

Materials and methods**Sampling**

Field surveys were conducted in September 2016 in Thuan Chau District, Son La Province; in November 2020 and December 2021 in Tuan Giao District, Dien Bien Province, northwestern Vietnam. Amphibian specimens were collected between 19:00 and 23:00 h. After having photographed the living specimens, they were anaesthetized and euthanized in a closed vessel with a piece of cotton wool containing ethyl acetate (Simmons 2002), fixed in 80% ethanol for five hours, and later transferred to 70% ethanol for permanent storage. Tissue samples were preserved separately in 70%

ethanol prior to fixation. Voucher specimens referred to in this paper were deposited in the collections of the Institute of Ecology and Biological Resources (**IEBR**) and the University of Science (**HUS**), Vietnam National University (**VNU**), Hanoi, Vietnam.

Molecular data and phylogenetic analyses

Three new samples from Dien Bien Province were included in the study. An additional 33 sequences of other species of *Gracixalus* were obtained from GenBank. Outgroup polarity was provided by three taxa, *Kurixalus eiffingeri*, *K. odontotarsus*, and *Philautus aurifasciatus* (Nguyen et al. 2013; Rowley et al. 2020). We used the protocols of Le et al. (2006) for DNA extraction, amplification, and sequencing. A fragment of the mitochondrial gene 16S was amplified using the primer pair 16Sar (5'-CGCCTGTTTATCAAAAACAT-3') + 16Sbr (5'-CCGGTCTGAACTCAGATCACGT-3') (Palumbi et al. 2002). To confirm genetic distinction of the new populations from other species with available samples, we also sequenced eight other species, *G. ananjevae*, *G. gracilipes*, *G. nonggangensis*, *G. quangi*, *G. sapaensis*, *G. supercornutus*, *G. trieng*, and *G. zieglerei*, using a fragment of the nuclear gene Rag1. A primer pair, Amp-RAG1 F (5'-AGCTGCAGYCARTAC CAYAARATGTA-3') and Amp-RAG1 R1 (5'-AACTCAGCTGCATTKCCAATRTCACA-3') (San Mauro et al. 2004), was employed to amplify DNA of targeted species. We included two species, *Philautus aurantium* and *P. ingeri*, whose sequences were obtained from GenBank, in the analyses as outgroups. After sequences were aligned by Clustal X v. 2 (Thompson et al. 1997), data were analyzed using maximum parsimony (MP) and Bayesian inference (BI), as implemented in PAUP*4.0b10 (Swofford 2001), maximum likelihood (ML), as implemented in IQ-TREE v. 1.6.7.1 (Nguyen et al. 2015), and Bayesian inference (BI), as implemented in MrBayes v. 3.2.7 (Ronquist et al. 2012) for 16S sequences. We performed BI and ML for Rag1 sequences. In addition, relationships amongst *Gracixalus* species were also inferred using the NeighborNet algorithm (Bryant and Moulton 2004) using SplitsTree v. 4.14.2 (Huson and Bryant 2006).

For MP analysis, heuristic analysis was conducted with 100 random taxon addition replicates using tree-bisection and reconnection (TBR) branch-swapping algorithm, with no upper limit set for the maximum number of trees saved. Bootstrap support was calculated using 1000 pseudo-replicates and 100 random taxon addition replicates. All characters were equally weighted and unordered. For ML analysis, we employed a single model for molecular evolution and 10,000 ultrafast bootstrap replications. The optimal model for nucleotide evolution was determined using jModeltest v. 2.1.4 (Darriba et al. 2012). For Bayesian analyses, we used the optimal model selected by jModeltest with parameters estimated by MrBayes 3.2.7. Two independent analyses with four Markov chains (one cold and three heated) were run simultaneously for 10 million generations with a random starting tree and sampled every 1000 generations. Log-likelihood scores of sample points were plotted against generation time to determine stationarity of Markov chains. Trees generated before log-likelihood scores reached stationarity were discarded from the final analyses using the burn-in function. The posterior probability values for all clades in the final majority rule consensus tree

were provided. The optimal models of nucleotide evolution were set to GTR+I+G and TPM1uf+G for ML and single-modelled Bayesian analyses as selected by Modeltest v. 2.1.4 for 16S and Rag1 matrices, respectively. The cutoff points for the burn-in function was set to 73 and 32 in the Bayesian analysis, as $-\ln L$ scores reached stationarity after 73,000 and 32,000 generations in both runs for 16S and Rag1 datasets, respectively. Nodal support was also evaluated using bootstrap replication (BP) as estimated in PAUP, ultrafast bootstrap (UFB) in IQ-TREE, and posterior probabilities (PP) in MrBayes v. 3.2.7. $BP \geq 70$ and PP and UFB $\geq 95\%$ were regarded as strong support for a clade (Hillis and Bull 1993; Ronquist et al. 2012; Nguyen et al. 2015). Uncorrected pairwise divergences were calculated in PAUP*4.0b10.

Rag1 data of nine species were first analyzed by DnaSP v. 6.12.03 (Rozas et al. 2017) to determine sequence variation. The network analysis was then performed in SplitsTree with the following settings: edge fitting as ordinary least squares, equal angle as chosen splits transformation, least squares to modify weights and four maximum dimensions as the filtering option. The generated split graph showed a visual representation of conflicting signals in the data by presenting them as a series of parallel edges. The program computed the least squares fit (LSfit) between the pairwise distances from the graph and the distances from the matrix to produce a distance-based unrooted tree diagram by means of the neighbor-joining algorithm (Saitou and Nei 1987). The method was selected because it has been shown to outperform statistical parsimony as implemented in the software TCS (Clement et al. 2000) when the evolutionary history had many missing intermediate descents (Cassens et al. 2005).

Morphological characters

Measurements were taken with a digital caliper to the nearest 0.1 mm. The following abbreviations were used (after Nguyen et al. 2013):

SVL	snout-vent length;
HL	head length (measured as a parallel line with the vertebral column from posterior margin of mandible to tip of snout);
HW	maximum head width (at rictus);
RL	rostral length (from anterior corner of orbit to tip of snout);
NS	distance from nostril to the tip of snout;
EN	distance from anterior corner of the eye to the nostril;
IN	internarial distance;
IOD	interorbital distance;
ED	eye diameter;
UEW	maximum width of upper eyelid;
DAE	distance between anterior corner of eyes;
DPE	distance between posterior corner of eyes;
MFE	distance between angle of jaws and anterior corner of the eye;
MBE	distance between angle of jaws and posterior corner of the eye;
MN	distance from the back of mandible to the nostril;

TYD	tympanum diameter;
TYE	distance from anterior margin of tympanum to posterior corner of the eye;
UAL	forelimb length (from axilla to elbow);
FAL	hand length (from elbow to the tip of third finger);
NPL	nuptial pad length;
fd3	width of discs of fingers III;
fw3	width of fingers III;
TFL	third finger length;
FeL	femur length (from vent to knee);
TbL	tibia length (from knee to tarsus);
TbW	tibia width;
FoL	foot length (from tarsus to the tip of fourth toe);
FTL	fourth toe length;
IMT	inner metatarsal tubercle length;
td4	width of discs of toes IV;
tw4	width of toes IV.

For the webbing formula, we followed Glaw and Vences (2007). Sex was determined by gonadal inspection.

Results

Phylogenetic analyses

The combined matrix contained 558 aligned characters with 175 parsimony-informative sites. MP analysis of the dataset recovered the 263 most parsimonious trees with 525 steps (Consistency index = 0.51; Retention index = 0.72). Similar to Yu et al. (2019) and Le et al. (2021), our study supported the division of the genus into three distinct lineages, Clades I, II, and III, with strong nodal support from the Bayesian analysis. While Clade II was also well corroborated by ML and MP analyses, BP and UFB values for Clade I and UFB value for Clade III were insignificant. Two new populations from Dien Bien and Son La provinces were placed in Clade III along with other species from southern China and Vietnam (Fig. 1). This species is significantly divergent from others within the clade III in terms of genetic distance with the minimum pairwise divergence of approximately 4.5% based on a fragment of the mitochondrial 16S rRNA gene (Table 1 and Suppl. material 2).

The matrix of Rag1 sequences consisted of 899 aligned characters. The number of polymorphic sites was 71, parsimony-informative sites 27, and nucleotide diversity was 0.028 as determined by DnaSP. Both BI and ML analyses recovered an identical topology, although support values were generally higher in BI. The new taxon was also corroborated as a separate taxonomic unit among existing species. However, the relationships between *Gracixalus* species supported by Rag1 data differ from those in the analyses using 16S sequences. Specifically, the new taxon clustered with

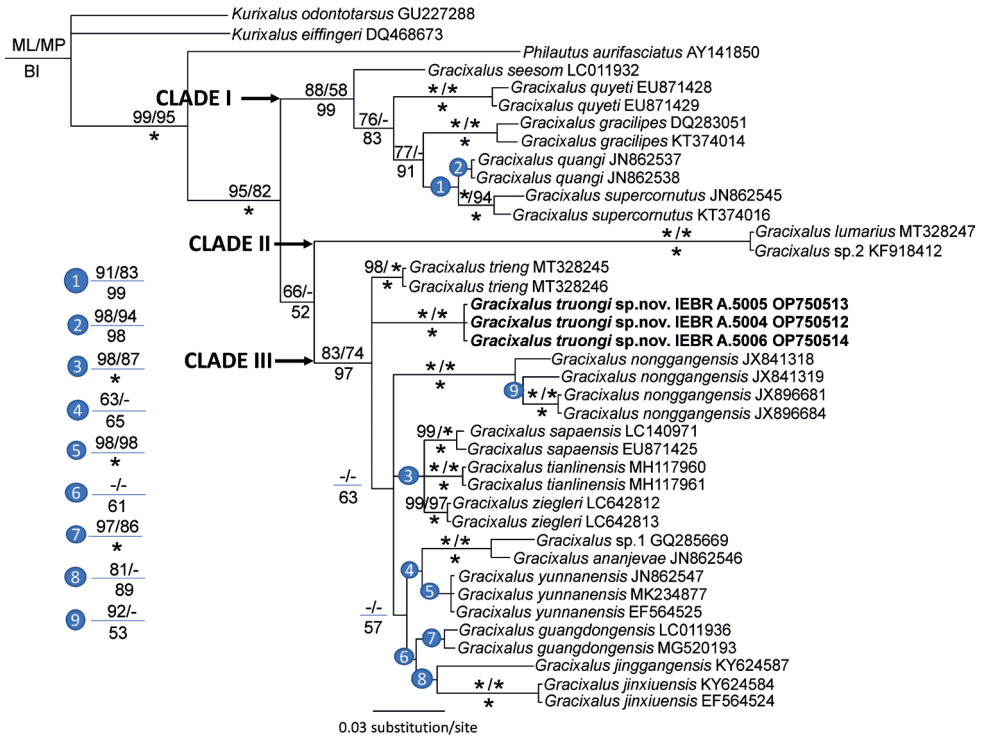


Figure 1. Phylogram based on the Bayesian analysis of 16S sequences. Number above and below branches are ML ultrafast bootstrap/MP bootstrap values and Bayesian posterior probabilities, respectively. Asterisk and dash represent 100% and < 50% values, respectively.

Table 1. Uncorrected (“p”) distance matrix showing average percentage pairwise genetic divergences (%) for the 16SrRNA gene between members of the genus *Gracixalus*. The highest distance within clades is italicized and shown in parenthesis. The new species described in this paper is in bold.

	1	2	3	4	5	6	7	8	9	10	11	12	13	14	15	16	17	18	19
1 <i>Gracixalus ananjevae</i>	(0.0)																		
2 <i>Gracixalus jinggangensis</i>	7.4	(0.0)																	
3 <i>Gracixalus jinxiuensis</i>	7.1	7.0	(0.0)																
4 <i>Gracixalus gracilipes</i>	10.6	10.8	10.7	(1.5)															
5 <i>Gracixalus guangdongensis</i>	4.8	5.3	5.7	10.1	(0.7)														
6 <i>Gracixalus lumarius</i>	14.7	14.9	16.3	15.0	14.7	(0.0)													
7 <i>Gracixalus nonggangensis</i>	8.2	7.5	7.8	12.3	6.7	16.5	(2.5)												
8 <i>Gracixalus quangi</i>	9.5	7.8	9.7	4.7	8.3	14.5	11.0	(0.0)											
9 <i>Gracixalus quyeti</i>	11.1	10.8	10.0	7.2	10.1	13.9	11.6	5.6	(0.6)										
10 <i>Gracixalus sapaensis</i>	5.4	6.3	6.9	10.1	4.6	15.7	7.0	8.9	10.2	(0.4)									
11 <i>Gracixalus seesom</i>	10.6	9.6	9.4	6.1	8.4	16.0	10.0	5.7	7.4	8.6	(0.0)								
12 <i>Gracixalus</i> sp. 1	2.3	7.7	7.4	11.4	5.7	14.6	9.1	9.9	10.7	6.1	9.8	(0.0)							
13 <i>Gracixalus</i> sp. 2	14.0	14.9	15.9	14.3	14.7	0.0	15.7	13.9	13.8	15.3	16.1	14.6	(0.0)						
14 <i>Gracixalus supercornutus</i>	10.7	9.2	10.8	6.2	9.5	15.4	11.9	2.5	5.9	10.4	6.6	10.8	14.9	(1.6)					
15 <i>Gracixalus tianlinensis</i>	6.3	6.5	5.9	10.5	4.5	15.2	6.8	9.6	9.6	2.7	7.6	6.7	15.3	10.6	(0.0)				
16 <i>Gracixalus trieng</i>	5.3	5.0	5.3	10.2	3.8	14.2	6.7	8.0	8.4	4.5	7.6	5.1	14.3	9.1	4.0	(0.0)			
17 <i>Gracixalus truongi</i> sp. nov.	6.4	6.5	7.6	11.4	5.2	15.9	8.5	9.0	10.3	6.0	10.0	6.8	15.9	10.0	5.9	4.5	(0.0)		
18 <i>Gracixalus yunnanensis</i>	3.9	5.0	5.8	10.1	2.2	14.3	6.6	8.0	9.7	4.3	8.7	5.1	13.9	8.9	4.4	4.0	4.7	(0.0)	
19 <i>Gracixalus ziegleri</i>	5.4	5.7	6.1	10.5	4.5	14.9	7.1	9.5	10.3	2.3	8.2	6.1	14.9	10.5	2.5	3.7	5.5	4.1	(0.0)

G. nonggangensis, *G. sapaensis*, and *G. ziegleri* with strong support from BI. In addition, *G. ananjevae*, and *G. trieng* formed a well-supported clade separated from the remaining congeners. The results derived from the network analysis also confirm the phylogenetic estimations (Fig. 2A, B; Suppl. materials 1, 3).

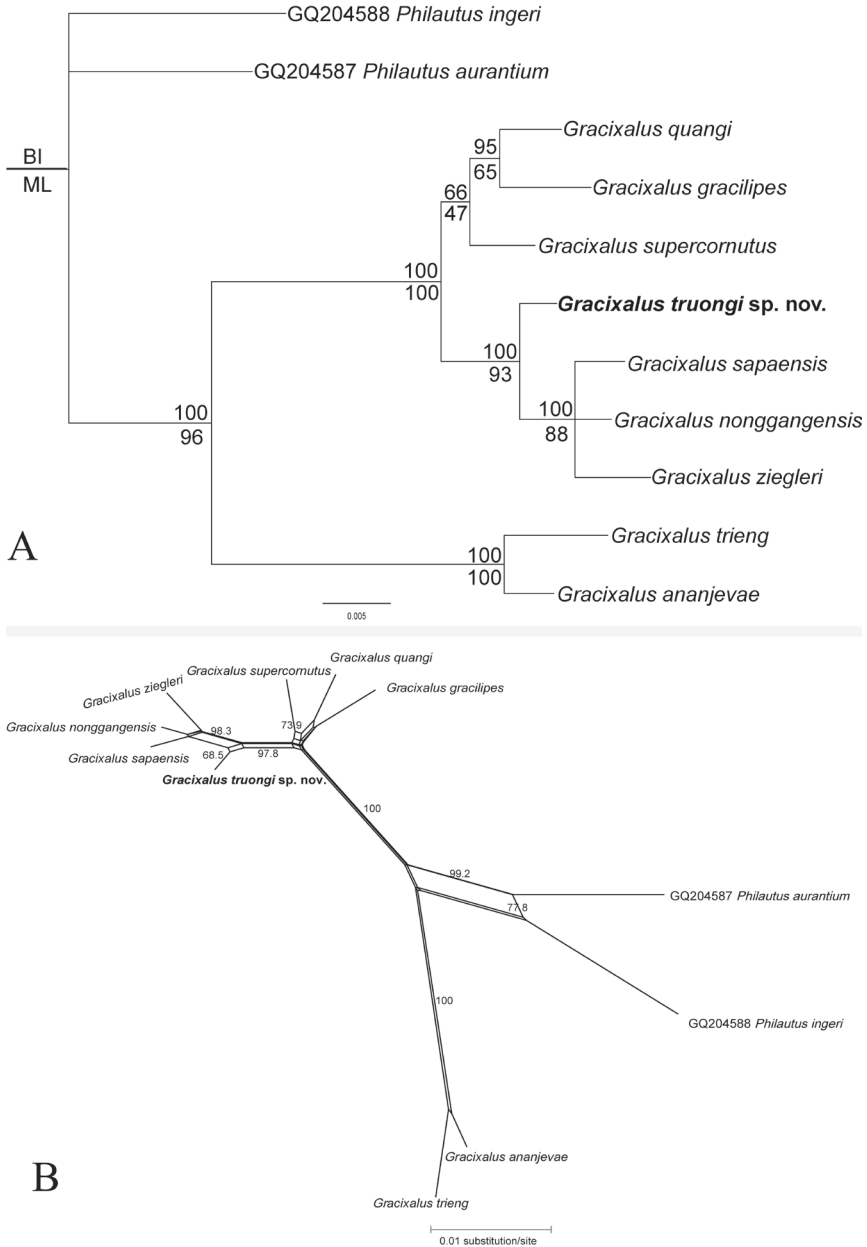


Figure 2. A phylogram based on the Bayesian analysis of Rag1 sequences. Number above and below branches are BI posterior probabilities and ML ultrafast bootstrap, respectively **B** split tree network based on Rag1 data. Numbers at major nodes are bootstrap values (1000 replicates).

Taxonomic account

Gracixalus truongi sp. nov.

<https://zoobank.org/2D02EBFB-DAC0-4297-A2EC-90CF183E68FF>

Figs 3, 4

Material. Holotype: IEBR A.5004 (Field number TN 2020.09), adult male, collected by N.H. Nguyen, H.N. Tran, H.Q. Nguyen on 11 November 2020 in the karst forest in Ta Ma Commune (21°40'36.0"N, 103°31'96.7"E, at an elevation of 1,164 m asl.), Tuan Giao District, Dien Bien Province, Vietnam. **Paratypes:** IEBR A.5005 (Field number TN 2020.08), adult female, collected on 11 November 2020 (the same data as the holotype); IEBR A.5006 (Field number ĐB 2021.7), adult male, collected by H. Q. Nguyen & T. Q. Phan, on 30 December 2021, in Tuan Giao District, Dien Bien Province, Vietnam; ZVNU 09 (Field numbers Co9.16.24) and ZVNU 10 (Field



Figure 3. *Gracixalus truongi* sp. nov., holotype (IEBR A.5004), male, in life **A** dorsolateral view **B** ventral view.



Figure 4. *Gracixalus truongi* sp. nov., dorsolateral view of paratypes in life **A** female (IEBR A.5005) from Dien Bien Province **B** female (ZVNU 09) from Son La Province.

Co9.16.36), two females, collected by A. V. Pham, N. B. Sung, L. M. Ha, T. Q. L. Hoang, and Q. T. Bui on 3 September 2016, in Long He Village (21°24'14.5"N, 103°28'41.5"E, at an elevation of 1,110 m asl.), Long He Commune, Thuan Chau District, Son La Province, Vietnam.

Diagnosis. The new species is assigned to the genus *Gracixalus* based on molecular phylogenetic analyses and the following morphological characters: the presence of intercalary cartilage between terminal and penultimate phalanges of digits, tips of digits expanded into large discs bearing circum-marginal grooves, the vomerine teeth being absent, horizontal pupil, tibia ~ 4–5× longer than wide, translucent skin, inner (first and second) and outer (third and fourth) fingers not opposable, and dorsum with an inversed Y-shaped dark brown marking (Fei et al. 2009; Rowley et al. 2011, 2020; Chen et al. 2018; Yu et al. 2019; Le et al. 2021).

Gracixalus truongi sp. nov. is distinguishable from its congeners by a combination of the following morphological characters: (1) size relatively small, SVL 32.2–33.1 mm in males, 37.6–39.3 mm in females; (2) head slightly wider than long; (3) vomerine teeth absent; (4) snout round and long RL/SVL 0.17–0.19 in males, 0.16–0.17 in females; (5) spines on upper eyelid absent; (6) supratympanic fold distinct; (7) tympanum distinct; (8) dorsal skin smooth; (9) throat skin smooth and venter skin granular; (10) tibiotarsal projection absent; (11) webbing of fingers rudimentary, toes with moderately developed webbing; (12) dorsum moss-green, with an inverse Y-shaped dark green marking extended from interorbital region to posterior region of dorsum; (13) external vocal sac absent in males; (14) males with a nuptial pad on finger I.

Description of holotype (male). *Size* small (SVL 33.1 mm), body robust, dorsoventrally compressed. Head slightly wider than long (HL 10.6 mm, HW 11.8 mm); snout round anteriorly in dorsal view, projecting beyond margin of the lower jaw; nostril round, without a lateral flap of skin, closer to tip of snout than to eye (NS 3.0 mm, EN 3.2 mm); canthus rostralis distinct and round; loreal region oblique and concave; rostral length greater than eye diameter (RL 4.8 mm, ED 4.5 mm); canthus rostralis round, loreal region oblique, concave; interorbital region flat, interorbital distance wider than internarial distance and upper eyelid width (IOD 3.9 mm, IND 3.7 mm, UEW 2.8 mm); distance between anterior corner of eyes (DAE 6.1 mm) ~ 57% distance between posterior corner of eyes (DPE 10.7 mm); pupil oval, horizontal; tympanum distinct (TYD 2.2 mm), round, half of the eye diameter but greater than tympanum-eye distance (TYE 1.5 mm); vomerine teeth absent; choanae small, oval; tongue cordate, deeply notched posteriorly; external vocal sacs absent.

Forelimbs robust; forearm and hand relative long (UAL/SVL 0.16), hand longer than forearm (FAL/SVL 0.45); relative finger lengths: I<II<IV<III; fingers webbing rudimentary; dermal ridge on sides of fingers absent; tips of all fingers with well-developed discs with distinct circum-marginal grooves, discs relatively wide compared to width of finger (fd3/fw3 1.9/1.2 mm), disc of finger III smaller than tympanum diameter; subarticular tubercles markedly elevated and prominent, round, one each on fingers I and II, two on fingers III and IV; nuptial pads prominent, oval; outer palmar tubercle divided into two.

Hindlimbs long (TbL/SVL 0.47, FoL/SVL 0.63); heels overlapping when held at right angles to the body; tibia length $\sim 4\times$ greater than tibia width (TbL/TbW 4.31), longer than thigh (FeL 15.1 mm) but shorter than foot length (FoL 20.8 mm); relative length of toes: I<II<III<V<IV; tips of all toes with well-developed discs with distinct circum-marginal grooves, discs slightly smaller than those of fingers; webbing formula I1–11/2II3/4–2III1–21/4IV2–1V; subarticular tubercles distinct, blunt, round: one on toes I and II, two on toes III and V, and three on toe IV; inner metatarsal tubercle small (IMT 1.3 mm); dermal ridge along outer side of tibia and tarsal fold absent; outer metatarsal and supernumerary tubercles absent; pointed projection at tibiotarsal articulation absent; tibio-tarsal articulation reaching between eye and nostril.

Skin texture: dorsal surface of head and body smooth; posterior part of tympanum, flank and lateral sides of limbs with small, flattened granules; spinules on upper eyelid absent; supratympanic fold distinct, extending from eye to angle of jaw; dorsolateral folds absent; throat and chest smooth, belly and ventral surface of thigh granular; dermal appendage at vent absent.

Coloration in life: background of dorsal surface of head, body and limbs moss-green with grey marking; with an inverse Y-shaped dark green marking, starting at the interorbital region, bifurcating into two branches on the shoulder, extending posteriorly; lateral side of body, dorsal surface of arms and limbs moss-green with dark green transverse bars; throat and chest white with dark brown marbling; belly immaculate white.

Coloration in preservative: Snout and dorsum grey with a dark brown pattern forming an inverse Y marking, notably a triangular pattern between eyes bifurcating into two bands continuing posteriorly; a dark pattern running from above cloaca forward to the middle of the back; lateral side of head and flank grey with dark spots; tympanum light brown; forelimb, dorsal surface of thigh, tibia and foot grey with some darker bands, posterior part of thigh below the vent yellowish brown with small white spots; throat and chest with dark brown marbling; belly immaculate cream to white; ventral part of forelimbs white; ventral surface of thighs white to grey; webbing grey.

Variation. Measurements and morphological characters of the type series are provided in Table 2 and photographs of the paratypes in life are presented in Fig. 4. Males are smaller than females (SVL 32.2–33.1 mm in males vs. 37.6–39.3 mm in females). The male specimens have a nuptial pad on finger I. The females contained yellowish cream eggs.

Etymology. We name this new species in honor of our colleague, Prof. Dr. Truong Quang Nguyen from the Institute of Ecology and Biological Resources, Vietnam Academy of Science and Technology, in recognition of his great contributions to the herpetofaunal exploration of the Indochina region. We recommend “Truong’s Treefrog” as the common English name of the new species and the common name in Vietnamese “Nhái cây trường”.

Ecological notes. The specimens were collected between 19:00 and 23:00 on a limestone cliff and on leaves, ~ 0.5 –1.2 m above the ground. The surrounding habitat was secondary karst forest of medium and small hardwoods mixed with shrubs and vines. Air temperature was 13–18 °C and relative humidity was 65–80%. Other amphibian species found at the site were *Leptobrachella* sp., *Kurixalus bisacculus* (Taylor, 1962), *Polyypedates megacephalus* Hallowell, 1861, and *Rhacophorus orlovi* (Ziegler & Köhler, 2001).

Table 2. Measurements (in mm) of the type series of *Gracixalus truongi* sp. nov.

	Males			Females			
	Holotype	Paratype	Min – Max	Paratype	Paratype	Paratype	Min – Max
	IEBR A.5004	IEBR A.5006		IEBR A.5005	ZVNU 09	ZVNU 10	
SVL	33.1	32.2	32.2–33.1	37.8	37.6	39.3	37.6–39.3
HW	11.8	13.0	11.8–13.0	14.6	14.6	14.8	14.6–14.8
HL	10.6	12.8	10.6–12.8	13.9	14.2	14.5	13.9–14.5
MN	9.5	10.8	9.5–10.8	11.9	12.1	12.9	11.9–12.9
MFE	7.4	8.2	7.4–8.2	9.3	9.2	9.9	9.2–9.9
MBE	4.1	5.0	4.1–5.0	4.9	5.1	5.5	4.9–5.5
RL	6.2	5.6	5.6–6.2	6.5	6.0	6.2	6.0–6.5
ED	4.5	5.1	4.5–5.1	5.1	5.1	5.3	5.1–5.3
UEW	2.8	3.2	2.8–3.2	3.7	3.5	3.9	3.5–3.9
IND	3.7	3.8	3.7–3.8	4.5	4.0	4.5	4.0–4.5
IOD	3.2	4.0	3.2–4.0	4.1	5.1	5.2	4.1–5.2
DAE	6.1	6.2	6.1–6.2	6.7	6.8	7.4	6.7–7.4
DPE	10.7	10.8	10.7–10.8	12.1	11.8	12.4	11.8–12.4
NS	3.0	2.6	2.6–3.0	3.0	2.8	2.9	2.8–3.0
EN	3.2	3.0	3.0–3.2	3.5	3.2	3.3	3.2–3.5
TYD	2.2	2.3	2.2–2.3	2.7	2.5	2.7	2.5–2.7
TYE	1.5	1.5	1.5–1.5	1.7	1.7	1.9	1.7–1.9
UAL	5.4	6.1	5.4–6.1	6.3	6.2	6.3	6.2–6.3
FAL	14.9	16.0	14.9–16.0	17.8	18.0	20.3	17.8–20.3
NPL	2.2	1.9	1.9–2.2				
TFL	8.3	8.9	8.3–8.9	8.9	8.9	10.2	8.9–10.2
fd3	1.9	1.7	1.7–1.9	2.0	1.8	1.9	1.8–2.0
fw3	1.2	1.0	1.0–1.2	1.3	1.2	1.3	1.2–1.3
FeL	15.1	15.2	15.1–15.2	17.7	17.1	20.2	17.1–20.2
TbL	15.5	18.0	15.5–18.0	18.1	19.2	21.9	18.1–21.9
TbW	3.6	4.0	3.6–4.0	4.2	4.0	4.8	4.0–4.8
FoL	20.8	23.2	20.8–23.2	24.2	25.1	28.3	24.2–28.3
FTL	12.6	13.0	12.6–13.0	14.8	15.4	16.7	14.8–16.7
td4	1.8	1.6	1.6–1.8	1.9	1.7	1.8	1.7–1.9
tw4	1.2	1.2	1.2–1.2	1.2	1.2	1.2	1.2–1.2
IMT	1.6	2.0	1.6–2.0	2.0	1.9	2.1	1.9–2.1
RL/SVL	0.19	0.17	0.17–0.19	0.17	0.16	0.16	0.16–0.17
ED/RL	0.73	0.91	0.73–0.91	0.78	0.85	0.85	0.78–0.85
TYE/TYD	0.68	0.65	0.65–0.68	0.63	0.68	0.70	0.63–0.70
UAL/SVL	0.16	0.19	0.16–0.19	0.17	0.16	0.16	0.16–0.17
FAL/SVL	0.45	0.50	0.45–0.50	0.47	0.48	0.52	0.47–0.52
TbL/TbW	4.31	4.50	4.31–4.50	4.31	4.80	4.56	4.31–4.80
TbL/SVL	0.47	0.56	0.47–0.56	0.48	0.51	0.56	0.48–0.56
FoL/SVL	0.63	0.72	0.63–0.72	0.64	0.67	0.72	0.64–0.72
fd3/TYD	0.86	0.74	0.74–0.86	0.74	0.72	0.70	0.70–0.74

Distribution. *Gracixalus truongi* sp. nov. is currently known only from Dien Bien and Son La provinces, northwestern Vietnam (Fig. 5).

Comparisons. We compared the new species with other members of the genus *Gracixalus* and data obtained from the literature (Boulenger 1893; Bourret 1937; Hu et al. 1978; Ye and Hu 1984; Matsui and Orlov 2004; Nguyen et al. 2008; Rowley et al. 2011, 2014, 2020; Mo et al. 2013; Nguyen et al. 2013; Matsui et al. 2015; Matsui et al. 2017; Zeng et al. 2017; Chen et al. 2018; Wang et al. 2018; Yu et al. 2019; Le et al. 2021) (Table 3).

Table 3. Morphological comparisons between *Gracixalus truongi* sp. nov., with other members of *Gracixalus*. The morphological data was obtained from the literature: Boulenger 1893; Bourret 1937; Hu et al. 1978; Ye and Hu 1984; Matsui and Orlov 2004; Nguyen et al. 2008, 2013; Rowley et al. 2011, 2014, 2020; Mo et al. 2013; Matsui et al. 2015, 2017; Zeng et al. 2017; Chen et al. 2018; Wang et al. 2018; Yu et al. 2019; Le et al. 2021). Abbreviations are as follows: ? = characters unobtainable from literature.

Species	Adult male SVL (mm)	Adult female SVL (mm)	Conical tubercles on dorsum	Dorsal color in life	Vocal sac	Skin of body sides	Skin of throat	Finger webbing	Linea masculina	Tibiotarsal articulation
<i>Gracixalus truongi</i> sp. nov.	32.2–33.1	37.6–39.3	absent	moss green with grey	internal	smooth	smooth	absent	absent	reaching between eye and nostril
<i>G. ananjevae</i>	20.0–32.0	43.4	absent	?	?	coarsely granular	plain	rudimentary	?	reaching eye
<i>G. carinensis</i>	30.2–38.1	?	absent	purplish, reddish, or greyish brown	internal	?	granular	rudimentary	?	reaching eye
<i>G. gracilipes</i>	20.0–24.0	26.4–28.8	absent	greenish	internal	smooth with white stripe	smooth	rudimentary	?	reaching eye
<i>G. quangdongensis</i>	26.1–34.7	34.9–35.4	absent	brown	?	rough, black blotches	granular	absent	present	reaching between eye and nostril
<i>G. jinggangensis</i>	27.9–33.8	31.6	absent	brown to beige	?	rough with tubercles	granular	rudimentary	?	reaching eye
<i>G. jinxiuensis</i>	23.5–26.3	29–30	?	brown	internal	rough with tubercles	granular	rudimentary	absent	reaching eye
<i>G. lamarius</i>	38.9–41.6	36.3	present	yellow	external	?	granular	rudimentary	?	?
<i>G. medogensis</i>	26.5	?	absent	grass green	internal	?	granular	absent	present	reaching eye
<i>G. nonggangensis</i>	27.1–35.3	26.8–27.3	absent	yellowish-olive with dark-green mark	internal	rough with tubercles	granular	absent	absent	reaching tip of snout
<i>G. quang</i>	21.0–24.0	26.8–27.3	present, small	olive-green	external	with black blotches	smooth	absent	?	?
<i>G. qiyeti</i>	28.5	34.0	present	brownish to moss-green	?	rough with sharp tubercles	smooth	rudimentary	?	reaching to snout
<i>G. sepauensis</i>	20.8–29.6	27.2–39.5	absent	Golden ochre	?	coarsely scattered with large tubercles	?	rudimentary	?	reaching eye
<i>G. sesom</i>	21.6–23.0	23.2–25.4	absent	tan	external	with large tubercles and white blotches	smooth	rudimentary	?	reaching between eye and nostril
<i>G. superarmatus</i>	22.0–24.1	?	present, bigger horn-like	green with brown spots	?	?	granular	?	?	?
<i>G. tianlinensis</i>	30.3–35.9	35.6–38.7	absent	brown to beige	external	?	granular	absent	?	?
<i>G. tring</i>	37.2–41.4		present	brown or yellowish	present	?	granular	rudimentary	?	?
<i>G. yunnanensis</i>	26.0–34.2	?	present, small	yellow brown or red brown	external	smooth, no black blotches	granular	rudimentary	present	reaching eye
<i>G. ziegleri</i>	28.1–30.0	36.7–41.2	present	yellowish brown	internal	rough, black blotches	granular	rudimentary	absent	reaching tip of snout

Species	Snout	White patch on temporal region	Tibiotarsal projection	Supratympanic fold	Venter	Nuptial pads	Heels	Iris	Linea masculina	Tibiotarsal articulation
<i>Gracixalus truongi</i> sp. nov.	rounded	absent	absent	distinct	immaculate white	on finger I	overlapping	brown and moss green	absent	reaching between eye and nostril
<i>G. manjane</i>	slightly pointed	absent	absent	distinct	immaculate	on finger I	overlapping	?	?	reaching eye
<i>G. carinensis</i>	round	absent	absent	distinct	immaculate white	?	?	?	?	reaching eye
<i>G. gracilipes</i>	triangularly pointed	absent	absent	distinct	yellowish white	on fingers I and II	overlapping	brown	?	reaching eye
<i>G. guangdongensis</i>	triangularly pointed	present	present	distinct	throat and chest creamy white, belly light brown, semi-transparent	on finger I	overlapping	brown	present	reaching between eye and nostril
<i>G. jinggangensis</i>	triangularly pointed	absent	absent	distinct	Throat and chest dirty white with dark specks, belly white anteriorly with dark marking and posteriorly yellowish, semi-transparent	on fingers I and II	just meeting	golden	?	reaching eye
<i>G. jinxiensis</i>	round	absent	absent	distinct	gray-brown with dark marbling	on finger I	just meeting	pale brown	absent	reaching eye
<i>G. lunantus</i>	round	absent	absent	indistinct	opaque pink	on finger I	?	dark gold	?	?
<i>G. medogensis</i>	round	absent	absent	distinct	pale green	on finger I	overlapping	?	present	reaching eye
<i>G. nonggangensis</i>	round	absent	absent	distinct	white with dark marbling, semi-transparent	on finger I	overlapping	olive	absent	reaching tip of snout
<i>G. quang</i>	triangularly pointed	present	present	distinct	opaque white with translucent pale green margins	on finger I	?	bronze	?	?
<i>G. qiyeti</i>	round	absent	absent	indistinct	belly immaculate white	?	overlapping	yellow moss green	?	reaching to snout
<i>G. sepaensis</i>	round	absent	absent	distinct	throat, chest, and belly light yellow, with dark marking	on finger I	overlapping	golden	?	reaching eye
<i>G. secom</i>	triangularly pointed	absent	absent	distinct	anterior belly opaque white and posterior belly translucent	absent	overlapping	golden	?	reaching between eye and nostril
<i>G. superarmatus</i>	pointed	present	present	distinct	light with white spots	?	?	Pale yellow	?	?
<i>G. taidinensis</i>	round	absent	absent	distinct	throat and chest gray with dark specks, belly creamy white, opaque	on fingers I and II	?	bronze	?	?
<i>G. trieng</i>	rounded	?	absent	distinct	throat and chest mostly yellowish brown, with dark mottling, belly pinkish brown	on fingers I and II	?	pale gold	?	?
<i>G. yunnanensis</i>	round	absent	absent	distinct	orangish with yellow spots, immaculate, semi-transparent	on finger I	overlapping	bronze	present	reaching eye
<i>G. zuegleri</i>	triangularly pointed	absent	absent	distinct	throat and chest dirty white with moderate dark specks, belly white cream with large dark blotches,	on finger I	overlapping	golden	absent	reaching tip of snout

Gracixalus truongi sp. nov. differs from *G. ananjevae* (Matsui & Orlov, 2004) by having skin of body sides smooth (vs. coarsely granular), snout round (vs. triangular pointed); tibio-tarsal articulation reaching between eye and nostril (vs. reaching eye). *Gracixalus truongi* sp. nov. differs from *G. carinensis* (Boulenger, 1893) by different dorsal color pattern (moss green with grey vs. purplish, reddish, or greyish brown), skin of throat smooth (vs. granular), tibio-tarsal articulation reaching between eye and nostril (vs. reaching eye). *Gracixalus truongi* sp. nov. differs from *G. gracilipes* (Bourret, 1937) by having a larger size (SVL 32.1–33.1 in males, 37.6–39.3 mm in females vs. 20.0–24.0 mm in males, 26.4–28.8 mm in females), different dorsal color pattern (moss green with grey vs. greenish with white stripe), round snout (vs. triangular pointed), tibio-tarsal articulation reaching between eye and nostril (vs. reaching eye), and iris moss green with brown marking (vs. brown). The new species differs from *G. guangdongensis* Wang, Zeng, Liu & Wang, 2018 by having a different dorsal color pattern (moss green with grey vs. brown with black blotches), skin of body sides smooth (vs. rough), skin of throat smooth (vs. granular), snout round (vs. triangular pointed), linea masculina absent (vs. present), white patch on temporal region absent (vs. present), tibiotarsal projection absent (vs. present), different venter color pattern (immaculate white vs. throat and chest creamy white, belly light brown, semi-transparent), and iris moss green with brown marking (vs. brown). *Gracixalus truongi* sp. nov. differs from *G. jinggangensis* Zeng, Zhao, Chen, Chen, Zhang & Wang, 2017 by different dorsal color pattern (moss green with grey vs. brown to beige), skin of body sides smooth (vs. rough with tubercles), skin of throat smooth (vs. granular), tibiotarsal articulation reaching between eye and nostril (vs. reaching eye), snout round (vs. triangular pointed), different venter color pattern (immaculate white vs. throat and chest dirty white with dark specks, belly white anteriorly with dark marking and posteriorly yellowish, semi-transparent), and iris moss green with brown marking (vs. golden). *Gracixalus truongi* sp. nov. differs from *G. jinxiuensis* (Hu, 1978) by having a larger size (SVL 32.1–33.1 in males, 37.6–39.3 mm in females vs. 23.5–26.3 mm in males, 29.0–30.0 mm in females), different dorsal color pattern (moss green with grey vs. brown), skin of body sides smooth (vs. rough with tubercles), skin of throat smooth (vs. granular), tibiotarsal articulation reaching between eye and nostril (vs. reaching eye), and different venter color pattern (immaculate white vs. gray-brown with dark marbling). *Gracixalus truongi* sp. nov. differs from *G. lumarius* Rowley, Le, Dau, Hoang & Cao, 2014 by having a smaller size in males (SVL 32.1–33.1 mm vs. 38.9–41.6 mm), different dorsal color pattern (moss green with grey vs. yellow), external vocal sac absent in males (vs. present), conical tubercles on dorsum absent (vs. present), skin of throat smooth (vs. granular), supratympanic fold distinct (vs. indistinct), different venter color pattern (immaculate white vs. opaque pink), and iris moss green with brown marking (vs. dark gold). *Gracixalus truongi* sp. nov. differs from *G. medogensis* (Ye & Hu, 1984) by having a larger size in males (SVL 32.1–33.1 mm vs. 26.5 mm), different dorsal color pattern (moss green with grey vs. grass green), skin of throat smooth (vs. granular), linea masculina absent (vs. present), tibio-tarsal articulation reaching between eye and nostril (vs. reaching eye), and different venter color pattern (immaculate white vs. pale green). *Gracixalus truongi* sp. nov. differs from

G. nonggangensis Mo, Zhang, Luo, Zhou & Chen, 2013 by different dorsal color pattern (moss green with grey vs. yellowish-olive with dark-green mark), skin of body sides smooth (vs. rough with tubercles), different venter color pattern (immaculate white vs. white with dark marbling, semi-transparent), tibio-tarsal articulation reaching between eye and nostril (vs. reaching tip of snout), and iris moss green with brown marking (vs. olive). *Gracixalus truongi* sp. nov. differs from *G. quangi* Rowley, Dau, Nguyen, Cao & Nguyen, 2011 by having a larger size (SVL 32.1–33.1 in males, 37.6–39.3 mm in females vs. 21.0–24.0 mm in males, 26.8–27.3 mm in females), different dorsal color pattern (moss green with grey vs. brown with black blotches), external vocal sac absent in males (vs. present), white patch on temporal region absent (vs. present), tibiotarsal projection absent (vs. present), different venter color pattern (immaculate white vs. opaque white with translucent pale green margins), and iris moss green with brown marking (vs. bronze). *Gracixalus truongi* sp. nov. differs from *G. quyeti* (Nguyen, Hendrix, Böhme, Vu & Ziegler, 2008) by having a larger size (SVL 32.1–33.1 in males, 37.6–39.3 mm in females vs. 21.0–24.0 mm in males, 34.0 mm in the female), conical tubercles on dorsum absent (vs. present), skin of body sides smooth (vs. rough with sharp tubercles), tibio-tarsal articulation reaching between eye and nostril (vs. reaching tip of snout), and supratympanic fold distinct (vs. indistinct). The new species differs from *G. sapaensis* Matsui, Ohler, Eto & Nguyen, 2017 from by having a larger size in males (SVL 32.1–33.1 mm vs. 20.8–29.6 mm), different dorsal color pattern (moss green with grey vs. golden ochre), skin of body sides smooth (vs. coarsely scattered with large tubercles), different venter color pattern (immaculate white vs. light yellow with dark marking), tibio-tarsal articulation reaching between eye and nostril (vs. reaching eye), and iris moss green with brown marking (vs. golden). *Gracixalus truongi* sp. nov. differs from *G. seesom* Matsui, Khonsue, Panha & Eto, 2015 by having a larger size (SVL 32.1–33.1 in males, 37.6–39.3 mm in females vs. 21.6–23.0 mm in males, 23.2–25.4 mm in females), different dorsal color pattern (moss green with grey vs. tan), external vocal sacs absent in males (vs. present), round snout (vs. triangular pointed), and iris moss green with brown marking (vs. golden). *Gracixalus truongi* sp. nov. differs from *G. supercornutus* (Orlov, Ho & Nguyen, 2004) by having a larger size in males (SVL 32.1–33.1 mm vs. 22.0–24.1 mm), conical tubercles on dorsum absent (vs. present), different dorsal color pattern (moss green with grey vs. green with brown spots), skin of throat smooth (vs. granular), round snout (vs. pointed), and tibiotarsal projection absent (vs. present). *Gracixalus truongi* sp. nov. differs from *G. tianlinensis* Chen, Bei, Liao, Zhou & Mo, 2018 by having different dorsal color pattern (moss green with grey vs. brown to beige), external vocal sacs absent in males (vs. present), skin of throat smooth (vs. granular), males with a nuptial pad on finger I (vs. males with a nuptial pad on finger I and II), tibio-tarsal articulation reaching between eye and nostril (vs. reaching eye), and iris moss green with brown (vs. bronze). *Gracixalus truongi* sp. nov. differs from *G. trieng* Rowley, Le, Hoang, Cao & Dau, 2020 by having a smaller size in males (SVL 32.1–33.1 mm vs. 37.2–41.4 mm), conical tubercles on dorsum absent (vs. present), different dorsal color pattern (moss green with grey vs. yellow or yellowish), external vocal sacs absent in males (vs. present), skin of throat smooth (vs. granular), different venter color pattern (immaculate



Figure 5. Map showing the type locality of *Gracixalus truongi* sp. nov. in Dien Bien Province (1) and the locality in Son La Province (2), Vietnam, where some of the paratypes were found.

white vs. throat and chest mostly yellowish brown with dark mottling, belly pinkish brown), and iris moss green with brown (vs. pale gold). *Gracixalus truongi* sp. nov. differs from *G. yunnanensis* Yu, Li, Wang, Rao, Wu & Yang, 2019 by conical tubercles on

dorsum absent (vs. present), different dorsal color pattern (moss green with grey vs. yellow brown or red brown), skin of throat smooth (vs. granular), and iris moss green with brown marking (vs. bronze). *Gracixalus truongi* sp. nov. differs from *G. zieglerei* Le, Do, Tran, Nguyen, Orlov, Ninh & Nguyen, 2021 by having a larger size in males (SVL 32.1–33.1 mm vs. 28.1–30.0 mm), conical tubercles on dorsum absent (vs. present), different dorsal color pattern (moss green with grey vs. yellowish brown with black blotches), skin of body sides smooth (vs. rough), skin of throat smooth (vs. granular), different ventral color pattern (immaculate white vs. throat and chest dirty white with moderate dark specks, belly white cream with large dark blotches), and iris moss green with brown (vs. golden).

In terms of dorsal color pattern *Gracixalus truongi* sp. nov. is similar to *Theloderma annae* Nguyen, Pham, Nguyen, Ngo & Ziegler, 2016 from Hoa Binh anh Ninh Binh provinces. In addition, *Gracixalus truongi* sp. nov. and *Theloderma annae* also have similar life histories, both inhabiting limestone karst forest far from water sources. However, *Gracixalus truongi* differs from *Theloderma annae* by a larger size (SVL 32.1–33.1 in males, 37.6–39.3 mm in females vs. 27.1–28.5 mm in males, 30.3–32.6 mm in females), the presence of a dark inverse Y-marking on dorsum (vs. absent), and a higher ratio of TYD/TYD (0.67 in males and 0.67 in females vs. 0.39 in males and 0.32 in females) (Nguyen et al. 2016).

Discussion

The discovery of *Gracixalus truongi* sp. nov. brings the number of species in the genus to a total of 19 with 13 occurring in Vietnam. It is clear that the diversity of *Gracixalus* peaks in Vietnam, including seven taxa present in the northern region, five in the central, and one in both regions of the country. The new species is most closely related to *G. trieng* in terms of genetic distance, but they are separated by 4.5% divergence based on a fragment of the mitochondrial 16S rRNA gene. Geographically, the two taxa are found in distant and distinct geographic regions. While *G. truongi* occurs in Dien Bien and Son La provinces, northwestern region, *G. trieng* is distributed in Kon Tum Province, the Central Highlands, Vietnam. In addition, the new species is recorded in the karstic landscape at elevations between 1,000 and 1,200 m, whereas *G. trieng* inhabits soil montane habitat at altitudes from 1,700 to 2,100 m. Morphologically, the former resembles *G. nonggangensis*, which occupies the same type of limestone habitat. The latter taxon is recorded between 500 and 700 m in northeastern Vietnam and 200–250 m in southern China. *G. truongi* differs from *G. nonggangensis* by 8.5% in genetic divergence based on a fragment of the mitochondrial 16S rRNA gene.

Acknowledgements

We are grateful to the directorate of the Forest Protection Department of Dien Bien and Son La provinces for supporting our field work. We thank T.Q. Phan, H.Q. Nguy-

en (Hanoi), N.B. Sung, L.M. Ha, T.Q. L. Hoang, and Q.T. Bui (Son La) for their assistance in the field and H.T. Ngo (Hanoi) for laboratory assistance. We thank T.A. Tran (Hanoi) for providing the map. For the fruitful collaboration within joint research projects, we cordially thank S.V. Nguyen (IEBR, Hanoi), as well as T. Pagel and C. Landsberg (Cologne Zoo). This research was funded by the National Foundation for Science and Technology Development (NAFOSTED, Grant No. 106.05-2021.19) to T.Q. Nguyen.

References

- Boulenger GA (1893) Concluding report on the reptiles and batrachians obtained in Burma by Signor L. Fea dealing with the collection made in Pegu and the Karin Hills in 1887–88. *Annali del Museo Civico di Storia Naturale di Genova* 13: 304–347. <https://doi.org/10.5962/bhl.part.9543>
- Bourret R (1937) Notes herpétologiques sur l’Indochine française. XIV. Les batraciens de la collection du Laboratoire des Sciences Naturelles de l’Université. Descriptions de quinze espèces ou variétés nouvelles. *Annexe au Bulletin Général de l’Instruction Publique* 1937: 5–56. <https://doi.org/10.5962/bhl.part.22065>
- Bryant D, Moulton V (2004) Neighbor-Net: An agglomerative method for the construction of phylogenetic networks. *Molecular Biology and Evolution* 21(2): 255–265. <https://doi.org/10.1093/molbev/msh018>
- Cassens I, Mardulyn P, Milinkovitch MC (2005) Evaluating intraspecific “network” construction methods using simulated sequence data: Do existing algorithms outperform the global maximum parsimony approach? *Systematic Biology* 54(3): 363–372. <https://doi.org/10.1080/10635150590945377>
- Chen W, Bei Y, Liao X, Zhou S, Mo Y (2018) A new species of *Gracixalus* (Anura: Rhacophoridae) from West Guangxi, China. *Asian Herpetological Research* 9: 74–84. <https://doi.org/10.11646/zootaxa.3616.1.5>
- Clement M, Posada D, Crandall KA (2000) TCS: A computer program to estimate genealogies. *Molecular Ecology* 9(10): 1657–1659. <https://doi.org/10.1046/j.1365-294x.2000.01020.x>
- Darriba D, Taboada GL, Doallo R, Posada D (2012) jModelTest 2: More models, new heuristics and parallel computing. *Nature Methods* 9(8): e772. <https://doi.org/10.1038/nmeth.2109>
- Delorme M, Dubois A, Grosjean S, Ohler A (2005) Une nouvelle classification générique et sub-générique de la tribu des Philautini (Amphibia, Anura, Rhacophorinae). *Bulletin Mensuel de la Société Linneenne de Lyon* 74: 165–171. <https://doi.org/10.3406/linly.2005.13595>
- Fei L, Hu S, Ye C, Huang Y (2009) *Fauna Sinica. Amphibia* (Vol. 2). Anura, Science Press, Beijing, 887 pp.
- Frost DR (2022) *Amphibian Species of the World: and Online Reference*. Version 6.1. American Museum of Natural History, New York. <http://research.amnh.org/herpetology/amphibia/index.html/> [Accessed on 16 August 2022]
- Glaw F, Vences M (2007) *A Field Guide to the Amphibians and Reptiles of Madagascar* (3rd edn.). FroschVerlag, Cologne, 496 pp.

- Hillis DM, Bull JJ (1993) An empirical test of bootstrapping as a method for assessing confidence in phylogenetic analysis. *Systematic Biology* 42(2): 182–192. <https://doi.org/10.1093/sysbio/42.2.182>
- Hu S, Fei L, Ye C (1978) Three new amphibian species in China. *Materials for Herpetological Research* 4: e20.
- Huson HD, Bryant D (2006) Application of phylogenetic networks in evolutionary studies. *Molecular Biology and Evolution* 23(2): 254–267. <https://doi.org/10.1093/molbev/msj030>
- Le M, Raxworthy CJ, McCord WP, Mertz L (2006) A molecular phylogeny of tortoises (Testudines: Testudinidae) based on mitochondrial and nuclear genes. *Molecular Phylogenetics and Evolution* 40(2): 517–531. <https://doi.org/10.1016/j.ympev.2006.03.003>
- Le DT, Do YT, Tran TT, Nguyen TQ, Orlov NL, Ninh TH, Nguyen TT (2021) A new species of *Gracixalus* (Anura: Rhacophoridae) from northern Vietnam. *Russian Journal of Herpetology* 28(3): 111–122. <https://doi.org/10.30906/1026-2296-2021-28-3-111-122>
- Matsui M, Orlov N (2004) A new species of *Chirixalus* from Vietnam (Anura: Rhacophoridae). *Zoological Science* 21(6): 671–676. <https://doi.org/10.2108/zsj.21.671>
- Matsui M, Khonosue W, Panha S, Eto K (2015) A new tree frog of the genus *Gracixalus* from Thailand (Amphibia: Rhacophoridae). *Zoological Science* 32(2): 204–210. <https://doi.org/10.2108/zs140238>
- Matsui M, Ohler A, Eto K, Nguyen TT (2017) Distinction of *Gracixalus carinensis* from Vietnam and Myanmar, with description of a new species. *Alytes* 33: 25–37.
- Mo Y, Zhang W, Luo Y, Zhou S, Chen W (2013) A new species of the genus *Gracixalus* (Amphibia: Anura: Rhacophoridae) from Southern Guangxi, China. *Zootaxa* 3616(1): 61–72. <https://doi.org/10.11646/zootaxa.3616.1.5>
- Nguyen TQ, Hendrix R, Böhme W, Vu TN, Ziegler T (2008) A new species of the genus *Philautus* (Amphibia: Anura: Rhacophoridae) from the Truong Son Range, Quang Binh Province, central Vietnam. *Zootaxa* 1925(1): 1–13. <https://doi.org/10.11646/zootaxa.1925.1.1>
- Nguyen TQ, Le MD, Pham CT, Nguyen TT, Bonkowski M, Ziegler T (2013) A new species of *Gracixalus* (Amphibia: Anura: Rhacophoridae) from northern Vietnam. *Organisms, Diversity & Evolution* 13(2): 203–214. <https://doi.org/10.1007/s13127-012-0116-0>
- Nguyen LT, Schmidt HA, von Haeseler A, Bui MQ (2015) IQ-TREE: A fast and effective stochastic algorithm for estimating maximum likelihood phylogenies. *Molecular Biology and Evolution* 32(1): 268–274. <https://doi.org/10.1093/molbev/msu300>
- Nguyen TQ, Pham TC, Nguyen TT, Ngo TT, Ziegler T (2016) A new species of *Theلودerma* (Amphibia: Anura: Rhacophoridae) from Vietnam. *Zootaxa* 4168(1): 171–186. <https://doi.org/10.11646/zootaxa.4168.1.10>
- Orlov NL, Ho TC, Nguyen QT (2004) A new species of the genus *Philautus* from central Vietnam (Anura: Rhacophoridae). *Russian Journal of Herpetology* 11: 51–64.
- Palumbi SR, Martin A, Romano S, McMillan WO, Stice L, Grabowski G (2002) *The Simple Fool's Guide to PCR*. Department of Zoology and Kewalo Marine Laboratory, Hawaii, 45 pp.
- Ronquist F, Teslenko M, van der Mark P, Ayres DL, Darling A, Höhna S, Larget B, Liu L, Suchard MA, Huelsenbeck JP (2012) MrBayes 3.2: Efficient Bayesian phylogenetic inference and model choice across a large model space. *Systematic Biology* 61(3): 539–542. <https://doi.org/10.1093/sysbio/sys029>

- Rowley JLL, Dau QV, Nguyen TT, Cao TT, Nguyen SN (2011) A new species of *Gracixalus* (Anura: Rhacophoridae) with a hyperextended vocal repertoire from Vietnam. *Zootaxa* 3125: 22–38. <https://doi.org/10.1163/15685381-00003007>
- Rowley JLL, Le DTT, Dau VQ, Hoang HD, Cao TT (2014) A striking new species of phytotelm breeding tree frog (Anura: Rhacophoridae) from central Vietnam. *Zootaxa* 3785(1): 25–37. <https://doi.org/10.11646/zootaxa.3785.1.2>
- Rowley JLL, Le DTT, Hoang HD, Cao TT, Dau QV (2020) A new species of phytotelm breeding frog (Anura: Rhacophoridae) from the Central Highlands of Vietnam. *Zootaxa* 4779: 341–354. <https://doi.org/10.11646/zootaxa.4779.3.3>
- Rozas J, Ferrer-Mata A, Sánchez-DelBarrio JC, Guirao-Rico S, Librado P, Ramos-Onsins SE, Sánchez-Gracia A (2017) DnaSP 6: DNA sequence polymorphism analysis of large data sets. *Molecular Biology and Evolution* 34(12): 3299–3302. <https://doi.org/10.1093/molbev/msx248>
- Saitou N, Nei M (1987) The neighbour-joining method: A new method for reconstructing phylogenetic trees. *Molecular Biology and Evolution* 4: 406–425.
- San Mauro D, Gower DJ, Oommen OV, Wilkinson M, Zardoya R (2004) Phylogeny of caecilian amphibians (Gymnophiona) based on complete mitochondrial genomes and nuclear RAG1. *Molecular Phylogenetics and Evolution* 33(2): 413–427. <https://doi.org/10.1016/j.ympev.2004.05.014>
- Simmons JE (2002) Herpetological collecting and collections management. Revised edition. Society for the Study of Amphibians and Reptiles. *Herpetological Circular* 31: 1–153.
- Swofford DL (2001) PAUP: Phylogenetic Analysis Using Parsimony (*and other Methods), Version 4.0. Sinauer Associates, Sunderland.
- Thompson JD, Gibson TJ, Plewniak F, Jeanmougin F, Higgins DG (1997) The ClustalX windows interface: Xexible strategies for multiple sequence alignment aided by quality analysis tools. *Nucleic Acids Research* 25(24): 4876–4882. <https://doi.org/10.1093/nar/25.24.4876>
- Wang J, Zeng Z, Lyu Z, Liu Z, Wang Y (2018) Description of a new species of *Gracixalus* (Amphibia: Anura: Rhacophoridae) from Guangdong Province, southeastern China. *Zootaxa* 4420(2): 251–269. <https://doi.org/10.11646/zootaxa.4420.2.7>
- Ye C, Hu S (1984) A new species of *Philautus* (Anura: Rhacophoridae) from Xizang Autonomous Region. *Acta Herpetologica Sinica* 3: 67–69.
- Yu G, Hui H, Wang J, Rao D, Wu Z, Yang J (2019) A new species of *Gracixalus* (Anura, Rhacophoridae) from Yunnan, China. *ZooKeys* 851: 91–111. <https://doi.org/10.3897/zookeys.851.32157>
- Zeng Z, Zhao J, Chen C, Chen G, Zhang Z, Wang Y (2017) A new species of the genus *Gracixalus* (Amphibia: Anura: Rhacophoridae) from Mount Jinggang, southeastern China. *Zootaxa* 4250(2): 171–185. <https://doi.org/10.11646/zootaxa.4250.2.3>

Supplementary material 1

Statistical parsimony network as reconstructed by TCS v1.21

Authors: Tung Thanh Tran, Anh Van Pham, Minh Duc Le, Nam Hai Nguyen, Thomas Ziegler, Cuong The Pham

Data type: figure (PDF file)

Copyright notice: This dataset is made available under the Open Database License (<http://opendatacommons.org/licenses/odbl/1.0/>). The Open Database License (ODbL) is a license agreement intended to allow users to freely share, modify, and use this Dataset while maintaining this same freedom for others, provided that the original source and author(s) are credited.

Link: <https://doi.org/10.3897/zookeys.1153.93566.suppl1>

Supplementary material 2

Uncorrected (“p”) distance matrix showing average percentage pairwise genetic divergences (%) for the 16SrRNA gene between members of the genus *Gracixalus*

Authors: Tung Thanh Tran, Anh Van Pham, Minh Duc Le, Nam Hai Nguyen, Thomas Ziegler, Cuong The Pham

Data type: table (word document)

Copyright notice: This dataset is made available under the Open Database License (<http://opendatacommons.org/licenses/odbl/1.0/>). The Open Database License (ODbL) is a license agreement intended to allow users to freely share, modify, and use this Dataset while maintaining this same freedom for others, provided that the original source and author(s) are credited.

Link: <https://doi.org/10.3897/zookeys.1153.93566.suppl2>

Supplementary material 3

Uncorrected (“p”) distance matrix showing average percentage pairwise genetic divergences (%) for the Rag1 gene between members of the genus *Gracixalus*

Authors: Tung Thanh Tran, Anh Van Pham, Minh Duc Le, Nam Hai Nguyen, Thomas Ziegler, Cuong The Pham

Data type: table (word document)

Copyright notice: This dataset is made available under the Open Database License (<http://opendatacommons.org/licenses/odbl/1.0/>). The Open Database License (ODbL) is a license agreement intended to allow users to freely share, modify, and use this Dataset while maintaining this same freedom for others, provided that the original source and author(s) are credited.

Link: <https://doi.org/10.3897/zookeys.1153.93566.suppl3>

The genus *Climaciella* Enderlein, 1910 (Neuroptera, Mantispidae) in French Guiana

Adrian Ardila-Camacho¹, Shaun L. Winterton², Atilano Contreras-Ramos³

1 Posgrado en Ciencias Biológicas, sede Instituto de Biología, Universidad Nacional Autónoma de México (UNAM), Apdo. Postal 70-153, 04510 Ciudad de México, Mexico **2** California State Collection of Arthropods, California Department of Food & Agriculture, Sacramento, 95832 CA, USA **3** Colección Nacional de Insectos, Departamento de Zoología, Instituto de Biología, Universidad Nacional Autónoma de México (UNAM), Apdo. Postal 70-153, 04510 Ciudad de México, Mexico

Corresponding author: Atilano Contreras-Ramos (acontreras@ib.unam.mx)

Academic editor: Davide Badano | Received 4 October 2022 | Accepted 21 February 2023 | Published 10 March 2023

<https://zoobank.org/00BE9805-F6E6-4621-B8EA-6B4026A25B12>

Citation: Ardila-Camacho A, Winterton SL, Contreras-Ramos A (2023) The genus *Climaciella* Enderlein, 1910 (Neuroptera, Mantispidae) in French Guiana. ZooKeys 1153: 37–64. <https://doi.org/10.3897/zookeys.1153.95960>

Abstract

The genus *Climaciella* Enderlein, 1910 is a remarkable group of mantidflies (Neuroptera: Mantispidae: Mantispinae) distributed from Canada to Argentina, including parts of the Caribbean. This genus comprises nine valid extant species plus an extinct species from the late Oligocene of France. Species exhibit Batesian mimicry with vespid wasps (Vespidae). Herein, six species of *Climaciella* from French Guiana are documented. Before this study only *C. semihyalina* (Le Peletier de Saint Fargeau & Audinet-Serville in Latreille et al. 1825) was known from this territory. Two new species, *C. elektroptera* Ardila-Camacho, Winterton & Contreras-Ramos, **sp. nov.** and *C. nigriflava* Ardila-Camacho, Winterton & Contreras-Ramos, **sp. nov.**, are described as well as the first records of *C. amapaensis* Penny, 1982, and *C. tincta* (Navás, 1914) provided from French Guiana. An unknown species recorded from a single female specimen is also presented. Based on the examination of material of *C. amapaensis* recorded here, a specimen previously recorded from Colombia as belonging to this species is herein proposed as a new species, *C. risaraldensis* Ardila-Camacho, **sp. nov.** A taxonomic key and high-resolution images of the species from French Guiana are provided.

Keywords

Lacewings, Neotropics, taxonomy

Introduction

Mantispidae (mantidflies) are a family of predatory insects included within the superfamily Mantispoidea (Winterton et al. 2018). This group is distinguished by the anteriorly curved ocular plane, a well-developed laminatentorium, a tubular pronotum set with maculae, and with forelegs inserted on an expanded anterior apex, presence of precoxal bridge and narrow-shaped postfurcasterna (Ardila-Camacho et al. 2021). On the forefemur, two primary processes on distal half of posteroventral row of processes, and a major, basal process on the anteroventral row of processes are present (Ardila-Camacho et al. 2021). The traditional classification scheme of Mantispidae proposed by Lambkin (1986a, b) considered four subfamilies, namely Symphrasinae, Drepanicinae, Calomantispinae, and Mantispinae, of which the former was always interpreted as sister of the remainder. Nonetheless, recent molecular and morphological studies recovered Symphrasinae as a subfamily of Rhachiberothidae, making Mantispidae non-monophyletic (Winterton et al. 2018; Ardila-Camacho et al. 2021). Even though thorough morphological data (Ardila-Camacho et al. 2021) and genomic scale data (Winterton et al. 2018) support the new position of Symphrasinae, several authors who recently described extinct species of Mantispoidea (Nakamine et al. 2021; Jouault 2022; Jouault et al. 2022; Baranov et al. 2022; Li et al. 2022) still follow the classification of Lambkin (1986a, b). In addition, previous phylogenetic studies based on different data systems (Lambkin 1986a; Liu et al. 2015; Shi et al. 2019; Lu et al. 2020) recovered Drepanicinae as sister to Calomantispinae + Mantispinae; however, the same aforementioned studies support Mantispinae as sister to Drepanicinae + Calomantispinae, with the latter two probably representing a single subfamily (Winterton et al. 2018; Ardila-Camacho et al. 2021).

Among the raptorial Mantispoidea, Mantispinae is the most diverse and widely distributed subfamily (Ohl 2004). This is a highly derived group, whose monophyly is supported by characters of the foreleg such as a ring-shaped groove on the coxa, a semi-triangular femur with anteroventral row of processes reduced to the major process, the anterior surface of the tibia is covered with clavate setae nearly over the entire extension, and the pretarsus is reduced to a single, simple claw (Ardila-Camacho et al. 2021). Currently, the subfamily includes around 319 species and 35 genera distributed in all biogeographical realms (Oswald and Machado 2018). Nine genera are recognized in the New World (Hoffman 1992, 2002) of which *Climaciella* Enderlein, 1910 contains nine species distributed from Southern Canada to northern Argentina including Cuba, Puerto Rico, and Dominican Republic (Hoffman 2002; Hoffman et al. 2017; Ardila-Camacho et al. 2018), plus an extinct species from France, badly preserved as a compression fossil from the late Oligocene (Nel 1988). The generic assignation of the fossil species was questioned by Hoffman (1992) based on venational characters, who proposed that it should be included into its own genus. The morphological characters supporting *Climaciella* as a monophylum include antennal flagellomeres along middle portion of flagellum $\geq 3\times$ as wide as long in anterior view, lateral parapsidal suture

(mesoscutal furrow *sensu* Hoffman (1992)) obsolete, and the female gonocoxites and gonapophyses VIII (both referred as sternite VIII by Hoffman (1992)) separated by thin membranous strip. Nevertheless, according to Hoffman (1992), these characters are also present in genera from other biogeographic regions such as *Euclimacia* Enderlein, 1910, *Pseudoclimaciella* Handschin, 1960, *Asperala* Lambkin, 1986, *Mantisquilla* Enderlein, 1910, and *Spaminta* Lambkin, 1986, and the monophyly of this genus would be probably supported by characters of the first instar larva.

The biology of *Climaciella* is known mostly from studies performed with *C. brunnea* (Say, 1824), a widely distributed species composed of a complex of morphs (or subspecies), which mimic polistine wasps and occur through North America, Mexico, and Central America (Opler 1981; Batra 1972; Redborg and MacLeod 1983; LaSalle 1986). According to Opler (1981), the Batesian mimicry of this species probably evolved because mimics and polistine models have similar habitats and habits. Adults of this species are diurnal and are often found on flowers or foliage, ambushing insect prey. Hoffman (1936) described some attributes of the behavior and morphology of the females, egg, and first instar larva, while Hoffman and Brushwein (1992) described the morphology of the first instar larva. Batra (1972) described the courtship, mating, and ovipositing behavior as well as the behavior of the first instar larvae. Additionally, this species was reported feeding on plant exudates, and *Polistes fuscatus utahensis* (Hayward, 1933) was determined as the model for the population studied by the author. In Costa Rica, the proportion of five different morphs of *C. brunnea* mimicking different species of Polistinae: *Polistes instabilis* Saussure, 1853, *P. canadensis* (Linnaeus), 1758, *P. carnifex* (Fabricius), 1775, *P. erythrocephalus* (Latreille), 1813, and *Synoeca septentrionalis* (Richards), 1978, varied among three different localities and could be related to differential abundance and aggressiveness of the models at each site (Opler 1981). Defensive behavior and displaying of the wasp-like warning colors, plus its capacity as occasional pollinators, was described by Boyden (1983).

After hatching, the first instar larva of *C. brunnea* adopts a vertical posture with the aid of the suctorial eversible process at the end of the abdomen while it maintains its legs extended (Batra 1972; Redborg and MacLeod 1983). Such questing behavior allows the larvae to board potential hosts that pass close by (Redborg and MacLeod 1983). This means that this species exhibits a phoretic behavior, in which the larvae first feed on spider hemolymph near the membranous areas of the carapace of the spider, and once the spider produces an egg-sac, they must reach the eggs before they are entirely encased with silk (Redborg and MacLeod 1983). This sequence is necessary for the larvae to be able to start feeding on the eggs, so it is classified as an obligate spider border, unable to penetrate egg-sacs like other genera of Mantispidinae (Redborg and MacLeod 1983). As the main objective of the larvae is to enter an egg-sac during its construction, larvae of this species are able to move from male to female spiders during copulation (Scheffer 1992). *Climaciella brunnea* has been found in the nature associated with species of the family Lycosidae, although laboratory experiments have shown that the larvae can board other spider families (e.g., Agelenidae and Salticidae), and complete their development

(Redborg and MacLeod 1983; LaSalle 1986; Redborg and Redborg 2020; Snyman et al. 2020). Nonetheless, two morphs of *Climaciella* were found attacking egg sacs of Ctenidae and Araneidae in Panama (Miranda 2007), one of them probably by *Climaciella porosa* Hoffman, 2002 (Ardila-Camacho and García 2015).

The taxonomy of the genus *Climaciella* was addressed in the classical studies of Mantispidae by Handschin (1960), and the works by Penny (1982) and Penny and da Costa (1983) which focused on the Amazonian fauna. Recent studies by Hoffman (2002) and Hoffman et al. (2017) treated this genus in Costa Rica and the West Indies, respectively, while Ardila-Camacho and García (2015) and Ardila-Camacho et al. (2018) dealt with taxonomy of the group in Colombia. In French Guiana, Thouvenot (2010) published a key to genera of Mantispidae, and thus far, only *C. semihyalina* has been reported in this territory (Ohl 2004). Herein, we update the knowledge on the diversity of *Climaciella* in French Guiana, describing two new species, providing new records and present a key to species. Furthermore, a new species from the Colombian Andes previously recorded as *Climaciella amapaensis* Penny, 1982 by Ardila-Camacho and García (2015) is herein proposed partly based on comparison with a specimen of this species from French Guiana.

Materials and methods

Specimens studied herein were collected in different localities of French Guiana between 2014 and 2016 using light traps, and then deposited in California State Collection of Arthropods, Sacramento CA (**CSCA**), Muséum national d'Histoire naturelle, Paris (**MNHN**), and Colección Nacional de Insectos, Instituto de Biología UNAM, Mexico City (**CNIN**). An additional specimen from Colombia is deposited in the private collection Colección Efraín Henao (CEH-085), Villamaría, Colombia. Other collections referred in this contribution are: Coleção Entomológica Pe. Jesus Santiago Moure, Curitiba, Paraná (**DZUP**), Museum of Comparative Zoology, Harvard University, Cambridge (**MCZ**), Naturhistorisches Museum, Bern (**NMBS**), and Museum für Naturkunde der Humboldt-Universität, Berlin (**ZMB**). Genitalia preparations were made by clearing the last abdominal segments in a hot solution of 10% potassium hydroxide (KOH). Residual alkaline solution was washed with distilled water and 80% ethyl alcohol. Then, the genitalia were stored in microvials filled with glycerin and mounted beneath the specimen. Wing venation was studied by spreading the wings of all specimens. Given the morphological peculiarities on the wing venation of *Climaciella*, the tracheation on the major traces of the specimens was compared to that of *C. brunnea* (Fig. 1), as this latter species is often used as example of the genus. External morphology and cleared genitalia were examined using a stereomicroscope. High-resolution images were produced using an AxioCam MRc5 digital camera attached to a Zeiss AxioZoom V16 stereomicroscope. Series of photographs were stacked and processed with the software ZENpro201. Morphological terminology and homology followed Ardila-Camacho et al. (2021).

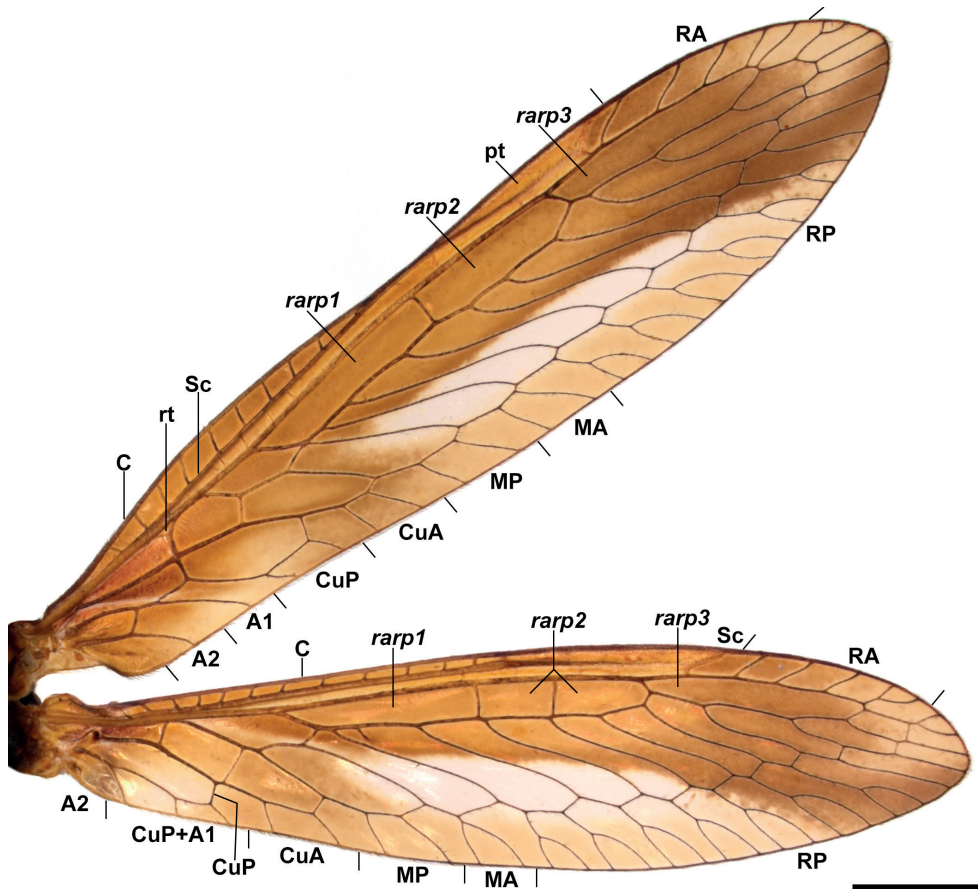


Figure 1. Wing venation in the genus *Climaciella*. *Climaciella brunnea* (Say, 1824) (specimen from Jalisco, Mexico) as an example for the genus. Scale bar: 2 mm.

Taxonomy

Family Mantispidae Leach, 1815

Subfamily Mantispinae Leach, 1815

Genus *Climaciella* Enderlein, 1910

Diagnosis. *Climaciella* is distinguished from other mantispines of the New World by the antennal flagellomeres ≥ 3 times as wide as long in frontal view, the lateral parapsidal furrow not developed, and the female gonocoxites and gonapophyses VIII separated by a membranous strip. Additionally, the membrane of the anterior half of the wings is amber colored, and all the species exhibit Batesian mimicry with polistine wasps.

Included species. *Climaciella amapaensis* Penny, 1982, *C. brunnea* (Say, 1824), *C. cubana* Enderlein, 1910, *C. elektroptera* sp. nov., *C. henrotayi* Nel, 1989, *C. nigri-flava* sp. nov., *C. obtusa* Hoffman, 2002, *C. personata* (Stitz, 1913), *C. porosa* Hoffman, 2002, *C. rafaeli* Calle et al. in Ardila et al. 2018, *C. risaraldensis* sp. nov., *C. semihyalina* (Le Peletier de Saint Fargeau & Audinet-Serville in Latreille et al. 1825), and *C. tincta* (Navás, 1914).

Key to the species of *Climaciella* Enderlein, 1910 from French Guiana

- 1 Prothorax straight or at least only slightly bent medially in lateral view 2
- Prothorax bent medially in lateral view 3
- 2 Body entirely black *Climaciella* sp.
- Body yellow with black stripes *Climaciella amapaensis* Penny, 1982
- 3 Head and prothorax black; anterior half of the wings smoky or dark amber 4
- Head and prothorax mostly yellow or entirely dark brown; wings with anterior half pale amber 5
- 4 Wings with anterior half smoky, the posterodistal margin of the pigmented area darker; abdomen orange *Climaciella tincta* (Navás, 1914)
- Wings with anterior half dark amber and hyaline posterodistal, triangular area; abdomen black *Climaciella semihyalina* (Le Peletier de Saint-Fargeau & Audinet-Serville, 1825)
- 5 Body mostly yellow with dark brown stripes and marks *Climaciella nigri-flava* sp. nov.
- Body entirely dark brown *Climaciella elektroptera* sp. nov.

Climaciella sp.

Fig. 2A

Specimens examined. FRENCH GUIANA: **Roura**, Montagne des Chevaux, Carrière du Galion, Créte avec foret sur quartzite érodée, 04°44'31.54"N, 52°25'53.02"W, 16.V.2015, automatic light trap (blue) (1 ♀ CNIN).

Remarks. Despite this species exhibits a similar coloration pattern as *C. semihyalina*, the straighter prothorax and the wing pattern easily differentiate the unknown species. Compared to *C. semihyalina*, the anterior half of both wings of the specimen examined have paler areas inside the cells and wing apexes (Fig. 2A). In *C. semihyalina*, these same areas are noticeably darker and uniformly colored. Furthermore, the infuscation on the posterior half of both wings differ in their overall extension, shape and intensity between both species. The cited specimen examined herein probably represents a new species; however, as a single female only was available for this study, we opted to not describe this species until male specimens are available to confirm this hypothesis.

Distribution. French Guiana.

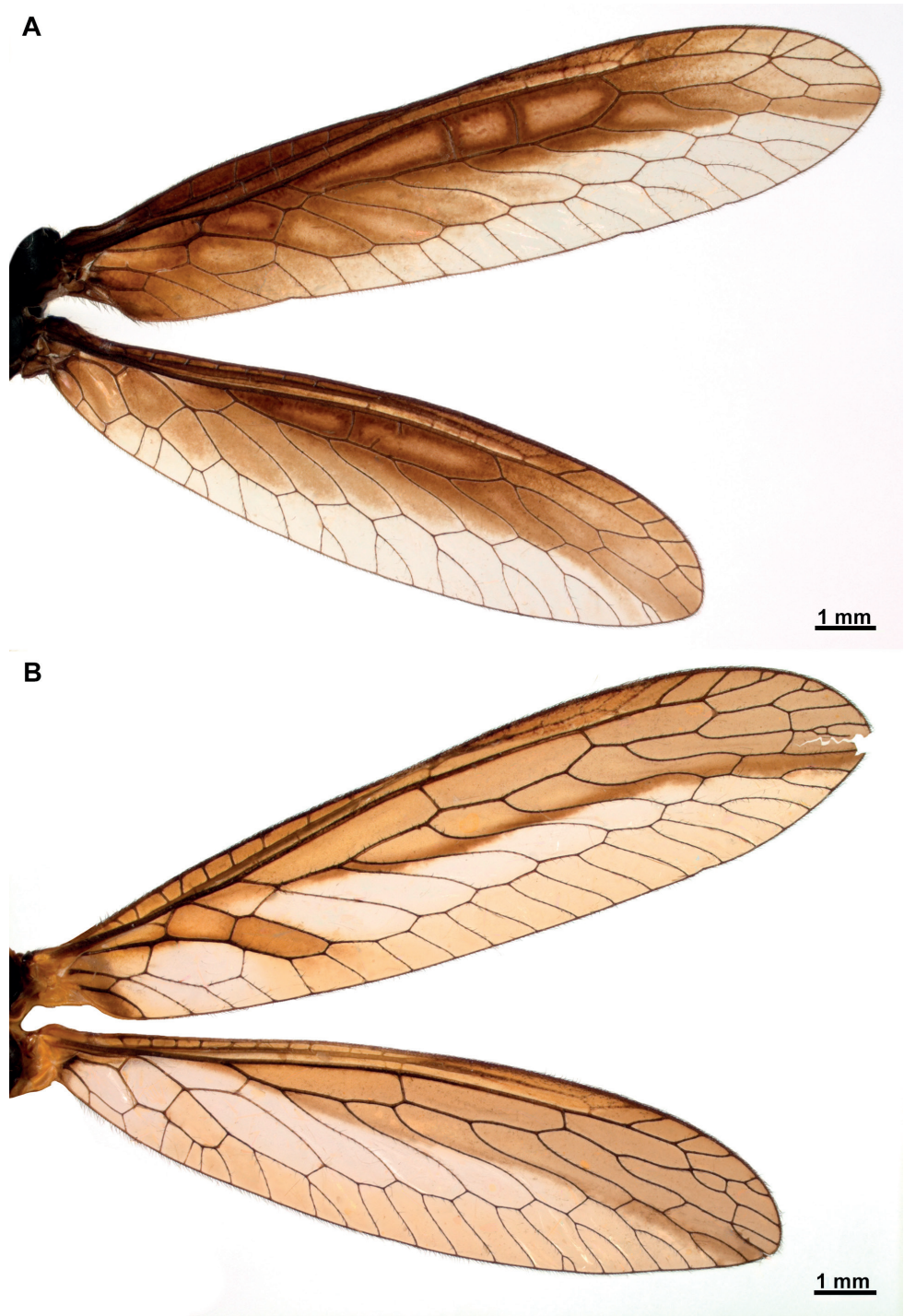


Figure 2. Wings of *Climaciella* species from French Guiana **A** *Climaciella* sp. **B** *Climaciella amapaensis* Penny, 1982.

***Climaciella amapaensis* Penny, 1982**

Fig. 2B

Climaciella amapaensis Penny, 1982: 450. Holotype: male, Brazil (DZUP).

Specimens examined. FRENCH GUIANA: **Maripasoula**, Mitaraka, Contreforts du Mitaraka, crique Alama, Foret vallonée au pied d'inselbergs, 20.VIII.2015, automatic light trap (GemLight) (1 sex? CNIN).

Diagnosis. Records of *Climaciella amapaensis* are scarce, but this species can be easily recognized by its coloration pattern that consists of a yellow body with black stripes and marks. Even though a similar color pattern is expressed by *C. nigriflava* sp. nov., *C. cubana*, *C. risaraldensis* sp. nov., and some morphs of *C. brunnea*, this species is distinguished because on the head there are two transversal bands at the level of the antennal insertion and on the upper portion of the region of the vertex, the compound eyes are enlarged and the region of the gena is narrow. In addition, the prothorax is straight in lateral view with longitudinal, lateral dark brown bands. This species is also unique within the genus due to the presence of narrow forefemur with thin processes. On the male genitalia, the apex of the gonocoxites X is not forked and blade-shaped, and the hypomeres are present as a single granule-shaped sclerite on the gonostyli X membrane laterally on each side.

Remarks. This species is herein reported from French Guiana for the first time. In the original description, this species was reported from Brazil (Amapá) (Penny 1982), and then Hoffman (1992) provided a further record from Peru (Cusco). Recently, Ardila-Camacho and García (2015) provided a redescription and the first record from Colombia (Risaralda); however, this species actually represents a new species despite its noticeably similitude in coloration and morphology.

Distribution. Brazil, French Guiana, Peru.

***Climaciella elektroptera* Ardila-Camacho, Winterton & Contreras-Ramos, sp. nov.**

<https://zoobank.org/8B20AC08-D64E-40FA-B4DD-1F1A4B48A5EC>

Figs 3–5

Type material. *Holotype* ♂, FRENCH GUIANA: **Maripasoula/Camopi**, Mont Itupé, Massif tabulaire, Pente oust (600 m), 28.XI.2014, light trap (MNHN). *Paratypes*. Same data as holotype (1♀ CNIN, 2♀ CSCA).

Diagnosis. This species is easily differentiated from its congeners based on its uniformly dark brown body coloration. The prothorax is bent medially like in *C. semihyalina* and *C. obtusa* and lacks a prominent hump as in *C. porosa*. The wing coloration pattern is similar to that of *C. porosa*, with the anterior half of both wings pale amber. On the male genitalia, the gonocoxites X are bifid at the apex, and the gonostyli X membrane is set with a granule-shaped hypomere laterally at each side. Additionally, the gonostyli X are ribbon-shaped and the female spermatheca is relatively short and simple.

A**2 mm****B****2 mm**

Figure 3. *Climaciella elektroptera* sp. nov. **A** female habitus, dorsal **B** fore- and hindwing.

Description. Measurements. Head width: 2.9–3.2 mm; Head length: 2.7–3.4 mm; Prothorax length: 3.4–3.9 mm; Forefemur length: 4.1–6.4 mm; Forefemur maximum width: 1.7–2.1 mm; Forewing length: 15.4–16.5–18.8 mm; Forewing maximum

width: 3.5–4.1 mm; Hindwing length: 13.3–15.8 mm; Hindwing maximum width: 3.2–3.9 mm.

Coloration (Figs 3, 4A–D). **Head.** Head capsule completely dark brown; antenna brown; flagellomeres with dark brown setae. Mouthparts dark brown. **Thorax.** Prothorax uniformly dark brown. **Foreleg.** Dark brown. **Mid- and hind leg.** Uniformly dark brown. **Wings.** Forewing membrane with anterior half and wing base pale brown, posterior half pale amber; venation brown, with paler and darker areas. Hind wing with costal, subcostal and radial fields, and *Ir-m* and area adjacent to RP branches pale brown; remaining membrane pale amber; venation brown, with paler and darker areas. **Abdomen.** Dark brown, except pleural region of abdominal base cream.

Morphology (Figs 3, 4). **Head.** Vertex region convex above compound eyes; compound eyes as wide as 0.75 of interocular distance at antennal insertion level. Antennal scape 2× as long as wide; pedicel as long as wide; basal flagellomere 1.5× as long as wide, the rest discoidal, with 31–33 flagellomeres, all covered with fine, short setae. Frons quadrangular, frontoclypeal ridge barely perceptible; clypeus trapezoidal, labrum ovoid; mandible elongate; region of the gena as long as clypeus; maxillary palpus with basal palpomere slightly longer than wide; second palpomere 2.5× as long as wide; third and fourth palpomere 3× as long as wide; fifth palpomere as long as third. Submentum rectangular; labial palpus with first palpomere 3× as long as wide, second palpomere 5× as long as wide, third palpomere slightly longer than second; palpimacula groove-shaped. **Thorax.** Pronotum tubular, 4× as long as wide at maculae, slightly bent at mid-length in lateral view; medial region coarsely wrinkled; dorsal surface densely covered with fine, short setae; postfurcasternum narrowly ovoid. Mesonotum as long as wide, anterolaterally produced; lateral parapsidal suture obsolete; entire surface covered with fine, short setae; metanotum rectangular, scutum glabrous, scutellum with fine, short setae. Pteropleuron with fine, short setae. **Foreleg.** Coxa cylindrical, elongate, with proximal ring-shaped sulcus; anterior and posterior surface with abundant fine, short setae distal to proximal sulcus; trochanter ovoid; femur semi-triangular, robust, with abundant fine, short setae; posteroventral row of processes present on distal 2/3 of femur length; medial region of the row with two primary processes, the rest of the row with alternate secondary, tertiary, and quaternary processes, and numerous Stitz organs arising from reduced processes. Anteroventral row of processes reduced to a prominent major process. Tibia short and arched, reaching the major process of femur; anterior surface covered with abundant, clavate setae; distal margin acutely produced; closing surface with abundant trichoid setae. Basitarsus subconical, as long as eutarsus, with abundant trichoid setae on closing surface; pretarsus reduced to a single, simple claw. **Mid- and hind leg.** Coxae and trochanter subconical; femora tubular, that of hind leg slightly longer than on mid leg; tibiae elongate, thin, that of hind leg longer than on mid leg; tibial spurs well-developed. Tarsi with basitarsus slightly longer than eutarsus; pretarsal claws with six apical denticles. **Wings.** Forewing elongate and narrow; costal space narrow with seven or eight subcostal veinlets; Sc vein running close to C on area adjacent to pterostigma, and not approaching or touching RA at pterostigma level; pterostigma wedge-shaped; subcostal space with five or six crossveins on medial region, five or six crossveins on substigmal area. Radial space with two crossveins; one

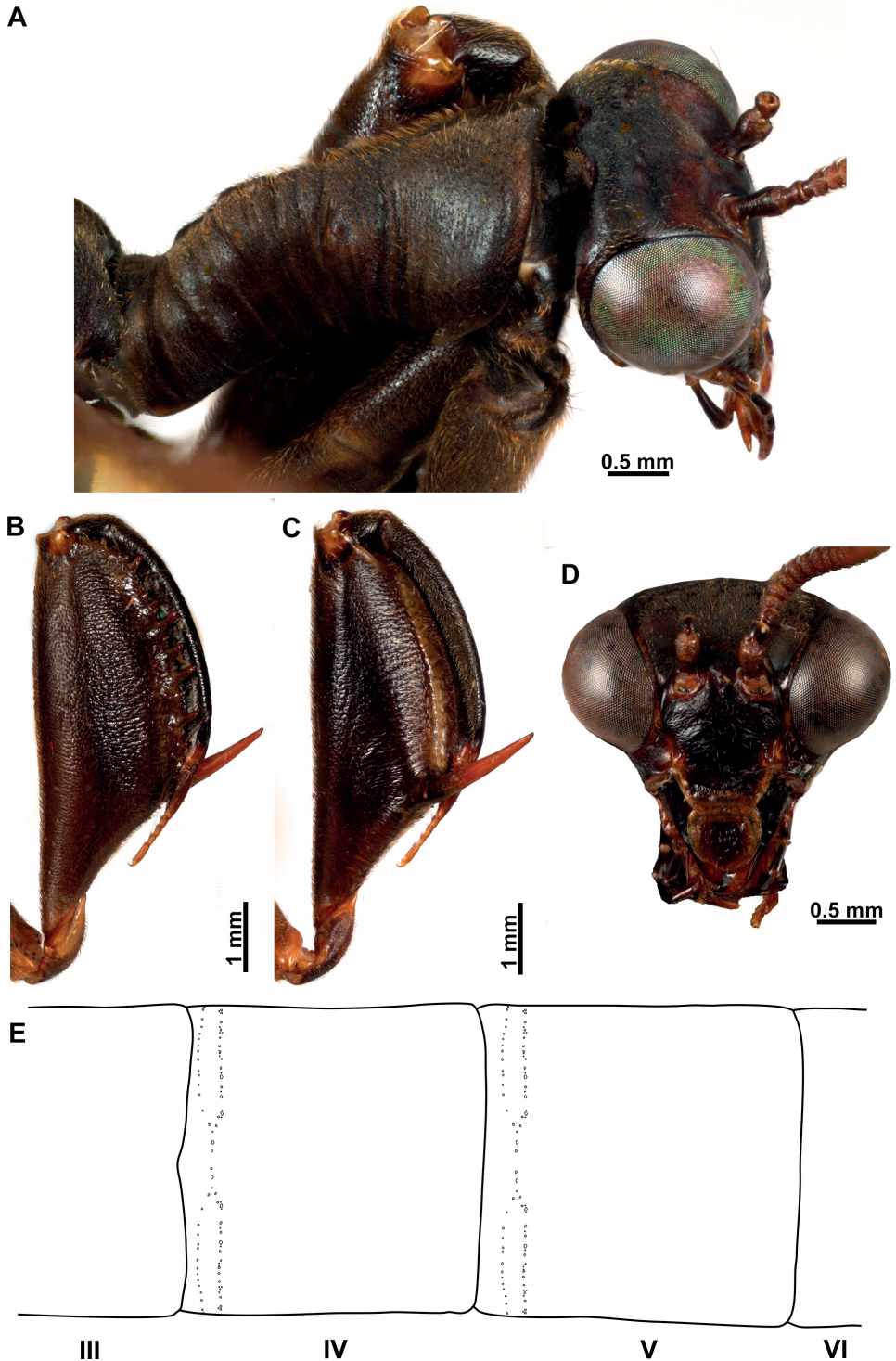


Figure 4. *Climaciella elektroptera* sp. nov. **A** prothorax and head, dorsolateral view **B** foreleg, posterior surface **C** same, anterior surface **D** head, frontal view **E** male pregenital abdominal apparatus.

or two RP branches arising from *rarp1*, three or four from *rarp2*, 1–3 from *rarp3*; six or seven gradate crossveins present. Media vein proximally fused to R, but inflexed forming a radial triangle; M diverging from R close R fork; M fork opposite to R fork; MA proximally fused to first RP stem for a short distance or connected to it through a short crossvein, forming a trapezoidal *rm2*. Cubitus forked near the level of radial triangle. Anal veins simple. Hind wing similar to forewing but shorter; costal space narrow, with nine subcostal veinlets; C and Sc not fused, running subparallel until pterostigma; pterostigma wedge-shaped; subcostal space with five crossveins on distal region. Radial space with three crossveins; two RP branches arising from *rarp1*, two or three from *rarp2*, one or two from *rarp3*; 5–7 gradate crossveins present. Media vein basally fused to R, forked slightly before level of R fork. Cubitus forked slightly beyond the level of 1m-cu, CuA terminating on posterior wing margin at level of 1r-m, CuP distally fused to anterior branch of A1. **Abdomen.** Male tergites IV and V with two parallel rows of pores anterolaterally on each side which converge on inner end, with 28–33 pores on each couple of rows (Fig. 4E); intertergal membrane between segments IV–VI expanded, apparently forming an eversible sac. In both sexes tergite III with two anteromedial glabrous marks; tergite IV with four glabrous marks, two medial and two lateral, all located at mid-length; tergites V and VI with a single glabrous mark, laterally on each side.

Male terminalia (Fig. 5A–F). Tergite IX half-ring shaped, medially narrower than laterally; sternite IX setose, approximately pentagonal, posteromedial region slightly protuberant. Gonocoxite IX elongated, curved, blunt on both apices, anterior apex somewhat expanded, posterior apex curved outwards. Ectoproct ovoid, ventromedial lobe with around 42 stout setae. Gonocoxites X forming an elongate, gently curved sclerite, which is slightly expanded towards anterior apex, posterior apex bifid; gonostyli X membrane ventrally with triangular slightly sclerotized area, covered with microspinulae and with lateral granule-shaped hypomere; gonostyli X elongated, ribbon-shaped; entire surface with microspinulae. Gonocoxites XI arch-shaped, median lobe, short, hook-shaped.

Female terminalia (Fig. 5G–I). Sternite VII (or gonocoxites VII) enlarged, pentagonal. Tergite VIII half-ring shaped, approximately as wide medially as laterally, enclosing the spiracle of the segment; gonocoxites VIII narrow, bar-shaped, subparallel-sided, slightly narrower at middle; gonapophyses VIII forming a bilobed, setose sclerite, connected to posteromedial region of gonocoxites VIII. Tergite IX half-ring shaped, posterolaterally connected to gonocoxites IX; gonocoxite IX a small and ovoid sclerite; gonapophyses IX probably represented by small, sclerotized areas on the anteroventral area of gonocoxites IX. Ectoprocts paired, ovoid. Bursa copulatrix short; spermatheca simple, entangled, with the same thickness on the different sections; fertilization canal duct and fertilization canal short.

Etymology. The specific name of this species is from the Greek *ἤλεκτρον* (*ēlektron*) meaning amber, and *πτερόν* (*pteron*), meaning wing, in allusion to the coloration of the wings of this species.

Remarks. This new species is similar to *C. porosa* based on its general coloration; however, the bent prothorax and the lack of a hump on the medial region of the

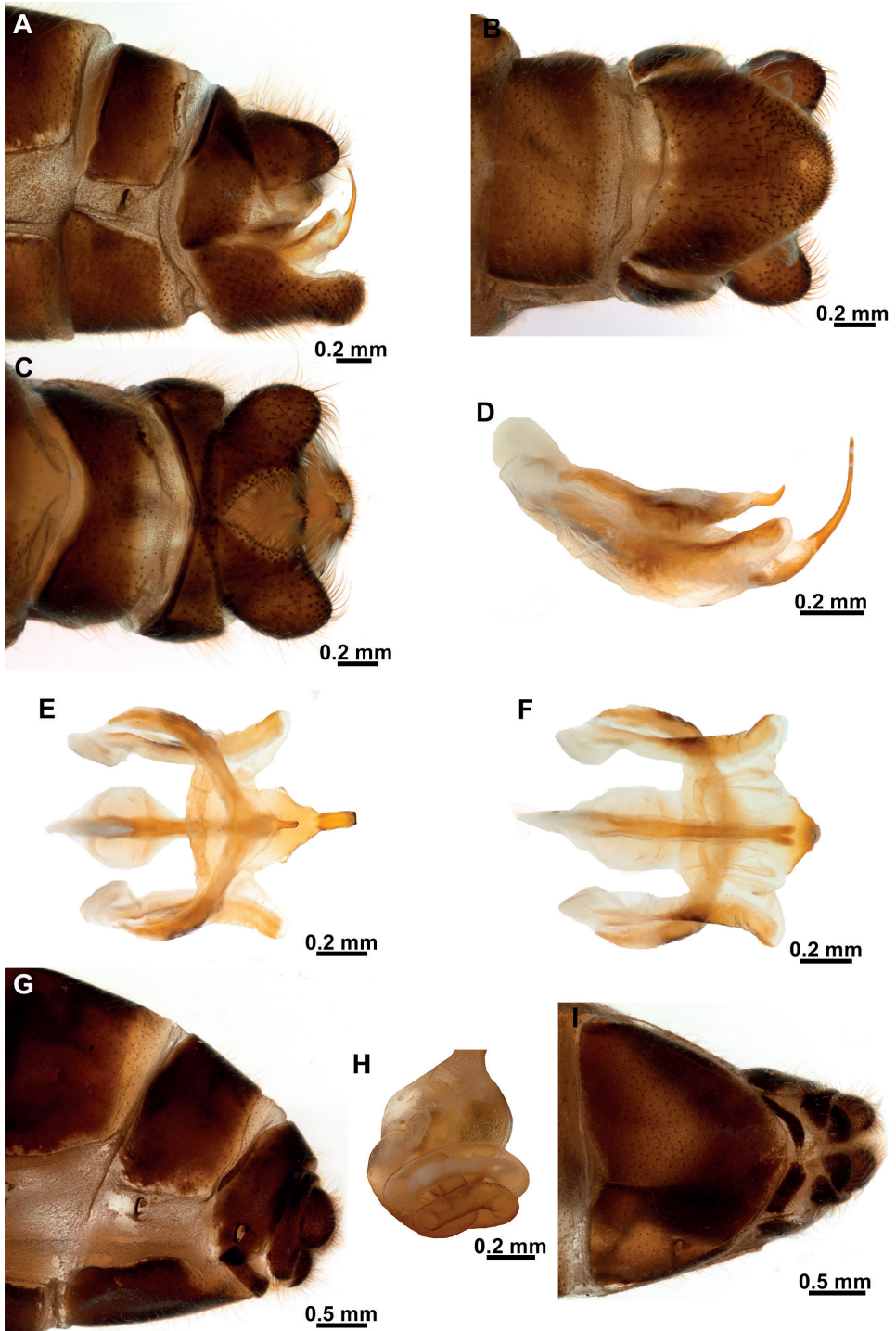


Figure 5. *Climaciella elektroptera* sp. nov. **A** male terminalia, lateral **B** same, ventral **C** same, dorsal **D** male genitalia, lateral **E** same, dorsal **F** same, ventral **G** female terminalia, lateral **H** spermtheca **I** female terminalia, ventral.

pronotum quickly differentiate it. Another species similar to *C. elektroptera* sp. nov. is *C. personata* from Bolivia, although the latter has a more patterned body coloration, and the posterior limit of the amber anterior area of the wings is darker and noticeably marked. Based on the bent prothorax, *C. elektroptera* sp. nov. is probably closely related to *C. obtusa*, *C. semihyalina*, *C. personata*, *C. rafaeli*, and *C. nigriflava* sp. nov.

Based on the coloration pattern, size, and distribution of *C. elektroptera* sp. nov., the possible wasp models for this species could be *Agelaia angulata* (Fabricius, 1804) or *Polistes deceptor* Schulz, 1905 (R. Lopes, pers. comm. 2022)

Distribution. French Guiana.

***Climaciella nigriflava* Ardila-Camacho, Winterton & Contreras-Ramos, sp. nov.**

<https://zoobank.org/01623019-404A-4378-BFE1-7363E84A18CE>

Figs 6–8

Type material. *Holotype* ♂, FRENCH GUIANA: Roura, Montagne des Chevaux, Carrière du Galion, Crête avec forêt sur quartzite érodée, 04°44'31.54"N, 52°25'53.02"W, 22.II.2016, automatic light trap (blue) (MNHN). *Paratypes*. FRENCH GUIANA: Maripasoula, Mitaraka, Contreforts du Mitaraka, crique Alama, Forêt vallonnée au pied d'inselbergs, 18.III.2015, light trap (1♀ CNIN); same data but 20.VIII.2015, automatic light trap (blue) (1♂ CSCA). Roura, Montagne des Chevaux, Carrière du Galion, Crête avec forêt sur quartzite érodée, 4°44'31,54"N, 52°25'53,02"W, 25.IV.2015, automatic light trap (blue) (1♂ CSCA).

Diagnosis. This new species has a similar body coloration pattern as *C. amapaensis*, *C. cubana*, and certain morphs of *C. brunnea*. However, the bent prothorax at midlength in lateral view distinguishes the new species from the aforementioned ones. Furthermore, the head in *C. nigriflava* sp. nov. is basically entirely yellow, while the remaining species with similar coloration exhibit dark stripes or marks. The coloration of the femur is also similar to that of *C. amapaensis*, yet the more robust femur with thickened processes distinguishes *C. nigriflava* sp. nov. from the former. Moreover, the wing coloration of this species is similar to that of *C. porosa* and *C. elektroptera* sp. nov. In the male genitalia, the gonocoxites X have the posterior apex truncate, the hypomeres are absent, and the gonostyli X are elongated, ribbon-shaped with the apex forming an obtuse angle.

Description. Measurements. Head width: 3.0–3.1 mm; Head length: 2.6–3.0 mm; Prothorax length: 3.6–3.8 mm; Forefemur length: 5.2 mm; Forefemur maximum width: 1.9 mm; Forewing length: 15.9–16.5 mm; Forewing maximum width: 3.5–3.7 mm; Hindwing length: 13.5–14.1 mm; Hindwing maximum width: 3.2–3.5 mm.

Coloration (Figs 6, 7A–D). **Head.** Head capsule completely yellow; antenna yellow, sometimes pale brown towards the flagellar apex; flagellomeres with dark brown setae. Clypeus and labrum yellow; mandible pale brown; maxilla and labium pale

A



B

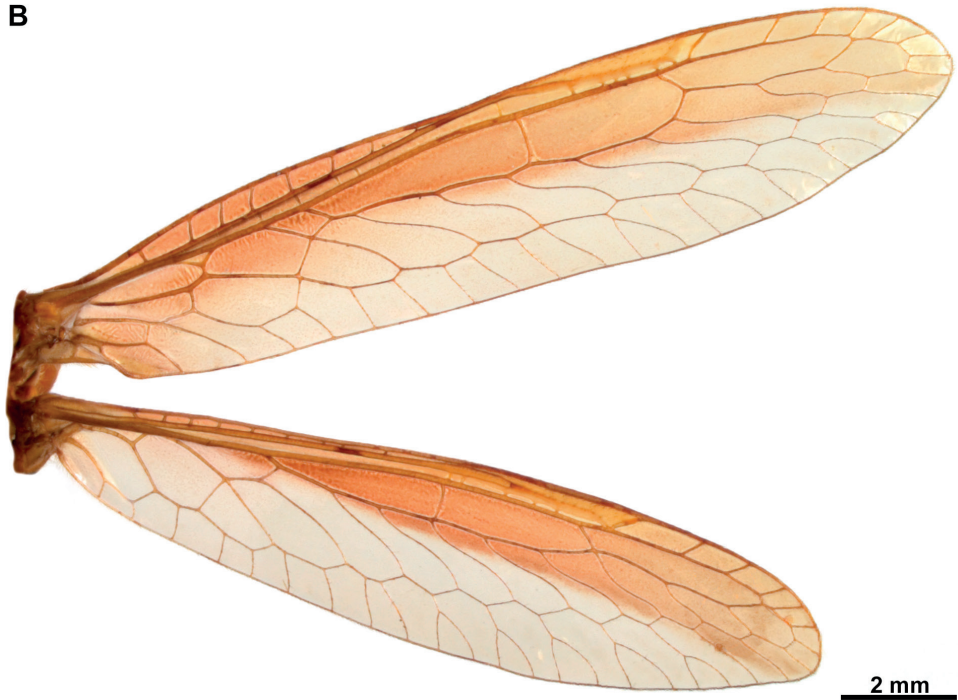


Figure 6. *Climaciella nigriflava* sp. nov. **A** female habitus, dorsal **B** fore- and hindwing.

brown. **Thorax.** Pronotum yellow, with pale brown, lateral areas on the prozona extended from macula to anterior pronotal margin; postfurcasternum yellow. Mesoscutum yellow with brown anterior margin and lateral spots; mesoscutellum yellow with brown, medial area. Metascutum yellow with lateral brown marks; mesoscutellum with anterior half brown, posterior half yellow. Pteropleuron yellow with brown on area adjacent to anapleural cleft and paracoxal suture. **Foreleg.** Coxa and trochanter yellow; femur yellow with small brown mark on medial region of posterior surface, and larger brown area on anterior surface; closing surface with processes yellow but changing to amber towards the apex; tibia mostly yellow with pale brown areas, except anterior surface with darker area. Tarsus pale brown. **Mid- and hind leg.** Coxa of both legs yellow to pale brown; trochanter, femur, tibia, and tarsus pale brown. **Wings.** Forewing membrane with anterior half and wing base pale brown, posterior half pale amber; venation brown, with paler and darker areas. Hind wing with costal, subcostal and radial fields, and *1r-m* and area adjacent to RP branches pale brown; remaining membrane pale amber; venation brown, with paler and darker areas. **Abdomen.** Abdominal segments I and II yellow with pale brown areas; male tergites III–V with striped pattern, exhibiting yellow anterior band and dark brown band on each segment; female tergites III yellow with broad, transversal dark brown band, tergite IV mostly dark brown; remaining tergites on both sexes completely dark brown. Male sternite III yellow, sternites IV and V brown, the remainder dark brown; female sternite III yellow, sternite IV with anterior yellow band and posterior brown band, remaining sternites dark brown.

Morphology (Figs 6, 7). **Head.** Vertex region convex above compound eyes; compound eyes as wide as 0.75 of interocular distance at antennal insertion level. Antennal scape 1.5× as long as wide; pedicel as long as wide; basal flagellomere as long as wide, the rest discoidal, with 32 or 33 flagellomeres, all covered with fine, short setae. Frons subquadrate, frontoclypeal ridge barely perceptible; clypeus trapezoidal, labrum ovoid; mandible elongate; region of the gena as long as clypeus; maxillary palpus with basal palpomere slightly wider than long; second palpomere 2× as long as wide; third and fourth palpomere subequal, both 2.5× as long as wide; fifth palpomere 1.2× as long as fourth. Submentum rectangular; labial palpus with first palpomere 4× as long as wide, second palpomere 5× as long as wide, third palpomere slightly longer than second; palpimacula groove-shaped. **Thorax.** Pronotum tubular, 3.5× as long as wide at maculae, slightly bent at mid-length in lateral view; medial region coarsely wrinkled; dorsal surface densely covered with fine, short setae; postfurcasternum narrowly ovoid. Mesonotum as long as wide, anterolaterally produced; lateral parapsidal suture obsolete; entire surface covered with fine, short setae; metanotum rectangular, scutum glabrous, scutellum with fine, short setae. Pteropleuron with fine, short setae. **Foreleg.** Coxa cylindrical, elongate, with proximal ring-shaped sulcus; anterior and posterior surface with abundant fine setae distal to proximal sulcus; trochanter ovoid; femur semi-triangular, robust, with abundant fine, short setae; posteroventral row of processes present on distal 2/3 of femur length; medial region of the row with two primary processes, the remainder of the row with alternate secondary, tertiary, and quaternary processes, and numerous Stitz organs arising from reduced processes. Anteroventral

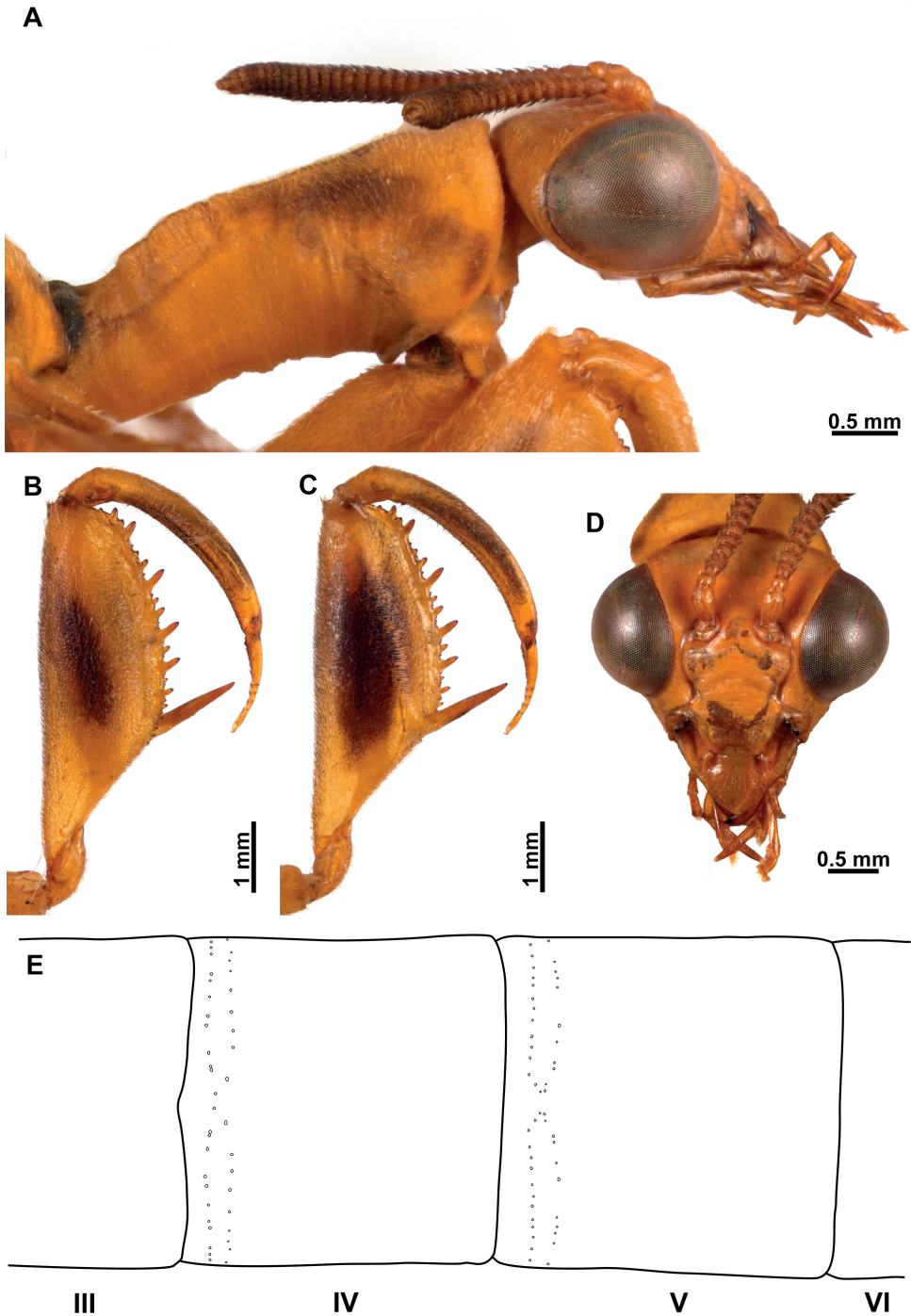


Figure 7. *Climaciella nigriflava* sp. nov. **A** prothorax and head, lateral view **B** foreleg, posterior surface **C** same, anterior surface **D** head, frontal view **E** male pregenital abdominal apparatus.

row of processes reduced to a prominent major process. Tibia short and arched, reaching the major process of femur; anterior surface covered with abundant, clavate setae; distal margin acutely produced; closing surface with abundant trichoid setae. Basitarsus subconical, as long as eutarsus, with abundant trichoid setae on closing surface; pretarsus reduced to a single, simple claw. **Mid- and hind leg.** Coxae and trochanter subconical; femora tubular, that of hind leg slightly longer than on mid leg; tibiae elongate, thin, that of hind leg longer than on mid leg; tibial spurs well-developed. Tarsi with basitarsus slightly shorter than eutarsus; pretarsal claws with five or six apical denticles. **Wings.** Forewing elongate and narrow; costal space narrow with 6–8 subcostal veinlets; Sc vein running close to C on area adjacent to pterostigma, and not approaching or touching RA at pterostigmal level; pterostigma wedge-shaped; subcostal space with four or five crossveins on medial region, six crossveins on substigmal area. Radial space with three crossveins; one or two RP branches arising from *rarp1*, two or three from *rarp2*, and two or three from *rarp3*; 6–8 gradate crossveins present. Media vein proximally fused to R, but inflexed forming a radial triangle; diverging from R close R fork; M fork opposite to R fork; MA proximally fused to first RP stem for a short distance, forming a trapezoidal *rm2*. Cubitus forked near the level of radial triangle. Anal veins simple. Hind wing similar to forewing but shorter; subcostal space narrow, with eight or nine subcostal veinlets; C and Sc not fused, running subparallel until pterostigma; pterostigma wedge-shaped; subcostal space with four or five crossveins on distal region. Radial space with three crossveins; two or three RP branches arising from *rarp1*, two or three from *rarp2*, 1–3 from *rarp3*; 6–8 gradate crossveins present. Media vein basally fused to R, forked slightly before level of R fork. Cubitus forked slightly beyond the level of 1m-cu, CuA terminating on posterior wing margin at level of 1r-m, CuP distally fused to anterior branch of A1. **Abdomen.** Male tergites IV and V with two parallel rows of pores anterolaterally on each side which converge on the inner end, with 22–30 pores on each couple of rows (Fig. 7E); intertergal membrane between segments IV–VI expanded, apparently forming an eversible sac. In both sexes tergite III with two anteromedial glabrous marks; tergite IV with four glabrous marks, two medial and two lateral, all located at mid-length; tergites V and VI with a single glabrous mark, laterally on each side.

Male terminalia (Fig. 8A–F). Tergite IX half-ring shaped, medially narrower than laterally; Sternite IX setose, approximately pentagonal, posteromedial region slightly protuberant. Gonocoxite IX elongated, sigmoid, blunt on both apices, anterior apex somewhat expanded. Ectoproct ovoid, ventromedial lobe with around 36 stout setae. Gonocoxites X forming an elongate and arched sclerite, which is slightly expanded towards anterior apex, posterior apex truncate; gonostyli X membrane ventrally slightly sclerotized covered with microspinulae; gonostyli X elongated, ribbon-shaped, slightly shorter than gonocoxites X, apex forming an obtuse angle; entire surface with microspinulae. Gonocoxites XI arch-shaped, median lobe, short, hook-shaped.

Female terminalia (Fig. 8G–I). Sternite VII (or gonocoxites VII) enlarged, U-shaped. Tergite VIII half-ring shaped, approximately as wide medially as laterally, enclosing the spiracle of the segment; gonocoxites VIII narrow, bar-shaped, subparallel-sided, slightly narrower at middle; gonapophyses VIII forming a rectangular, setose

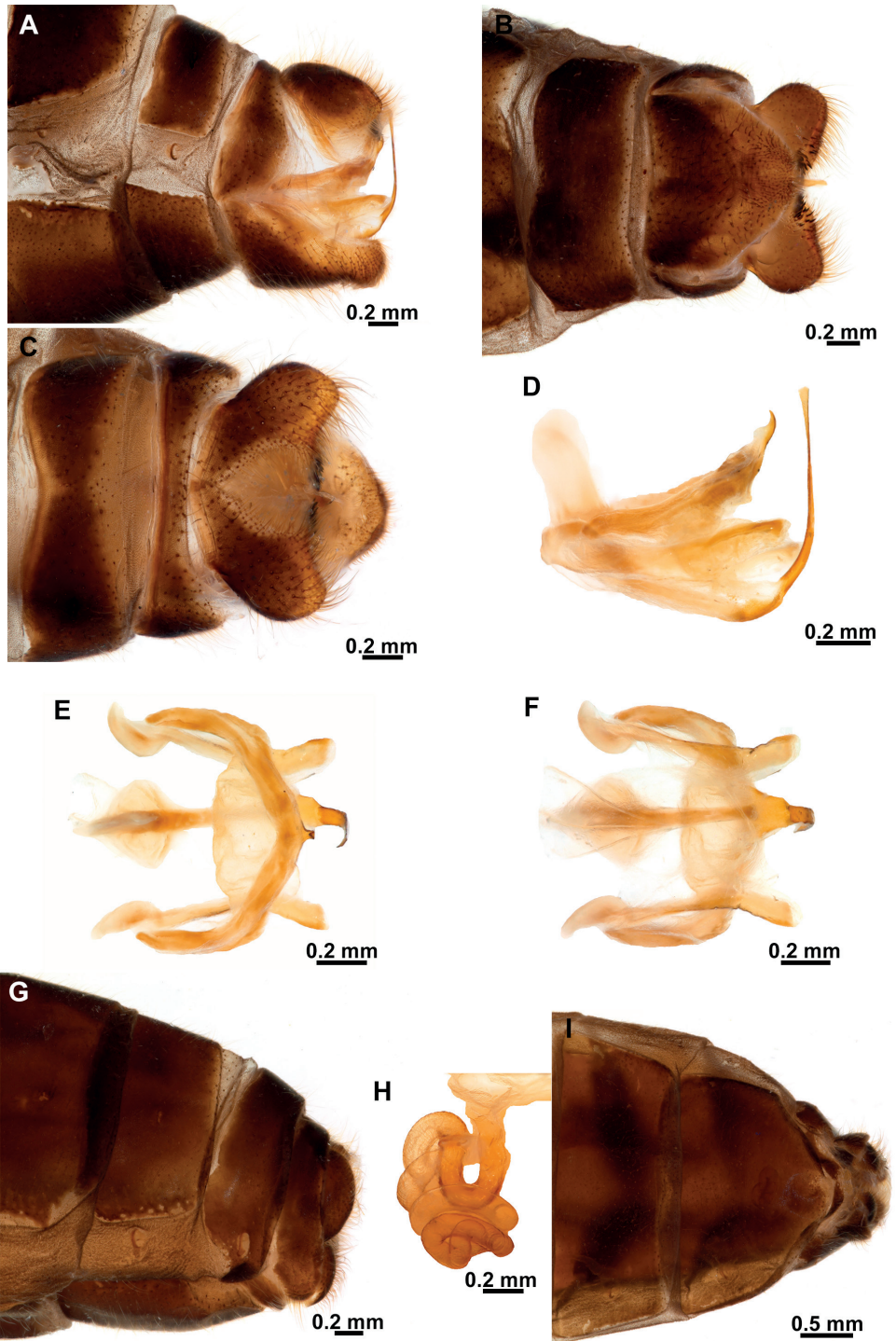


Figure 8. *Climaciella nigriflava* sp. nov. **A** male terminalia, lateral **B** same, ventral **C** same, dorsal **D** male genitalia, lateral **E** same, dorsal **F** same, ventral **G** female terminalia, lateral **H** spermatheca **I** female terminalia, ventral.

sclerite, connected to posteromedial region of gonocoxites VIII. Tergite IX half-ring shaped, posterolaterally connected to gonocoxites IX; gonocoxite IX a small and ovoid sclerite; gonapophyses IX probably represented by small, sclerotized areas on the anteroventral area of gonocoxites IX. Ectoprocts paired, ovoid. Bursa copulatrix short; spermatheca simple, spiral-shaped, progressively narrowed towards the apex; fertilization canal duct and fertilization canal short.

Etymology. The specific epithet of this species is a combination of the Latin words *niger* which means black, and *flavus* meaning yellow, in allusion to the coloration pattern of the body of this species.

Remarks. Based on the prothorax morphology, this new species appears to be closely related to *C. obtusa*, *C. semihyalina*, *C. personata*, *C. rafaeli*, and *C. elektroptera* sp. nov. The body coloration pattern of the new species with head and thorax predominantly yellow, and a large dark area on the abdomen indicates this species could be a mimic of the vespid wasps *Agelaia pallipes* (Olivier, 1792) or *Mischocyttarus cerberus* Ducke, 1918 in the case of smaller specimens, or *Polistes testaceicolor* Bequaert, 1937 or *Agelaia testacea* (Fabricius, 1804) in the case of larger specimens (R. Lopes, pers. comm. 2022).

***Climaciella semihyalina* (Le Peletier de Saint-Fargeau & Audinet-Serville in Latreille et al. 1825)**

Fig. 9A

Mantispa semihyalina Le Peletier de Saint-Fargeau & Audinet-Serville in Latreille et al. 1825: 270, sex not indicated. Holotype (or syntypes): sex unknown, Brazil (MNHN).

Mantispa chalybea Erichson, 1839: 160, sex not indicated. Syntypes: sex unknown, Brazil, Suriname (ZMB, MCZ). Synonymized by Enderlein 1910: 367.

Mantispa grandis; Burmeister, 1839: 967. Not available with Burmeister as author. Synonymized by Westwood 1852: 253.

Nobrega tinctus Navás, 1914: 233, sex not indicated (see *C. tinctus* below). Holotype: sex unknown, Brazil (NHMUK). Synonymized by Penny 1982: 453. (non).

Specimens examined. FRENCH GUIANA: Maripasoula, Mitaraka, Contreforts du Mitaraka, crique Alama, Forêt vallonnée au pied d'inselbergs, 12.III.2015, light trap (1♂ CNIN); same data but automatic light trap (blue) (1♂ CSCA).

Diagnosis. The overall black coloration of the body of this species is shared with *C. obtusa*, *C. rafaeli*, and the *synoeca* morph of *C. brunnea*. However, the wing pattern of *C. semihyalina* easily separates it from the former two, whereas the bent prothorax distinguishes this species from the latter. This species is rapidly recognized by the dark amber anterior half of the wings, while in the posterior half, the basal region is pale amber, while a preapical triangular area is hyaline. On the male genitalia, the apex of the gonocoxites X is bifid, and the gonostyli X are spine-shaped.

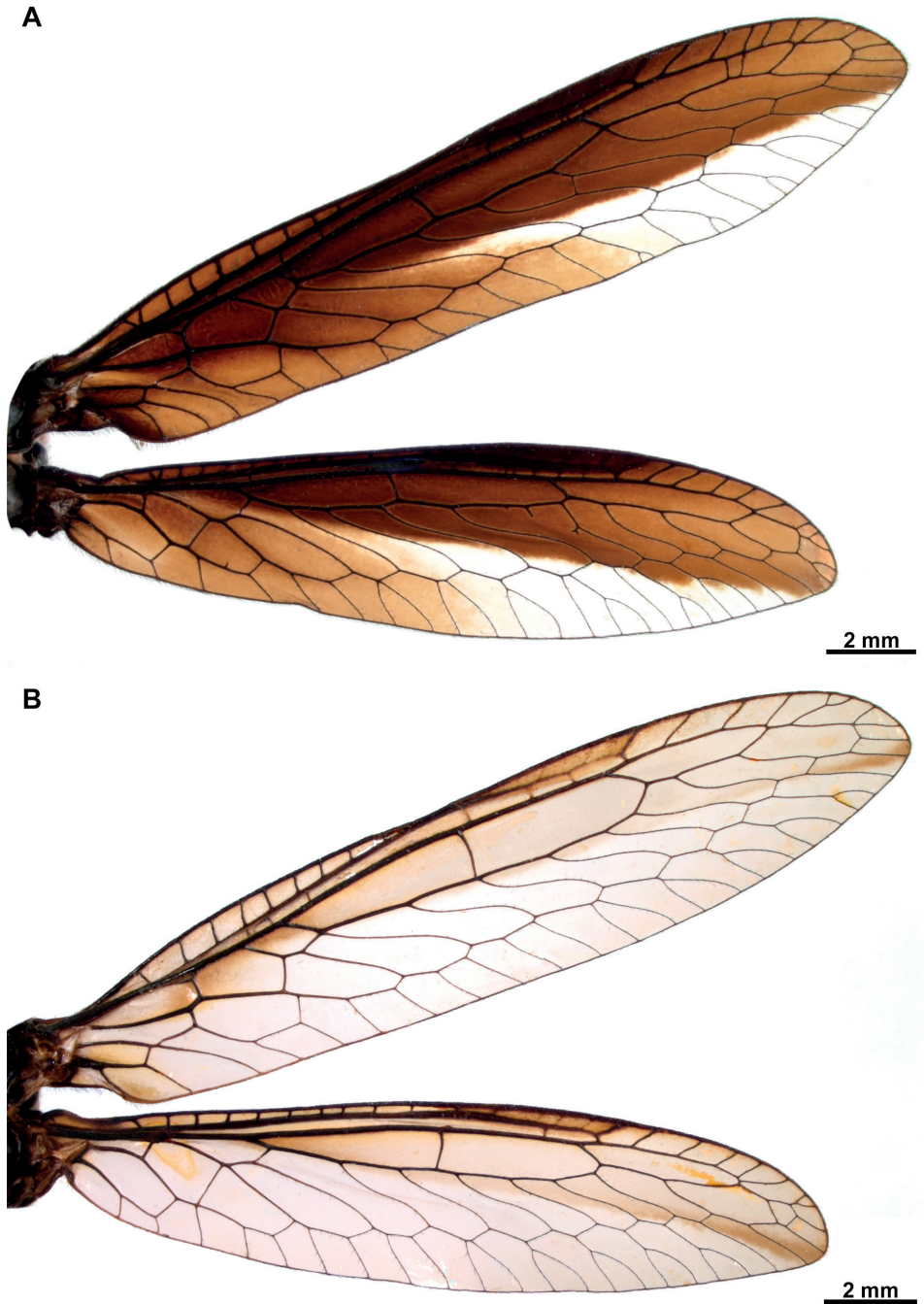


Figure 9. Wings of *Climaciella* species from French Guiana **A** *Climaciella semihyalina* (Le Peletier de Saint-Fargeau & Audinet-Serville in Latreille et al. 1825) **B** *Climaciella tincta* (Navás, 1914).

Remarks. *Climaciella semihyalina*, is the most commonly encountered species of the genus in South America, being widely distributed in the Amazon. The bent prothorax together the robust forefemora of this species resemble the shape of the head of its potential models, i.e., the vespids *Polybia simillima* Smith, 1862, *P. ignobilis* (Haliday, 1836) (Ardila-Camacho and García 2015), *Synoeca surinama* (Linnaeus, 1767), or *Polistes goeldii* Ducke, 1904 (R. Lopes, pers. comm. 2022). The basal orange-reddish region of the forefemur apparently resembles the mandibles of the wasp model. This species was already known in French Guiana, with the first record from this territory published by Navás (1926). The wide distribution of this species from the Amazon to Argentina, calls into attention about the possibility that the different populations could represent actually different species.

Distribution. Argentina, Bolivia, Brazil, Colombia, Ecuador, French Guiana, Paraguay, Peru, Suriname, Uruguay.

Climaciella tincta (Navás, 1914)

Figs 9B, 10

Nobrega tinctus Navás, 1914: 233. Holotype: sex unknown, Brazil (NHMUK).

Climaciella duckei Navás, 1915: 196. Holotype: sex unknown, Peru (NMBS). Synonymized by Alvim, 2021: 31.

Climaciella tincta (Navás, 1914); Alvim 2021: 31.

Specimens examined. FRENCH GUIANA: Maripassoula/Camopi, Mont Itoupé, Massif tabulaire, Pente oust (600 m), 23.XI.2014, light trap (1♂, 1♀ CNIN); same data but 24.XI.2014, light trap (1♀ CSCA); same data but 29.XI.2014, light trap (2♀ CSCA). Roura, Montagne des Chevaux, Carrière du Galion, Crête avec forêt sur quartzite érodée, 4°44'31,54"N, 52°25'53,02"W, 10.X.2015, automatic light trap (blue) (1♀ CSCA).

Diagnosis. This species has a distinctive coloration of the body with black head and thorax and orange abdomen. The prothorax is bent like in *C. semihyalina*, *C. obtusa*, *C. personata*, *C. rafaeli*, and the new species described herein. The wings have smoky anterior half, with the posterodistal margin of this pigmented area more marked. On the male genitalia, the apex of the gonocoxites X is bifid, the hypomeres are present as a lateral granule-shaped sclerite at each side, and the gonostyli X is elongated and narrow.

Remarks. Based on the prothorax morphology, *C. tincta* is apparently closely related with *C. semihyalina*, *C. obtusa*, *C. personata*, *C. rafaeli*, *C. elektroptera* sp. nov., and *C. nigriflava* sp. nov. This species was originally described by Navás (1914) as *Nobrega tinctus* Navás, 1914; however, Penny (1982) proposed this species as a synonym of *C. semihyalina* based on the coloration of the head and the thorax. It is noteworthy that the type of *Nobrega tinctus* lacks an abdomen, so the coloration and genitalic morphology were unknown by Penny (1982). Furthermore, he considered the wing coloration of the type of *N. tinctus* as intraspecific variation. Hoffman (1992) revalidated this species and transferred it to the genus *Climaciella* after the examination of the type. Additionally, he synonymized *Climaciella duckei* Navás, 1915 under *C. tincta*. These



Figure 10. Habitus of female *Climaciella tincta* in dorsal view.

results were corroborated by Alvim (2021), who redescribed this species and provided illustrations of the male and female genitalia for the first time. Herein, we provide the first record of *C. tincta* from French Guiana.

Based on the distribution and coloration pattern exhibited by *C. tincta* (Fig. 10), the possible models for this species could be *Polybia rejecta* (Fabricius, 1798) in the case of small specimens, while *Polybia dimidiata*, *Polistes occipitalis* Ducke, 1904, and *Polistes bicolor* Fox, 1898 could be the models for larger specimens (R. Lopes, pers. comm. 2022).

Distribution. Brazil, French Guiana.

***Climaciella risaraldensis* Ardila-Camacho, sp. nov.**

<https://zoobank.org/07366DDF-2CDC-416F-9D77-6DD21026F018>

Type material. *Holotype* ♂, COLOMBIA: **Risaralda**, Tatamá, Centro de visitantes planes de San Rafael, 5°4'20,87"N, 75°57'44,45"W, 2400 m, 10.VI.2010, F. Gaviria, entomological net (CEH-085).

Diagnosis. This new species may be distinguished from the majority of the species in the genus by the general coloration pattern that is yellow with black stripes and marks. Furthermore, *C. risaraldensis* sp. nov. is easily separated from *C. nigriflava* sp. nov. by the black vertex region and the straight prothorax. On the other hand, this new species can be separated from *C. amapaensis* by having smaller compound eyes and

broadened region of the gena, pronotum dark brown with small diffuse yellow areas, anterior half of the wing pale amber, the forked apex of the male gonocoxites X, and hypomeres present as two granules on each side of the gonostyli X membrane.

Description. See Ardila-Camacho and García (2015).

Etymology. This species is named after the department of Risaralda, a region of the central Andes of Colombia where the type locality of this species is located.

Remarks. Based on the descriptions of Penny (1982) and Hoffman (1992), this species was initially identified as *C. amapaensis* by Ardila-Camacho and García (2015) as both have a quite similar coloration and patterning, and because the former authors did not provide enough details of the male pregenital, abdominal apparatus and genitalia. *Climaciella risaraldensis* sp. nov. is noticeably morphologically differentiated from its Amazonian congeners exhibiting a yellow and black coloration pattern. Furthermore, this species is found at high elevation (2400 m) in the mountains of the Western Cordillera of Colombia, an area remarkably isolated from the Amazon.

Based on the morphology of the prothorax, this species is probably closely related to *C. amapaensis*, *C. brunnea*, *C. cubana*, and *C. porosa*. Among these, the new species is similar to certain morphs of *C. brunnea*; however the wing coloration, the male pregenital apparatus, and the genitalic morphology are markedly differentiated between both species.

Distribution. Colombia.

Discussion

In the present study, the number of species of *Climaciella* in French Guiana is increased from one to six, based on considerable collecting efforts performed in this small portion of the Amazon. The diversity of species in this territory is quite remarkable compared to other, larger Neotropical countries. In Colombia and Brazil for example, five species of this genus have been reported to date (Ardila-Camacho and García 2015; Ardila-Camacho et al. 2018; Alvim 2021). By contrast, in a smaller and well-sampled country such as Costa Rica, three species have been reported (Hoffman 2002). It is likely that the number of species recorded in the Neotropics is influenced by the collecting efforts, and a considerable diversity of this genus is expected to be found, primarily in countries of Northern South America, where this genus appears to have its higher diversity.

The two Guianese new species described herein are apparently closely related based on genitalic morphology. Both species appear to form a group of species together with *C. semihyalina*, *C. obtusa*, *C. rafaelli*, *C. personata*, and *C. tincta* based on the bent prothorax, a hypothesis supported in the cladistic analysis performed by Hoffman (1992). By contrast, *C. amapaensis*, *C. brunnea*, *C. cubana*, *C. porosa*, and *C. risaraldensis* sp. nov. form a group of species distinguished by a straight prothorax, although this still needs to be tested in a phylogenetic framework. In the phylogenetic analysis performed by Hoffman (1992), *C. cubana* was recovered as sister of the other species, while *C. brunnea* and *C. porosa* were recovered as sister based on the presence of five or more transverse rows of pores anterolaterally on tergite IV at each side, and the forked apex of the male gonocoxite IX.

Climaciella was recovered as sister of the remainder of mantispine genera of the New World by Hoffman (1992) based on morphological characters. This genus exhibits a series character states such as the MA of the FW fused or nearly fused (i.e., separated by short crossvein) to the RP stem and the overall morphology of the fusion between the CuP and the anterior branch of the A1 of the HW, which are shared with genera from other realms such as *Austroclimaciella* Handschin, 1961, *Euclimacia*, *Pseudoclimaciella*, *Nampista* Navás, 1914, *Tuberontha* Handschin, 1961, and *Mimetispa* Handschin, 1961 (Hoffman 1992; Snyman et al. 2012; Snyman et al. 2018). Interestingly, all these genera also express Batesian mimicry, begging the question if this attribute arose a single time in all these taxa or if it arose multiple times independently. Moreover, in the New World, the mimicry with vespid wasps is also expressed by *Entanoneura* and likely by *Paramantispa* Williner & Kormilev, 1958, of which the latter appears to be closely related to *Climaciella* based on venational characters, especially the close association between the MA and the RP stem of the FW. Furthermore, species of *Paramantispa* and *Climaciella* have relatively small compound eyes and broadened genal region, with the exception of *C. amapaensis* that has enlarged compound eyes and narrow genal region. Based on the work of Hoffman (1992), *Entanoneura* and *Paramantispa* are sister groups and are more related to other mantispine genera of the New World lacking Batesian mimicry. This would suggest, that at least, in the New World this condition arose independently in different genera.

Acknowledgements

We thank Rogério Botion Lopes for his help recognizing the possible wasp models of the species studied herein. Sincere thanks to Renato Machado for sharing information about the genus *Climaciella* from Brazil, to Michael Ohl for kindly providing high resolution images of the holotypes of *C. personata* and *C. tincta*, as well as for useful reviews to this contribution, and to associate editor D. Badano for encouraging feedback on a previous manuscript version. AAC acknowledges Posgrado en Ciencias Biológicas, UNAM, for support during his doctoral studies, and Consejo Nacional de Ciencia y Tecnología (CONACYT-Mexico) for support through a doctoral scholarship. We thank Susana Guzmán-Gómez (Laboratorio de Microscopía y Fotografía de la Biodiversidad, LaNaBio-IBUNAM) for help with high resolution stereomicroscope photography. AAC and ACR acknowledge Instituto de Biología, UNAM for general support for this research. General support is also acknowledged through the project “Biodiversidad de Neuroptera en México: un enfoque taxonómico integrativo” (CONACYT CB2017-2018, A1-S-32693) and “Biodiversidad de grupos selectos de Neuropteroidea de la Península de Baja California” (PAPIIT IN209721). Specimens were collected under ABS permit number APA 973-1 as part of the “Our Planet Reviewed” Guyane-2015 expedition in the Mitaraka range, in the core area of the French Guiana Amazonian Park, organized by the MNHN and Pro-Natura International. The expedition was funded by the European Fund for Regional Development (ERDF), the Conseil régional de Guyane, the Conseil général de Guyane, the Direction de l’Environnement, de l’Aménagement et du Logement and by the ministère de

l'Éducation nationale, de l'Enseignement supérieur et de la Recherche. It was realized in collaboration with the Parc amazonien de Guyane and the Société entomologique Antilles-Guyane (SEAG).

References

- Alvim BGC (2021) Estudo taxonômico dos gêneros *Climaciella* Enderlein, 1910 e *Entanoneura* Enderlein, 1910 (Neuroptera: Mantispidae: Mantispinae) no Brasil. Master's Thesis, Universidade Federal do Tocantins, Porto Nacional, Tocantins, Brazil.
- Ardila-Camacho A, García A (2015) Mantidflies of Colombia (Neuroptera, Mantispidae). *Zootaxa* 3937(3): 401–455. <https://doi.org/10.11646/zootaxa.3937.3.1>
- Ardila-Camacho A, Calle-Tobón A, Wolff M, Stange LA (2018) New species and new distributional records of Neotropical Mantispidae (Insecta: Neuroptera). *Zootaxa* 4413(2): 295–324. <https://doi.org/10.11646/zootaxa.4413.2.4>
- Ardila-Camacho A, Martins CC, Aspöck U, Contreras-Ramos A (2021) Comparative morphology of extant raptorial Mantispoidea (Neuroptera: Mantispidae, Rhachiberothidae) suggests a non-monophyletic Mantispidae and a single origin of the raptorial condition within the superfamily. *Zootaxa* 4992(1): 1–89. <https://doi.org/10.11646/zootaxa.4992.1.1>
- Baranov V, Pérez-de la Fuente R, Engel M, Hammel JU, Kiesmüller C, Hörnig MK, Pazinato PG, Stahlecker C, Haug C, Haug JT (2022) The first adult mantis lacewing from Baltic amber, with an evaluation of the post-Cretaceous loss of morphological diversity of raptorial appendages in Mantispidae. *Fossil Record (Weinheim)* 25(1): 11–24. <https://doi.org/10.3897/fr.25.80134>
- Batra SWT (1972) Notes on the behavior and ecology of the mantispid, *Climaciella brunnea occidentalis*. *Journal of the Kansas Entomological Society* 45: 334–340. <https://www.jstor.org/stable/25082507> [sic]
- Boyden TC (1983) Mimicry, predation and potential pollination by the mantispid, *Climaciella brunnea* var. *instabilis* (Say) (Mantispidae: Neuroptera). *Journal of the New York Entomological Society* 91: 508–511. <https://www.jstor.org/stable/25009393>
- Handschin E (1960) Zur Revision süd-amerikanischer Mantispiden. *Revue Suisse de Zoologie* 67: 523–560. <https://doi.org/10.5962/bhl.part.75281>
- Hoffman KM (1992) Systematics of the Mantispinae (Neuroptera: Mantispidae) of North, Central, and South America. PhD Thesis, Clemson University, Clemson, South Carolina, USA.
- Hoffman KM (2002) Family Mantispidae. In: Penny ND (Ed.) *A guide to the lacewings (Neuroptera) of Costa Rica*. *Proceedings of the California Academy of Sciences* 53(12): 251–275.
- Hoffman KM, Brushwein JR (1992) Descriptions of the larvae and pupae of some North American Mantispinae (Neuroptera: Mantispidae) and development of a system of larval chaetotaxy for Neuroptera. *Transactions of the American Entomological Society* 118: 159–196. <https://www.jstor.org/stable/25078557>
- Hoffman KM, Flint OS, Pérez-Gelabert DE (2017) The Mantispidae of the West Indies with special reference to de Dominican Republic (Neuroptera: Mantispidae). *Insecta Mundi* 0559: 1–15. <https://digitalcommons.unl.edu/insectamundi/1076/>
- Hoffman CH (1936) Notes on *Climaciella brunnea* var. *occidentalis* [sic] Banks (Mantispidae – Neuroptera). *Bulletin of the Brooklyn Entomological Society* 31: 202–203.

- Jouault C (2022) A new species of thorny lacewing (Neuroptera: Rhachiberothidae: Paraberotherinae) from mid-Cretaceous Burmese amber with novel raptorial foreleg structure. *Proceedings of the Geologists' Association* 133: 32–39. <https://doi.org/10.1016/j.pgeola.2021.11.001>
- Jouault C, Pouillon JM, Nel A (2022) Beautiful wing coloration pattern in a new doratomantispine species (Neuroptera: Mantispidae) from the mid-Cretaceous Burmese amber. *Zootaxa* 5100(3): 390–400. <https://doi.org/10.11646/zootaxa.5100.3.4>
- Lambkin KJ (1986a) A revision of the Australian Mantispidae (Insecta: Neuroptera) with a contribution to the classification of the family. I. General and Drepanicinae. *Australian Journal of Zoology, Supplementary Series* 116: 1–142. <https://doi.org/10.1071/AJZS116>
- Lambkin KJ (1986b) A revision of the Australian Mantispidae (Insecta: Neuroptera) with a contribution to the classification of the family. II. Calomantispinae and Mantispininae. *Australian Journal of Zoology, Supplementary Series* 117: 1–113. <https://doi.org/10.1071/AJZS117>
- LaSalle MW (1986) Note on the mantispid *Climaciella brunnea* (Neuroptera: Mantispidae) in a coastal marsh habitat. *Entomological News, Philadelphia* 97: 7–10.
- Latreille PA, Le Peletier de Saint Fargeau ALM, Audinet-Serville JG, Guérin-Méneville FE (1825) *Encyclopedie méthodique. Histoire naturelle (Vol. 10 (Insectes))*. Paris, 344 pp. https://lacewing.tamu.edu/neuropterida/neur_bibliography/edoc12/latreille1825ref3681-5034.pdf
- Li H, Zhuo D, Cao L, Wang B, Poinar Jr G, Ohl M, Liu X (2022) New Cretaceous fossil mantispids highlight the palaeodiversity of the extinct subfamily Doratomantispinae (Neuroptera: Mantispidae). *Organisms, Diversity & Evolution* 22(3): 681–730. <https://doi.org/10.1007/s13127-022-00546-y>
- Liu XY, Winterton SL, Chao W, Ross P, Ohl M (2015) A new genus of mantidflies discovered in the Oriental region, with a higher-level phylogeny of Mantispidae (Neuroptera) using DNA sequences and morphology. *Systematic Entomology* 40(1): 183–206. <https://doi.org/10.1111/syen.12096>
- Lu X, Wang B, Zhang W, Ohl M, Engel MS, Liu X (2020) Cretaceous diversity and disparity in a lacewing lineage of predators (Neuroptera: Mantispidae). *Proceedings. Biological Sciences* 287(1928): e20200629. <https://doi.org/10.1098/rspb.2020.0629>
- Miranda RJ (2007) *Insectos depredadores y parasitoides de huevos de arañas (Arachnida: Araneae: Araneomorphae) en Panamá*. Master's Thesis, Universidad de Panamá, Panamá, República de Panamá. http://up-rid.up.ac.pa/2954/5/roberto_miranda.pdf
- Nakamine H, Yamamoto S, Takayashi Y, Li H, Liu X (2021) A remarkable new thorny lacewing from mid-Cretaceous amber from northern Myanmar (Neuroptera: Rhachiberothidae). *PalZ* 96: 207–217. <https://doi.org/10.1007/s12542-021-00589-0>
- Navás L (1914) *Neurópteros sudamericanos. Primera [I] serie. Brotéria (Zoológica)* 12: 45–56. [215–234.]
- Navás L (1926) *Insectos exóticos neurópteros y afines. Brotéria (Zoológica)* 23: 79–93.
- Nel A (1988) Deux nouveaux Mantispidae (Planipennia) fossiles de l'Oligocene du sud-est de la France. *Neuroptera International* 5: 103–109. https://lacewing.tamu.edu/neuropterida/neur_bibliography/edoc12/nel1988ref4431-20917.pdf
- Ohl M (2004) Annotated catalog of the Mantispidae of the world (Neuroptera). *Contributions on Entomology, International* 5(3): 131–262. https://lacewing.tamu.edu/neuropterida/neur_bibliography/edoc12/ohl2004ref11556-961.pdf

- Opler PA (1981) Polymorphic mimicry of polistine wasps by a neotropical neuropteran. *Biotropica* 13(3): 165–176. <https://doi.org/10.2307/2388121>
- Oswald JD, Machado RJP (2018) Biodiversity of the Neuropterida (Insecta: Neuroptera: Megaloptera, and Raphidioptera). In: Footitt RG, Adler PH (Eds) *Insect Biodiversity: Science and Society* (Vol. II. 1st Edn.). John Wiley and Sons, New York, 627–671. <https://doi.org/10.1002/9781118945582.ch21>
- Penny ND (1982) Neuroptera of the Amazon basin. Part 6. Mantispidae (1). *Acta Amazonica* 12(2): 415–463. <https://doi.org/10.1590/1809-43921982122415>
- Penny ND, da Costa CA (1983) Mantispídeos do Brasil (Neuroptera: Mantispidae). *Acta Amazonica* 13(3–4): 601–687. <https://doi.org/10.1590/1809-439219831334601>
- Redborg KE, Macleod EG (1983) *Climaciella brunnea* (Neuroptera: Mantispidae): a mantispid that obligately boards spiders. *Journal of Natural History* 17(1): 63–73. <https://doi.org/10.1080/00222938300770041>
- Redborg KE, Redborg AH (2000) Resource partitioning of spider hosts (Arachnida, Araneae) by two mantispid species (Neuroptera, Mantispidae) in an Illinois woodland. *The Journal of Arachnology* 28(1): 70–78. [https://doi.org/10.1636/0161-8202\(2000\)028\[0070:RPOSHA\]2.0.CO;2](https://doi.org/10.1636/0161-8202(2000)028[0070:RPOSHA]2.0.CO;2)
- Say T (1824) Order Neuroptera. In: Keating WH (Ed.) *Narrative of an Expedition to the Source of St. Peter's River, Lake Winnepeek, Lake of the Woods, &c. &c. Performed in the Year 1823, by Order of the Hon. J. C. Calhoun, Secretary of War, Under the Command of Stephen H. Long, Major U.S.T.E.* (Vol. 2). Carey and Lea, Philadelphia, 303–310. https://lacewing.tamu.edu/neuropterida/neur_bibliography/edoc12/say1824ref5533-368.pdf
- Scheffer S (1992) Transfer of a larval mantispid during copulation of its spider host. *Journal of Insect Behavior* 5(6): 797–800. <https://doi.org/10.1007/BF01047988>
- Shi C, Yang Q, Winterton SL, Pang H, Ren D (2019) Stem-group fossils of Symphrasinae shed light on early evolution of Mantispidae (Insecta, Neuroptera). *Papers in Palaeontology* 6(1): 143–154. <https://doi.org/10.1002/spp2.1265>
- Snyman LP, Ohl M, Mansell MW, Scholtz CH (2012) A revision and key to the genera of Afro-tropical Mantispidae (Neuropterida, Neuroptera), with the description of a new genus. *ZooKeys* 184: 67–93. <https://doi.org/10.3897/zookeys.184.2489>
- Snyman LP, Sole CL, Ohl M (2018) A revision of and keys to the genera of the Mantispinae of the Oriental and Palearctic regions (Neuroptera: Mantispidae). *Zootaxa* 4450(5): 501–549. <https://doi.org/10.11646/zootaxa.4450.5.1>
- Snyman LP, Ohl M, Pirk CWW, Sole CL (2020) A review of the biology and biogeography of Mantispidae (Neuroptera). *Insect Systematics & Evolution* 52(2): 125–166. <https://doi.org/10.1163/1876312X-bja10002>
- Thouvenot M (2010) Mantispidae de Guyane (Neuroptera). *Entomologiste* 66: 165–168. [= Mantispidae of Guyana (Neuroptera)]
- Winterton SL, Lemmon AR, Gillung JP, Garzon IJ, Badano D, Bakkes DK, Breitkreuz LCV, Engel MS, Lemmon EM, Liu X, Machado RJP, Skevington JH, Oswald JD (2018) Evolution of lacewings and allied orders using anchored phylogenomics (Neuroptera, Megaloptera, Raphidioptera). *Systematic Entomology* 43(2): 330–354. <https://doi.org/10.1111/syen.12278>

Description of one new species of the genus *Orthozona* Hampson, 1895 (Lepidoptera, Erebidae, Herminiinae) from China

Ting-Ting Zhao¹, Xin-Yu Zhang², Hui-Lin Han^{1,3,4}

1 School of Forestry, Northeast Forestry University, Harbin, 150040, China **2** Simianshan Forest Resource Service Center, Jiangjin District, Chongqing, 402296, China **3** Key Laboratory of Sustainable Forest Ecosystem Management-Ministry of Education, Northeast Forestry University, Harbin, 150040, China **4** Northeast Asia Biodiversity Research Center, Northeast Forestry University, Harbin, 150040, China

Corresponding author: Hui-Lin Han (hanhuilin@aliyun.com)

Academic editor: Pavel Stoev | Received 28 December 2021 | Accepted 22 February 2023 | Published 13 March 2023

<https://zoobank.org/AA538D0F-56CF-4A53-9626-B685BDFE0E64>

Citation: Zhao T-T, Zhang X-Y, Han H-L (2023) Description of one new species of the genus *Orthozona* Hampson, 1895 (Lepidoptera, Erebidae, Herminiinae) from China. ZooKeys 1153: 65–72. <https://doi.org/10.3897/zookeys.1153.79856>

Abstract

A new species of the genus *Orthozona* Hampson, 1895, *O. parallelineata* **sp. nov.**, is described from China. The new species is illustrated with images of adults and genitalia, and it is compared to similar species, *O. quadrilineata* and *Paracolax curvilineata*. A distribution map of this new species is also presented.

Keywords

Herminine moths, new species, southwest China, taxonomy

Introduction

The genus *Orthozona* was erected by Hampson (1895) with *Madopa quadrilineata* Moore, 1882 as the type species from Darjiling, India. The genus has included as many as five species, namely *Orthozona bilineata* Wileman, 1915; *O. curvilineata* Wileman, 1915; *O. quadrilineata* (Moore, 1882); *O. karapina* Strand, 1920, and *O. rufilineata* (Hampson, 1895) (Poole 1989; Beccaloni et al. 2003). However, *O. bilineata* and *O. curvilineata* were transferred to *Paracolax* Hübner, [1825] by Owada (1992a) and

Owada et al. (2021). To date, two species are known to occur in China: *O. karapina* and *O. quadrilineata* (Owada 1992b; Chen 1999; Wu et al. 2013). Smetacek and Kitching (2012) recorded a male specimen of *O. quadrilineata* from northwestern India and illustrated a female syntype of *O. quadrilineata* from Darjeeling, but they did not show the male and female genitalia. In the present study, a new species is described from Xizang Autonomous Region, China. Further study is needed to understand the relatedness of *Orthozona* with *Paracolax*.

Materials and methods

Specimens were collected in Xizang Autonomous Region, China, using a 220 V/450 W mercury lamp and a DC black light. Standard methods for dissection of the genitalia and preparation of the slide mounts were used (Kononenko and Han 2007). Photographs of the adults were taken with a Nikon D700 camera; genitalia slides were photographed with an Olympus photo-microscope, composited with Helicon Focus, and further processed with Adobe Photoshop CS6. The types of the two new species are deposited in the collection of Northeast Forestry University, Harbin, China.

Abbreviations for institutional collections are as follows:

- NEFU Northeast Forestry University (Harbin, China);
NSMT National Museum of Nature and Science (Tsukuba, Japan).

Taxonomic account

Genus *Orthozona* Hampson, 1895

Orthozona Hampson, 1895, 94. Type species: *Madopa quadrilineata* Moore, 1882.

Diagnosis. In morphology, both *Orthozona* and *Paracolax* Hübner, [1825] share some characters as follows: the color of the forewings is ochre to dark ochre, the antemedial and postmedial line are distinct; the distal part of valva are tongue-like, the sacculus process are developed; and the ductus bursae have a pair of sclerotized stripes. However, these genera can be distinguished by the following features: the antemedial and postmedial lines in *Orthozona* are inwardly oblique or slightly curved but always parallel with each other, whereas the two lines in *Paracola* are oblique or wavy and seldom parallel; the reniform spots in *Orthozona* are not obvious, while these spots in *Paracola* are obvious; the sacculus process of *Orthozona* is finger-shaped, slightly separated from the valva, and slightly sclerotized, whereas the sacculus process in *Paracola* is variously shaped, e.g. digitiform, conical, truncate, etc.; and the corpus bursae of *Orthozona* is sac-like, with a single signum, while the corpus bursae of *Paracola* is very long, more than twice as long as the ductus bursae, and with or without signum (Owada 1992a; Chen 1999; Smetacek and Kitching 2012; Wu 2014).

Description. The proboscis is developed; the labial palpus in males is sickle-shaped, mostly covered with scale tufts ventrally; labial palpus in females with the 2nd segments straight and the 3rd segments upturned; the antenna is filiform. Thorax: quite stout; the forewing is broad, with the outer margin broad and slightly excurved; in many species of this genus, the medial line of the hindwing is indistinct and the subterminal line is slightly arched. Abdomen: slender, slightly lighter than the thorax; the uncus is slender, with a hooked apex; the tegumen is narrow and triangular; the saccus is U-shaped; the valva is simple and weakly sclerotized, with saccular process; the vesica is covered minutely granular and bears a basal cornutus; in females, the analis papili is short, the apophyses posteriores and anteriores are moderate in length, the ductus bursae is short, the corpus bursae have more extensive microspines, and a signum is present.

***Orthozona parallelineata* Zhao, Zhang & Han, sp. nov.**

<https://zoobank.org/5DE18C80-120E-445A-A501-54900F5F7D91>

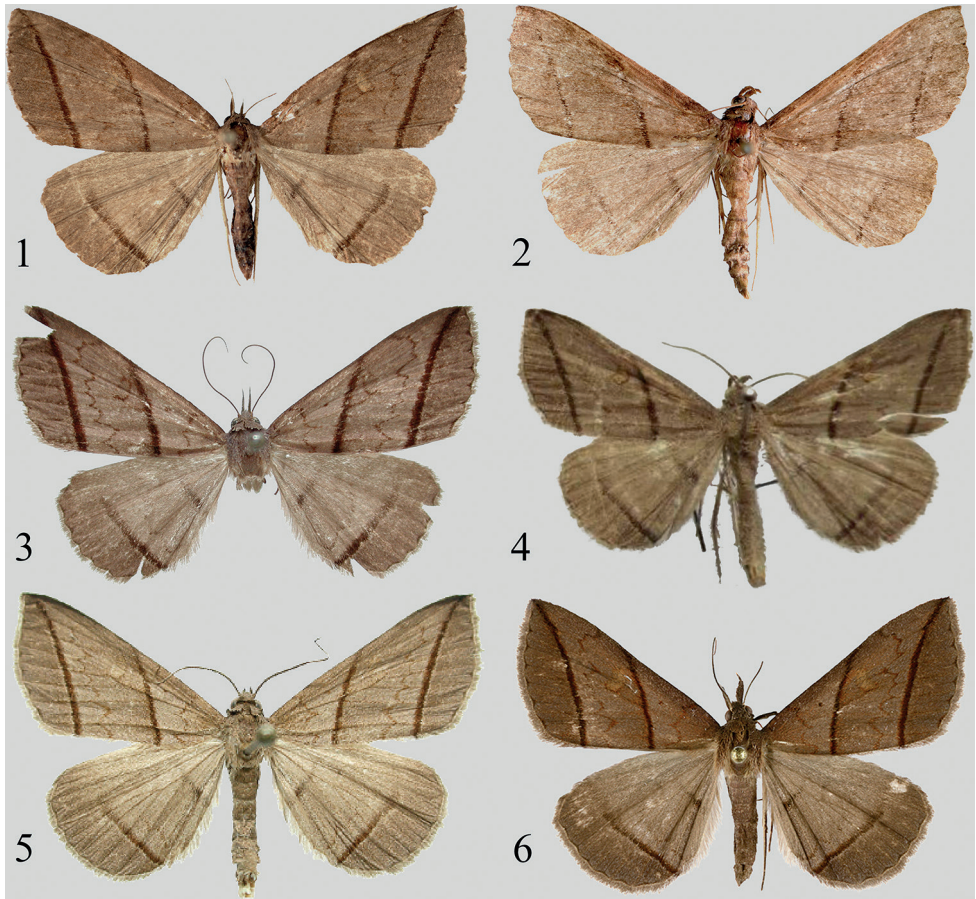
Figs 1, 2, 7, 9, 12–14

Material examined. Holotype: ♀, CHINA; Xizang Autonomous Region, Linzhi City, Lulang Town; 19.VIII.2014; H.L. Han leg.; genitalia No. zxy-0132-2; coll. NEFU.

Paratypes: 1 ♀, CHINA; Xizang Autonomous Region, Linzhi City, Pailong Countryside; 22–23.IX.2011; H.L. Han leg.; genitalia No. ztt-5280-2; 1 ♀ • Xizang Autonomous Region, Linzhi City, Nadengzuo Village; 14–15.VIII.2014; H.L. Han leg.; genitalia No. ztt-5286-2; 3 ♂♂, 2 ♀♀ • Xizang Autonomous Region, Linzhi City, Nadengzuo Village; 17.VIII.2014; H.L. Han leg.; genitalia No. zxy-0099-2, zxy-0103-1, ztt-5278-2, ztt-5281-1, ztt-5284-1; 3 ♀♀, 1 ♂ • Xizang Autonomous Region, Linzhi City, Mount Sejila; 20.VIII.2014; H.L. Han leg.; genitalia No. hhl-5279-1, hhl-5282-2, hhl-5283-2, hhl-5291-2; 1 ♀ • Xizang Autonomous Region, Linzhi City, Mount Sejila; 22.IX.2016; Z.H. Pan leg.; genitalia No. hhl-5289-2; 3 ♂♂ • Xizang Autonomous Region, Linzhi City, 13.VIII.2017; H.L. Han leg.; genitalia No. hhl-5285-1, hhl-5288-1, hhl-5293-1; coll. NEFU.

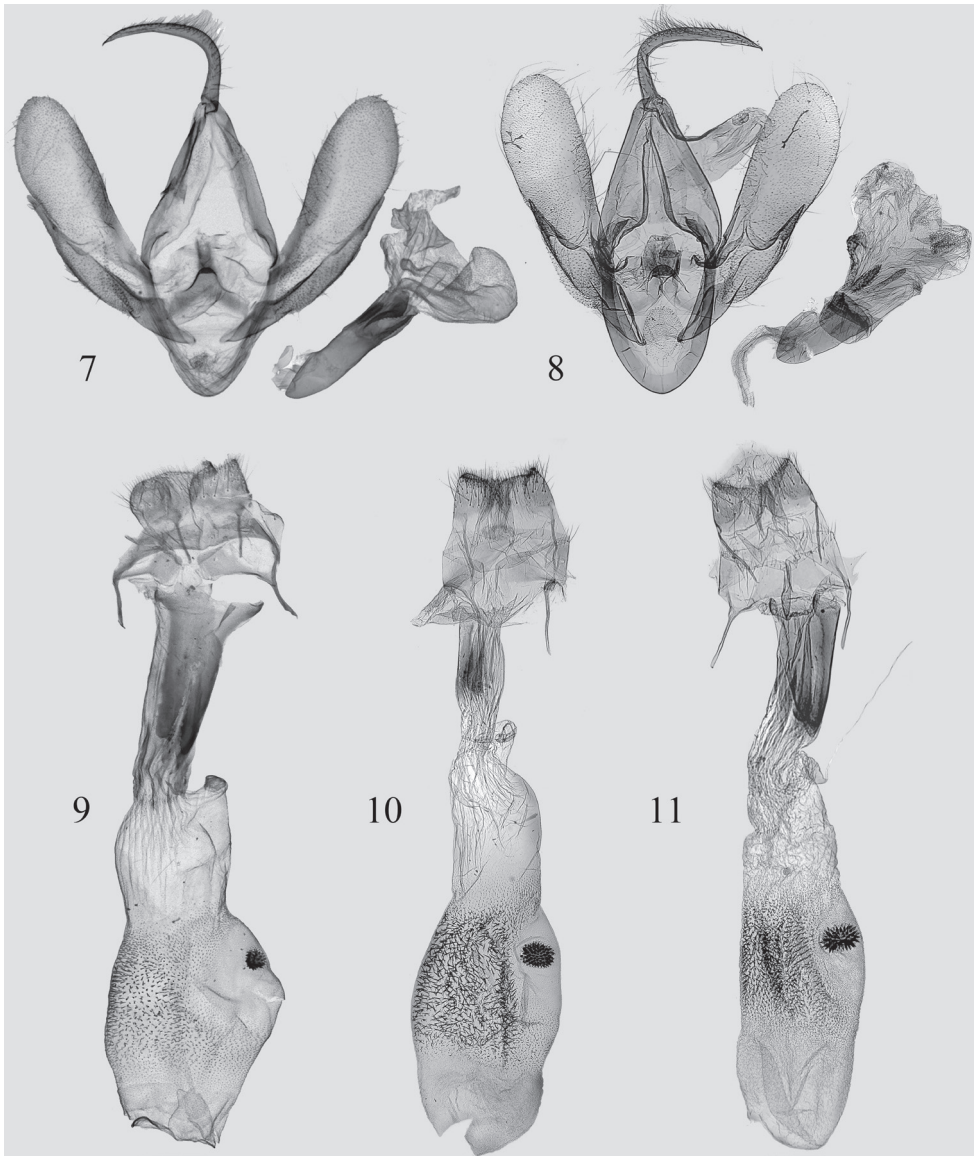
Diagnosis. *O. parallelineata* sp. nov. (Figs 1, 2) is superficially similar to *O. quadrilineata* (Figs 3, 4) and *P. curvilineata* (Figs 5, 6) but can be separated from these species by the following characters. In the male genitalia (Fig. 7), the valva is narrower (in *P. curvilineata*, the cucullus is roundish and broader); the sacculus process is approximately 3/4 the length of valva, narrow, and the distal part is thin, finger-shaped (in *P. curvilineata*, the length of sacculus processes is obviously less than 1/2 of the valva, and the sclerotized is apically pointed); the saccus is narrower (in *P. curvilineata*, the saccus is broader); the phalli are slightly longer (in *P. curvilineata*, the phalli are shorter and stouter).

The characters of female genitalia (Fig. 9) are very similar to those of *O. quadrilineata* (Fig. 10) and *P. curvilineata* (Fig. 11); the corpus bursae is covered with sparse spinules (in *O. quadrilineata* and *P. curvilineata*, the spinules are more dense); the ductus bursae has two long, sclerotized longitudinal bands, which is similar to that of *P. curvilineata* (in *O. quadrilineata*, the ductus bursae has a small sclerotized band).



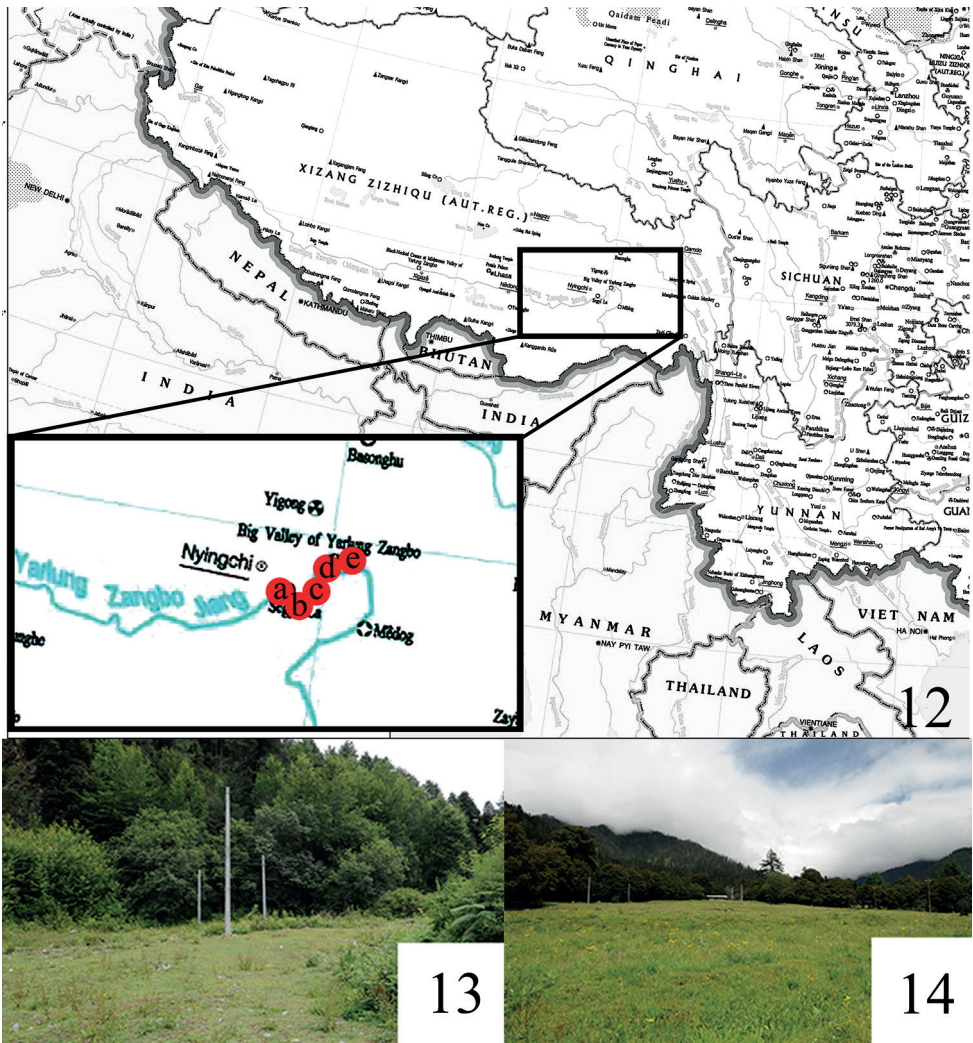
Figures 1–6. *Orthozona* and *Paracolax* spp., adults **1** *O. parallellilineata* sp. nov., female, holotype, Xizang **2** *O. parallellilineata* sp. nov., male, paratype, Xizang **3** *O. quadrilineata* (Moore, 1882), female, Sikkim (from Dr Mamoru Owada) **4** *O. quadrilineata* (after Smetacek and Kitching 2012) **5** *P. curvilineata* (Wileman, 1915), male, Taiwan (from Dr Shipher Wu) **6** *P. curvilineata*, female, Taiwan (from Dr Shipher Wu).

Description. Adult (Figs 1, 2). Wingspan 37–39 mm in both sexes. Head: dark brown; labial palpus sickle-shaped in male, extended forward in female; antenna filiform. Thorax: patagium and tegula dark brown; mesothorax and metathorax light ochre-grey. Forewing light ochre-brown, diffused with brown scales; antemedial line dark brown, excurved, with a deep, excurved dent in $Cu_2-1A+2A$ area; medial line inwardly oblique, dark blackish brown, broadly band-shaped, slightly curved inwards; postmedial line narrow, brown, waved on the vein, with a large, excurved dent at the costal margin region, and a large, incurved dent in $Cu_2-1A+2A$ area; subterminal line inwardly oblique, dark blackish brown, broadly band-shaped, slightly curved inwards, parallel to the medial line, and running from the apex to inner margin close to the tornus; terminal line grey, narrow; orbicular spot small, brown, distinct, encircled with



Figures 7–11. Genitalia of *Orthozona* and *Paracolax* spp. **7** *O. parallelilineata* sp. nov., paratype, genit. prep. zxy-0103-1 **8** *P. curvilineata* (Wileman, 1915), Taiwan (from Dr Mamoru Owada, genit. prep. NSMT4187, in NSMT) **9** *O. parallelilineata* sp. nov., holotype, genit. prep. zxy-0132-2 **10** *O. quadrilineata* (Moore, 1882), Sikkim (from Dr Mamoru Owada, genit. prep. NSMT4373, in NSMT) **11** *P. curvilineata* (from Dr Mamoru Owada).

a halo; reniform spot oval; a flap with a fringe of scales underlapping the forewing costa below over ca 2/3 of its length in male. Hindwing slightly lighter than forewing; media line brown, more prominent in inner margin region; postmedial line very narrow,



Figures 12–14. Distribution and collecting sites of *Orthozona* spp. **12** distribution map: a = Mount Sejila; b = Nadengzuo Village; c = Lulang Town; d = Layue Village; e = Pailong Countryside **13** collection site at Nadengzuo Village, Linzhi City, Xizang Autonomous Region **14** collection site in Luluang countryside, Linzhi City, Xizang Autonomous Region.

almost not visible; subterminal line broad, blackish brown to brown, gradually noticeable from costal to inner margin; discal spot obscure. Both forewing and hindwing with a discal spot on the ventral side, respectively. Abdomen: light ochre-grey, rather slender, terminus with yellow tufts.

Male genitalia (Fig. 7). Tegumen broad, slightly longer than vinculum. Vinculum narrow, U-shaped. Saccus with a rounded and rough central plate. Valva narrow,

insole-shaped, gradually widening from base to cucullus; sacculus moderately sclerotized, narrow, band-shaped, ca $3/4$ length of valva; sacculus process sclerotized, narrow, finger-shaped, weakly split from the valva; costa flattened, tapering from basal to terminal part, ca $2/3$ length of valva; cucullus smoothly arched. Uncus long and slender, tapering from basal part to top, curved at $1/3$ from base, apically sharp. Juxta inverted V-shaped, slightly concave on both sides, papillate and sclerotized apically. Phallus straight; coecum narrow, ca $1/3$ length of aedeagus; carina with a short and narrow spine, and with a sclerotized and short band ventrally. Vesica has four membranous diverticula, densely covered with small grains; basal part of vesica with a reversed, curved, saw-toothed cornutus; subbasal diverticulum is the largest.

Female genitalia (Fig. 9). Ostium bursae broad and straight. Dorsal side of 8th segment with a pair of subcircular, slightly sclerotized areas, connected to base of apophysis anterior. Ductus bursae flattened, shorter than $1/2$ length of corpus bursae, with two long, sclerotized longitudinal bands ca $2/3$ length of ductus bursae. Corpus bursae membranous; anterior part densely covered with small granulations, with an oval signum covered with small, stout spines; posterior half smooth, covered with longitudinal wrinkles. Apophysis anterior thicker and longer than apophysis posterior. Papilla analis thick and short.

Distribution. China (Xizang: Linzhi) (Fig. 12). This species occurs in grasslands around coniferous and broad-leaved mixed forests in the Xizang Autonomous Region (Figs 13, 14). It flies in the dry season. Specimens were captured with UV light in August.

Etymology. The species is named for the parallel medial and subterminal lines.

Remarks. *Orthozona quadrilineata* and *Paracolax curvilineata* are very similar in external appearance and genitalia in both sexes. However, they are not discussed further here due to the poor condition of their materials; the relationship between these three species deserves in-depth study when the materials become available. In this paper, one female of *O. quadrilineata* was collected by Dr M. Owada on 25 September 1983 in Sikkim, India (genitalia slide no. NSMT4373).

Acknowledgements

This research was supported by grants from the National Natural Science Foundation of China (No. 31872261), the project of the Northeast Asia Biodiversity Research Center (NABRI202203) and the Fundamental Research Funds for the Central Universities (No. 2572019CP11, 2572021DJ08, 2572021AW28). We sincerely thank Dr Shipher Wu (Biodiversity Research Center, Academia Sinica, Taipei) for providing the images of *P. curvilineata*, and Dr. Mamoru Owada (NSMT, Tsukuba) for the images of *O. quadrilineata* and *P. curvilineata*. We also would like to thank Dr Alberto Zilli (Natural History Museum, London, UK) for his valuable comments and precise linguistic adjustments.

References

- Beccaloni GW, Scoble MJ, Robinson GS, Pitkin B (2003) The Global Lepidoptera Names Index (Lep Index). <http://www.nhm.ac.uk/entomology/lepindex> [Accessed 31 March 2011]
- Chen YX (1999) Lepidoptera: Noctuidae: Fauna Sinica (Insecta) 16. Science Press, Beijing, 1596 pp.
- Hampson GF (1895) The Fauna of British India Including Ceylon and Burma. Moths (Vol. 2). Taylor and Francis, London, 546 pp. <https://doi.org/10.5962/bhl.title.100745>
- Kononenko VS, Han HL (2007) Atlas Genitalia of Noctuidae in Korea (Lepidoptera). In: Park K-T (Ed.) Insects of Korea (Series 11). Junhaeng-Sa, Seoul, 464 pp.
- Moore F (1882) Descriptions of Indian Lepidoptera Heterocera from the collection of the late Mr. W.S. Atkinson [part 2]. In: Hewitson WC, Moore F (Eds) (1879–1888) Descriptions of New Indian Lepidopterous Insects from the Collection of the Late Mr. W.S. Atkinson. M.A., F.L.S., &c. Asiatic Society of Bengal, Calcutta, 89–198.
- Owada M (1992a) Synonymic notes on the herminiine moths (Noctuidae) of Japan with descriptions of three new species. *Tinea* 13: 183–203.
- Owada M (1992b) Herminiinae. In: Heppner JB, Inoue H (Eds) Lepidoptera of Taiwan (Vol. 1). Part 2: Checklist. Association for Tropical Lepidoptera, Gainesville, 172–173.
- Owada M, Wu S, Fu CM (2021) Herminiinae. In: Fu CM, Owada M, Shih LC, Lin HH (Eds) Moths of Nanheng Part 2. Endemic Species Research Institute, Nantou, 261–331.
- Poole RW (1989) Noctuidae. In: Heppner JB (Ed.) Lepidopterorum Catalogus (New Series), 118. E.J. Brill/Flora & Fauna Publications, Leiden, 745 pp.
- Smetacek P, Kitching IL (2012) The hitherto undescribed male of *Orthozona quadrilineata* (Moore, 1882) (Lepidoptera: Erebidae). *Journal of Threatened Taxa* 4(14): 3366–3368. <https://doi.org/10.11609/JoTT.o2749.3366-8>
- Wileman AE (1915) New species of Heterocera from Formosa. *Entomologist* 48: 12–40.
- Wu S (2014) Systematics of Herminiinae of the Palaearctic and Oriental regions, with a taxonomic revision of the Taiwanese fauna (Lepidoptera, Erebidae). PhD thesis, National Taiwan University, Department of Entomology, College of Bioresources and Agriculture, [ix +] 357 pp.
- Wu S, Fu CM, Owada M (2013) Erebidae: Herminiinae. In: Fu CM, Ronkay L, Lin HH (Eds) Moths of Hehuanshan. Endemic Species Research Institute, Nantou, 333–363.

Three new species of cave-adapted pseudoscorpions (Pseudoscorpiones, Chthoniidae) from eastern Yunnan, China

Yanmeng Hou¹, Zegang Feng^{1,2,3}, Feng Zhang¹

1 The Key Laboratory of Zoological Systematics and Application, Institute of Life Science and Green Development, College of Life sciences, Hebei University, Baoding, Hebei 071002, China **2** Key Laboratory of Zoological Systematics and Evolution, Institute of Zoology, Chinese Academy of Sciences, Beijing 100101, China **3** College of Life Sciences, University of Chinese Academy of Sciences, Beijing, 100049, China

Corresponding author: Feng Zhang (dudu06042001@163.com)

Academic editor: J. Christophoryová | Received 3 January 2023 | Accepted 24 February 2023 | Published 15 March 2023

<https://zoobank.org/D9BFB547-5F3F-45F1-A556-3F05839B4413>

Citation: Hou Y, Feng Z, Zhang F (2023) Three new species of cave-adapted pseudoscorpions (Pseudoscorpiones, Chthoniidae) from eastern Yunnan, China. ZooKeys 1153: 73–95. <https://doi.org/10.3897/zookeys.1153.99537>

Abstract

Three new cave-adapted chthoniid pseudoscorpions from four karst caves of Yunnan Province (China) are described, including detailed diagnosis and illustrations: *Tyrannochthonius calvatus* **sp. nov.** from an unnamed cave and Dongtianfu Cave (Fuyuan County), *T. capito* **sp. nov.** from Xianren Cave (Xichou County), and *Lagynochthonius daidaiensis* **sp. nov.** from Daidai Cave (Qiubei County). All three species are endemic to Yunnan. *Tyrannochthonius calvatus* **sp. nov.**, lacking the carapaceal antero-medial setae and having intercalary teeth on the movable chelal finger only, is a peculiar chthoniid species.

Keywords

Cavernicolous, karst caves, *Lagynochthonius*, taxonomy, *Tyrannochthonius*

Introduction

The genus *Tyrannochthonius* Chamberlin, 1929 contains 149 species and two subspecies, with at least 58 species occurring in caves, and is distributed in all continents except Antarctica (Li 2022; WPC 2022). This genus can be diagnosed as follows: trichobothrium *sb* situated midway between *st* and *b*, or closer to *st*; trichobothria *ib* and *isb*

situated close together in a median or sub-basal position on the dorsum of the chelal hand; chelal hand not distally constricted and the movable finger without a complex or strongly sclerotized apodeme at the base; fixed finger usually with one large, medial acuminate spine-like seta at its base, but can be reduced or absent in some cave-dwelling species; coxal spines generally long and present on coxae II only; epistome pointed, triangular or rounded, inconspicuous and usually with two closely-flanking setae at its base (Chamberlin 1962; Muchmore 1984, 1991; Muchmore and Chamberlin 1995; Edward and Harvey 2008). So far, 15 species and one subspecies of this genus have been described from China, of which 12 are exclusively known from karst caves (Mahnert 2009; Gao et al. 2018, 2020; Hou et al. 2022a; Li 2022; WPC 2022).

The genus *Lagynochthonius* Beier, 1951 was erected by Beier (1951) as a subgenus of *Tyrannochthonius* but was later elevated to generic status by Chamberlin (1962). The genus is diagnosed by trichobothrium *sb* situated midway between *st* and *b*, or closer to *st*; trichobothria *ib* and *isb* situated close together in a median or sub-basal position on the dorsum of the chelal hand; coxal spines generally long and present on coxae II only; chelal hand distally constricted (or flask-shaped) and movable finger with complex or strongly sclerotized apodeme at its base and the modified tooth (*td*) of the fixed chelal finger displaced onto the dorso-antiaxial face (Chamberlin 1962; Harvey 1989; Muchmore 1991; Judson 2007; Edward and Harvey 2008). At present, this genus contains 67 species (19 species living in caves) distributed in Asia, Australia, Africa, and America. Twenty species of this genus have been described from China, 13 of which are exclusively known from karst caves (Li et al. 2019; Hou et al. 2022a, b; WPC 2022).

Yunnan, located in southwest China, was once an ancient shallow sea during the Sinian (= Ediacaran) to Triassic periods and the area is characterized by massive karst landforms today (11.09×10^4 km²) (Wang 2001). The influence of subtropical and tropical monsoon climates as well as the presence of rivers and precipitation regimes have probably fostered the development of karst caves. According to a survey, more than 1000 karst caves have been found in Yunnan Province (Ming 1997). To date, more than 750 cave-dwelling animals have been identified in China (nearly 15% of them are from Yunnan), including 54 cave-dwelling pseudoscorpion species (25 of them are from Yunnan) (Schawaller 1995; Mahnert 2003, 2009; Mahnert and Li 2016; Gao et al. 2017, 2018, 2020; Li et al. 2017, 2019; Feng et al. 2019, 2020; Latella 2019; Zhang et al. 2020; Li and Wang 2021; Hou et al. 2022a, b; Li 2022; WPC 2022; Xu et al. 2022).

Three new cavernicolous species of Chthoniidae have been recently found from the karst caves survey in Yunnan in 2021 and are here described.

Materials and methods

The specimens examined for this study were cleared with a fine, soft-bristle brush and preserved in 75% alcohol and deposited in the Museum of Hebei University (MHBU) (Baoding, China) and the Museum of Southwest University (MSWU) (Chongqing, China). Photographs, drawings, and measurements were taken using a Leica M205A

stereo-microscope equipped with a Leica DFC550 camera and the Inkscape software (v. 1.0.2.0). Detailed examination was carried out with an Olympus BX53 general optical microscope. All images were edited and formatted using Adobe Photoshop 2022.

Terminology and measurements follow Chamberlin (1931) with some minor modifications to the terminology of trichobothria (Harvey 1992; Judson 2007) and chelicera (Judson 2007). The chela and legs are measured in lateral view and others are taken in dorsal view. All measurements are given in mm unless noted otherwise. Proportions and measurements of chelicerae, carapace and pedipalps correspond to length/breadth, and those of legs, chela, and hand to length/depth.

The following abbreviations are used in the text: *b* basal trichobothrium; *sb* sub-basal trichobothrium; *st* sub-terminal trichobothrium; *t* terminal trichobothrium; *ib* interior basal trichobothrium; *isb* interior sub-basal trichobothrium; *ist* interior sub-terminal trichobothrium; *it* interior terminal trichobothrium; *eb* exterior basal trichobothrium; *esb* exterior sub-basal trichobothrium; *est* exterior sub-terminal trichobothrium; *et* exterior terminal trichobothrium; *dx* duplex trichobothria; *sc* microsetae (chemosensory setae); *td* modified tooth.

Taxonomy

Family Chthoniidae Daday, 1889

Subfamily Chthoniinae Daday, 1889

Tribe Tyrannochthoniini Chamberlin, 1962

Genus *Tyrannochthonius* Chamberlin, 1929

Type species. *Chthonius terribilis* With, 1906, by original designation.

Tyrannochthonius calvatus sp. nov.

<https://zoobank.org/789C8A08-776E-47A8-BCC3-B73E4940FB3D>

Figs 2–5

Chinese name: 秃头暴伪蝎

Type material. Holotype: CHINA • ♂; Yunnan Province, Fuyuan County, Mo-hong Town, Puchong Village, unnamed cave; 25°22.301'N, 104°6.380'E; 2060 m a.s.l.; 07 Oct. 2021; Zegang Feng, Yanmeng Hou, Lu Zhang and Liu Fu leg.; under a stone in the dark zone; Ps.-MHBU-HBUARA#2021-429-01 (Figs 1C, 2A).

Paratypes: • 4 ♂; the same data as the holotype; Ps.-MHBU-HBUARA#2021-429-02-HBUARA#2021-429-05 • 1 ♂, 2 ♀; the same collection date and collectors as the holotype; Puchong Village, Dongtianfu Cave; 25°22.105'N, 104°6.447'E; 2035 m a.s.l.; under stones and clods in the dark zone; Ps.-MSWU-HBUARA#2021-428-01-HBUARA#2021-428-03 (Figs 1D, 2B).

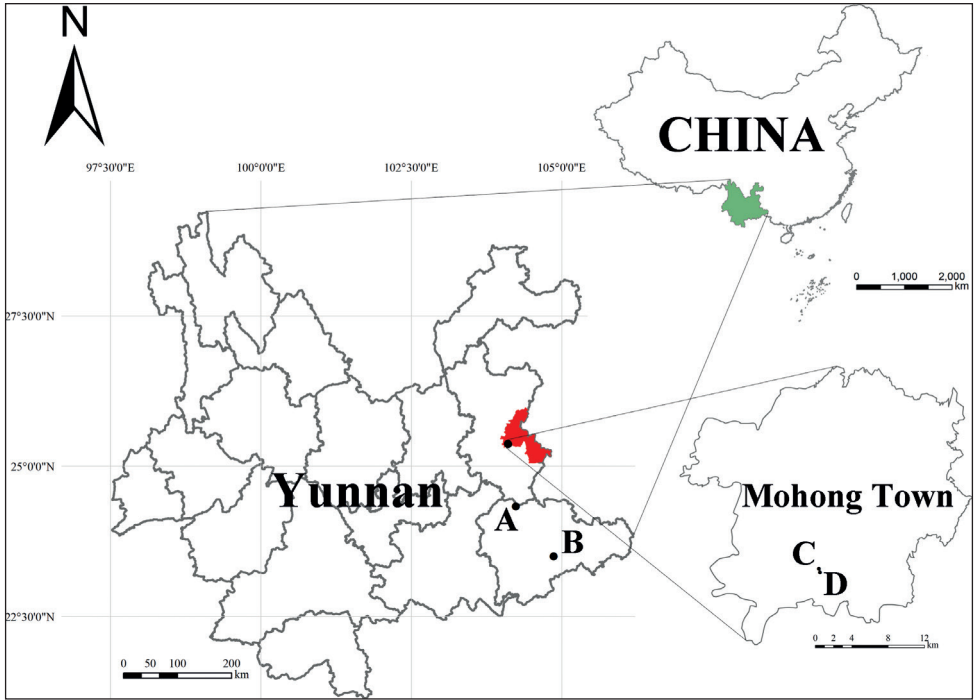


Figure 1. Study area, general cave locations, and type locality for each species, Yunnan Province, China. Each color represents an administrative region (green: Yunnan Province; red: Fuyuan County) **A** Daidai Cave (*Lagynochthonius daidaiensis* sp. nov.) **B** Xianren Cave (*Tyrannochthonius capito* sp. nov.) **C, D** unnamed cave and Dongtianfu Cave (*T. calvatus* sp. nov.).

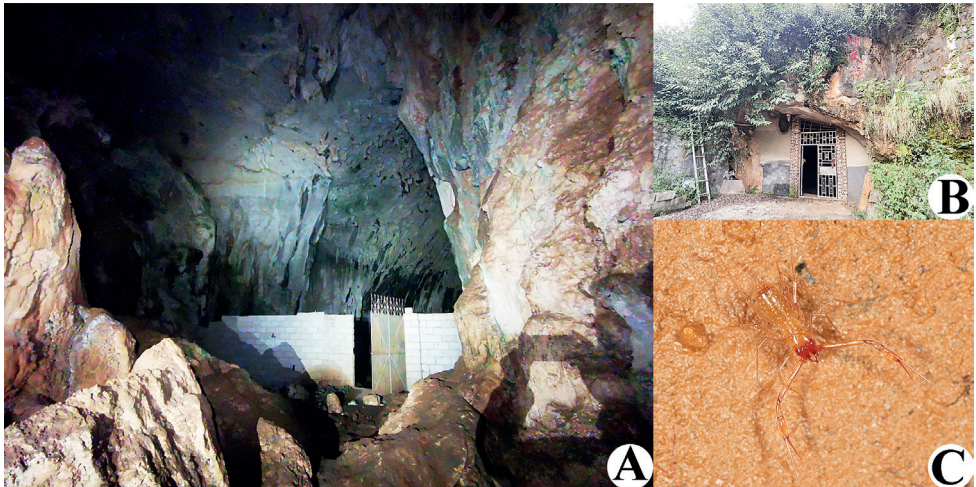


Figure 2. Unnamed cave (type locality) and Dongtianfu Cave, habitats of *Tyrannochthonius calvatus* sp. nov. **A** unnamed cave **B** Dongtianfu Cave **C** live female of *T. calvatus* sp. nov. in its natural environment from Dongtianfu Cave.

Diagnosis (♂♀). Moderately sized troglomorphic species with elongated appendages; carapace without eyes or eyespots; anterior margin of carapace thin, finely denticulated, with four setae (including preocular setae) only, without epistome and flanking basal setae; posterior margin of carapace with two setae; tergites I–III each with two setae. Pedipalps slender, femur 8.06–8.44 (♂), 7.94–8.38 (♀) × longer than broad; chela 8.05–8.33 (♂), 8.05–8.71 (♀) × longer than deep only movable chelal finger with intercalary teeth; movable chelal finger teeth markedly smaller than fixed chelal finger teeth and strongly retrorse and contiguous.

Etymology. The specific name is derived from the Latin adjective *calvatus* (bald) and refers to the absence of two antero-median setae on the carapace.

Description. Adult males (Figs 3A, 4A–F, 5). **Color:** generally pale yellow, chelicerae, pedipalps and tergites slightly darker, soft parts pale. **Cephalothorax** (Figs 4C, 5A): carapace 0.98× longer than broad, gently narrowed posteriorly; surface smooth, without furrows; no traces of eyes; anterior margin slightly serrate; epistome absent, without two setae flanking base; with 14–15 setae arranged s2s:4:4:0–1:2 (with 14–17 setae arranged s2s:4:4:0–3:2 in females), most setae heavy, long and gently curved, anterolateral setae much shorter than others; with three pairs of lyrifissures, the first two pairs situated middle and lateral to the setae of ocular row respectively, the third situated exterior to the sole pair of setae of posterior row. Chaetotaxy of coxae: P 3, I 3, II 3–4, III 5, IV 5; manducatory process with two acuminate distal setae, anterior seta more than 1/2 length of medial seta; apex of coxa I with small, rounded anteromedial process; coxae II with 12 or 13 terminally indented coxal spines on each side, set as an oblique and arc row, longer spines present in the middle of the row, becoming shorter distally and proximally and incised for ca. half their length (Fig. 5C); intercoxal tubercle absent; without sub-oral seta. **Chelicera** (Figs 4D, 5B, D): large, ca. as long as carapace, 2.43–2.48× longer than broad; five setae and two lyrifissures (exterior condylar lyrifissure and exterior lyrifissure) present on hand, all setae acuminate, ventrobasal seta shorter than others; movable finger with one medial seta. Cheliceral palm with moderate hispid granulation on both ventral and dorsal sides. Both fingers well provided with teeth, fixed finger with 14–16 teeth, distal one largest; movable finger with 13–15 retrorse contiguous small teeth; galea absent (Fig. 5B). Serrula exterior with 25–28 blades and serrula interior with 17 or 18 blades. Rallum with eight blades, the distal one longest and recumbent basally, with fine barbules and slightly set apart from the other blades, latter tightly grouped and with long pinnae, some of which are subdivided (Fig. 5D). **Pedipalp** (Figs 4A, B, E, 5E–G): long and slender, trochanter 1.74–1.88, femur 8.06–8.44, patella 2.37–2.61, chela 8.05–8.33, hand 3.00–3.10× longer than deep femur 2.87× longer than patella; movable chelal finger 1.64–1.66× longer than hand and 0.61–0.62× longer than chela. Setae generally long and acuminate; one distal lyrifissure present on patella (Figs 4E, 5E). Chelal palm not constricted towards fingers, apodeme complex of movable chelal finger only slightly sclerotized, with weak granulation dorsally at base of fixed chelal finger. Fixed chelal finger and hand with eight trichobothria, movable chelal finger with four trichobothria, *ib* and *isb* situated close together, submedially



Figure 3. *Tyrannochthonius calvatus* sp. nov. **A** holotype male, habitus (dorsal view) **B** paratype female, habitus (dorsal view). Scale bars: 0.50 mm.

on dorsum of chelal hand; *eb*, *esb*, and *ist* forming a nearly straight oblique row at base of fixed chelal finger; *it* slightly distal to *est*, situated subdistally; *et* slightly near to tip of fixed chelal finger, very close to chelal teeth; *dx* situated distal to *et*; *sb* situated midway between *b* and *st*; *b* and *t* situated subdistally, *t* situated distal to *b* and proximal to *est* (Fig. 5F). A tiny antiaxial lyrifissure present at base of fixed chelal finger (situated distal to *ist*). Both chelal fingers with a row of teeth, heterodontate, spaced regularly along the margin, larger and well-spaced teeth present in the middle of the row, becoming smaller and closer distally and proximally: fixed chelal finger with 32–36 macrodenticles, long and pointed, without intercalary teeth; movable chelal finger with 37–41 macrodenticles (smaller than teeth on fixed chelal finger), retrorse and contiguous, plus 10–12 intercalary microdenticles (roughly extending to *b*), 47–53 in total (Fig. 5F). Chelal fingers straight in dorsal view; microsetae (*sc*) present on dorsum of chelal hand (Figs 4B, 5G). **Opisthosoma:** generally typical, pleural membrane finely granulated. Tergites and sternites undivided; setae uniseriate and acuminate. Tergal chaetotaxy I–XII: 2:2:2:2:4:4:4:4:4–5:4:T2–3T:0; tergite IX with an unpaired median seta. Sternal chaetotaxy III–XII: 12–14:11–12:8:9:9:9–10:9:7–9:0: 2. Anterior genital operculum with ten setae, genital opening slit-like, with 10–12 marginal setae on each side, 31–33 in total (Fig. 4F). **Legs** (Fig. 5H, 5I): generally typical, long and slender. Fine granulation present on anterodorsal faces of femur IV and patella IV. Femur of leg I 1.88× longer than patella and with one lyrifissure at the base of femur; tarsus 2.45× longer than tibia. Femoropatella of leg IV 4.83–5.04× longer than deep; tibia 7.60× longer than deep; with basal tactile setae on both tarsal segments: basitarsus 4.00–4.25× longer than deep (TS = 0.24–0.28),

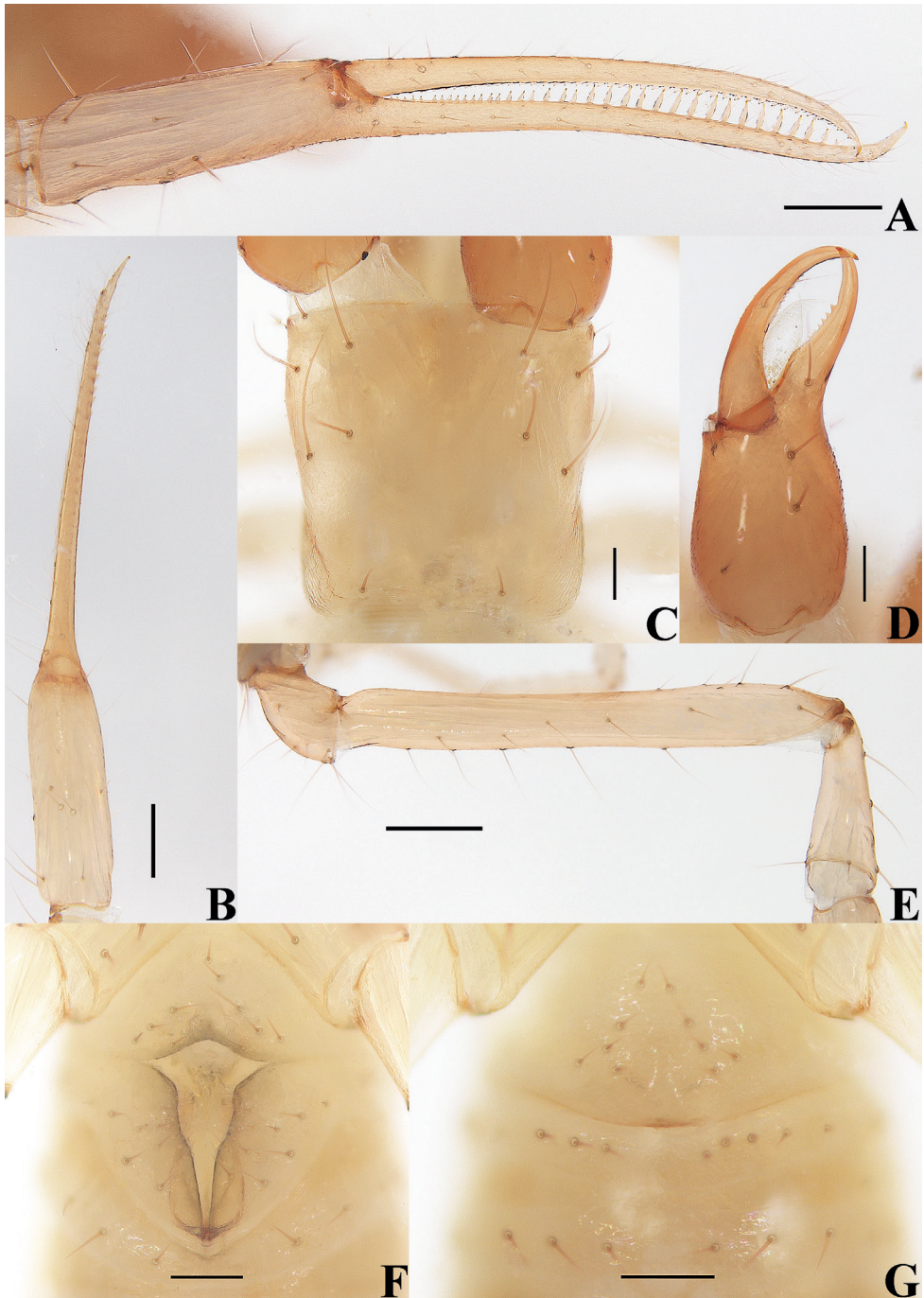


Figure 4. *Tyrannochthonius calvatus* sp. nov., holotype male (**A–F**), paratype female (**G**) **A** left chela (lateral view) **B** left chela (dorsal view) **C** carapace (dorsal view) **D** left chelicera (dorsal view) **E** left pedipalp (minus chela, dorsal view) **F** male genital area (ventral view) **G** female genital area (ventral view). Scale bars: 0.25 mm (**E**); 0.20 mm (**A, B**); 0.10 mm (**C, D, F, G**).

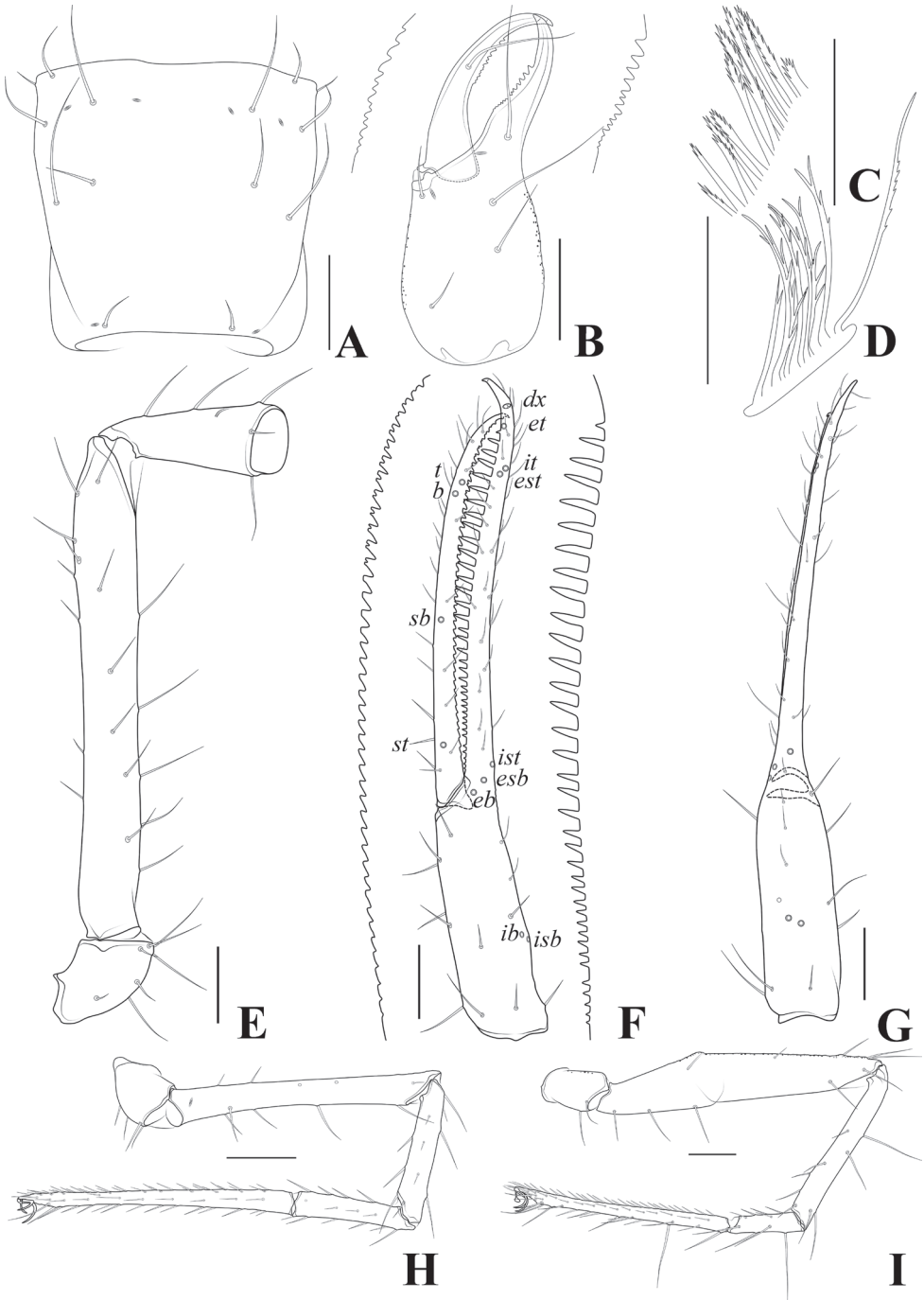


Figure 5. *Tyrannochthonius calvatus* sp. nov., holotype male **A** carapace (dorsal view) **B** left chelicera (dorsal view) with details of dentation **C** coxal spines on coxae II (ventral view) **D** rallum **E** left pedipalp (minus chela, dorsal view) **F** left chela (lateral view) with details of dentation and trichobothrial pattern **G** left chela (dorsal view) **H** leg I (lateral view) **I** leg IV (lateral view). Scale bars: 0.20 mm (**A, B, E–I**); 0.10 mm (**C, D**).

telotarsus 15.33–15.50× longer than deep and 2.71–2.91× longer than basitarsus (TS = 0.27–0.28). Arolium slightly shorter than the claws, not divided; claws simple.

Adult females (Figs 2C, 3B, 4G). Mostly same as males, but a little larger; chaetotaxy of coxae: P 3, I 3, II 4, III 5, IV 5; tergal chaetotaxy I–XII: 2:2:2:2–3:4:4:3–4:4:4–5:4:T2T:0; sternal chaetotaxy IV–XII: 10–12:9–10:7–10:9:9:6–8:0:2; anterior genital operculum with 10–13 setae, posterior margin with 10–14 marginal setae, 22–24 in total; leg IV with a long tactile seta on both tarsal segments: basitarsus 3.56–5.00× longer than deep (TS = 0.23–0.25), telotarsus 14.00–16.17× longer than deep and 2.77–2.88× longer than basitarsus (TS = 0.27–0.29).

Dimensions (length/breadth or, in the case of the legs, also for chela and hand, length/depth in mm). Males (females in parentheses): body length 2.16–2.21 (2.13–2.26). Pedipalps: trochanter 0.32–0.33/0.17–0.19 (0.32–0.34/0.18–0.20), femur 1.29–1.35/0.16 (1.34–1.37/0.16–0.17), patella 0.45–0.47/0.18–0.19 (0.49–0.52/0.18–0.20), chela 1.75–1.77/0.21–0.22 (1.77–1.84/0.21–0.22), hand 0.65–0.66/0.21–0.22 (0.65–0.68/0.21–0.22), movable chelal finger length 1.08 (1.11–1.16). Chelicera 0.72–0.73/0.29–0.30 (0.73–0.76/0.29–0.32), movable finger length 0.40 (0.40–0.41). Carapace 0.59/0.59–0.60 (0.59–0.65/0.62–0.66). Leg I: trochanter 0.21/0.13–0.14 (0.20–0.22/0.12–0.16), femur 0.75–0.77/0.09 (0.77–0.82/0.08–0.10), patella 0.40–0.41/0.08 (0.41–0.44/0.07–0.09), tibia 0.33/0.07 (0.34–0.37/0.06–0.07), tarsus 0.81/0.06 (0.79–0.82/0.06–0.07). Leg IV: trochanter 0.29–0.32/0.18 (0.28–0.30/0.15–0.18), femoropatella 1.11–1.16/0.23 (1.11–1.15/0.20–0.24), tibia 0.76/0.10 (0.77–0.81/0.10), basitarsus 0.32–0.34/0.08 (0.32–0.35/0.07–0.09), telotarsus 0.92–0.93/0.06 (0.92–0.98/0.06–0.07).

Remarks. *Tyrannochthonius calvatus* sp. nov. can be easily distinguished from other Chinese cave-dwelling *Tyrannochthonius* species by lacking two carapaceal antero-medial setae and the presence of intercalary teeth on the movable chelal finger only.

Distribution. Known only from the unnamed cave (type locality) and Dongtianfu Cave.

***Tyrannochthonius capito* sp. nov.**

<https://zoobank.org/9D5EEEF-13A3-4C9C-895D-897EC8C8DF0E>

Figs 6–9

Chinese name: 大头暴伪蝎

Type material. Holotype: CHINA • ♂; Yunnan Province, Xichou County, Jijie Township, Xianrendong Village, Xianren Cave; 23°30.124'N, 104°52.082'E; 1345 m a.s.l.; 16 Oct. 2021; Zegang Feng, Yanmeng Hou, Lu Zhang and Liu Fu leg.; under a stone in the dark zone; Ps.-MHBV-HBUARA#2021-443-01 (Figs 1B, 6). **Paratypes:** • 1 ♂, 2 ♀; the same data as the holotype; Ps.-MSWU-HBUARA#2021-443-02-HBUARA#2021-443-04.

Diagnosis (♂♀). Small-sized cavernicolous species with slightly elongated appendages; carapace with two anterior corneate eyes only; anterior margin of carapace thin,

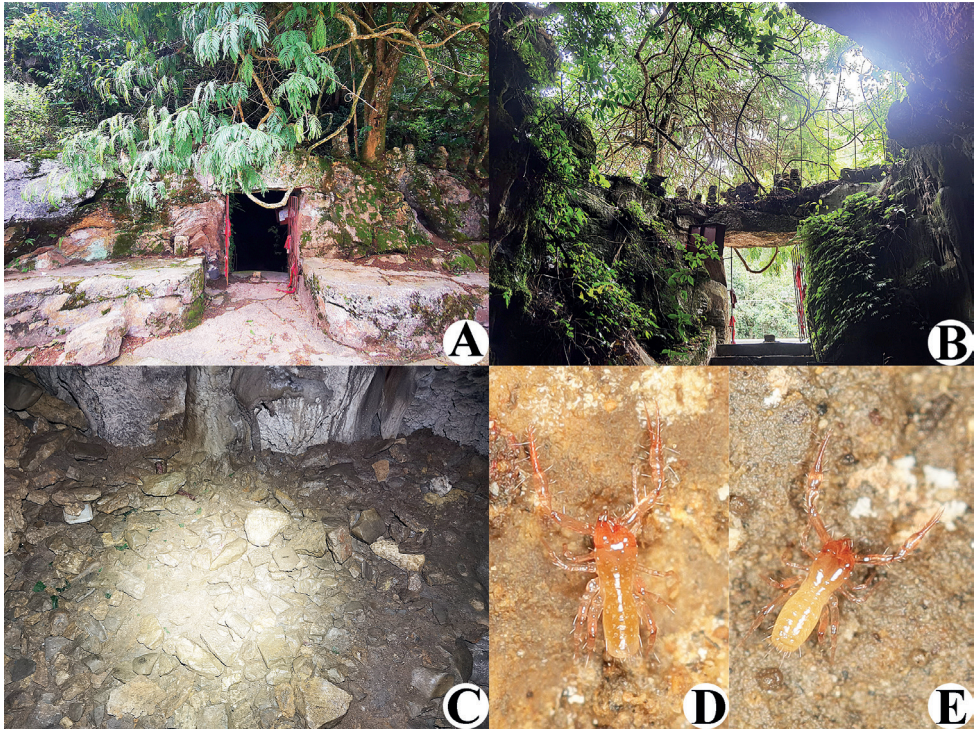


Figure 6. Xianren Cave (type locality), habitat of *Tyrannochthonius capito* sp. nov. **A** entrance **B** inside the cave entrance **C** area where *T. capito* sp. nov. specimens were collected **D** live male of *T. capito* sp. nov. in its natural environment **E** live female of *T. capito* sp. nov. in its natural environment.

finely denticulated, epistome small, pointed, triangular; posterior margin of carapace with two setae; tergites I–III each with four setae. Pedipalps slender, femur 4.30–4.67 (♂), 4.27–4.60 (♀) × longer than broad; chela 4.77–5.23 (♂), 4.53–4.73 (♀) × longer than deep; both chelal fingers with intercalary teeth.

Etymology. The specific name is derived from the Latin noun *capito* (big head) and refers to the presence of a large cephalothorax.

Description. Adult males (Figs 6D, 7A, 8A–F, 9). **Color:** generally pale yellow, chelicerae, pedipalps and tergites slightly darker, soft parts pale. **Cephalothorax** (Figs 8C, 9A): carapace 0.88–0.95× longer than broad, gently narrowed posteriorly; surface smooth, without furrows; with two anterior eyes only; anterior margin slightly serrate; epistome small, pointed, triangular; with 18 setae arranged s4s:4:4:2:2, most setae heavy, long and gently curved, anterolateral setae much shorter than others; with three pairs of lyrifissures, the first two pairs situated middle and lateral to the setae of ocular row respectively, the third situated exterior to the sole pair of setae of posterior row. Chaetotaxy of coxae: P 3, I 3–5, II 4, III 5, IV 5; mandatory process with two acuminate distal setae, anterior seta more than 1/2 length of medial seta; apex of coxa I with small, rounded anteromedial process; coxa II with seven or eight terminally

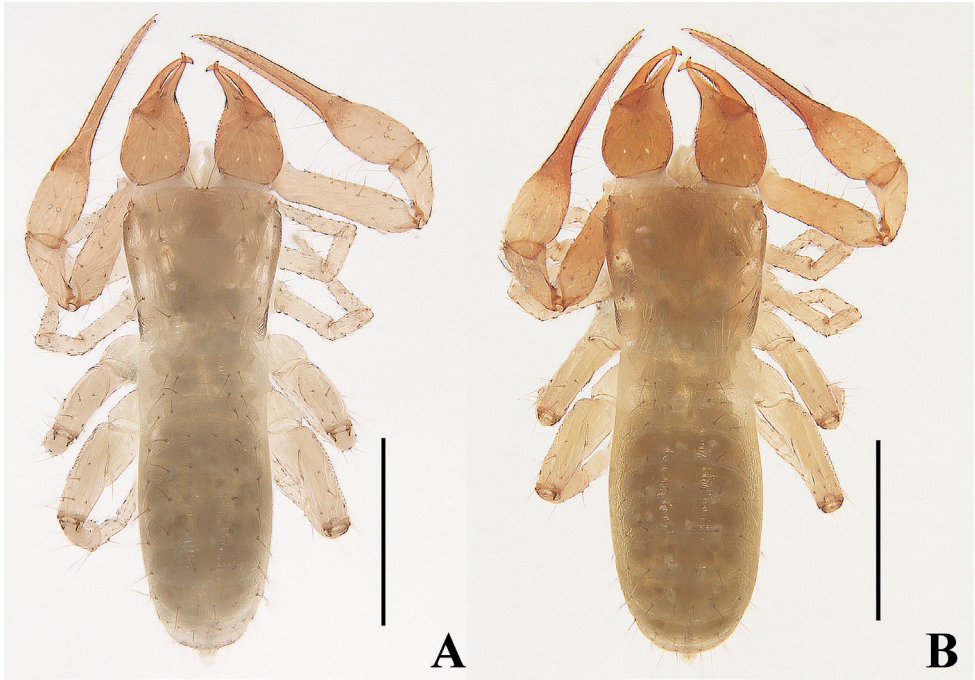


Figure 7. *Tyrannochthonius capito* sp. nov. **A** holotype male, habitus (dorsal view) **B** paratype female, habitus (dorsal view). Scale bars: 0.50 mm.

indented coxal spines on each side, set as an oblique and arc row, longer spines present in the middle of the row, becoming shorter distally and proximally and incised for ca. half their length (Fig. 9C); intercoxal tubercle absent; without sub-oral seta. **Chelicera** (Figs 8D, 9B, D): large, ca. as long as carapace, $2.00\times$ longer than broad; five setae and two lyrifissures (exterior condylar lyrifissure and exterior lyrifissure) present on hand, all setae acuminate, ventrobasal seta shorter than others; movable finger with one medial seta. Cheliceral palm with moderate hispid granulation on both ventral and dorsal sides. Both fingers well provided with teeth, fixed finger with seven or nine acute teeth, distal one largest; movable finger with seven or eight rounded and contiguous small teeth; galea represented by a very slight bump on movable finger (Fig. 9B). Serrula exterior with 19 or 20 blades and serrula interior with 16 blades. Rallum with eight blades, the distal one longest and recumbent basally, with fine barbules and slightly set apart from the other blades, latter tightly grouped and with long pinnae, some of which are subdivided (Fig. 9D). **Pedipalp** (Figs 8A, B, E, 9E–G): long and slender, trochanter $1.64\text{--}1.70$, femur $4.30\text{--}4.67$, patella $1.67\text{--}2.00$, chela $4.77\text{--}5.23$, hand $1.62\text{--}1.77\times$ longer than broad; femur $2.10\text{--}2.15\times$ longer than patella; movable chelal finger $2.00\text{--}2.04\times$ longer than hand and $0.68\text{--}0.69\times$ longer than chela. Setae generally long and acuminate; one distal lyrifissure present on patella (Figs 8E, 9E). Chelal palm not constricted towards fingers, apodeme complex of movable chelal finger only

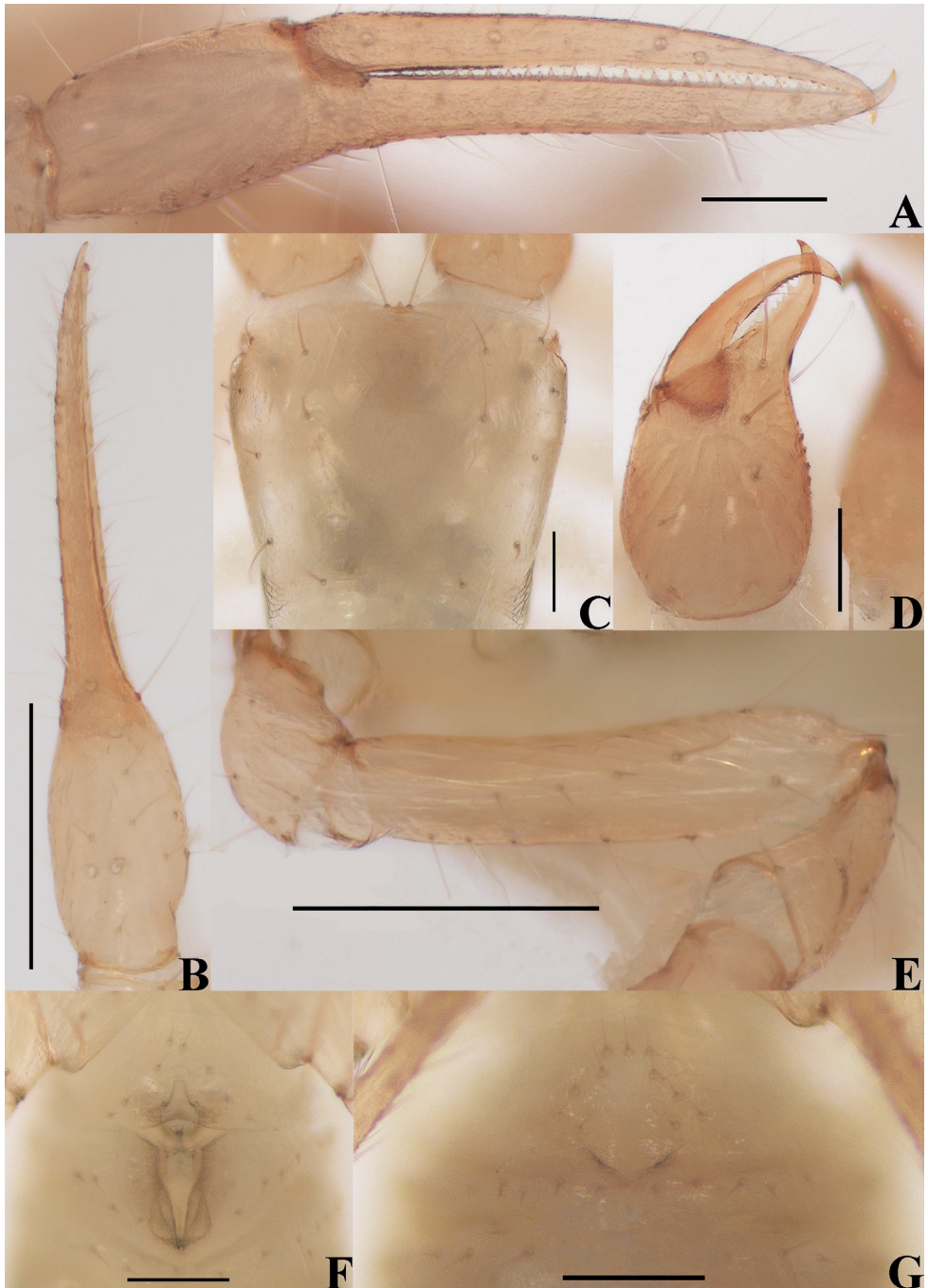


Figure 8. *Tyrannochthonius capito* sp. nov., holotype male (A–F), paratype female (G) **A** left chela (lateral view) **B** left chela (dorsal view) **C** carapace (dorsal view) **D** left chelicera (dorsal view) **E** left pedipalp (minus chela, dorsal view) **F** male genital area (ventral view) **G** female genital area (ventral view). Scale bars: 0.25 mm (B, E); 0.10 mm (A, C, D, F, G).

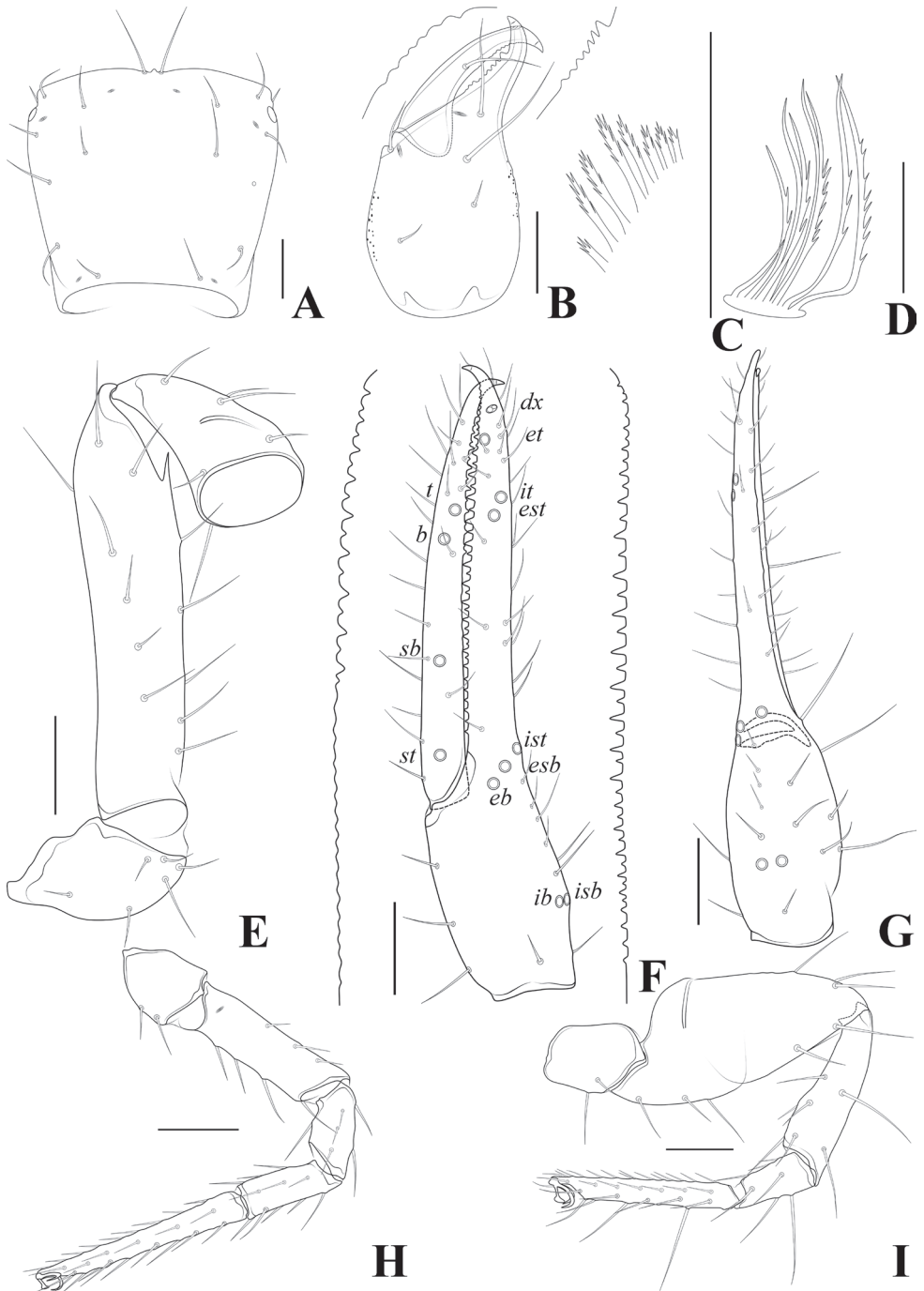


Figure 9. *Tyrannochthonius capito* sp. nov., holotype male **A** carapace (dorsal view) **B** left chelicera (dorsal view) with details of dentation **C** coxal spines on coxae II (ventral view) **D** rallum **E** left pedipalp (minus chela, dorsal view) **F** left chela (lateral view) with details of dentation and trichobothrial pattern **G** left chela (dorsal view) **H** leg I (lateral view) **I** leg IV (lateral view). Scale bars: 0.10 mm.

slightly sclerotized, with weak granulation dorsally at base of fixed chelal finger. Fixed chelal finger and hand with eight trichobothria, movable chelal finger with four trichobothria, *ib* and *isb* situated close together, submedially on dorsum of chelal hand; *eb*, *esb*, and *ist* forming a straight oblique row at base of fixed chelal finger; *it* slightly distal to *est*, situated subdistally; *et* slightly near to tip of fixed chelal finger, very close to chelal teeth; *dx* situated distal to *et*; *sb* situated closer to *st* than to *b*; *b* and *t* situated subdistally, *t* situated distal to *b* and at same level as *est* (Fig. 9F). A tiny antiaxial lyrifissure present at base of fixed chelal finger (situated distal to *ist*). Both chelal fingers with a row of teeth, heterodontate, spaced regularly along the margin, larger and well-spaced teeth present in the middle of the row, becoming smaller and closer distally and proximally: fixed chelal finger with 22 or 23 macrodenticles, pointed and slightly retrorse, plus 19 or 20 intercalary microdenticles, 42 in total; movable chelal finger with nine or ten macrodenticles (slightly smaller than teeth on fixed chelal finger), pointed and slightly retrorse, plus nine intercalary microdenticles and 17 or 18 vestigial, rounded and contiguous basal teeth, 36 in total (Fig. 9F). Chelal fingers straight in dorsal view; microsetae (*sc*) present on dorsum of chelal hand (Figs 8B, 9G). **Opisthosoma:** generally typical, pleural membrane finely granulated. Tergites and sternites undivided; setae uniseriate and acuminate. Tergal chaetotaxy I–XII: 4:4:4:6:6:6:6:6:7:T2T:0. Sternal chaetotaxy III–XII: 13:12–14:10:9:9–10:10–12:11–12:10:0:2. Anterior genital operculum with 8 setae, genital opening slit-like, with 11 or 12 marginal setae on each side, 31 in total (Fig. 8F). **Legs** (Fig. 9H, I): generally typical, long and slender. Fine granulation present on anterodorsal faces of femur IV and patella IV. Femur of leg I 1.83–1.92× longer than patella and with one lyrifissure at the base of femur; tarsus 2.00–2.25× longer than tibia. Femoropatella of leg IV 1.89–2.20× longer than deep; tibia 3.25–3.71× longer than deep; with basal tactile setae on both tarsal segments: basitarsus 2.00–2.20× longer than deep (TS = 0.33–0.36), telotarsus 6.25–7.00× longer than deep and 2.27–2.33× longer than basitarsus (TS = 0.28–0.29). Arolium slightly shorter than the claws, not divided; claws simple.

Adult females (Figs 6E, 7B, 8G). Mostly same as males, but a little larger; chaetotaxy of coxae: P 3, I 3, II 4, III 5, IV 5; tergal chaetotaxy I–XII: 4:4:4:6:6–7:6:6–7:6:6–7:7:T2T:0; sternal chaetotaxy IV–XII: 12–13:9–11:9:9–11:12–13:13:11–13:0:2; anterior genital operculum with 10 or 11 setae, posterior margin with 14 marginal setae, 24 or 25 in total; leg IV with a long tactile seta on both tarsal segments: basitarsus 2.00–2.17× longer than deep (TS = 0.31–0.33), telotarsus 7.00–9.00× longer than deep and 2.08–2.33× longer than basitarsus (TS = 0.25–0.26).

Dimensions (length/breadth or, in the case of the legs, also for chela and hand, length/depth in mm). Males (females in parentheses): body length 1.08–1.25 (1.31–1.37). Pedipalps: trochanter 0.17–0.18/0.10–0.11 (0.19–0.20/0.10), femur 0.42–0.43/0.09–0.10 (0.46–0.47/0.10–0.11), patella 0.20/0.10–0.12 (0.23–0.24/0.11–0.12), chela 0.62–0.68/0.13 (0.68–0.71/0.15), hand 0.21–0.23/0.13 (0.24/0.15), movable chelal finger length 0.42–0.47 (0.46–0.49). Chelicera 0.34–0.38/0.17–0.19 (0.40–0.41/0.20), movable finger length 0.19–0.21 (0.22–0.23). Carapace 0.37/0.39–0.42 (0.38–0.39/0.45–0.46). Leg I: trochanter 0.10–0.11/0.08–0.09

(0.11–0.12/0.08–0.09), femur 0.22–0.23/0.06 (0.25–0.26/0.07), patella 0.12/0.05 (0.13–0.14/0.06), tibia 0.12–0.15/0.04 (0.13–0.15/0.04), tarsus 0.27–0.30/0.03–0.04 (0.27–0.28/0.04). Leg IV: trochanter 0.14/0.10–0.11 (0.14–0.16/0.10–0.11), femoropatella 0.33–0.34/0.15–0.18 (0.36–0.38/0.14–0.16), tibia 0.26/0.07–0.08 (0.27/0.07–0.08), basitarsus 0.11–0.12/0.05–0.06 (0.12–0.13/0.06), telotarsus 0.25–0.28/0.04 (0.27–0.28/0.03–0.04).

Remarks. *Tyrannochthonius capito* sp. nov. is similar to an epigean species *T. robustus* Beier, 1951 (from Vietnam and China) in having intercalary teeth on both chelal fingers and similar body size (e.g., body length 1.08–1.25 mm vs. 1.20 mm (♂), 1.31–1.37 mm vs. 1.20 mm (♀)), but differs by the number of eyes (2 vs. 4), the presence of a hypopigmented body cuticle and the ratio of movable chelal finger and chelal hand (2.00–2.04× vs. 1.52× (♂), 1.92–2.04× vs. 1.80× (♀)) (Beier 1951; Song 1996).

Tyrannochthonius capito sp. nov. can be easily distinguished from other Chinese cave-dwelling *Tyrannochthonius* species by the presence of a pair of anterior corneate eyes.

Distribution. Known only from the type locality.

Genus *Lagynochthonius* Beier, 1951

Type species. *Chthonius johni* Redikorzev, 1922, by original designation.

Lagynochthonius daidaiensis sp. nov.

<https://zoobank.org/D23220D7-2AF6-47AE-B848-941BED5096E1>

Figs 10–13

Chinese name: 呆呆拉伪蝎

Type material. *Holotype*: CHINA • ♀; Yunnan Province, Qiubei County, Shuanglongying Town, Pingtan Village, Daidai Cave; 24°19.772'N, 104°14.355'E; 1228 m a.s.l.; 20 Jul. 2021; Zegang Feng, Hongru Xu, Liu Fu and Nana Zhan leg.; under a stone in the dark zone; Ps.-MHBH-HBUARA#2021-176-01 (Figs 1A, 10).

Paratypes: • 2 ♀; the same data as the holotype; Ps.-MSWU-HBUARA#2021-176-02-HBUARA#2021-176-03.

Diagnosis (♀). Moderately sized troglomorphic species with elongated appendages; carapace without eyes or eyespots; anterior margin of carapace thin, finely denticulated, epistome pointed and small, triangular; posterior margin of carapace with two setae; tergites I–IV each with two setae. Pedipalps slender, femur 7.79–8.07× longer than broad; chela 7.67–8.39× longer than deep; both chelal fingers without intercalary teeth but fixed chelal finger with a modified accessory tooth (*ta*) on dorso-antiaxial face.

Etymology. Named after the type locality, Daidai Cave.

Description. **Adult females** (male unknown) (Figs 10C, 11–13). **Color:** generally pale yellow, chelicerae, pedipalps and tergites slightly darker, soft parts pale. **Cephalothorax** (Figs 12C, 13A, C): carapace 0.97× longer than broad, gently

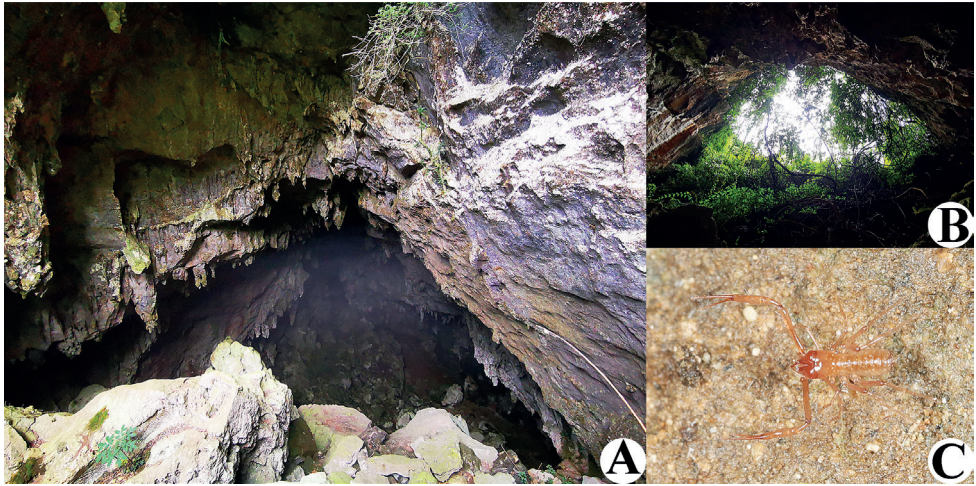


Figure 10. Daidai Cave (type locality), habitat of *Lagynochthonius daidaiensis* sp. nov. **A** entrance **B** inside the cave entrance **C** live female of *L. daidaiensis* sp. nov. in its natural environment.



Figure 11. *Lagynochthonius daidaiensis* sp. nov., holotype female, habitus (dorsal view). Scale bar: 0.50 mm.

narrowed posteriorly; surface smooth, without furrows; no traces of eyes; anterior margin slightly serrate; epistome pointed and small, triangular; with 18 setae arranged $s_4s_3:4:4:2:2$, most setae heavy, long and gently curved, anterolateral setae much shorter than others; with three pairs of lyrifissures, the first two pairs situated middle and lateral to the setae of ocular row respectively, the third situated exterior to the sole pair of setae of posterior row. Chaetotaxy of coxae: P 3, I 3, II 3–4, III 5, IV 5; manducatory process with two acuminate distal setae, anterior seta less than $1/2$ length of medial seta; apex of coxa I with small, rounded anteromedial process; coxae II with 11 or 12 terminally indented coxal spines on each side, set as an oblique and arc row, longer spines present in the middle of the row, becoming shorter distally and proximally and incised for ca. half their length (Fig. 13C); intercoxal tubercle absent; without sub-oral seta. **Chelicera** (Figs 12D, 13B, D): large, ca. as long as carapace, $2.41\times$ longer than broad; five setae and two lyrifissures (exterior condylar lyrifissure and exterior lyrifissure) present on hand, all setae acuminate, ventrobasal seta shorter than others; movable finger with one medial seta. Cheliceral palm with moderate hispid granulation on both ventral and dorsal sides. Both fingers well provided with teeth, fixed finger with 15–17 teeth, distal one largest; movable finger with 12 retrorse contiguous small teeth; galea absent (Fig. 13B). Serrula exterior with 21 blades and serrula interior with 13 or 14 blades. Rallum with seven blades, the distal one longest and recumbent basally, with fine barbules and slightly set apart from the other blades, latter tightly grouped and with long pinnae, some of which are subdivided (Fig. 13D). **Pedipalp** (Figs 12A, B, F, 13E–G): long and slender, trochanter 1.25–1.41, femur 7.79–8.07, patella 2.35–2.53, chela 7.67–8.39, hand 3.29–3.61 \times longer than broad; femur 2.83–2.87 \times longer than patella; movable chelal finger 1.32–1.35 \times longer than hand and 0.57–0.58 \times longer than chela. Setae generally long and acuminate; one distal lyrifissure present on patella (Figs 12F, 13E). Chelal palm gradually constricted towards fingers, apodeme complex of movable chelal finger strongly sclerotized, with weak granulation dorsally at base of fixed chelal finger. Fixed chelal finger and hand with eight trichobothria, movable chelal finger with four trichobothria, *ib* and *isb* situated close together, submedially on dorsum of chelal hand; *eb*, *esb*, and *ist* forming an oblique row at base of fixed chelal finger; *it* slightly distal to *est*, situated subdistally; *et* slightly near to tip of fixed chelal finger, very close to chelal teeth; *dx* situated distal to *et*; *sb* situated midway between *b* and *st*; *b* and *t* situated subdistally, *t* situated distal to *b*; *est* and *it* situated between *b* and *t* (Fig. 13F). A tiny antiaxial lyrifissure present at base of fixed chelal finger (situated distal to *ist*). Both chelal fingers with a row of teeth, homodontate, spaced regularly along the margin, larger teeth present in the middle of the row, becoming smaller and closer distally and proximally: fixed chelal finger with 35 or 36 macrodenticles, slightly retrorse and pointed, plus a modified accessory tooth on dorso-antiaxial face (*td*, close to *dx*), 36 or 37 in total; movable chelal finger with 20–22 macrodenticles (slightly smaller than teeth on fixed chelal finger), slightly retrorse and pointed, plus nine or ten vestigial, rounded and contiguous basal teeth, 30 or 31 in total (Fig. 13F). Chelal fingers slightly curved in dorsal view;

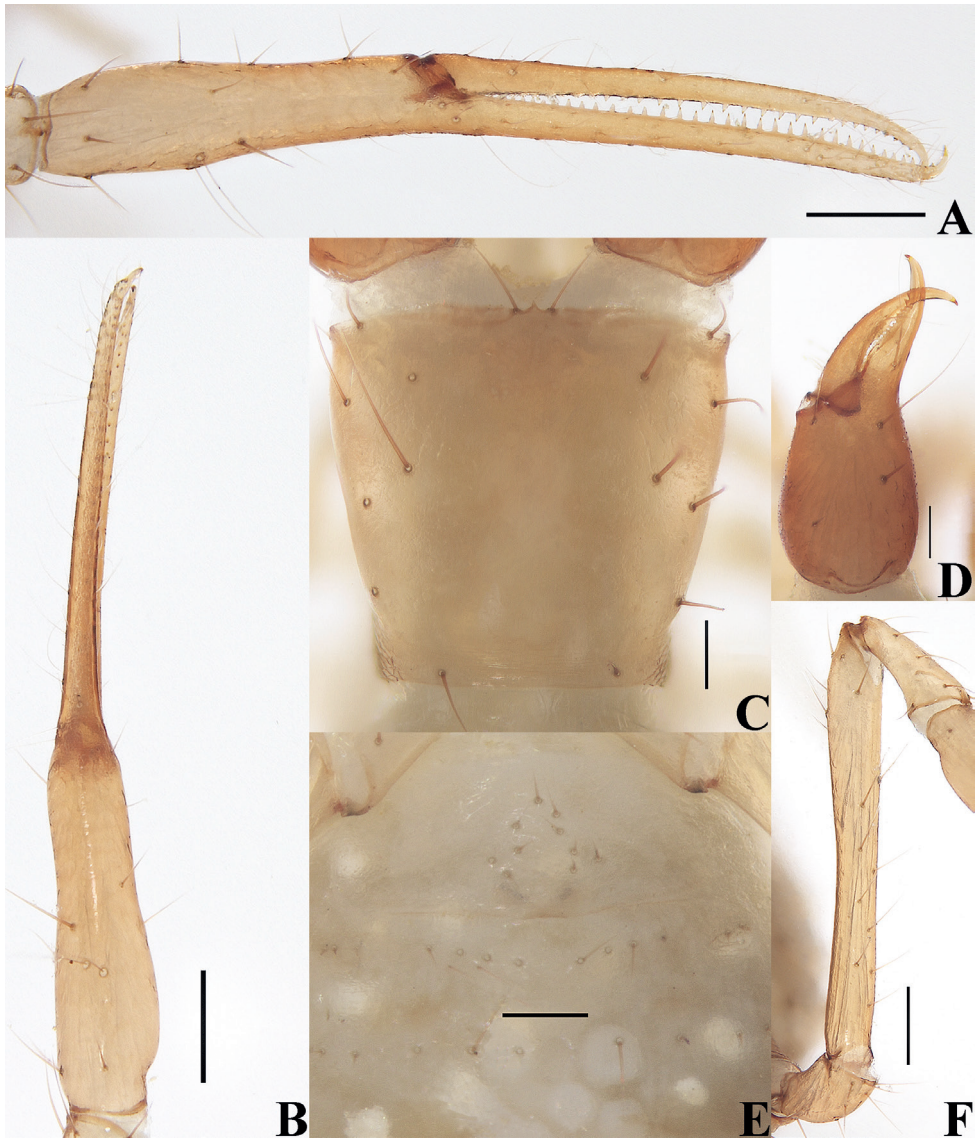


Figure 12. *Lagynochthonius daidaiensis* sp. nov., holotype female **A** left chela (lateral view) **B** left chela (dorsal view) **C** carapace (dorsal view) **D** left chelicera (dorsal view) **E** female genital area (ventral view) **F** left pedipalp (minus chela, dorsal view). Scale bars: 0.20 mm (**A, B, F**); 0.10 mm (**C–E**).

microsetae (*sc*) present on dorsum of chelal hand (Figs 12B, 13G). **Opisthosoma:** generally typical, pleural membrane finely granulated. Tergites and sternites undivided; setae uniseriate and acuminate. Tergal chaetotaxy I–XII: 2:2:2:2:4:4–5:4–5:5:5:4:T2T:0, tergites VIII and IX each with an unpaired median seta. Sternal chaetotaxy IV–XII: 11–12:7–8:7:7–8:7–8:7:7–8:0:2. Anterior genital operculum with 10 setae, posterior margin with 13–14 marginal setae, 23–24 in total (Fig. 12E).

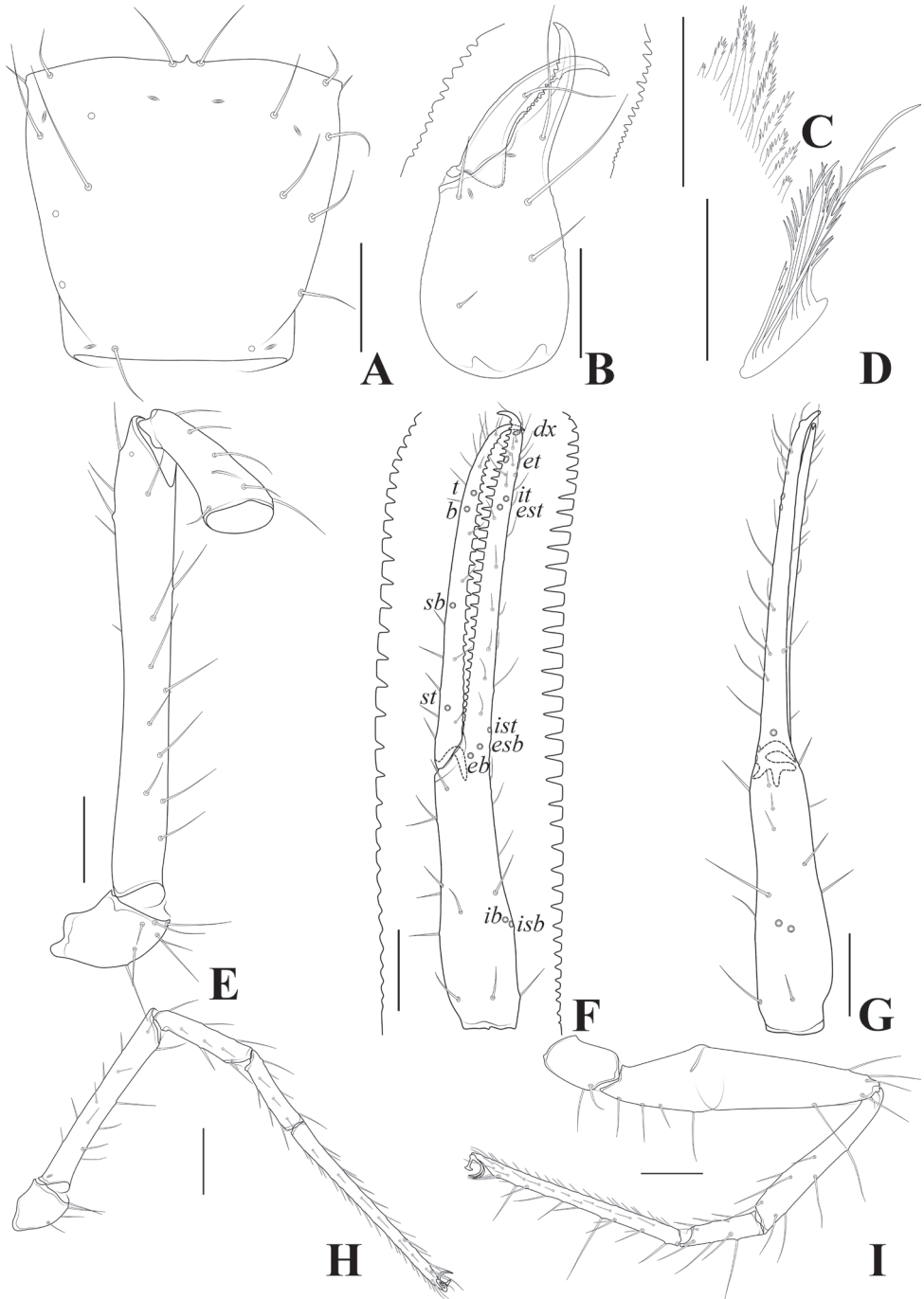


Figure 13. *Lagynochthonius daidaiensis* sp. nov., holotype female **A** carapace (dorsal view) **B** left chelicera (dorsal view) with details of dentation **C** coxal spines on coxae II (ventral view) **D** rallum **E** left pedipalp (minus chela, dorsal view) **F** left chela (lateral view) with details of dentation and trichobothrial pattern **G** left chela (dorsal view) **H** leg I (lateral view) **I** leg IV (lateral view). Scale bars: 0.20 mm (**A, B, E-I**); 0.10 mm (**C, D**).

Legs (Fig. 13H, I): generally typical, long and slender. Fine granulation present on anterodorsal faces of femur IV and patella IV. Femur of leg I 1.88–1.97× longer than patella and with one lyrifissure at the base of femur; tarsus 2.72–2.73× longer than tibia. Femoropatella of leg IV 4.00× longer than deep; tibia 6.20–6.33× longer than deep; with basal tactile setae on both tarsal segments: basitarsus 3.50–3.71× longer than deep (TS = 0.29–0.35), telotarsus 14.60–15.20× longer than deep and 2.71–2.81× longer than basitarsus (TS = 0.36). Arolium slightly shorter than the claws, not divided; claws simple. **Dimensions of adult females** (length/breadth or, in the case of the legs, also for chela and hand, length/depth in mm): body length 1.85–2.04. Pedipalps: trochanter 0.20–0.24/0.16–0.17, femur 1.09–1.13/0.14, patella 0.38–0.40/0.15–0.17, chela 1.51–1.61/0.18–0.21, hand 0.65–0.69/0.18–0.21, movable chelal finger length 0.86–0.93. Chelicera 0.65–0.70/0.27–0.29, movable finger length 0.34–0.36. Carapace 0.56–0.58/0.58–0.60. Leg I: trochanter 0.16–0.18/0.15, femur 0.60–0.65/0.08, patella 0.32–0.33/0.07, tibia 0.25–0.26/0.05–0.06, tarsus 0.68–0.71/0.05. Leg IV: trochanter 0.25–0.26/0.15, femoropatella 0.84–0.92/0.21–0.23, tibia 0.57–0.62/0.09–0.10, basitarsus 0.26–0.28/0.07–0.08, telotarsus 0.73–0.76/0.05.

Remarks. *Lagynochthonius daidaiensis* sp. nov. is similar to *L. laoxueyanensis* Hou, Gao & Zhang, 2022 (from Yunnan, China), but differs by the number of setae on tergites III–IV (2 vs. 4), a shorter chela (chela 7.67–8.39 vs. 6.88–7.22 (♀) × longer than deep, length 1.51–1.61 vs. 1.65–1.66 mm) and the number of coxal spines blades (11 or 12 vs. 9) (Hou et al. 2022a).

Lagynochthonius daidaiensis sp. nov. can be easily distinguished from *L. fengi* Hou, Gao & Zhang, 2022, *L. retrorsus* Hou, Gao & Zhang, 2022, *L. serratus* Hou, Gao & Zhang, 2022, *L. spinulentus* Hou, Gao & Zhang, 2022, *L. xiaolinensis* Hou, Gao & Zhang, 2022 and *L. yaowangguensis* Hou, Gao & Zhang, 2022 by the absence of intercalary teeth on both chelal fingers; from *L. crassus* Hou, Gao & Zhang, 2022 by lacking a pair of anterior eyespots; from *L. magnidentatus* Hou, Gao & Zhang, 2022 and *L. xinjiaoensis* Hou, Gao & Zhang, 2022 by the presence of two carapaceal antero-medial setae; from *L. bailongtanensis* Li, Liu & Shi, 2019, *L. minimus* Hou, Gao & Zhang, 2022 and *L. xibaiensis* Hou, Gao & Zhang, 2022 by the number of setae on tergites I–II (2 vs. 3–4) (Li et al. 2019; Hou et al. 2022b).

Distribution. Known only from the type locality.

Acknowledgements

We are grateful to Hongru Xu, Lu Zhang, Liu Fu, and Nana Zhan for their assistance in the field, to subject editor Dr. Jana Christophoryová and three reviewers, Dr. Mark S. Harvey, Dr. Giulio Gardini, and Dr. Ilya Turbanov for their helpful suggestions that greatly improved this paper. This work was supported by the National Natural Science Foundation of China (No. 31872198), and the Natural Science Foundation of Hebei Province (No. C2021201030).

References

- Beier M (1951) Die Pseudoscorpione Indochinas. Mémoires du Muséum National d'Histoire Naturelle, Paris, nouvelle série 1: 47–123.
- Chamberlin JC (1931) The arachnid order Chelonethida. Stanford University Publications. Biological Sciences 7(1): 1–284.
- Chamberlin JC (1962) New and little-known false scorpions, principally from caves, belonging to the families Chthoniidae and Neobisiidae (Arachnida, Chelonethida). Bulletin of the American Museum of Natural History 123: 303–352.
- Edward KL, Harvey MS (2008) Short-range endemism in hypogean environments: the pseudoscorpion genera *Tyrannochthonius* and *Lagynochthonius* (Pseudoscorpiones: Chthoniidae) in the semiarid zone of Western Australia. Invertebrate Systematics 22(2): 259–293. <https://doi.org/10.1071/IS07025>
- Feng ZG, Wynne JJ, Zhang F (2019) Two new subterranean-adapted pseudoscorpions (Pseudoscorpiones: Neobisiidae: *Parobisium*) from Beijing, China. Zootaxa 4661(1): 145–160. <https://doi.org/10.11646/zootaxa.4661.1.7>
- Feng ZG, Wynne JJ, Zhang F (2020) Cave-dwelling pseudoscorpions of China with descriptions of four new hypogean species of *Parobisium* (Pseudoscorpiones, Neobisiidae) from Guizhou Province. Subterranean Biology 34: 61–98. <https://doi.org/10.3897/subtbiol.34.49586>
- Gao ZZ, Chen HM, Zhang F (2017) Description of two new cave-dwelling *Bisotocreagris* species (Pseudoscorpiones: Neobisiidae) from China. Turkish Journal of Zoology 41: 615–623. <https://doi.org/10.3906/zoo-1602-39>
- Gao ZZ, Wynne JJ, Zhang F (2018) Two new species of cave-adapted pseudoscorpions (Pseudoscorpiones: Neobisiidae, Chthoniidae) from Guangxi, China. The Journal of Arachnology 46(2): 345–354. <https://doi.org/10.1636/JoA-S-17-063.1>
- Gao ZZ, Zhang F, Chen HM (2020) Two new cave-dwelling species of *Tyrannochthonius* Chamberlin 1929 (Pseudoscorpiones: Chthoniidae) from the Guizhou karst, China. Zootaxa 4853(4): 572–580. <https://doi.org/10.11646/zootaxa.4853.4.6>
- Harvey MS (1989) Two new cavernicolous chthoniids from Australia, with notes on the generic placement of the south-western Pacific species attributed to the genera *Paraliochthonius* Beier and *Morikawia* Chamberlin (Pseudoscorpionida: Chthoniidae). Bulletin – British Arachnological Society 8: 21–29.
- Harvey MS (1992) The phylogeny and classification of the Pseudoscorpionida (Chelicerata: Arachnida). Invertebrate Taxonomy 6(6): 1373–1435. <https://doi.org/10.1071/IT9921373>
- Hou YM, Gao ZZ, Zhang F (2022a) Two new species of cave-adapted pseudoscorpions (Pseudoscorpiones, Chthoniidae) from Yunnan, China. ZooKeys 1097: 65–83. <https://doi.org/10.3897/zookeys.1097.82527>
- Hou YM, Gao ZZ, Zhang F (2022b) Diversity of cave-dwelling pseudoscorpions from eastern Yunnan in China, with the description of eleven new species of the genus *Lagynochthonius* (Pseudoscorpiones, Chthoniidae). Zootaxa 5198(1): 001–065. <https://doi.org/10.11646/zootaxa.5198.1.1>

- Judson MLI (2007) A new and endangered species of the pseudoscorpion genus *Lagynochthonius* from a cave in Vietnam, with notes on chelal morphology and the composition of the Tyrannochthoniini (Arachnida, Chelonethi, Chthoniidae). *Zootaxa* 1627(1): 53–68. <https://doi.org/10.11646/zootaxa.1627.1.4>
- Latella L (2019) Biodiversity: China. In: White WB, Culver DC, Pipan T (Eds) *Encyclopedia of Caves* (Third Edition). Academic Press, Amsterdam, 127–135. <https://doi.org/10.1016/B978-0-12-814124-3.00016-9>
- Li YC (2022) Five new troglobitic species of *Tyrannochthonius* (Arachnida, Pseudoscorpiones, Chthoniidae) from the Yunnan, Guizhou and Sichuan Provinces, China. *ZooKeys* 1131: 173–195. <https://doi.org/10.3897/zookeys.1131.91235>
- Li YC, Wang ML (2021) Description of a new cave-dwelling pseudoscorpion, *Anatemnus hemuensis* sp. nov. (Pseudoscorpiones, Atemnidae) from Gaoligong Mountain, China. *Carso-logica Sinica* 40(6): 1058–1062.
- Li YC, Shi AM, Liu H (2017) A new cave-dwelling species of *Bisetocreagris* Ćurčić (Arachnida, Pseudoscorpiones: Neobisiidae) from Yunnan Province, China. *Entomologica Fennica* 28(4): 212–218. <https://doi.org/10.33338/ef.84688>
- Li YC, Liu H, Shi AM (2019) A new cave-dwelling species of *Lagynochthonius* (Arachnida: Pseudoscorpiones: Chthoniidae) from Yunnan Province, China. *Zootaxa* 4571(1): 28–34. <https://doi.org/10.11646/zootaxa.4571.1.2>
- Mahnert V (2003) Four new species of pseudoscorpions (Arachnida, Pseudoscorpiones: Neobisiidae, Chernetidae) from caves in Yunnan Province, China. *Revue Suisse de Zoologie* 110: 739–748. <https://doi.org/10.5962/bhl.part.80209>
- Mahnert V (2009) New species of pseudoscorpions (Arachnida, Pseudoscorpiones, Chthoniidae, Chernetidae) from caves in China. *Revue Suisse de Zoologie* 116(2): 185–201. <https://doi.org/10.5962/bhl.part.79492>
- Mahnert V, Li YC (2016) Cave-inhabiting Neobisiidae (Arachnida: Pseudoscorpiones) from China, with description of four new species of *Bisetocreagris* Ćurčić. *Revue Suisse de Zoologie* 123: 259–268. <https://doi.org/10.5281/zenodo.155299>
- Ming QZ (1997) Study on tourism resources exploitation of karst caves in Yunnan. *Geography and Territorial Research* 13(1): 33–36. [In Chinese]
- Muchmore WB (1984) Pseudoscorpions from Florida and the Caribbean area. 13. New species of *Tyrannochthonius* and *Paraliochthonius* from the Bahamas, with discussion of the genera (Chthoniidae). *The Florida Entomologist* 67(1): 119–126. <https://doi.org/10.2307/3494110>
- Muchmore WB (1991) Pseudoscorpions from Florida and the Caribbean area. 14. New species of *Tyrannochthonius* and *Lagynochthonius* from caves in Jamaica [sic], with discussion of the genera (Chthoniidae). *The Florida Entomologist* 74(1): 110–121. <https://doi.org/10.2307/3495247>
- Muchmore WB, Chamberlin JC (1995) The genus *Tyrannochthonius* in the eastern United States (Pseudoscorpionida: Chthoniidae). Part 1. The historical taxa. *Insecta Mundi* 9: 249–257.
- Schawaller W (1995) Review of the pseudoscorpion fauna of China (Arachnida: Pseudoscorpionida). *Revue Suisse de Zoologie* 102(4): 1045–1063. <https://doi.org/10.5962/bhl.part.80489>

- Song DX (1996) On five species of soil pseudoscorpions from China. *Acta Arachnologica Sinica* 5(1): 75–80. [In Chinese]
- Wang Y (2001) Analysis and Evaluation of Development and Utilization Conditions of Karst Water in Yunnan Province. *Journal of Hydraulic Engineering* 1: 49–52. [In Chinese]
- WPC (2022) World Pseudoscorpiones Catalog. Natural History Museum Bern. <https://wac.nmbe.ch/order/pseudoscorpiones/3> [Accessed on 01 Jan. 2023]
- Xu HR, Gao ZZ, Zhang F (2022) Two new species of the pseudoscorpion subfamily Lamprochernetinae Beier, 1932 from Guizhou, China (Pseudoscorpiones: Chernetidae). *Zootaxa* 5105(4): 581–592. <https://doi.org/10.11646/zootaxa.5105.4.7>
- Zhang C, Feng ZG, Zhang F (2020) Two new cave-dwelling pseudoscorpions (Pseudoscorpiones: Neobisiidae: *Parobisium*) from Yunnan, China. *Zootaxa* 4834(1): 107–120. <https://doi.org/10.11646/zootaxa.4834.1.7>

Tricosa uniseriata, a new species of xyleborine ambrosia beetle from Thailand (Coleoptera, Curculionidae, Scolytinae, Xyleborini)

Wisut Sittichaya¹, Anthony I. Cognato²

1 Agricultural Innovation and Management Division, Faculty of Natural Resources, Prince of Songkla University, Had Yai, Songkhla, 90112, Thailand **2** Department of Entomology, Michigan State University, 288 Farm Lane, 243 Natural Science Bldg., East Lansing, MI 48824, USA

Corresponding author: Wisut Sittichaya (wisut.s@psu.ac.th)

Academic editor: M. Alonso-Zarazaga | Received 15 February 2023 | Accepted 4 March 2023 | Published 15 March 2023

<https://zoobank.org/60080833-6C7E-423D-91EE-B48F9D96A7CB>

Citation: Sittichaya W, Cognato AI (2023) *Tricosa uniseriata*, a new species of xyleborine ambrosia beetle from Thailand (Coleoptera, Curculionidae, Scolytinae, Xyleborini). ZooKeys 1153: 97–103. <https://doi.org/10.3897/zookeys.1153.101985>

Abstract

A new species, *Tricosa uniseriata* **sp. nov.**, is described here. A list of *Tricosa* species found in Thailand with distributions and an updated key to *Tricosa* are also provided.

Keywords

Ambrosia beetles, key, new species, Thailand, *Tricosa*, Xyleborini

Introduction

The xyleborine ambrosia beetle genus *Tricosa* Cognato, Smith & Beaver, 2020 (Curculionidae, Scolytinae) contains six species (Cognato et al. 2020; Smith et al. 2022). Two species were originally described as *Xyleborus* Eichhoff, 1864 and *Cyclorhipidion* Hagedorn, 1912, and four species were subsequently described (Cognato et al. 2020; Smith et al. 2022). *Tricosa* shares diagnostic characters with three xyleborine genera, *Cyclorhipidion* Hagedorn, 1912, *Cryptoxyleborus* Schedl, 1937, and *Fraudatrix* Cognato, Smith & Beaver, 2020, including either a setose and/or an attenuate appearance. *Tricosa* is distinguished from *Cyclorhipidion* by the slightly tapering elytra, from *Cryptoxyleborus* by the obliquely triangular protibial and attenuate elytra, and from *Fraudatrix* by the four-segmented antennal

Table 1. Synoptic list of the *Tricosa* fauna of Thailand.

Species	First record	Thai distribution
<i>Tricosa cattienensis</i>	Cognato et al. 2020	N: Chiang Mai; N-E: Chaiyaphum; W: Phetchaburi; S: Surat Thani
<i>Tricosa indochinensis</i>	Cognato et al. 2020	N: Chiang Mai
<i>Tricosa metacuneolus</i>	Beaver et al. 2014	S: Chumphon, Nakhon Sri Thammarat
<i>Tricosa uniseriata</i> sp. nov.	This publication	S: Narathiwat

funicle, the type 3 antennal club with one or two sutures visible on the posterior face, and the pronotal disc being as long as or shorter than the anterior slope (Cognato et al. 2020). *Tricosa* species are mainly distributed in southern Asia and eastern Papua New Guinea (Cognato et al. 2020; Smith et al. 2020, 2022). Three species have been previously recorded from Thailand, *Tricosa cattienensis* Cognato, Smith & Beaver, 2020, *T. indochinensis* Cognato, Smith & Beaver, 2020, and *T. metacuneolus* (Eggers, 1940) (Beaver et al. 2014; Cognato et al. 2020). In this present study, we describe a new species, increasing the number of Thai *Tricosa* species to four and adding a seventh member to the genus (Table 1).

Materials and methods

A specimen was collected from a small branch of *Artocarpus integer* (Moraceae) in the lowland tropical rain forest of the Hala-Bala Wildlife Sanctuary, Narathiwat province, Thailand. Photographs were taken with a Canon 5D digital camera with a Canon MP-E 65 mm macro lens (Canon, Tokyo, Japan) and StackShot-Macrorail (Cognisys Inc., MI, USA) The photos were then combined with Helicon Focus 6.8.0. (Helicon Soft, Ukraine), and all photos were improved with Adobe Lightroom classic (Adobe Systems, CA, USA). The antennal and pronotum types and characters follow those proposed by Hulcr et al. (2007) and subsequently elaborated upon by Smith et al. (2020). Length was measured from the pronotal apex to the apex of the declivity, and width was measured at the widest part of the specimen.

Results

Taxonomic treatment

Tricosa Cognato, Smith & Beaver, 2020

Type species. *Xyleborus metacuneolus* Eggers, 1940.

Diagnosis. Antennal funicle four-segmented; antennal club with one or two sutures visible on the posterior face; protibia distinctly or obliquely triangular with six or fewer denticles on outer margin and posterior face flattened and unarmed; scutellum small, flush with elytra surface; mycangial tufts absent; elytra attenuate; posterolateral costa absent.

Similar genera. *Cryptoxyleborus*, *Cyclorhipidion*, and *Fraudatrix*.

***Tricosa uniseriata* Sittichaya & Cognato, sp. nov.**

<https://zoobank.org/B97E9080-B657-4301-A775-CA9C057A644C>

Fig. 1A–F

Type material. *Holotype*, female, THAILAND, Narathiwat Province, Hala-Bala Wildlife Sanctuary, 5°48'02.4"N, 101°49'58.2"E, lowland tropical rainforest, 140 m a.s.l., 12.x.2021, ex. small branch of *Artocarpus integer* (W. Sittichaya) (NHMW, Naturhistorisches Museum Wien, Wien).

Similar species. *T. hipparion* Smith, Beaver & Cognato, 2022.

Diagnosis. This species is distinguished by its stoutness: 2.35 mm long, 2.40× as long as wide. The combination of the following characters is diagnostic: lateral margin of elytra feebly broadened apically; elytral disc convex; discal striae and interstriae uniseriate punctate; stria weakly impressed and interstriae elevated; anterior margin of pronotum with six moderate serrations.

Description (female). 2.35 mm long, 2.40× as long as wide. Body dark brown, except appendages yellowish brown. Body more robust, less elongate. **Head:** epistoma entire, transverse, lined with a row of short, hair-like setae. Frons flat from epistoma to middle level of eye, then slightly convex upward to vertex; lower portion of surface at medial line shagreened, subshining; sides of medial line glabrous, strongly shining; upper portion shagreened, subshining; frons with widely separated, small granules, with each granule decorated with long, fine, hair-like setae. Eyes weakly emarginate above level of antennal insertion; upper portion of eyes slightly smaller than lower part. Submentum slightly impressed below genae, widely triangular at base. Antennal club type 3 (Hulcr et al. 2007; Smith et al. 2020); scape regularly thick, as long as club. Antennal funicle four-segmented; first segment longest and other segments approximately equal in length. Pedicel shorter than funicle. Club flattened, approximately circular (type 3) (Hulcr et al. 2007; Smith et al. 2020); segment 1 corneous, transverse on anterior face, occupying basal $\sim 1/3$; segment 2 slightly concave, corneous and corneous line very narrow; segments 1 and 2 present on posterior face.

Pronotum: 1.0× as long as wide; elongate and parallel sided in dorsal view, type 7 (Hulcr et al. 2007; Smith et al. 2020); sides parallel in basal $2/3$, rounded anteriorly; anterior margin with a row of six serrations. In lateral view, elongate, disc longer than anterior slope, type 7, summit low, on apical $2/5$. Surface alutaceous, anterior $1/2$ asperate; asperities robust, close together, arranged in concentric arcs from midpoint of pronotum to anterior and anterolateral areas; disc evenly punctate, punctures moderate in size, round and deep, sparse and separated by glabrous, shining areas 3–5× the size of puncture, each puncture with short, erect, hair-like seta, some longer hair-like setae at margins. Lateral margins obliquely costate. Base transverse, posterior angles acutely rounded. **Scutellum:** small, narrow, linguiform, flush with elytra, shiny. **Elytra:** 1.36× as long as wide, 1.44× as long as pronotum. Base transverse, margins oblique; humeral angles rounded. Sides subparallel, slightly broader from base to apical $3/4$, then attenuate at apical $1/4$, apex attenuate, broadly rounded. Disc convex, surface smooth, shining, striae and interstriae uniseriate. Striae feebly impressed, punctate, punctures round, broad, and shallow, separated by $1/2$ the width



Figure 1. *Tricosa uniseriata* sp. nov. holotype female **A** dorsal view **B** ventro-lateral view **C** posterolateral view **D** front **E** declivity **F** antenna.

of a puncture, each puncture with a short, fine, inconspicuous, hair-like seta. Interstriae feebly elevated, elevation more evident apically; interstriae minutely uniseriate punctate-granulate, widely spaced, near elytral base with fine punctures and small

granules on apical 1/2, granules slightly increasing in size apically; each puncture or granule with a very long, hair-like seta. Declivity occupying $\sim 1/3$ of elytra, gradual, face feebly convex, subshining; striae feebly impressed, punctate, punctures similar in size with those on the disc, each with short, fine, hair-like seta; interstriae feebly elevated, with small granules, granule apices curved ventrad, each granule with very long hair-like seta; setae on declivity twice as long as those of disc. Posterolateral margins rounded and granulate. **Legs:** procoxae contiguous, prosternal posterocoxal piece conical, slightly inflated. Protibiae distinctly triangular, broadest at apical 1/3, posterior face flat, unarmed; outer margin armed with five large denticles at apical 1/3. Meso- and metatibiae obliquely triangular, flattened, posterior face unarmed; outer margin armed with 6 and 10 moderately socketed denticles.

Male. Unknown.

Etymology. *L. uniseriata*: *uni-* = one; *series* = row. Refers to the arrangement of striae and interstitial punctures in one line. A variable adjective.

Distribution. Thailand (Narathiwat Province).

Host plants. The holotype was collected from a small branch of *Artocarpus integer* (Thunb.) Merr. (Moraceae).

Discussion

Tricosa uniseriata is the smallest and stoutest *Tricosa* species. The proportion of this species' body is 2.40 \times as long as wide as compared to the other species. The elytra are feebly widened 3/4 from the base and slightly tapered to apex as compared to *T. hipparion* where the elytra are parallel sided 2/3 from the base and tapered to the apex (Cognato et al. 2020; Smith et al. 2022). Its pronotum is less posteriorly elongate, which is similar to *T. hipparion* and *T. mangoensis* (Schedl, 1942), and different from the other species, which have a more posteriorly elongated pronotum. The elytral apex is less tapering, broadly rounded, and similar to *T. hipparion*.

Key to the species of *Tricosa* (females only)

Modified from Cognato et al. (2020).

- | | | |
|---|--|--|
| 1 | Elytral disc slightly convex without transverse impression | 2 |
| – | Elytral disc deeply transversely impressed with a saddle-like depression..... | |
| | | <i>T. hipparion</i> |
| 2 | Elytral discal striae and interstriae uniseriate punctate..... | 3 |
| – | Elytral discal striae and interstriae punctures confused | 6 |
| 3 | Pronotum anterior margin unarmed, protibia broad, appearing distinctly triangular..... | <i>T. jacula</i> Cognato, Smith & Beaver, 2020 |
| – | Pronotum anterior margin serrate, protibia narrow, appearing obliquely triangular..... | 4 |

- 4 Discal striae and interstriae flat, body more elongate 2.53–2.78× as long as wide, elytra more tapering, apex broadly acute..... **5**
- Discal striae feebly impressed, interstriae feebly elevate, body shorter and stouter 2.40× as long as wide, elytra less tapering, apex broadly round.....
..... *T. uniseriata* sp. nov.
- 5 Smaller in size, 2.40–2.50 mm, and declivital interstriae moderately setose...
..... *T. metacuneolus*
- Larger, 3.80 mm, and declivital striae and interstriae densely setose.....
..... *T. mangoensis*
- 6 Pronotum anterior margin armed by a row of six serrations. Smaller, 2.70–3.10 mm long, and stouter, 2.50–2.70× as long as wide..... *T. cattienensis*
- Pronotum anterior margin armed by a row of eight serrations. Larger, 3.20–3.40 mm long, and more slender, 2.83–2.91× as long as wide
..... *T. indochinensis*

Acknowledgements

We are most grateful to Dr H. Schillhammer (NHMW) for access to specimens. We give special thanks to Mr Sunate Karapan, the senior author's best friend, for his consistent support and facilitation of collecting specimens in Hala-Bala Wildlife Sanctuary as part of multiple research projects at various times. This research was supported by Faculty of Natural Resources Research Fund, and a Cooperative Agreement (IP00533923 to Anthony Cognato) from the United States Department of Agriculture's Animal and Plant Health Inspection Service (APHIS). It may not necessarily express views of APHIS.

References

- Beaver R, Sittichaya W, Liu L-Y (2014) A synopsis of the scolytine ambrosia beetles of Thailand (Coleoptera: Curculionidae: Scolytinae). *Zootaxa* 3875(1): 1–82. <https://doi.org/10.11646/zootaxa.3875.1.1>
- Cognato AI, Smith SM, Beaver RA (2020) Two new genera of Oriental xyleborine ambrosia beetles (Coleoptera, Curculionidae: Scolytinae). *Zootaxa* 4722: 540–554. <https://doi.org/10.11646/zootaxa.4722.6.2>
- Eggers H (1940) Neue indomalayische Borkenkäfer (Ipidae) III Nachrag (Forstsetzung). *Tijdschrift voor Entomologie* 83: 132–154.
- Hagedorn M (1912) Neue Borkenkäfergattungen und Arten aus Afrika (Col.). *Deutsche Entomologische Zeitschrift* 1912: 351–356. [pls 6, 7] <https://doi.org/10.1002/mmnd.48019120313>
- Hulcr J, Dole SA, Beaver RA, Cognato AI (2007) Cladistic review of generic taxonomic characters in Xyleborina (Coleoptera: Curculionidae: Scolytinae). *Systematic Entomology* 32(3): 568–584. <https://doi.org/10.1111/j.1365-3113.2007.00386.x>

- Schedl KE (1937) Scolytidae and Platypodidae. 34 Contribution Fauna Borneensis, part I. Sarawak Museum Journal, Kuching 4: 543–552.
- Smith SM, Beaver RA, Cognato AI (2020) A monograph of the Xyleborini (Coleoptera, Curculionidae, Scolytinae) of the Indochinese Peninsula (except Malaysia) and China. ZooKeys 983: 1–442. <https://doi.org/10.3897/zookeys.983.52630>
- Smith SM, Beaver RA, Pham TH, Cognato AI (2022) New species and new records of from the Oriental region, Japan and Papua New Guinea (Coleoptera: Curculionidae: Scolytinae). Zootaxa 5209: 001–033. <https://doi.org/10.11646/zootaxa.5209.1.1>

A new species of the genus *Lindaspio* Blake & Maciolek, 1992 (Annelida, Spionidae) from a cold seep near Hainan Island, China

Jixing Sui^{1,2}, Dong Dong^{1,2}, Xuwen Wu^{1,2}, Xinzheng Li^{1,2,3}

1 Laboratory of Marine Organism Taxonomy and Phylogeny, Qingdao Key Laboratory of Marine Biodiversity and Conservation, Institute of Oceanology, Chinese Academy of Sciences, Qingdao 266071, China **2** Laboratory for Marine Biology and Biotechnology, Pilot National Laboratory for Marine Science and Technology (Qingdao), Qingdao, China **3** University of Chinese Academy of Sciences, Beijing, China

Corresponding authors: Xuwen Wu (wuxuwen@qdio.ac.cn); Xinzheng Li (lixzh@qdio.ac.cn)

Academic editor: Greg Rouse | Received 3 February 2023 | Accepted 23 February 2023 | Published 16 March 2023

<https://zoobank.org/3CA5E635-BECD-40AA-80B3-A36E0F3E8198>

Citation: Sui J, Dong D, Wu X, Li X (2023) A new species of the genus *Lindaspio* Blake & Maciolek, 1992 (Annelida, Spionidae) from a cold seep near Hainan Island, China. ZooKeys 1153: 105–112. <https://doi.org/10.3897/zookeys.1153.101406>

Abstract

A new species of the spionid genus *Lindaspio* Blake & Maciolek, 1992 was collected from a cold seep near the Hainan Island at a depth of 1758 m. Morphologically, *Lindaspio polybranchiata* sp. nov. differs from the congeners in having a narrow, folded caruncle and more neuropodial branchiae (from chaetiger 20). The 18S, COI, and 16S sequences of the new species have been submitted to GenBank. It is the first record of the genus *Lindaspio* from Chinese waters. A key to all species of *Lindaspio* is given.

Keywords

Cold seep, *Lindaspio polybranchiata* sp. nov., Polychaeta, taxonomy

Introduction

Spionidae Grube, 1850 is a group of polychaetes which have a worldwide marine distribution from the intertidal zone to the deep sea, including hydrothermal vent and cold seep environments (Blake and Maciolek 1992; Blake and Ramey-Balci 2020). They are very common and frequently dominant within polychaete communities (Meißner

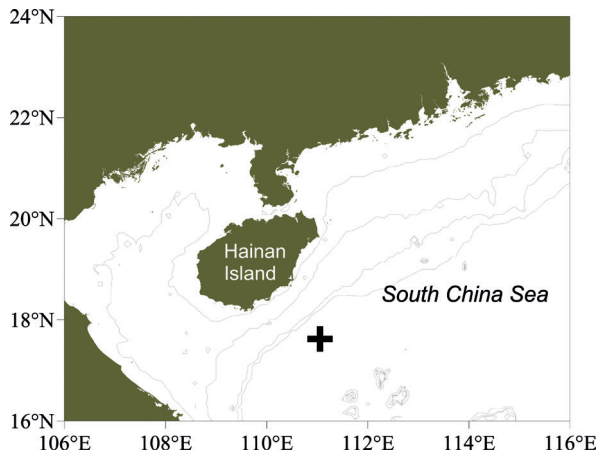


Figure 1. Sampling site of *Lindaspio polybranchiata* sp. nov.

et al. 2014). The genus *Lindaspio* was established by Blake and Maciolek (1992) for *Lindaspio dibranchiata*, which was collected from a hydrothermal mound in the Guaymas Basin (27°01'N, 111°24'W, 2008 m depth). At present, *Lindaspio* comprises three valid species: *L. dibranchiata* Blake & Maciolek, 1992 and *L. southwardorum* Blake & Maciolek, 1992 from a high-heat-flow area in the Middle Valley segment of the Juan de Fuca Ridge (48°25.8'N, 128°40.9'W, 2425 m depth), as well as *L. sebastiena* Bellan, Dauvin & Laubier, 2003 from an oil field off Congo (5°16.390'N, 11°33.848'W, 150 m depth).

In May 2021, a biodiversity survey in the area of a cold-seep (named “Lingshui”) near Hainan Island was conducted by the Institute of Oceanology, Chinese Academy of Sciences (IOCAS) using the R/V Kexue. During the cruise, some specimens of an undescribed species of polychaetes were collected by the ROV Faxian at a depth of 1758 m (Fig. 1).

Materials and methods

All the specimens were fixed and preserved in 75% ethanol solution and are deposited in the Marine Biological Museum of the Chinese Academy of Sciences (**MBMCAS**) in the Institute of Oceanology, Chinese Academy of Sciences (**IOCAS**). The specimens were observed, measured, and photographed with a Nikon AZ100 stereomicroscope. The fine morphology of anterior end, notochaetae, and neurochaetae was observed using a Hitachi S-3400N scanning electron microscope (SEM).

Total DNA was extracted with the DNeasy Blood and Tissue Kit (Qiagen, Hilden, Germany) and stored at -20 °C. Partial fragments of COI (~700 bp), 16S (~450 bp), and 18S (~1800 bp) genes were amplified by the polymerase chain reaction (PCR) using primers polyLCO/polyHCO (Carr et al. 2011), 16S-AnnF/AnnR (Sjölin et al. 2005), and 18S-A/B (Medlin et al. 1988), respectively. Amplifications were carried out in a reaction mixture containing 2 µl of template DNA, 12.5 µl of Premix Taq™ (Takara,

Otsu, Shiga, Japan), 0.5 μ l of each primer (10 mM), and sterile distilled H₂O to a total volume of 25 μ l with cycling conditions as follows: initial denaturation at 94 °C for 10 min, followed by 35–45 cycles of denaturation at 94 °C for 30 sec, annealing at 45 °C for 40 sec, and extension at 72 °C for 90 sec. A final extension at 72 °C for 5 min was included. PCR products with distinct bands after electrophoresis on 1.5% agarose gels were sent to Qingke Laboratory (Qingdao, China) for sequencing using the same set of primers that were used for PCR amplifications. Fragments with overlapping sequences (forward and reverse) were merged into consensus sequences using CONTIG EXPRESS (a component of Vector NTI Suite 6.0, Life Technologies, Carlsbad, CA, USA). The assembled sequences were checked by BLASTing in GenBank to ensure that the DNA was not contaminated. Finally, all the new sequences were submitted to GenBank.

Systematics

Taxonomy

Family Spionidae Grube, 1850

Genus *Lindaspio* Blake & Maciolek, 1992

Type species. *Lindaspio dibranchiata* Blake & Maciolek, 1992.

Generic diagnosis (according to Gérard et al. 2003). Prostomium incised, developed into two frontal lobes or weak horns; caruncle present or absent; occipital tentacle absent. Peristomial wings absent. Notopodia of chaetigers 2–4 with fascicles of heavy spines. Anterior neuropodial spines present. Dorsal branchiae starting from chaetiger 2; ventral branchiae starting from an anterior segment, branchiae closely associated with parapodial lamellae, continuing to posterior end. Chaetiger 1 reduced, with notopodia reduced to single lamellae lacking notochaetae. Following notopodia and neuropodia with capillaries and hooded hooks. Pygidium simple, conical, lacking cirri.

Lindaspio polybranchiata sp. nov.

<https://zoobank.org/601C3193-EE40-4088-9029-2CB1BDDC8641>

Figs 2–4

Material examined. Holotype: Complete, Lingshui cold seep cruise, Faxian Dive 252, 1758 m, 17°37'N, 111°03'E, coll. crew of R/V Kexue, 28 May 2021, MBM 304666.

Paratypes: 4 specimens, complete, same collection data as holotype, MBM 304662–MBM 304665.

Non-type: 14 incomplete specimens depositing in one specimen bottle, MBM304661.

Description of holotype. Total length 55 mm, maximum width 4 mm, including chaetae. More than 350 crowded chaetigers. Color pale in alcohol.

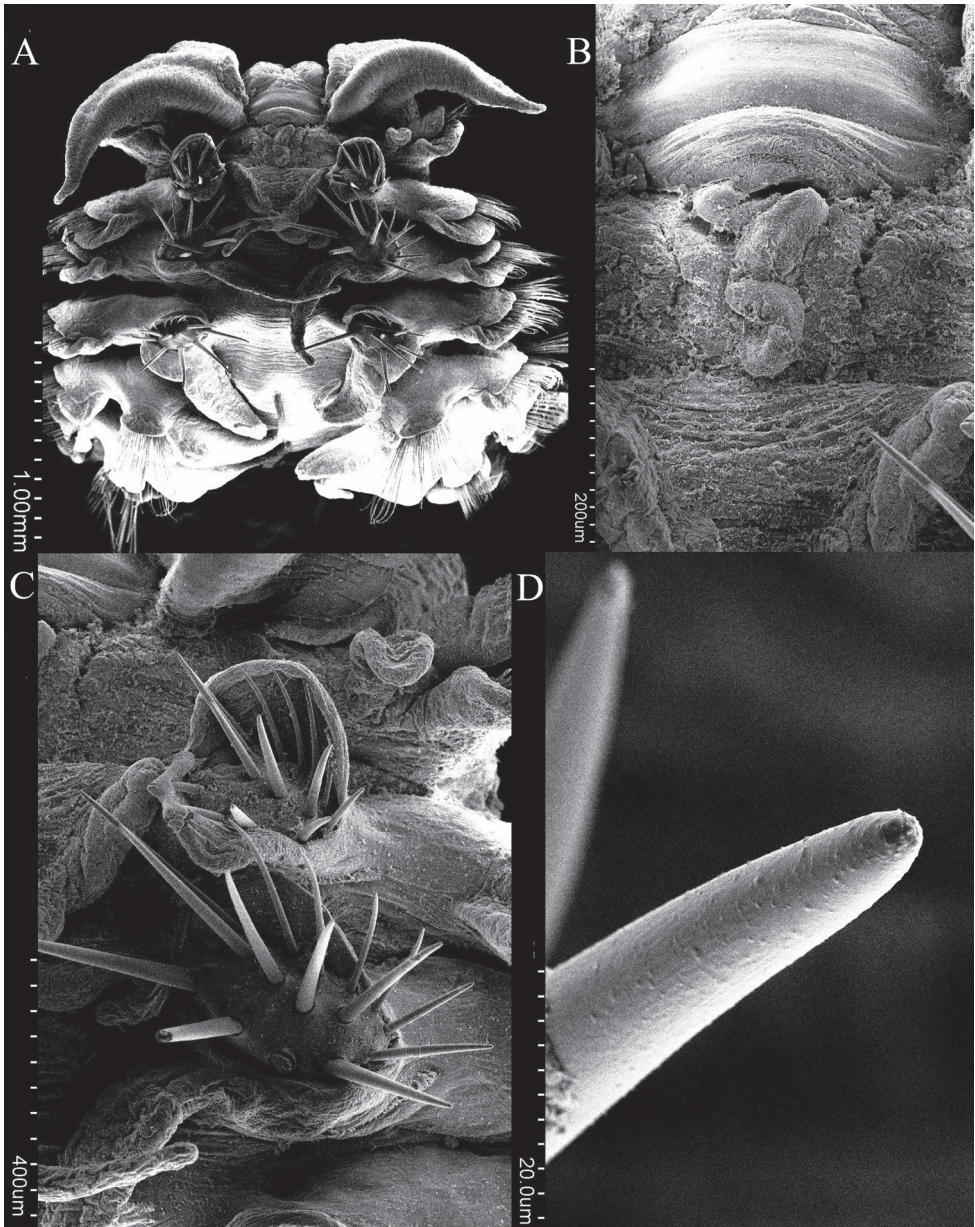


Figure 2. *Lindaspio polybranchiata* sp. nov. (Paratype, MBM 304662) **A** anterior end, dorsal view **B** caruncle **C** modified notopodial spines from anterior chaetiger **D** tip of modified notopodial spine.

Prostomium anteriorly bilobed, forming two broadly swollen lobes (Fig. 2A), continuing posteriorly as narrow, undulating caruncle to anterior margin of chaetiger 2 (Fig. 2B). Palps short, thick, tapering to pointed tip, not extending beyond chaetiger 3 (Figs 2A, 3A). Chaetiger 1 reduced, notopodia reduced to flattened lamella, lacking

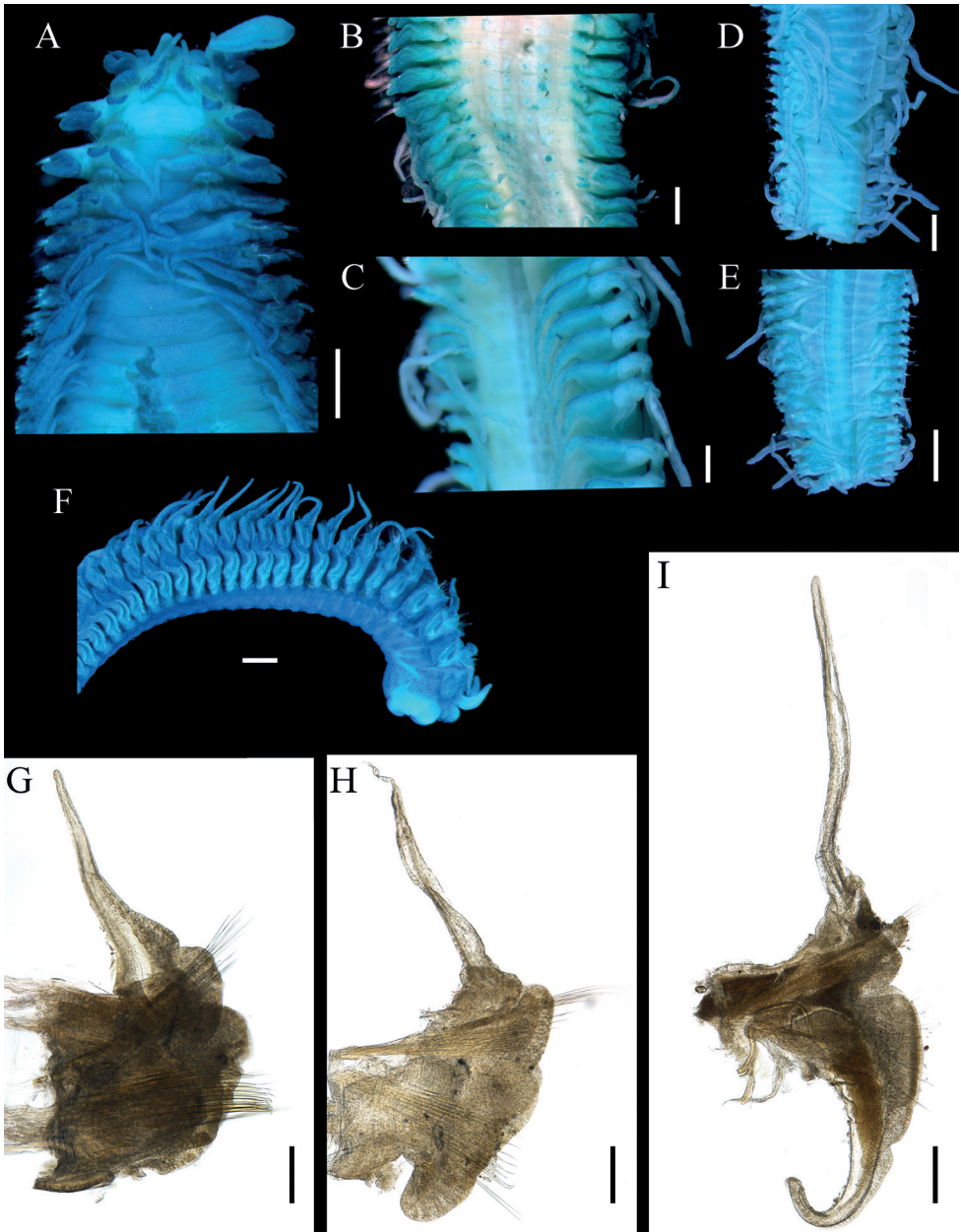


Figure 3. *Lindaspio polybranchiata* sp. nov. (Paratype, MBM 304663) **A** anterior end in dorsal view **B** anterior segments in ventral view, starting from segment 20 **C** median segments in ventral view **D** posterior end in dorsal view **E** posterior end in ventral view **F** anterior end in lateral view **G** parapodium from segment 12 **H** parapodium from segment 31; **I**. parapodium from segment 51. Scale bars: 1 mm (**A**, **E**); 500 µm (**B–D**, **F**); 250 µm (**G–I**).

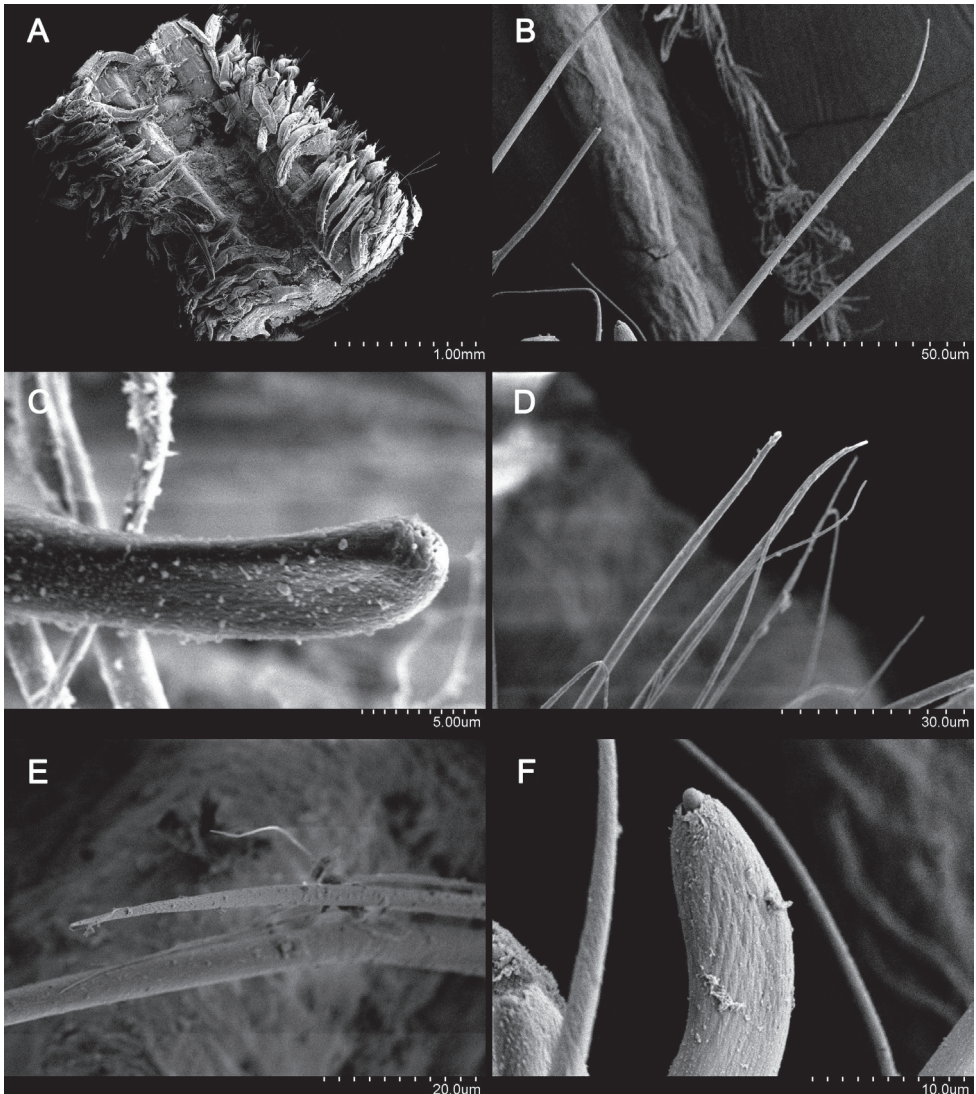


Figure 4. *Lindaspio polybranchiata* sp. nov. (Paratype, MBM 304662) **A** ventral view, middle part **B** anterior notochaetae **C** notopodial hooded hooks **D** anterior neurochaetae **E** details of neurochaetae **F** neuropodial hooded hook.

notochaetae (Fig. 3A); neuropodia with well-developed pre- and postchaetal lamellae (Fig. 3F) and fascicles of capillaries. Notopodia of chaetigers 2–4 shifted dorsally to medial position, with pre- and postchaetal lamellae forming three rows enclosing cluster of modified spines (Figs 2C, D, 3A, F). Notopodia of chaetigers 5–8 gradually shifted to lateral position (Fig. 3A, F). Notopodia from chaetiger 5 and neuropodia from chaetiger 2 with well-developed pre- and postchaetal lobes.

Dorsal branchiae fingerlike, appear from chaetiger 2 (Fig. 3A) and remaining short to chaetiger 30, thereafter branchiae becoming thinner, longer, extending to dorsal midline. Ventral branchiae absent in the anterior part (Fig. 3G). From chaetiger 20 small

neuropodial expansion (Fig. 3B), becoming well-developed neuropodial branchiae (Fig. 3C) at chaetiger 40, until about chaetiger 80, becoming longer, more cylindrical, nearly reaching ventral midline, but never as long as dorsal branchiae (Figs 3H, I, 4A).

Notochaetae of chaetigers 2–4 modified into cluster of about 15 heavy spines (Figs 2C, 3A); subsequent notochaetae numerous, thin capillaries (Fig. 4B) until about chaetiger 60 where hooded hooks appear; capillaries become heavier and more limbate in far posterior segments; individual notopodial hooks strongly curved, with pointed tips without minute teeth (Fig. 4C).

Anterior neurochaetae include row of heavy spines and ventral bundle of thin capillaries (Fig. 4D); neuropodial spines each with smooth shaft that tapers gradually, then continues as fine, pointed tip with fine bristles sometimes visible along edge (Fig. 4E); spines present until about chaetiger 40, then accompanied with thin capillaries; these capillaries accompanied by neuropodial hooded hooks from about chaetiger 65; each hook smaller, more delicate than notopodial hooks, without minute teeth (Fig. 4F). Pygidium simple, conical, lacking cirri (Fig. 3D, E).

GenBank Accession Number: COI OQ582086, 16S OQ592054, 18S OQ592055.

Remarks. As mentioned above, three species have been reported in the genus *Lindaspio*. The new species is easily distinguished from *L. dibranchiata* and *L. sebastiena* in having a narrow, undulating caruncle, while *L. sebastiena* has no caruncle and *L. dibranchiata* has a short, mounded caruncle. The new species resembles *L. southwardorum* in having similar caruncle, ventral branchiae and dorsal clusters of spines in anterior notopodia, while the latter differs in having first neuro-branchiae from chaetiger 55 (vs. chaetiger 20 in the new species) and having more modified spines on chaetigers 2–4 (20 vs. 15).

The BLAST percent identity of the 18S sequence between the new species and *Lindaspio dibranchiata* is 99% (1758/1762 bp), suggesting that they are congeneric. Additionally, the COI and 16S sequences of our specimen are identical to those of *Lindaspio* sp. (GenBank accession number OK032597.1), which confirms that the unverified species of *Lindaspio* in GenBank is a *Lindaspio polybranchiata* sp. nov.

Etymology. The species is so named because it has more neuropodial branchiae than the congeners.

Distribution. Currently only known from the type locality, near Hainan Island, China, at a depth of 1758 m (Fig. 1).

Key to *Lindaspio* species

- 1 Caruncle absent *L. sebastiena* Bellan, Dauvin & Laubier, 2003
- Caruncle present 2
- 2 Caruncle oval *L. dibranchiata* Blake & Maciolek, 1992
- Caruncle undulating 3
- 3 First neuro-branchiae starting from about chaetiger 55
..... *L. southwardorum* Blake & Maciolek, 1992
- First neuro-branchiae starting from about chaetiger 20
..... *L. polybranchiata* sp. nov.

Acknowledgements

Many thanks are due to Dr Qi Kou and Yong Xu (IOCAS) for their help with photography. We are grateful to the operation team of the ROV Faxian and the crews of the R/V Kexue for their support in collecting the deep-sea specimens during the cruise in May 2021. This work is financially supported by the National Key R&D Program of China, project number 2018YFC0310800, the National Natural Science Foundation of China, project number 31872194 and the Biological Resources Program, Chinese Academy of Sciences, project number KFJ-BRP-017-46.

References

- Blake JA, Maciolek NJ (1992) Polychaeta from deep-sea hydrothermal vents in the Eastern Pacific. III: A new genus and two new species of Spionidae from the Guaymas Basin and Juan de Fuca Ridge with comments on a related species from the western North Atlantic. *Proceedings of the Biological Society of Washington* 105(4): 723–732.
- Blake JA, Ramey-Balci PA (2020) A new genus and species of spionid polychaete (Annelida, Spionidae) from a deep-water cold seep site in the eastern Mediterranean sea off Turkey. *Zoosymposia* 19(1): 121–134. <https://doi.org/10.11646/zoosymposia.19.1.14>
- Carr CM, Hardy SM, Brown TM, Macdonald TA, Hebert PD (2011) A tri-oceanic perspective: DNA barcoding reveals geographic structure and cryptic diversity in Canadian polychaetes. *PLoS ONE* 6(7): e22232. <https://doi.org/10.1371/journal.pone.0022232>
- Gérard B, Jean-Claude D, Lucien L (2003) The genus *Lindaspio* (Annelida: Polychaeta: Spionidae), and a new species from an oil field off Congo, western Africa. *Journal of Natural History* 37(20): 2413–2424. <https://doi.org/10.1080/00222930210155666>
- Medlin L, Elwood HJ, Stickel S, Sogin ML (1988) The characterization of enzymatically amplified eukaryotic 16S-like rRNA-coding regions. *Gene* 71(2): 491–499. [https://doi.org/10.1016/0378-1119\(88\)90066-2](https://doi.org/10.1016/0378-1119(88)90066-2)
- Meißner KBA, Guggolz T, Götting G (2014) Spionidae (Polychaeta: Canalipalpata: Spionida) from seamounts in the NE Atlantic. *Zootaxa* 3786(3): 201–245. <https://doi.org/10.11646/zootaxa.3786.3.1>
- Sjölin E, Erséus C, Källersjö M (2005) Phylogeny of Tubificidae (Annelida, Clitellata) based on mitochondrial and nuclear sequence data. *Molecular Phylogenetics and Evolution* 35(2): 431–441. <https://doi.org/10.1016/j.ympev.2004.12.018>

A new species of *Physomerinus* Jeannel (Coleoptera, Staphylinidae, Pselaphinae) from Jiulong National Wetland Park, China

Zi-Wei Yin¹

¹ *Laboratory of Systematic Entomology, College of Life Sciences, Shanghai Normal University, Shanghai 200234, China*

Corresponding author: Zi-Wei Yin (pselaphinae@gmail.com)

Academic editor: Adam Brunke | Received 9 January 2023 | Accepted 24 February 2023 | Published 16 March 2023

<https://zoobank.org/0EE0C6EF-EA13-411B-8655-D6AFC9DB0B3A>

Citation: Yin Z-W (2023) A new species of *Physomerinus* Jeannel (Coleoptera, Staphylinidae, Pselaphinae) from Jiulong National Wetland Park, China. ZooKeys 1153: 113–120. <https://doi.org/10.3897/zookeys.1153.100073>

Abstract

Physomerinus jiulongensis sp. nov. is described from a series of overwintering individuals collected in decomposing wood at Jiulong National Wetland Park, East China. The new species is characterized and separated from related congeners by the unique form of the sexually dimorphic maxillary palpi, greatly swollen male metafemora, as well as by the shape of the genitalia of both sexes. A key to, and a distributional map of, *Physomerinus* species occurring in China and on the Ryukyu Islands, Japan is provided.

Keywords

Ant-loving beetle, Batrisina, Batrisini, East China, new taxon, taxonomy, Zhejiang

Introduction

The ant-loving beetle genus *Physomerinus* Jeannel, 1952 (Batrisitae: Batrisini) contains 12 species distributed in the Oriental and East Palaearctic regions (Newton 2022). The genus was placed in Jeannel's fifth division of the Batrisina (Jeannel 1958), or as a member of Nomura's (1991) '*Batrisocenus* complex' of genera. Species of this genus have the pronotum with distinct median and two lateral longitudinal sulci, and a complete transverse antebasal sulcus, the sides of the pronotum lack spines, each elytron has two basal foveae, and the first visible tergite (IV) is longest. The males possess variously

modified metafemora, and often a constricted basal capsule of the aedeagus. The latter indicates a close relationship to the genus *Batriscenaulax* Jeannel, 1958 which includes six species from Japan and China (Nomura 1991; Yin 2022). One major taxonomic problem of *Physomerinus* is that the type species, *P. septemfoveolatus* (Schaufuss L. W., 1877) from Southeast Asia, has a secretory trichome on the anterolateral margin of the scape, and the aedeagus bears a large basal capsule (Jeannel 1952: fig. 42; Nomura pers. com.), which are congruent with the defining features of a group of genera centered on *Batrisiella* Raffray, 1904. A revision of the genus is needed to clarify this problem.

Within *Physomerinus* several species may indeed form monophyletic subgroups by their shared male features. *Physomerinus hasegawai* Nomura, 1991 from China (Taiwan) and Japan (Ryukyu Islands) and *P. clavipes* Zhang & Yin, 2022 from China (Guangxi) are linked by the smoothly broadened lateral portions of maxillary palpomeres 4, and greatly swollen metafemora with a large lateral cavity (Nomura 1991, 2010, 2012, 2013; Zhang and Yin 2022).

During December 2022 to January 2023, a team of IZCAS led by Hong-Bin Liang surveyed the beetle fauna of Jiulong National Wetland Park in Zhejiang Province, East China. A series of overwintering pselaphine beetles were collected from decomposing wood along a riverbank and were later sent to me for identification. The result revealed a new species of *Physomerinus* closely related to *P. hasegawai* and *P. clavipes*, which is diagnosed, described, and illustrated in this paper.

Material and methods

The holotype of the new species described here is deposited in the Institute of Zoology, Chinese Academy of Science (IZCAS), Beijing, China, and the paratypes in IZCAS and the Insect Collection of Shanghai Normal University (SNUC), Shanghai, China. The label data of the material are quoted verbatim.

Dissected parts were mounted in Euparal on plastic slides pinned with the specimen. The habitus image of the beetle was taken using a Canon 5D Mark III camera, equipped with a 7.5× Mitutoyo M Plan Apo lens, and two Godox V860III-C TTL Li-Ion flashes were used as the light source. Images of the morphological details were produced using a Canon G9 camera mounted to an Olympus CX31 microscope under reflected or transmitted light. Helicon Focus v. 8.2.0 Pro was used for image stacking. All images were modified and grouped into plates using Adobe Photoshop CC 2020.

Measurements were taken as follows: total body length was measured from the anterior margin of the clypeus to the apex of the abdomen; head length was measured from the anterior margin of the clypeus to the head base, excluding the occipital constriction; head width was measured across the eyes; the length of the pronotum was measured along the midline, the width of the pronotum is its maximum width; the length of the elytra was measured along the suture; the width of the elytra was measured as the maximum width across both elytra; the length of the abdomen is the length of the dorsally exposed part of the abdomen along its midline, the width of

the abdomen is its maximum width. Terminology follows Chandler (2001) and Yin (2022). The abdominal tergites and sternites are numbered in Arabic (starting from the first visible segment) and Roman (reflecting true morphological position) numerals, e.g., tergite 1 (IV), or sternite 1 (III). Paired appendages in the description of the new species are treated as singular.

Taxonomy

Physomerinus jiulongensis Yin, sp. nov.

<https://zoobank.org/A558FA35-B929-44A5-B490-613DE3074175>

Figs 1, 2

Chinese common name: 九龙奇腿蚁甲

Type material (25 exx.). Holotype: CHINA: ♂, 'China: Zhejiang, Lishui, Bihu To., Hongyu Vill., Jiulong Wetland Park, 28.38479°N, 119.8247°E, 60 m, 31.xii.2022, wood, Liang, Qin, Wang leg. [丽水九龙湿地公园, 梁红斌, 秦雨瑶, 王凯 采]' (IZCAS). **Paratypes:** CHINA: 9 ♂♂, 8 ♀♀, same collecting data as for holotype; 4 ♂♂, 3 ♀♀, same collecting data as for holotype, except '4.i.2023' (4 exx. in IZCAS, 20 exx. in SNUC).

Diagnosis. Male. Body length approximately 1.8 mm. Head subtruncate at base; vertex with transverse sulcus posterior antennal tubercles, with short mediobasal carina, vertexal foveae small and asetose; antenna relatively long, antennomeres each elongate, lacking modification; maxillary palpomere 4 protuberant on lateral margin. Discal stria of elytron extending posteriorly to near posterior margin. Metafemur greatly swollen and with large cavity on lateral side. Abdomen dorsally with tergite 1 (IV) longer than 2–4 (V–VII) combined in dorsal view, simple. Aedeagus strongly asymmetric, ventral stalk much shorter than dorsal lobe. **Female.** Body length slightly over 1.8 mm, maxillary palpus and metafemur lacking modification, genital complex as in Fig. 1G.

Description. Male. Body (Fig. 1A) length 1.77–1.81 mm; color reddish-brown, tarsi and mouthparts lighter in color. Dorsal surface of body covered with relatively short pubescence.

Head (Fig. 1B) subtruncate at base, much wider than long, length 0.35–0.36 mm, width across eyes 0.40–0.43 mm; vertex finely punctate, smoothly convex, with small, asetose and broadly separated vertexal foveae (dorsal tentorial pits), with short, straight transverse sulcus posterior antennal tubercles, mediobasal carina extending posteriorly to occipital constriction and anteriorly to level of slightly posterior midlength of eyes, antennal tubercle moderately raised, surrounding area roughly punctate; frons broadly and shallowly impressed medially, confluent with clypeus; clypeus with smooth surface, its anterior margin carinate and moderately raised; ocular-mandibular carina complete. Venter with tiny gular foveae (posterior tentorial pits) originating from shared transverse slit, with distinct median carina extending from foveae anteriorly to mouthparts. Compound eyes greatly prominent, composed of approximately 35 large

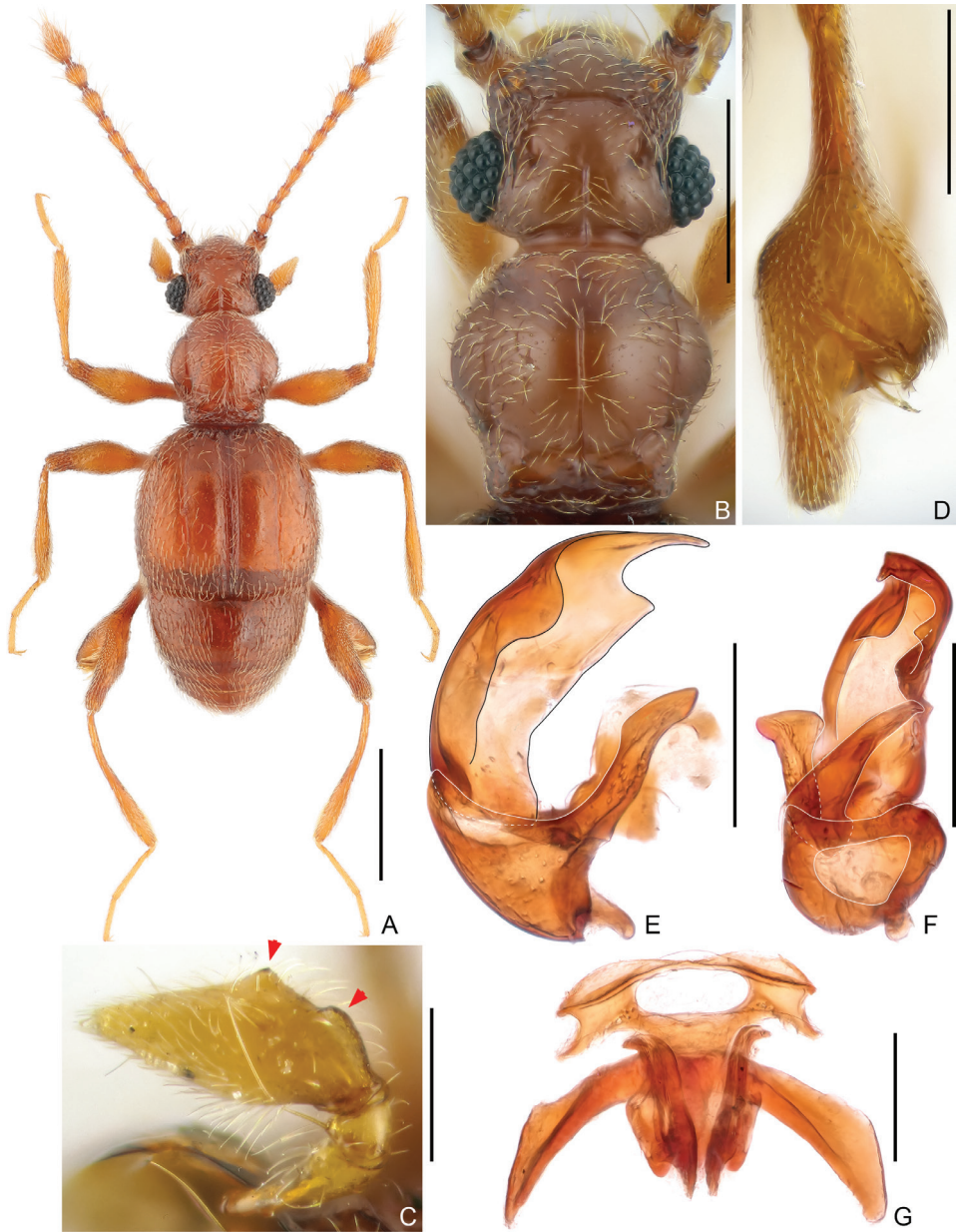


Figure 1. Morphology of *Physomerinus jiulongensis* sp. nov. (**A–F** male **G** female) **A** habitus **B** head and pronotum **C** maxillary palpus **D** metafemur **E, F** aedeagus, lateral (**E**) and ventral (**F**) **G** genital complex. Scale bars: 0.5 mm (**A**); 0.3 mm (**B**); 0.1 mm (**C, E, F, G**); 0.2 mm (**D**).

ommatidia. Antenna 0.97–1.01 mm long, lacking modification; antennomere 1 thick, subcylindrical, 2–7 each slightly elongate, successively longer, 8 shortest, slightly elongate, enlarged 9–11 forming distinct club, 9 and 10 of subequal size, each moderately expanded on mesal margin, 11 largest, 1.7× as long as 10, fusiform, truncate at base.

Pronotum (Fig. 1B) slightly longer than wide, length 0.41–0.44 mm, width 0.40–0.42 mm, widest at middle; lateral margins rounded; disc moderately convex, finely punctate, with median longitudinal sulcus much shorter than semicircular lateral sulci in dorsal view; lacking median antebasal fovea, with complete, deep transverse antebasal sulcus connecting lateral antebasal foveae, with small, blunt antebasal tubercles; outer and inner pair of basolateral foveae small. Prosternum with anterior part as long as coxal part, with small lateral procoxal foveae; hypomerid ridge complete, with lateral antebasal hypomerid pit; margin of coxal cavity thinly carinate.

Elytra much wider than long, length 0.61–0.62 mm, width 0.69–0.72 mm; each elytron with two large, widely separated basal foveae, lacking subbasal fovea; humeral protuberance small, acute; discal stria long, extending from outer basal fovea to approximately apical 4/5 of elytral length; subhumeral fovea small, carinate marginal stria extending posteriorly from fovea to apex of elytron. Metathoracic wings fully developed.

Mesoventrite short, demarcated from metaventrite by ridged anterior edges of impressed areas where large, setose lateral mesocoxal foveae situated at mesal portions of impression, with pair of admesal carinae; setose median mesoventral foveae broadly separated, lateral mesoventral foveae large and setose, forked internally. Metaventrite moderately impressed at middle, with pair of setose lateral metaventral foveae, posterior margin with small and narrow split at middle.

Legs elongate; mesotrochanter with tiny, indistinct protuberance on ventral margin; metafemur greatly swollen laterally and with large cavity (Fig. 1D), dorsal side with short sensory setae, with tufts of setae along mesal and posterior margin of cavity.

Abdomen much narrower than elytra, widest at basolateral margins of tergite 1 (IV), length 0.44–0.52 mm, width 0.62–0.65 mm; lacking modification. Tergite 1 (IV) in dorsal view longer than 2–4 (V–VII) combined; setose basal sulcus separated by mediobasal and one pair of basolateral foveae, with pair of thin, triangular discal carinae; tergites 2 and 3 (V and VI) each short, lacking fovea, 4 (VII) as long as 2 and 3 combined along middle, with one pair of small basolateral foveae, 5 (VIII) semicircular, posterior margin roundly emarginate at middle. Sternite 2 (IV) with one pair of mediobasal and one pair of basolateral foveae, and large basolateral sockets, with one pair of short and one pair of long lateral carinae; midlength of sternite 2 shorter than 3 (V) and 4 (VI) combined, 3–5 (VII) each short, successively shorter, lacking fovea, 6 (VIII) greatly transverse, posterior margin roundly convex at middle, sternite 7 (IX) membranous, indistinct.

Aedeagus (Fig. 1E, F) 0.21 mm long, strongly asymmetric; median lobe with constricted basal capsule and sub-triangular foramen, with long basoventral projection, ventral stalk short, in lateral view curved and narrowing towards apex; dorsal lobe much longer than ventral stalk, broad, sides incurved, with narrowed apex; parameres fused to form broad, semi-sclerotized plate.

Female. Similar to male in external morphology; antenna slightly shorter; maxillary palpus and metafemur lacking modification; each compound eye composed of approximately 30 ommatidia; humeral protuberance small and weak; metathoracic wings reduced. Measurements (as for male): body length 1.83–1.85 mm; length/width of head 0.35–0.37/0.41–0.43 mm, pronotum 0.40–0.43/0.40–0.43 mm, elytra

0.54–0.57/0.66–0.71 mm; abdomen 0.50–0.54/0.65–0.67 mm; length of antenna 0.92–0.96 mm; maximum width of genital complex (Fig. 1G) 0.29 mm, genital plate much wider than sternite 9, lateral arms broadened distally.

Comparative notes. This species shares with *P. hasegawai* from Taiwan and Japan and *P. clavipes* from Guangxi the sexually dimorphic fourth segments of the maxillary palpi and greatly swollen metafemora of the male, and together these species may form a monophyletic group. The male of *Physomerinus jiulongensis* sp. nov. can be readily separated by the presence of two protuberances on the lateral margins of maxillary palpomeres 4, and short ventral lobe of the aedeagus. In contrast, both *P. hasegawai* and *P. clavipes* have smoothly swollen lateral margins of maxillary palpomeres 4, and the ventral stalks of the aedeagi are as long as or slightly longer than the dorsal lobes.



Figure 2. Distribution and habitat of *Physomerinus* **A** map showing the distribution of *Physomerinus* species occurring in China and on the Ryukyu Islands, Japan **B, C** collecting environment (**B**) and habitat (**C**) of *P. jiulongensis* sp. nov. in Jiulong National Wetland Park, Zhejiang, China. Yu-Yao Qin (left) and Kai Wang (right) were searching for pselaphines from decomposing wood.

Distribution. East China: Zhejiang (Fig. 2A).

Bionomics. All overwintering adults were collected in decomposing wood near a river bank (Fig. 2B, C).

Etymology. The new species is named after its type locality, i.e., Jiulong National Wetland Park.

Key to males of *Physomerinus* species from China and the Ryukyu Islands, Japan

- 1 Lateral margin of maxillary palpomere 4 smoothly expanded or protuberant.....2
- Maxillary palpomere 4 fusiform; lateral margin not expanded and lacking protuberance 4
- 2 Lateral margin of maxillary palpomere 4 smoothly expanded; aedeagus with ventral stalk as long as or slightly longer than dorsal lobe 3
- Lateral margin of maxillary palpomere 4 with two protuberances (Fig. 1C); aedeagus with ventral stalk much shorter than dorsal lobe (Fig. 1E, F) (Zhejiang) *P. jiulongensis* sp. nov.
- 3 Hind legs relatively much longer (Zhang and Yin 2022: fig. 2A); aedeagus with ventral stalk slightly longer than dorsal lobe, and expanded at middle in dorso-ventral view (Zhang and Yin 2022: fig. 2F) (Guangxi) *P. clavipes* Zhang & Yin
- Hind legs relatively much shorter; aedeagus with ventral stalk as long as dorsal lobe, and slightly broadened from base toward apical portion in dorso-ventral view (Nomura 1991: fig. 134G) (Taiwan; Ryukyu Islands) *P. basegawai* Nomura
- 4 Metafemur with large cavity and mushroom-like projection in cavity (Yin et al. 2017: figs 1B, 3C) (Shanghai, Zhejiang) *P. predator* (Sharp)
- Metafemur swollen, lacking cavity or projection 5
- 5 Body size larger, length approximately 2 mm; pronotum with short median longitudinal sulcus not reaching anterior margin of pronotum; metafemur with oblique furrow on lateral side (Taiwan) *P. cruralis* (Raffray)
- Body size smaller, length 1.5–1.7 mm; pronotum with long median longitudinal sulcus almost reaching anterior margin of pronotum; metafemur with transverse furrow on upper side (Taiwan; Ryukyu Islands) *P. schenklingsi* (Raffray)

Acknowledgements

I would like to thank Hong-Bin Liang, Yu-Yao Qin and Kai Wang (all IZCAS) for the collection and providing of the material used in this study. The field work was supported by the management office of Jiulong National Wetland Park of Lishui, Zhejiang. Shûhei Nomura (National Museum of Nature and Science, Tsukuba-shi, Japan), Peter Hlaváč (National Museum, Natural History Museum, Praha, Czech Republic), and an anonymous reviewer read the draft manuscript and provided helpful

comments. Shûhei Nomura also pointed out the distribution of *P. hasegawai* in Taiwan. The present study was supported by the National Natural Science Foundation of China (no. 31872965).

References

- Chandler DS (2001) Biology, morphology, and systematics of the antlike litter beetles of Australia (Coleoptera: Staphylinidae: Pselaphinae). *Memoirs on Entomology International* 15: 1–560.
- Jeannel R (1952) Pselaphides de Saïgon. *Revue Française d'Entomologie* 19(2): 69–113.
- Jeannel R (1958) Révision des Pselaphides du Japon. *Mémoires du Muséum National d'Histoire Naturelle (A: Zoologie)* 18(1): 1–138.
- Newton A (2022) Staphyliniformia world catalog database. In: Bánki O, Roskov Y, Döring M, Ower G, Vandepitte L, Hobern D, Remsen D, Schalk P, DeWalt RE, Keping M, Miller J, Orrell T, Aalbu R, Adlard R, Adriaenssens EM, Aedo C, Aescht E, Akkari N, Alexander S et al. (Eds) *Catalogue of Life Checklist (Aug 2022)*. <https://www.catalogueoflife.org/data/dataset/1204> [Last accessed 1st March 2022]
- Nomura S (1991) Systematic study on the genus *Batrisoplisus* and its allied genera from Japan (Coleoptera, Pselaphidae). *Esakia* 30: 1–462. <https://doi.org/10.5109/2550>
- Nomura S (2010) Pselaphine species (Staphylinidae) collected by Nakase style light traps (NLT) from Ishigakijima Island, the Ryukyus, SW Japan. *Coleopterists' News* 172: 1–6. [In Japanese, with English subtitle]
- Nomura S (2012) A faunistic review of pselaphine species known from Nansei Islands, SW Japan, with new distributional records of *Physomerinus hasegawai* Nomura, 1991. *Sayabane, N. S.* 8: 38–47. [In Japanese, with English subtitle]
- Nomura S (2013) Pselaphine species (Staphylinidae) collected by Nakase system light traps (NLT) from Miyako Island and its adjacent Islands, the Ryukyus, SW Japan. *Sayabane, N. S.* 12: 11–17. [In Japanese, with English subtitle]
- Yin Z-W (2022) The Batrisini of Tibet: Unveiling an enigmatic ant-loving beetle diversity at Earth's "Third Pole" (Coleoptera, Staphylinidae, Pselaphinae). *Zootaxa* 5111(1): 1–211. <https://doi.org/10.11646/zootaxa.5111.1.1>
- Yin Z-W, Jiang R-X, Chen Z-B (2017) Notes on the Pselaphinae (Coleoptera: Staphylinidae) in Shanghai, China. *Zootaxa* 4238(3): 433–439. <https://doi.org/10.11646/zootaxa.4238.3.10>
- Zhang W-X, Yin Z-W (2022) Two new species of Batrisini (Coleoptera: Staphylinidae: Pselaphinae) from Nanling Mountain Area, China. *Insects* 13(2): 119. <https://doi.org/10.3390/insects13020119>

New species, a new combination, and DNA barcodes of *Parachironomus* Lenz, 1921 (Diptera, Chironomidae)

Wen-Bin Liu¹, Ying Wang¹, Kang-Zhu Zhao¹, Cheng-Yan Wang¹,
Jun-Yu Zhang¹, Chun-Cai Yan¹, Xiao-Long Lin^{2,3}

1 Tianjin Key Laboratory of Conservation and Utilization of Animal Diversity, College of Life Sciences, Tianjin Normal University, Tianjin, 300387, China **2** Shanghai Universities Key Laboratory of Marine Animal Taxonomy and Evolution, Shanghai Ocean University, Shanghai 201306, China **3** Engineering Research Center of Environmental DNA and Ecological Water Health Assessment, Shanghai Ocean University, Shanghai 201306, China

Corresponding authors: Chun-Cai Yan (skyycc@tjnu.edu.cn); Xiao-Long Lin (lin880224@gmail.com)

Academic editor: F. L. da Silva | Received 8 December 2022 | Accepted 28 February 2023 | Published 16 March 2023

<https://zoobank.org/33E8B084-33BA-4CD7-8021-7AD989C2E826>

Citation: Liu W-B, Wang Y, Zhao K-Z, Wang C-Y, Zhang J-Y, Yan C-C, Lin X-L (2023) New species, a new combination, and DNA barcodes of *Parachironomus* Lenz, 1921 (Diptera, Chironomidae). ZooKeys 1153: 121–140. <https://doi.org/10.3897/zookeys.1153.98542>

Abstract

The genus *Parachironomus* has a cosmopolitan distribution including 85 valid described species worldwide. Species records and studies of the genus in the Tibetan Plateau are scarce. In this study, the genus *Parachironomus* from China is revised and two new species, *Parachironomus wangi* Liu & Lin, **sp. nov.** and *Parachironomus nankaiensis* Liu & Lin, **sp. nov.**, are described based on adult morphology and molecular data. *Paracladopelma demissum* Yan, Wang & Bu is placed in the genus *Parachironomus* as a new combination. A neighbor-joining tree was reconstructed based on all known *Parachironomus* COI DNA barcodes. A key to adult males of the genus *Parachironomus* from China is also provided.

Keywords

COI, new combination, new species, taxonomy, Tibetan Plateau

Introduction

The genus *Parachironomus* was erected by Lenz (1921) based on the characters of larvae and pupae with *Chironomus cryptotomus* Kieffer, 1915 as type species. Subsequently, the genus was studied by a number of authors in different life stages and geographical areas (Edwards 1929; Townes 1945; Cranston et al. 1989; Sæther and Spies 2013). Larvae of *Parachironomus* can be found in a variety of habitats, such as standing and flowing waters, soft sediments, or within aquatic macrophytes, while others are endo- or ectoparasites on snails (Orel 2017). Among the *Harnischia* generic group, members of *Parachironomus* can be separated from the similar genus *Demicryptochironomus* Lenz by the extended superior volsella with several distal setae always arising from distinct pits, and the inferior volsella with a pointed or blunt caudal projection (Yan et al. 2015). To date, 85 valid species have been reported worldwide (Lehmann 1970; Ashe and Cranston 1990; Kikuchi and Sasa 1990; Oliver et al. 1990; Sæther et al. 2000; Wang 2000; Sasa et al. 2001; Sasa and Tanaka 2001; Makarchenko et al. 2005; Spies 2008; Trivinho-Strixino et al. 2010; Yan et al. 2015; Orel 2017).

The DNA barcodes corresponding to the 658-bp fragment of the mitochondrial gene cytochrome c oxidase I (COI) has been identified as the core of a global bio-identification system at the species level (Hebert et al. 2003a, b). DNA barcodes also proved to be useful in the delimitation of non-biting midge species and has provided important evidence to confirm new species (Anderson et al. 2013; Lin et al. 2015, 2021; Gilka et al. 2018; Liu et al. 2021).

The Tibetan Plateau is located in southwest China, with a vast territory and diverse terrain. The Tibetan Plateau is one of the most important areas of biodiversity in the world because of its unique environmental and regional units, which breed unique biological communities and many unique and rare wild animals and plants. Some interesting species were discovered during the investigations of insect diversity in the Tibetan Plateau. In this paper, one new combination and two new species are proposed and described. The partial COI sequences of species in *Parachironomus* with DNA barcode analysis is conducted. A key to the known Chinese adult males of the genus is presented.

Materials and methods

The examined specimens were caught using sweep net and light trap, stored in the dark at 4 °C, and preserved in 85% ethanol before molecular and morphological analyses. Genomic DNA was extracted from the thorax and leg using a Qiagen DNA Blood and Tissue Kit at Tianjin Normal University, Tianjin, China (TJNU), following the standard protocol except for the final elution volume of 100 µl. After DNA extraction, the exoskeleton of each specimen was mounted in Euparal on a microscope slide together with the corresponding antennae, legs, wing, and abdomen, following the procedures outlined by Sæther (1969). Morphological terminology follows Sæther (1980).

The color pattern of all species is described based on the specimen preserved in ethanol. Digital photographs of slide-mounted specimens were taken with a 300-dpi resolution using Nikon Eclipse 80i with Nikon Digital Sight DS-Fil camera at TJNU.

The universal primers LCO1490 and HCO2198 (Folmer et al. 1994) were adopted to amplify the standard 658-bp mitochondrial COI barcode region. Polymerase chain reaction (PCR) amplifications followed Song et al. (2018) and were conducted in a 25 μ l volume including 12.5 μ l 2 \times Es Taq MasterMix (CoWin Biotech Co., Beijing, China), 0.625 μ l of each primer, 2 μ l of template DNA, and 9.25 μ l of deionized H₂O. PCR products were electrophoresed in 1.0% agarose gel, purified, and sequenced in both directions at Beijing Genomics Institute Co. Ltd., Beijing, China.

Raw sequences were assembled and edited in Geneious Prime 2020 (Biomatters Ltd., Auckland, New Zealand). Alignment of the sequences was carried out using the MUSCLE (Edgar 2004) algorithm on amino acids in MEGA v. 7.0 (Kumar et al. 2016). Some published DNA barcodes of *Parachironomus* were downloaded from the Barcode of Life Data Systems (BOLD) (Ratnasingham and Hebert 2013). Before phylogenetic analysis, nucleotide substitution saturation analysis of gene sequences was performed by DAMBE version 6 (Xia 2017). The pairwise distances were calculated using the Kimura 2-Parameter (K2P) substitution model in MEGA. The neighbor-joining (NJ) tree was constructed using the K2P substitution model, 1000 bootstrap replicates, and the “pairwise deletion” option for missing data in MEGA. Novel sequences, trace-files, and metadata of the new species were uploaded to the BOLD platform.

In this study, the partial COI sequences of *Parachironomus* were submitted to on-line ABGD web interface (<https://bioinfo.mnhn.fr/abi/public/abgd/abgdweb.html>). We used the K2P nucleotide substitution model. The prior intraspecific divergence was set at between 0.001 and 0.1. The minimum relative gap width was 1.0 and other parameters were defaulted.

The holotype of two new species is deposited at the College of Fisheries and Life Science, Shanghai Ocean University (**SHOU**) and College of Life Sciences, Tianjin Normal University, Tianjin, China (**TJNU**).

Results

DNA barcode analysis

In this study, five COI sequences were obtained, and 19 COI sequences of *Parachironomus* were downloaded from BOLD, totaling 24 COI sequences. All sequences could be translated successfully into amino acids without indels and stop codons. MEGA analysis showed that the average total length of the sequence was 658 bp, and that there were 427 conserved sites, 231 variable sites, 196 parsimony informative sites, and 35 singleton sites. The mean nucleotide base compositions were 27.1% A, 17.9% C, 16.2% G, and 38.8% T for COI genes (Table 1). The ratio of A + T was 65.9%, which was

Table 1. The contents and nucleotide substitutions of COI gene sequences of *Parachironomus*.

	T (%)	C (%)	A (%)	G (%)	ii	si	sv	R
1 st	48.3	8.2	40.0	3.5	144	30	44	0.7
2 nd	25.3	18.5	27.6	28.6	205	11	1	13.3
3 rd	42.9	27.0	13.6	16.5	216	0	0	3
Avg	38.8	17.9	27.1	16.2	565	41	44	0.9
	TT	TC	TA	TG	CT	CC	CA	CG
1 st	76	11	18	1	10	5	2	0
2 nd	49	5	0	0	5	35	0	0
3 rd	93	0	0	0	0	58	0	0
Avg	218	16	18	2	14	98	2	0
	AT	AC	AA	AG	GT	GC	GA	GG
1 st	18	2	62	5	1	0	4	2
2 nd	0	0	59	1	0	0	1	61
3 rd	0	0	29	0	0	0	0	36
Avg	18	2	151	6	2	0	4	98

significantly higher than that of G + C (34.1%), showing obvious AT bias, which was consistent with the bias of base composition of mitochondrial genes in most insects.

The neighbor joining tree based on available COI DNA barcodes of the *Parachironomus* revealed two species new to science (Fig. 1). *Parachironomus wangi* Liu & Lin, sp. nov. is closer to *Parachironomus biannulatus* Staeger, 1839; and *Parachironomus nankaiensis* Liu & Lin, sp. nov. is closer to *Parachironomus cayapo* Spies, Fittkau & Reiss, 1994. The new species separate from the other sequenced species by more than 11% divergence in the COI barcode sequences (Table 2).

When the interspecific genetic distance is greater than the intraspecific genetic distance, barcode gaps will appear through the frequency histogram of genetic data. There is an obvious barcode gap in the genetic distance of all *Parachironomus* COI sequences, which fully confirms the feasibility of COI as a DNA barcode (Fig. 2).

Taxonomic descriptions

Parachironomus demissum Yan, Wang & Bu, 2012, comb. nov.

Figs 3–5

Paracladopelma demissum Yan, Wang & Bu, 2012: 291.

Material examined. Holotype. Male (TJNU: 11430), CHINA, Sichuan Province, Yajiang County, Sandaoqiao Town, 30.01532°N, 101.05134°E, 2460 m a.s.l., 9.VI.1996, light trap, leg: X. H. Wang. **Paratypes.** One male (TJNU: 11730), CHINA, Sichuan Province, Ya'an City, Baoxing County, Xinglong Elementary School, Xihe River, 30.25800°N, 102.50387°E, 1100 m a.s.l., 19.VI.1996, light trap, leg: X. H. Wang. One male (TJNU: 12886), CHINA, Sichuan Province, Kangding County, Wasigou River, 30.04191°N, 102.09454°E, 2000 m a.s.l., 15.VI.1996, light trap, leg: X. H. Wang. One male (TJNU: 13079), CHINA, Sichuan Province, Shimian County, Nanyuhe River, 29.11156°N, 102.23265°E, 1040 m a.s.l., 16.VI.1996, light trap, leg: X. H. Wang.

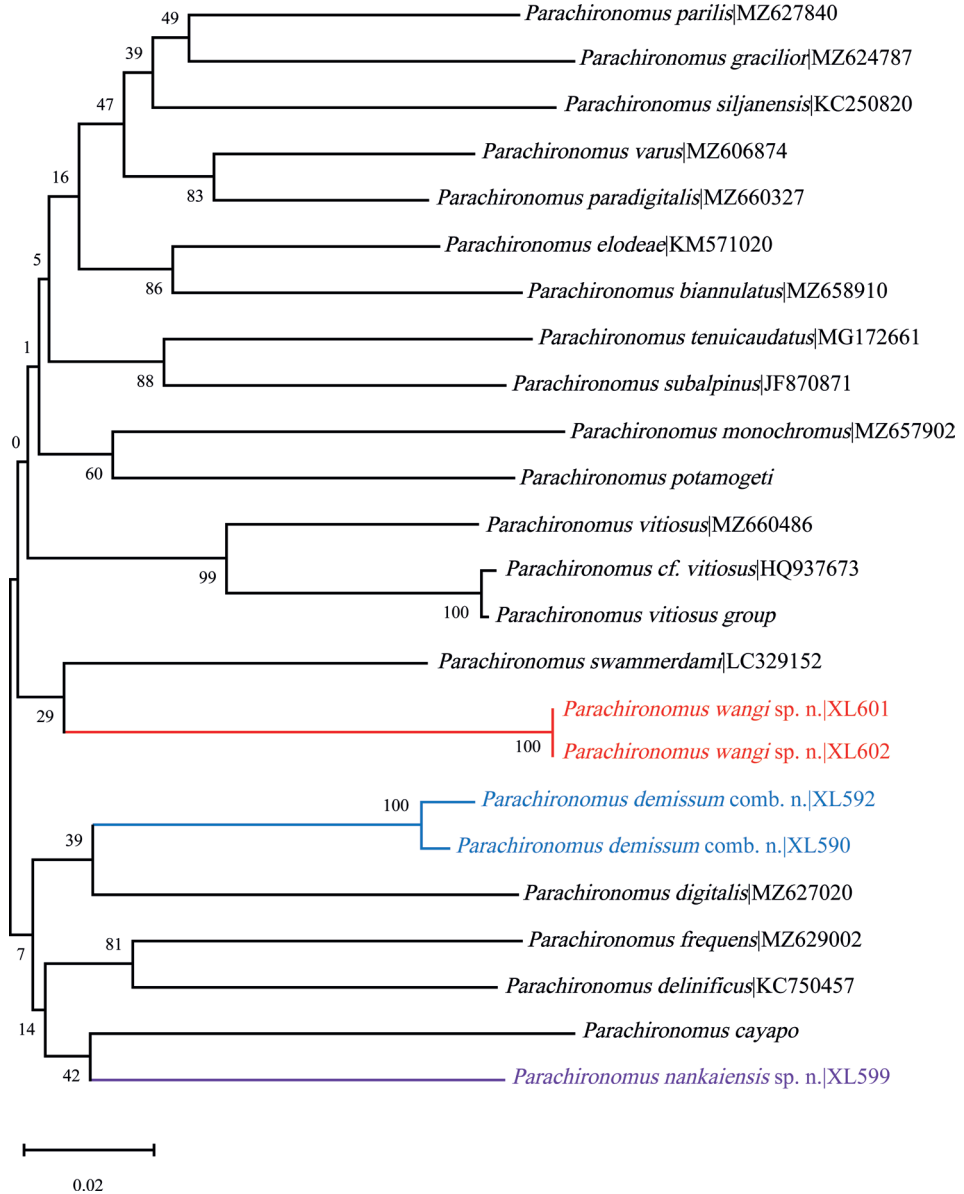


Figure 1. Neighbor-joining tree for 20 species of the genus *Parachironomus* based on K2P distance in DNA barcodes. Numbers on branches represent bootstrap support (> 70%) based on 1000 replicates; scale equals K2P genetic distance.

Additional materials. Two males (SHOU: XL590, XL592), CHINA, Xizang Autonomous Region, Rikaze City, Yadong County, Xiasima Town, 27.48986°N, 88.90572°E, 3032 m a.s.l., 20.VII.2014, light trap, leg: X. L. Lin.

Diagnostic characters. The species can be distinguished from known species of *Parachironomus* by the following combination of characters: AR 0.58–0.67, 0.62;

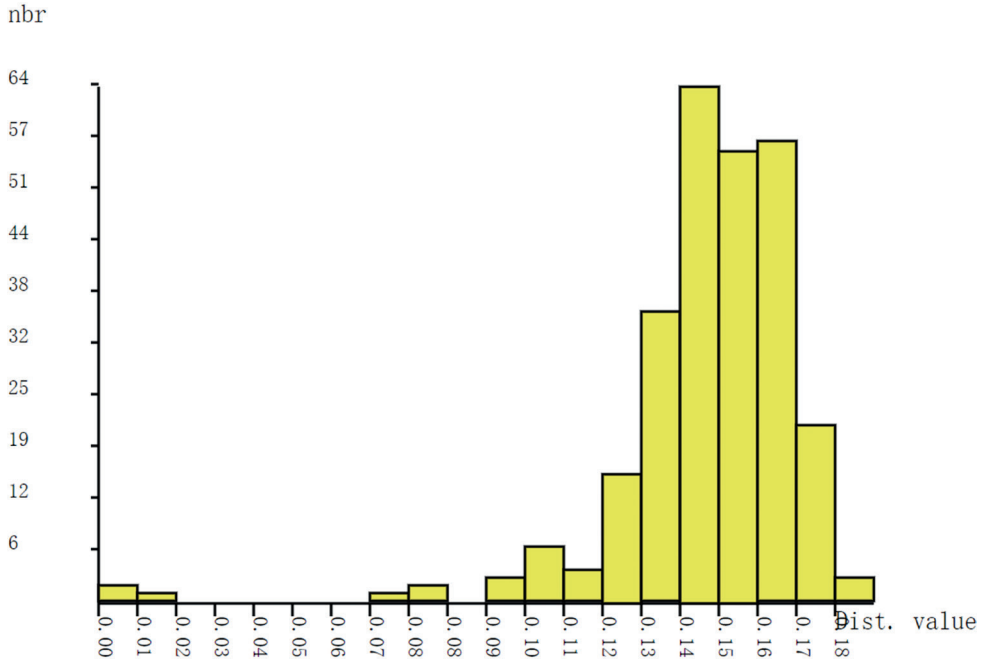


Figure 2. Histogram of pairwise K2P distances of 24 COI barcodes of *Parachironomus*.

tergite IX with shoulder-like posterior margin; anal point triangular base, constricted in the middle, with a ridge mesally; anal tergite bands V-shaped and fused; superior volsella with a bare triangular projection apically; gonostylus slender, parallel-sided, curved medially, gradually tapered to the top.

Description. Adult males ($n = 6$, unless otherwise stated). Total length 3.08–3.60, 3.35 mm. Wing length 1.60–1.89, 1.75 mm. Total length/wing length 1.81–2.10, 1.93. Wing length/length of profemur 2.16–2.63, 2.32.

Coloration. Thorax yellowish brown with pale brown spots. Femora and tibiae of front legs yellowish green with distal parts brown, anterior 1/2 of tarsi I yellowish green, remainder of front legs dark brown; femora, tibiae and basal 1/2 of tarsi I of mid and hind legs yellowish green, remaining dark brown. Abdomen yellowish green to dark brown, with tergites I–V yellowish green, tergites VII, VIII, and hypopygium dark brown.

Head (Fig. 3A). Antenna with 11 flagellomeres, ultimate flagellomere 250–290, 273 (3) μm long. AR 0.58–0.67, 0.62 (3). Frontal tubercles conical, 13–25, 18 (5) μm long, 8–20, 17 (5) μm wide at base. Temporal setae 17–20, 18; including 3–4, 3 inner verticals; 5–8, 8 outer verticals; and 6–9, 8 postorbitals. Clypeus with 12–16, 15 setae. Tentorium 105–132, 118 (5) μm long, 22–28, 24 (5) μm wide. Palpomere lengths (in μm): 30–42, 37 (5); 35–45, 39 (5); 95–119, 109 (5); 130–148, 139 (5); 155–220, 190 (5); Pm5/ Pm3 1.48–2.05, 1.76 (5).

Thorax (Fig. 3D). Anteprenotals with 2–3, 2 setae, acrostichals 5–7, 6, dorsocentrals 7–8, 8, prealars 3. Scutellum with 12–14, 13 setae.

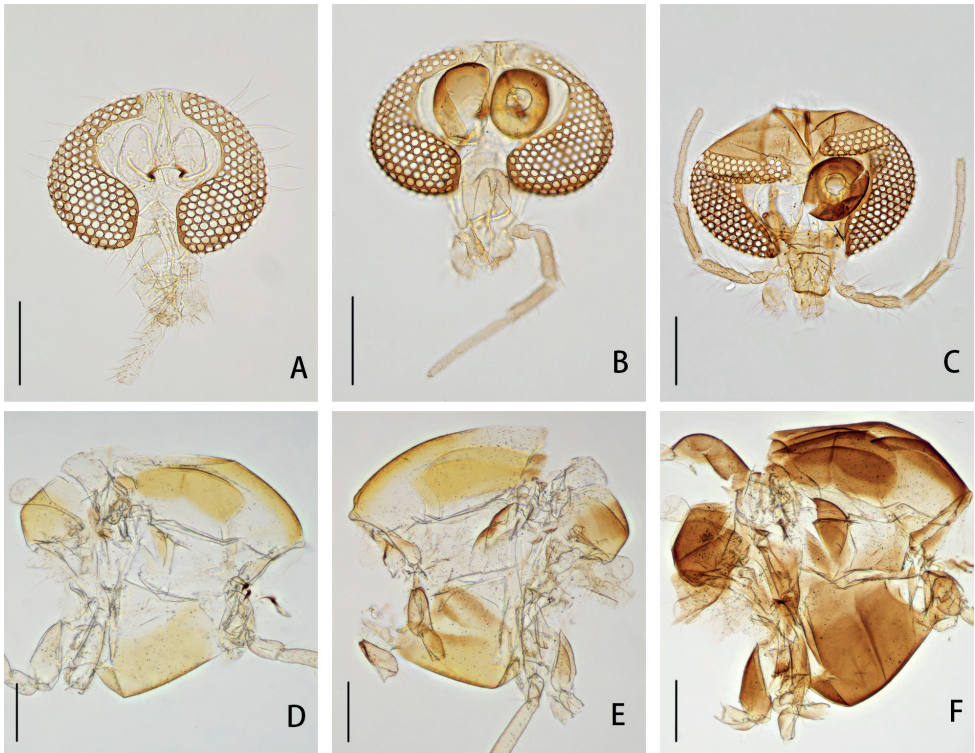


Figure 3. Head (A–C) and thorax (D–F) of *Parachironomus* species **A** *P. demissum* (Yan, Wang & Bu), comb. nov. **B** *P. wangi* Liu & Lin, sp. nov. **C** *P. nankaiensis* Liu & Lin, sp. nov. **D** *P. demissum* (Yan, Wang & Bu), comb. nov. **E** *P. wangi* Liu & Lin, sp. nov. **F** *P. nankaiensis* Liu & Lin, sp. nov. Scale bars: 200 μ m.

Wing (Fig. 5A). VR 1.18–1.34, 1.26. R with 13–18, 16 setae, R_1 with 12–18, 15 setae, R_{4+5} with 12–22, 16 setae. Brachiolum with 2–3, 2 setae. Squama with 3–5, 4 setae.

Legs. Front tibia with 3 subapical setae, 80–84, 82; 83–97, 91 and 85–112, 101 (5) μ m long. Combs of mid tibia 37–41, 39 μ m wide with 18–25, 22 μ m long spur, and 41–55, 48 μ m wide with 20–34, 27 μ m long spur; combs of hind tibia 37–41, 39 μ m wide with 23–27, 25 μ m long spur, 60–66, 63 μ m wide with 28–34, 32 μ m long spur. Tarsomere 1 of mid and hind legs without sensilla chaetica. Lengths (in μ m) and proportions of legs as in Table 3.

Hypopygium (Figs 4A, D, 5B, C). Tergite IX with shoulder-like posterior margin, bearing 16–24, 20 setae at base of anal point. Laterosternite IX with 2 or 3, 3 setae. Anal point 55–67, 63 μ m long, 12–25, 19 μ m wide at base, 10–14, 13 μ m wide apically, originating from caudal margin of anal tergite, triangular base, constricted in the middle, with a ridge mesally, moderately widen to distal and apically swollen (Fig. 4D). Anal tergite bands V-shaped and fused. Phallapodeme 52–70, 61 μ m long. Transverse sternapodeme 30–52, 42 μ m long. Superior volsella 55–65, 61 μ m long, curved medially, expanded in the apical part, apically with a bare triangular projection, bearing

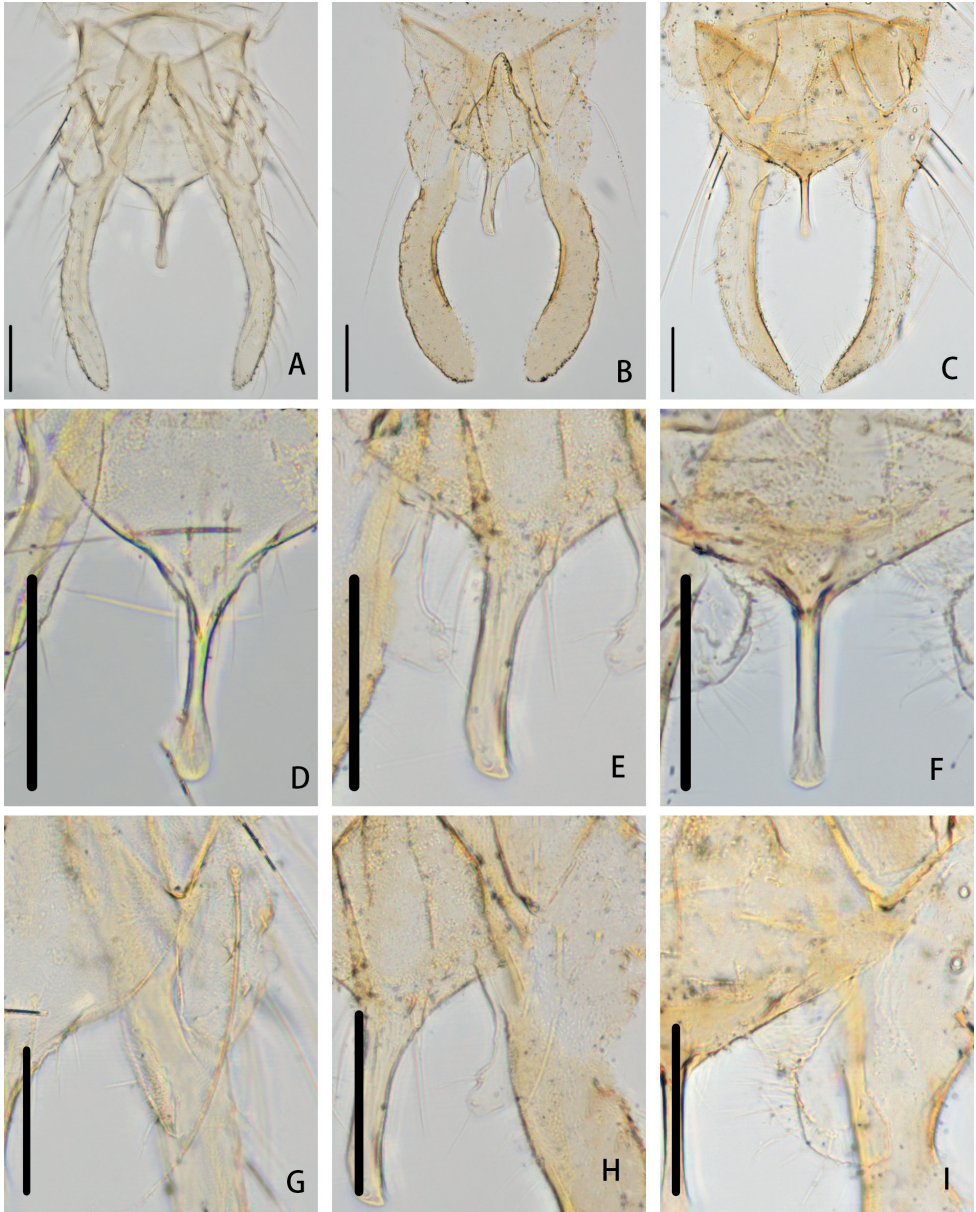


Figure 4. Hypopygium **A** *P. demissum* (Yan, Wang & Bu), comb. nov. **B** *P. wangi* Liu & Lin, sp. nov. **C** *P. nankaiensis* Liu & Lin, sp. nov. Anal point **D** *P. demissum* (Yan, Wang & Bu), comb. nov. **E** *P. wangi* Liu & Lin, sp. nov. **F** *P. nankaiensis* Liu & Lin, sp. nov. Superior volsella **G** *P. demissum* (Yan, Wang & Bu), comb. Nov. **H** *P. wangi* Liu & Lin, sp. nov. **I** *P. nankaiensis* Liu & Lin, sp. nov. Scale bars: 50 μ m.

two subapical setae, covered with microtrichia on inner margin. Inferior volsella with moderately blunt caudal projection, not reaching beyond anal tergite margin, and covered by microtrichia (Fig. 4G). Gonocoxite 90–131, 107 μ m long, with three setae

Table 3. Lengths (in μm) and proportions of legs of *Parachironomus demissum* (Yan, Wang & Bu), comb. nov., adult male ($n = 6$).

	fe	ti	ta ₁	ta ₂	ta ₃
P ₁	632–815, 755	498–640, 586	901–1049, 996	341–434, 407	276–352, 329
P ₂	575–810, 731	524–660, 600	317–370, 349	134–180, 169	99–133, 122
P ₃	730–910, 841	698–890, 802	496–549, 521	245–290, 275	187–246, 221
	ta ₄	ta ₅	LR	BV	SV
P ₁	273–326, 305	152–170, 162	1.63–1.81, 1.69	1.94–1.95, 1.94	1.25–1.37, 1.34
P ₂	64–90, 84	66–70, 69	0.55–0.64, 0.58	3.75–3.90, 3.79	3.47–3.93, 3.81
P ₃	112–140, 126	80–96, 87	0.61–0.71, 0.65	3.01–3.07, 3.05	2.88–3.22, 3.15

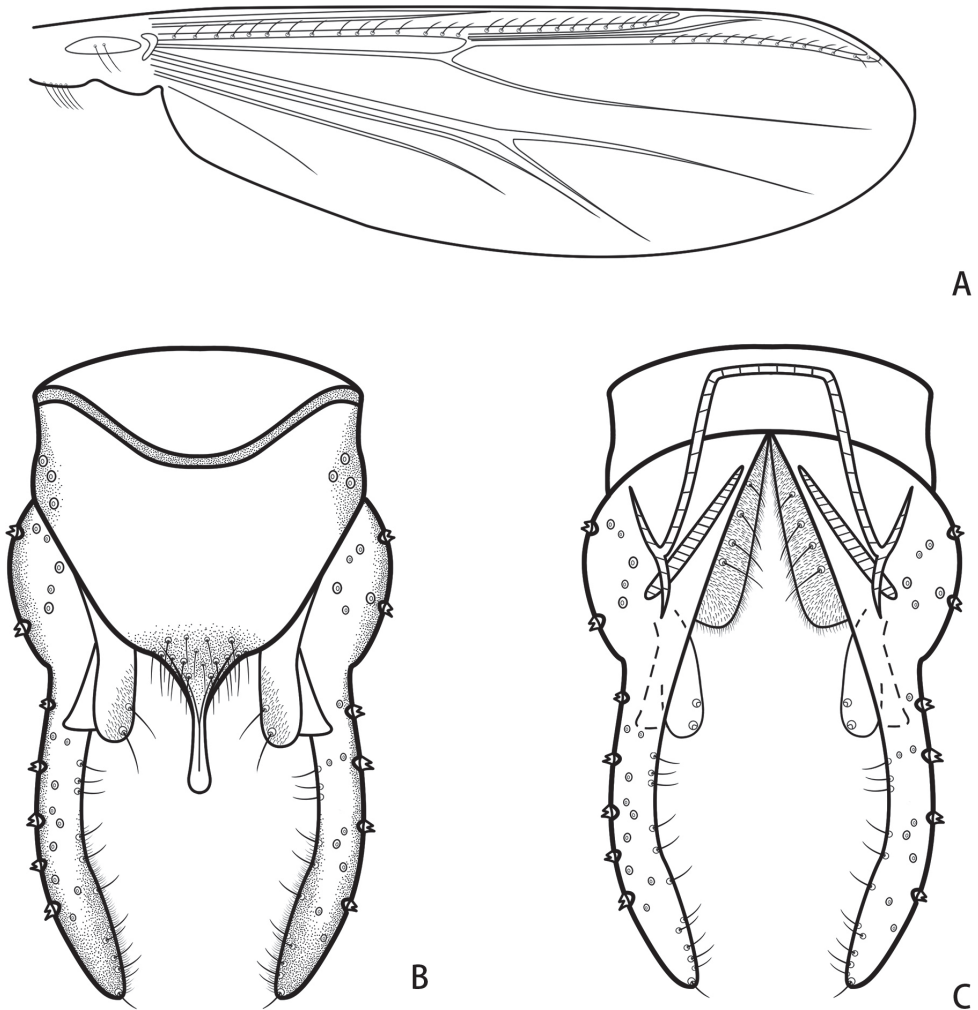


Figure 5. *Parachironomus demissum* (Yan, Wang & Bu), comb. nov. holotype male **A** wing **B** hypopygium, dorsal view **C** hypopygium, ventral view.

on inner margin. Gonostylus 140–174, 168 μm long, slender, parallel-sided, curved medially, gradually tapered to the top, bearing 12–24, 20 setae along inner margin and one stronger seta at apex. HR 0.55–0.94, 0.68. HV 1.86–2.50, 2.09.

Distribution. China (Sichuan and Xizang).

***Parachironomus wangi* Liu & Lin, sp. nov.**

<https://zoobank.org/DE07AF99-393F-407D-826E-FCA5C9B45FE1>

Figs 3, 4, 6

Material examined. Holotype. Male (SHOU: XL601), CHINA, Xizang Autonomous Region, Shannan City, Gongga County, Gangdui Town, 29.27888°N, 90.82323°E, 3586 m a.s.l., 18.VII.2014, sweep net, leg: X.L. Lin. **Paratypes.** One male (TJNU: XL602), collecting data as holotype.

Diagnostic characters. The species can be distinguished from known species of *Parachironomus* by the following combination of characters: frontal tubercles absent; tergite IX with triangular posterior margin; anal point slightly wider at base, parallel-sided, swollen apically; superior volsella wide, parallel-sided, bent inward at 1/3 distance from apex, apically rounded, free microtrichia; inferior volsella not reaching beyond anal tergite margin; gonostylus gradually widened distally, curved and parallel-sided, apically rounded.

Description. Adult males ($n = 2$, unless otherwise stated). Total length 3.63–3.91, 3.77 mm. Wing length 1.85–1.91, 1.88 mm. Total length/wing length 1.96–2.05, 2.01. Wing length/length of profemur 2.74–2.79, 2.77.

Coloration. Thorax yellowish brown with pale brown spots. Front legs dark brown; femora and basal 1/3 of tarsi I of mid and hind legs yellowish brown, remaining dark brown. Abdomen pale yellow to yellowish brown, with tergites I–VI pale yellow, tergites VII, VIII, and hypopygium yellowish brown.

Head (Fig. 3B). Antenna with 11 flagellomeres, ultimate flagellomere 502–536, 519 μm long. AR 1.54–1.55, 1.55. Frontal tubercles absent. Temporal setae 13–14, 14; including 2–4, 3 inner verticals; 4–6, 5 outer verticals; and 5 or 6, 6 postorbitals. Clypeus with 7–9, 8 setae. Tentorium 95–128, 112 μm long, 31–34, 33 μm wide. Palpomere lengths (in μm): 26–28, 27; 37–39, 38; 92–98, 95; 106–109, 108; 176–193, 185; Pm5/ Pm3 1.91–1.97, 1.94.

Thorax (Fig. 3E). Anteprenotals with 1 or 2, 2 setae, acrostichals 4, dorsocentrals 8, prealars 3. Scutellum with 12 setae.

Wing (Fig. 6A). VR 1.10–1.16, 1.13. R with 5 or 6, 6 setae, R_1 with 1 or 2, 2 setae, R_{4+5} with 2 setae. Brachiolum with two setae. Squama with 7–9, 8 setae.

Legs. Front tibia with three subapical setae, 82–91, 87; 84 (1) and 105 (1) μm long. Combs of mid tibia 26–33, 30 μm wide with 15–25, 20 μm long spur, and 21 μm wide with 28 μm long spur; combs of hind tibia 22–26, 24 μm wide with 22–34, 28 μm long spur, 38–42, 40 μm wide with 34–38, 36 μm long spur. Tarsomere 1 of mid and hind legs without sensilla chaetica. Lengths (in μm) and proportions of legs as in Table 4.

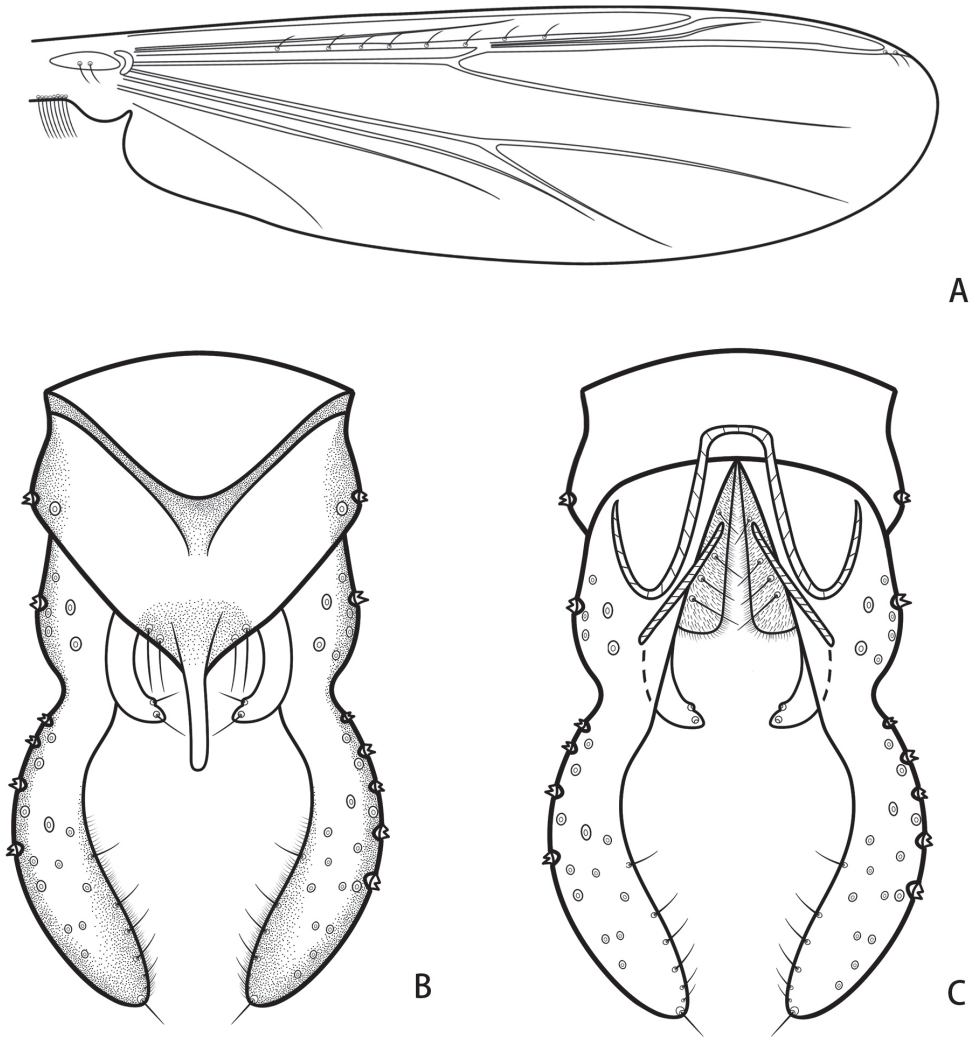


Figure 6. *Parachironomus wangi* Liu & Lin, sp. nov. holotype male **A** wing **B** hypopygium, dorsal view **C** hypopygium, ventral view.

Table 4. Lengths (in μm) and proportions of legs of *Parachironomus wangi* Liu & Lin, sp. nov., adult male ($n = 2$).

	fe	ti	ta ₁	ta ₂	ta ₃
P ₁	664–695, 680	469–503, 486	858–940, 899	455–489, 472	337–355, 346
P ₂	692–700, 696	604–638, 621	348–362, 355	171–189, 180	126–135, 131
P ₃	726–751, 739	783–801, 792	560–594, 577	291–302, 297	220–231, 226
	ta ₁	ta ₂	LR	BV	SV
P ₁	282–290, 286	147–152, 150	1.83–1.87, 1.85	1.62–1.67, 1.65	1.27–1.32, 1.30
P ₂	83–84, 84	75–78, 77	0.57–0.58, 0.57	3.50–3.61, 3.56	3.70–3.72, 3.71
P ₃	127–130, 129	90–93, 92	0.72–0.74, 0.73	2.82–2.86, 2.84	2.61–2.69, 2.65

Hypopygium (Figs 4B, E, H, 6B, C). Tergite IX with triangular posterior margin, bearing 4–8, 6 setae at base of anal point. Laterosternite IX with two setae. Anal point originating from caudal margin of anal tergite, slightly wider at base, parallel-sided, swollen apically, 56–60, 58 μm long, 17–21, 19 μm wide at base, 10 μm wide at apex (Fig. 4E). Anal tergite bands V-shaped, fused in the middle. Phallapodeme 79–81, 80 μm long. Transverse sternapodeme 39–45, 42 μm long. Superior volsella wide, parallel-sided, bent inward at 1/3 distance from apex, apically rounded, 50–61, 56 μm long, 12–14, 13 μm wide at apex, bearing an apical seta and a proximal lateral seta, both arising from distinct setal pits, free microtrichia. Inferior volsella with distinct blunt caudal projection, not reaching beyond anal tergite margin, and covered by microtrichia (Fig. 4H). Gonocoxite 119–135, 127 μm long, with 4 strong medial setae. Gonostylus 171–174, 173 μm long, narrower at base, gradually widened distally, curved and parallel-sided, apically rounded, bearing 6–8, 7 setae along inner margin and one stronger seta at apex. HR 0.70–0.78, 0.74. HV 2.12–2.25, 2.18.

Etymology. Name after Prof. Xin-Hua Wang, for his outstanding contribution towards increasing our knowledge of aquatic insect taxonomy; noun in nominative case.

Distribution. China (Xizang).

***Parachironomus nankaiensis* Liu & Lin, sp. nov.**

<https://zoobank.org/9524FD76-DA2D-4E37-90CD-EB6F4765A95D>

Figs 3, 4, 7

Material examined. Holotype. Male (SHOU: XL599), China, Xizang Autonomous Region, Shannan City, Gongga County, Gangdui Town, 29.27888°N, 90.82323°E, 3586 m a.s.l., 18.VII.2014, sweep net, leg: X.L. Lin.

Diagnostic characters. The species can be distinguished from known species of *Parachironomus* by the following combination of characters: frontal tubercles small; squama with seven setae; anal tergite bands V-shaped, separated; superior volsella narrower at base, curved and expanded in the distal part, with a bare lamellar projection as wide as apex of volsella; inferior volsella reaching slightly beyond anal tergite margin; gonostylus slender, slightly curved in the middle, tapered to the apex.

Description. Adult male ($n = 1$). Total length 3.90 mm. Wing length 2.51 mm. Total length/wing length 1.56. Wing length/length of profemur 2.64.

Coloration. Thorax dark brown with dark spots. Legs brown. Abdomen yellowish green to brown, tergites I–V yellowish green, tergites VI–VIII yellowish brown, hypopygium brown.

Head (Fig. 3C). Antenna with 11 flagellomeres, ultimate flagellomere 699 μm long. AR 1.60. Frontal tubercles small, 9 μm long, 8 μm wide. Temporal setae 14, including 4 inner verticals; 4 outer verticals; and 6 postorbitals. Clypeus with 11 setae. Tentorium 154 μm long, 39 μm wide. Palpomere lengths (in μm): 30; 42; 115; 146; 235; Pm5/ Pm3 2.04.

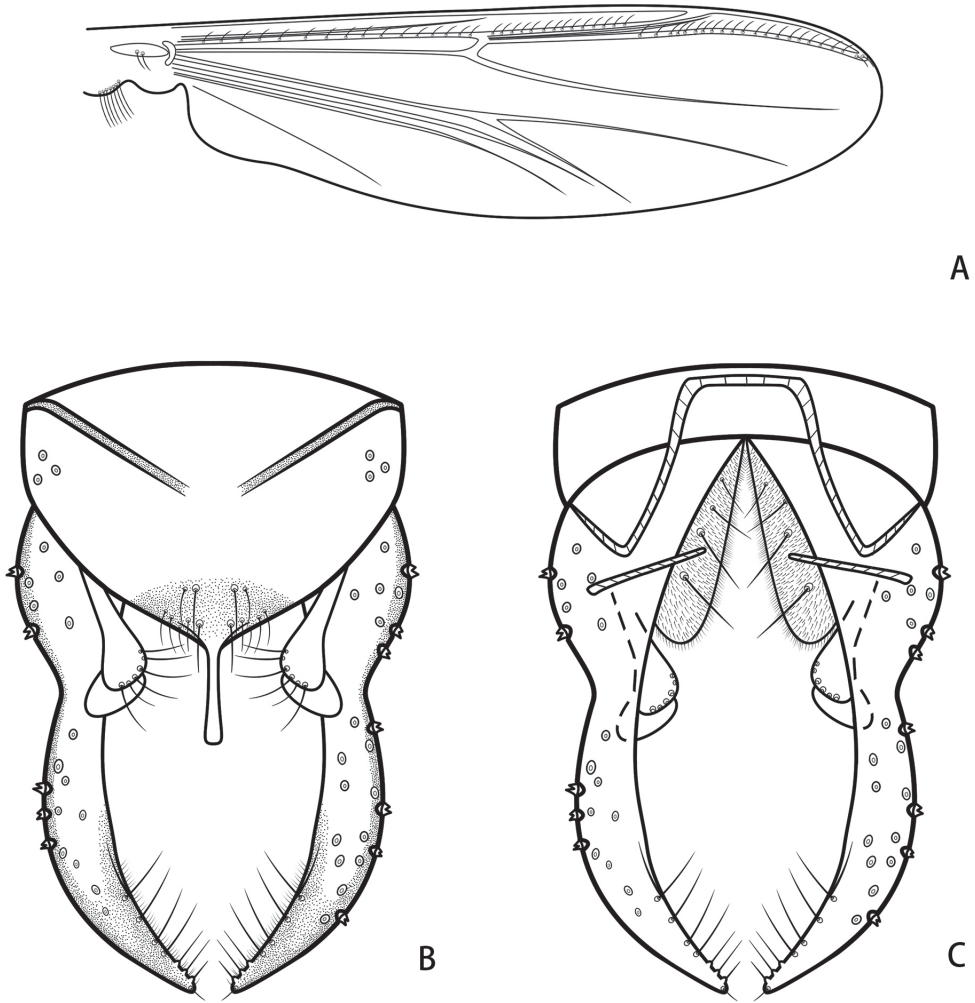


Figure 7. *Parachironomus nankaiensis* Liu & Lin, sp. nov. holotype male **A** wing **B** hypopygium, dorsal view **C** hypopygium, ventral view.

Thorax (Fig. 3F). Antepronotals with 3 setae, acrostichals 6, dorsocentrals 10, prealars 3. Scutellum with 10 setae.

Wing (Fig. 7A). VR 1.11. R with 16 setae, R_1 with 14 setae, R_{4+5} with 22 setae. Brachiolum with two setae. Squama with seven setae.

Legs. Front tibia with three subapical setae, 80, 87 and 93 μm long. Combs of mid tibia 33 μm wide with 19 μm long spur, and 29 μm wide with 27 μm long spur; combs of hind tibia 30 μm wide with 20 μm long spur, 65 μm wide with 36 μm long spur. Tarsomere 1 of mid and hind legs without sensilla chaetica. Lengths (in μm) and proportions of legs as in Table 5.

Table 5. Lengths (in μm) and proportions of legs of *Parachironomus nankaiensis* Liu & Lin, sp. nov., adult male ($n = 1$).

	fe	ti	ta ₁	ta ₂	ta ₃
P ₁	950	744	1135	576	431
P ₂	889	825	448	258	187
P ₃	1056	1072	675	385	292
	ta ₄	ta ₅	LR	BV	SV
P ₁	315	140	1.53	1.94	1.49
P ₂	120	91	0.54	3.30	3.83
P ₃	162	89	0.63	3.02	3.15

**Figure 8.** Habitat for *Parachironomus wangi*, Liu & Lin, sp. nov.

Hypopygium (Figs 4C, F, I, 7B, C). Tergite IX with 14 setae at base of anal point and shoulder-like posterior margin of anal tergite. Laterosternite IX with three setae. Anal point originating from caudal margin of anal tergite, almost parallel-sided, moderately expanded at apex, 50 μm long, 9 μm wide at base, 10 μm wide apically. Anal tergite bands V-shaped, separated (Fig. 4F). Phallapodeme 80 μm long. Transverse sternapodeme 59 μm long. Superior volsella narrower at base, curved and expanded in the distal part, with a bare lamellar projection as wide as apex of volsella, 80 μm long, 22 μm wide at apex; and bearing six long setae at apex, free microtrichia. Inferior volsella with fairly blunt caudal projection, reaching slightly beyond anal tergite margin,

and covered with microtrichia (Fig. 4I). Gonocoxite 143 μm long, with four stout setae placed along inner margin. Gonostylus 169 μm long, slender, slightly curved in the middle, tapered to the apex, bearing seven setae along inner margin and one single seta at apex. HR 0.85. HV 2.31.

Etymology. Name after Nankai University, the institution of study and work for Prof. Xin-Hua Wang; noun in nominative case.

Distribution. China (Xizang).

Key to known adult males of *Parachironomus* from China

- 1 Tergite IX with shoulder-like caudal margin 2
- Tergite IX with triangle caudal margin 4
- 2 Superior volsella without projection; gonostylus with constriction in middle...
..... *P. frequens* (Johannsen)
- Superior volsella with a projection; gonostylus gradually tapered to the top 3
- 3 AR 0.58–0.67; anal tergite bands fused; inferior volsella not reaching beyond
anal tergite margin *P. demissum* (Yan, Wang & Bu), **comb. nov.**
- AR 1.60; anal tergite bands separated; inferior volsella reaching slightly be-
yond anal tergite margin *P. nankaiensis* Liu & Lin, **sp. nov.**
- 4 Superior volsella short, bearing two apical setae and with folds on inner mar-
gin; gonostylus widened basally *P. gracilior* (Kieffer)
- Superior volsella elongate, bearing an apical seta and a subapical seta and
without folds; gonostylus widened distally 5
- 5 Mid and hind tibiae each with 1 spur; superior volsella straightly, widened at
base *P. poyangensis* Yan
- Mid and hind tibiae each with 2 spurs; superior volsella curved, widened in
the distal part 6
- 6 Superior volsella slightly curved; gonostylus slender, with distinct expansion
in distal 1/3 *P. monochromus* (van der Wulp)
- Superior volsella bent inward at 1/3 distance from apex; gonostylus parallel-
sided, gradually widened distally *P. wangi* Liu & Lin, **sp. nov.**

Discussion

In this study, the holotype of *Paracladopelma demissum* were examined, and the original description has been modified. The distinguishing feature of *Parachironomus* are that the superior volsella usually has a distinct preapical tooth as well as setae arising from distinct pits (Yan et al. 2012; pers. comm. Martin Spies July. 2022). We re-checked the holotype, and the characters of tergite IX with shoulder-like posterior margin, superior volsella slender and with 2 distal setae arising from distinct pits, inferior volsella with blunt or pointed caudal projection conform to the characters of *Parachironomus*; therefore, *Paracladopelma demissum* should be placed in *Parachironomus*. *Parachironomus demissum* **comb. nov.** resembles *Parachironomus digitalis* Edwards, 1929 in having

similarly shaped tergite IX, anal point and superior volsella, but the antenna ratio and some other measurements are different.

Parachironomus wangi Liu & Lin, sp. nov. resembles *Parachironomus biannulatus* Staeger, 1839 in having similar shapes of the superior volsella and posterior margin of tergite IX, but can be separated by the following combination characters: AR 1.54–1.55, anal point parallel-sided and gonostylus expanded apically in *P. wangi* Liu & Lin, sp. nov, whereas AR 3.0–3.6, the anal point is constricted in the middle, and the gonostylus is tapered to the apex in *P. biannulatus*.

Parachironomus nankaiensis Liu & Lin, sp. nov. resembles *Parachironomus cayapo* Spies, Fittkau & Reiss, 1994 in having similar shapes of anal point, inferior volsella, and anal tergite bands, but can be separated from the latter by the following combination characters: squama seven setae, the superior volsella expanded in the distal part and with a bare lamellar projection, plus with the gonostylus tapered to the apex. In contrast, the squama of *P. cayapo* is bare, the superior volsella is not widened in the distal part and has no projection, and the gonostylus has a protruding hump.

The results of molecular identification and morphological taxonomy are consistent, indicating that DNA barcodes and traditional morphological taxonomy are complementary in this case; therefore, the DNA barcode can be used as a simple method to supplement traditional morphological taxonomy for *Parachironomus*.

Biogeographically, the three species examined in this study are all distributed in the Tibetan Plateau at an altitude of more than 3,000 meters (Fig. 8). With the gradual increase of altitude, the climate gradually deteriorates, and *Parachironomus* living in high altitude areas have strong cold tolerance. The high biodiversity in Tibetan Plateau is demonstrated, as well as the distribution range of this genus extended.

In conclusion, this study not only enriches the database of Chironomidae in China, but also provides baseline data for the protection of the environment and biodiversity in the Tibetan Plateau.

Acknowledgements

We thank Dr. M. Spies (Zoologische Staatssammlung München, Germany) for providing input on various levels of this work. Financial support from National Natural Science Foundation of China is gratefully acknowledged (grant numbers: 32170473, 31801994, 31900344).

References

- Anderson AM, Stur E, Ekrem T (2013) Molecular and morphological methods reveal cryptic diversity and three new species of Nearctic *Micropsectra* (Diptera: Chironomidae). *Freshwater Science* 32(3): 892–921. <https://doi.org/10.1899/12-026.1>
- Ashe P, Cranston PS (1990) Family Chironomidae. In: Soós A, Papp L (Eds) *Catalogue of Palaearctic Diptera* (Vol. 2). Psychodidae-Chironomidae. Akadémiai Kiadó, Budapest, 113–355.

- Cranston PS, Dillon ME, Pinder LCV, Reiss F (1989) The adult males of Chironominae (Diptera: Chironomidae) of the Holarctic region – Keys and diagnoses. In: Wiederholm T (Ed.) Chironomidae of the Holarctic region. Keys and diagnoses. Part 3 – Adult males. Entomologica Scandinavica Supplement 34: 353–502.
- Edgar RC (2004) MUSCLE: Multiple sequence alignment with high accuracy and high throughput. *Nucleic Acids Research* 32(5): 1792–1797. <https://doi.org/10.1093/nar/gkh340>
- Edwards FW (1929) British non-biting midges (Diptera: Chironomidae). *Transactions of the Royal Entomological Society of London* 7: 279–439. <https://doi.org/10.1111/j.1365-2311.1929.tb00692.x>
- Folmer O, Black M, Hoeh W, Lutz R, Vrijenhoek R (1994) DNA primers for amplification of mitochondrial cytochrome c oxidase subunit I from diverse metazoan invertebrates. *Molecular Marine Biology and Biotechnology* 3: 294–299.
- Gilka W, Paasivirta L, Gadawski P, Grabowski M (2018) Morphology and molecules say: *Tanytarsus latens*, sp. nov. from Finland (Diptera: Chironomidae). *Zootaxa* 4471(3): 569–579. <https://doi.org/10.11646/zootaxa.4471.3.8>
- Hebert PDN, Cywinska A, Ball SL, deWaard JR (2003a) Biological identifications through DNA barcodes. *Proceedings of the Royal Society of London, Series B, Biological Sciences* 270(1512): 313–321. <https://doi.org/10.1098/rspb.2002.2218>
- Hebert PDN, Ratnasingham S, de Waard JR (2003b) Barcoding animal life: Cytochrome c oxidase subunit I divergences among closely related species. *Proceedings of the Royal Society of London, Series B, Biological Sciences* 270: S96–S99. <https://doi.org/10.1098/rsbl.2003.0025>
- Kikuchi M, Sasa M (1990) Studies on the chironomid midges (Diptera, Chironomidae) of the Lake Toba area, Sumatra, Indonesia. *Japanese Journal of Sanitary Zoology* 41(4): 291–329. <https://doi.org/10.7601/mez.41.291>
- Kumar S, Stecher G, Tamura K (2016) MEGA7: Molecular evolutionary genetics analysis version 7.0 for bigger datasets. *Molecular Biology and Evolution* 33(7): 1870–1874. <https://doi.org/10.1093/molbev/msw054>
- Lehmann J (1970) Revision der Europäischen Arten (Imagines ♂♂) der Gattung Parachironomus Lenz (Diptera, Chironomidae). *Hydrobiologia* 33(1): 129–158. <https://doi.org/10.1007/BF00751287>
- Lenz F (1921) Chironomidenpuppen und –larven. Bestimmungstabellen. *Deutsche Entomologische Zeitschrift* 1921: 148–162. <https://doi.org/10.1002/mmnd.48019210303>
- Lin XL, Stur E, Ekrem T (2015) Exploring genetic divergence in a species-rich insect genus using 2790 DNA Barcodes. *PLoS ONE* 10(9): e0138993. <https://doi.org/10.1371/journal.pone.0138993>
- Lin XL, Yu HJ, Wang XH, Bu WJ, Yan CC, Liu WB (2021) New or little-known *Boreoheptagyia* (Diptera, Chironomidae) in China inferred from morphology and DNA barcodes. *ZooKeys* 1040: 187–200. <https://doi.org/10.3897/zookeys.1040.66527>
- Liu WB, Yao Y, Yan CC, Wang XH, Lin XL (2021) A new species of *Polypedilum* (*Cerobregma*) (Diptera, Chironomidae) from Oriental China. *ZooKeys* 1011: 139–148. <https://doi.org/10.3897/zookeys.1011.59554>

- Makarchenko EA, Makarchenko MA, Zorina OV, Sergeeva IV (2005) Preliminary Data on Fauna and Taxonomy of Chironomids (Diptera, Chironomidae) of the Russian Far East. Vladimir Ya. Levanidov's Biennial Memorial Meetings, 394–420.
- Oliver DR, Dillon ME, Cranston PS (1990) A Catalog of Nearctic Chironomidae. Research Branch Agriculture Canada Publication, Ottawa, 89 pp.
- Orel O (2017) Two new species and new records of the genus *Parachironomus* Lenz, 1921 (Diptera, Chironomidae) from northern Russia. *Zootaxa* 4312(3): 531–546. <https://doi.org/10.11646/zootaxa.4312.3.7>
- Ratnasingham S, Hebert PDN (2013) A DNA-based registry for all animal species: The barcode index number (BIN) system. *PLoS ONE* 8(7): e66213. <https://doi.org/10.1371/journal.pone.0066213>
- Sæther OA (1969) Some Nearctic Podonominae, Diamesinae and Orthocladiinae (Diptera: Chironomidae). *Bulletin – Fisheries Research Board of Canada* 170: 1–154.
- Sæther OA (1980) Glossary of Chironomid morphology terminology (Diptera: Chironomidae). *Entomologica Scandinavica (Supplement 14)*: 1–51.
- Sæther OA, Spies M (2013) Fauna Europaea: Chironomidae. In: Beuk P, Pape T (Eds) *Fauna Europaea: Diptera Nematocera*. Fauna Europaea version 2.6. <http://www.faunaeur.org/> [Accessed 2 October 2022]
- Sæther OA, Ashe P, Murray DA (2000) Family Chironomidae. In: Papp L, Darvas B (Eds) *Contributions to a Manual of Palaearctic Diptera (with Special Reference to the Flies of Economic Importance)*. Appendix. Science Herald, Budapest, 113–334.
- Sasa M, Tanaka N (2001) Studies on the chironomids midges collected with light Annual Report of Gunma Prefectural Institute of Public Health and Environmental Sciences 33: 41–73.
- Sasa M, Kitami K, Suzuki H (2001) Additional Studies on the Chironomid Midges Collected on the Shore of Lake Inawashiro. Institute of Tropical Medicine, Nagasaki University, Nagasaki, 38 pp.
- Song C, Lin XL, Wang Q, Wang XH (2018) DNA barcodes successfully delimit morphospecies in a superdiverse insect genus. *Zoologica Scripta* 47(3): 311–324. <https://doi.org/10.1111/zsc.12284>
- Spies M (2008) *Parachironomus valdiviensis*, spec. n., and other changes to nomenclature of Neotropical Chironomidae (Insecta, Diptera). *Spixiana* 31: 173–175.
- Spies M, Fittkau EJ, Reiss F (1994) The adult males of *Parachironomus* Lenz, 1921, from the Neotropical faunal region (Insecta, Diptera, Chironomidae). *Spixiana (Supplement 20)*: 61–98.
- Staeger C (1839) Systematisk fortegnelser over de i Danmark hidtil fundne Diptera. (Systematic listing of Diptera hitherto found in Denmark.). *Naturhistorisk Tidsskrift*. Copenhagen. 2: 549–600.
- Townes HK, Townes Jr HK (1945) The Nearctic species of Tendipedini (Diptera, Tendipedidae = Chironomidae). *American Midland Naturalist* 34(1): 1–206. <https://doi.org/10.2307/2421112>
- Trivinho-Strixino S, Silva F, Roque F (2010) A new species of *Parachironomus* Lenz, 1921 (Diptera: Chironomidae: Chironominae), and description of immature stages of two other species from the Neotropical Region. *Zootaxa* 2689: 1–14.

- Wang XH (2000) A revised checklist of Chironomids from China (Diptera). Late 20th Century Research on Chironomidae: Anthology from the 13th International Symposium on Chironomidae. Odwin Hoffrichter Shaker Verlag, Aachen, 629–652.
- Xia X (2017) DAMBE6: New Tools for Microbial Genomics, Phylogenetics, and Molecular Evolution. The Journal of Heredity 108(4): 431–437. <https://doi.org/10.1093/jhered/esx033>
- Yan CC, Wang XH, Bu WJ (2012) A new species in the genus *Paracladopelma* Harnisch (Diptera: Chironomidae) from China. Entomotaxonomia 34(2): 291–295.
- Yan CC, Yan J, Jiang L, Guo Q, Liu T, Ge XY, Wang XH, Pan BP (2015) *Parachironomus* Lenz from China and Japan (Diptera, Chironomidae). ZooKeys 494: 31–50. <https://doi.org/10.3897/zookeys.494.6837>

Unrecognized for centuries: distribution and sexual caste descriptions of the West European *Aphaenogaster* species of the *subterranea* group (Hymenoptera, Formicidae)

Enrico Schifani^{1,2}, Antonio Alicata³, Lech Borowiec⁴, Fede García⁵, Vincenzo Gentile⁶, Kiko Gómez⁷, Elia Nalini⁸, Fabrizio Rigato⁹, Sämi Schär¹⁰, Antonio Scupola¹¹, Roger Vila², Mattia Menchetti²

1 Department of Chemistry, Life Sciences, and Environmental Sustainability, University of Parma, Parma, Italy **2** Institut de Biologia Evolutiva (CSIC-Univ. Pompeu Fabra), Barcelona, Spain **3** Department of Biological, Geological and Environmental Sciences, University of Catania, Catania, Italy **4** Department of Biodiversity and Evolutionary Taxonomy, Myrmecological Laboratory, University of Wrocław, Wrocław, Poland **5** Blesa 45, Barcelona, Spain **6** C.so Umberto I, 301, Torre Annunziata, Naples, Italy **7** Falconera 2, Garraf, Barcelona, Spain **8** Department of Biosciences, University of Milan “La Statale”, Milan, Italy **9** Museo Civico di Storia Naturale, Milano, Italy **10** Dietikon, Zürich, Switzerland **11** Natural History Museum, Verona, Italy

Corresponding authors: Enrico Schifani (enrico.schifani@unipr.it; enrsc8@gmail.com);
Mattia Menchetti (mattiamen@gmail.com; mattia.menchetti@ibe.upf-csic.es)

Academic editor: B. Boudinot | Received 6 December 2022 | Accepted 20 February 2023 | Published 16 March 2023

<https://zoobank.org/8AB17CC0-E18B-4936-90E7-408C4CA638CA>

Citation: Schifani E, Alicata A, Borowiec L, García F, Gentile V, Gómez K, Nalini E, Rigato F, Schär S, Scupola A, Vila R, Menchetti M (2023) Unrecognized for centuries: distribution and sexual caste descriptions of the West European *Aphaenogaster* species of the *subterranea* group (Hymenoptera, Formicidae). ZooKeys 1153: 141–156. <https://doi.org/10.3897/zookeys.1153.98297>

Abstract

There are only two *Aphaenogaster* species from the *subterranea* group in the western Mediterranean: *A. ichnusa* Santschi, 1925, from south-western Europe, and *A. subterranea* (Latreille, 1798), also occurring in central and eastern Europe. Historically, the two species have been widely misunderstood: *A. ichnusa* was long considered a Sardinian endemic subspecies of *A. subterranea*, while its continental populations were misidentified as *A. subterranea* s. str. Recently, *A. ichnusa* was elevated to species rank and its worker caste was redescribed with that of *A. subterranea*, allowing for their correct identification. Yet their distribution was documented in detail only for France and Sardinia. Furthermore, no morphological characters were described to distinguish the males and queens of the two species. By investigating private

and museum collections, 276 new records of *A. ichnusa* are provided here and 154 of *A. subterranea* from the western Mediterranean. Additionally, qualitative and quantitative morphological characters were combined to identify their males and queens. We present the new southernmost, easternmost, and westernmost distribution limits for *A. ichnusa*. Based on our results, this species is widely distributed in Italy and Catalonia (Spain), also occurring on several Mediterranean islands, avoiding areas with continental climate and high altitudes. Sicily is the only island to host the less thermophilous *A. subterranea*, which otherwise extends westward to Galicia (Spain). Sympatric occurrence is not rare along the contact zone. Additional natural history observations are reported regarding foraging habits, associated myrmecophiles, habitat preferences, and colony structure in the two species.

Keywords

Ants, *Aphaenogaster ichnusa*, biogeography, Mediterranean, Myrmicinae, Stenammini

Introduction

The genus *Aphaenogaster* Mayr, 1853 belongs to the myrmicine tribe Stenammini Ashmead, 1905 (Ward et al. 2015) and currently counts 206 valid species and 16 valid subspecies (Bolton 2023). The true genus *Aphaenogaster* is almost exclusively Holarctic, while the tropical species belong to the “*Deromyrma*” clade that awaits formal separation (Branstetter et al. 2022). Most *Aphaenogaster* ant species inhabit the West Palearctic, where six species groups have been identified (Schifani et al. 2022a).

The *subterranea* group currently includes eight species [*A. epirotes* (Emery, 1895), *A. holtzi* (Emery, 1898), *A. ichnusa* Santschi, 1925, *A. kurdica* Ruzsky, 1905, *A. lesbica* Forel, 1913, *A. maculifrons* Kiran & Aktaç, 2008, *A. subcostata* Viehmeyer, 1922, *A. subterranea* (Latreille, 1798)], mostly residing in the eastern Mediterranean and Caucasus region, where several putative undescribed species also exist (Borowiec and Salata 2017; Schifani et al. 2022a). Ten taxa formerly included in this group that are distributed in the Maghreb region and around Sicily, were recently assigned to the distinct *crocea* group according to morphological and genetic evidence (Alicata and Schifani 2019; Schifani et al. 2022a). The only three North African records of *A. subterranea* are based on outdated taxonomy (Forel 1890; Bernard 1967; Cagniant 1970; Henine-Maouche et al. 2022), and most likely represent misidentifications of species of the *crocea* group (Alicata and Schifani 2019; Schifani et al. 2022a). For instance, a worker labeled *A. subterranea* in the Forel’s collection of Geneva Natural History Museum (AntWeb identifier CASENT0907686) is in fact *A. strioloides* (see Schifani et al. 2021a).

Only two species belonging to the *subterranea* group are recognized in West Europe: *A. subterranea* (Latreille, 1798) (terra typica: mainland France) and *A. ichnusa* Santschi, 1925 (terra typica: Sardinia). The first was described using the spelling “*subteranea*” (Latreille 1798), which was later corrected by Latreille himself (Latreille 1802).

Aphaenogaster subterranea has a wide distribution, from Iberia to Anatolia, and north to central Europe, while the range of *A. ichnusa* is restricted to West Europe and

does not occur in the Balkans (Borowiec and Salata pers. comm., 2022; MM unpublished data). Until recent years *A. ichnusa* was considered as a Sardinian endemic and a subspecies of *A. subterranea*. Their separation as two distinct species was only recently demonstrated based on worker morphology and mitochondrial DNA (Galkowski et al. 2019). The recent recognition implies that reliable data over the distribution of the two species is scarce in the sympatric range, where they were historically confused. Apart from Sardinia, Galkowski et al. (2019) reported the presence of *A. ichnusa* in Corsica and southern mainland France. More recently, only a few scattered records were published from mainland Italy, Sicily, and mainland Spain (Schifani and Alicata 2018; García et al. 2020; Schär et al. 2020; Zara et al. 2021; Bazzato et al. 2022; Scupola et al. 2022). However, a detailed picture of the distribution of *A. ichnusa* and *A. subterranea* in these regions is lacking.

The investigation of specimens from private and museum collections allowed us to gather reliable distribution data of *A. ichnusa* and *A. subterranea* from the west Mediterranean basin, and to fill the current gaps of knowledge. Among them, we investigated several complete nest samples allowing us to morphologically characterize the sexual castes of the two species and provide tools for their identification.

Materials and methods

In this study, we focused our investigation on the West European region, where *A. ichnusa* is present and co-occurs with *A. subterranea*. We re-identified worker specimens belonging to the *subterranea* species group found in the authors' personal collections and the Natural History Museum of Milan. Specimen identification was performed using the morphological characters illustrated by Galkowski et al. (2019): *A. ichnusa* differs from *A. subterranea* in the shorter and thicker propodeal spines, which are triangular, the feebler surface sculpturing of the pronotal sides, and paler pigmentation (Fig. 1).

Queens and males associated with identified workers were examined to detect further distinctive morphological features. In total, we studied 16 queens from nine colonies and 17 males from seven colonies of *A. ichnusa*, as well as 16 queens from eight colonies and 19 males from nine colonies of *A. subterranea*. Samples were chosen from across the study region and included specimens from their *terrae typicae* (see Suppl. material 1). Due to the unknown, but possibly significant, dispersal capabilities, queens and males unassociated with workers as proof of successful colony establishment were not considered informative for the distribution range of the two species. Morphometric data for the descriptions was produced by taking pictures with a Carl Zeiss Stemi 2000-C stereomicroscope equipped with a CMEX PRO-5 DC.5000p digital camera and measurements taken with ImageFocus 4 software. Three quantitative morphological characters were defined for this study based on those presented by Wagner et al. (2017) and Seifert (2019) (Fig. 2):

- PrW** Males only. In dorsal view, maximum width of the dorsal plate of the propodeum at the level of the propodeal spiracles.
- SPWI** Males only. In dorsal view, maximum distance between the tips of the propodeal spines (whether well-developed or not).
- MCMssctm** Queens only. In dorsal view, quantification of stickman-like or reticulate microsculpture units on the mesoscutum: the number of connected lines building units and being separated by line intersections and by fleccions angled $> 30^\circ$ is counted. Very short lines are also considered full counts. Arithmetic means of three units per specimen are taken.

In addition to means to distinguish males and queens of *A. ichnusa* from those of *A. subterranea*, we provide identification keys that tell them apart from the other *Aphaenogaster* species occurring in the study area (i.e., *A. cardenai*, *A. italica*, *A. ovaticeps*, and species from the *crocea*, *gibbosa*, *pallida*, *splendida*, and *sardoa* groups; see Schifani et al. 2022a).



Figure 1. Workers of *Aphaenogaster ichnusa* (on the left, sample from Monte Petroso, Sicily) and of *A. subterranea* (on the right, sample from Parma, Italian peninsula). Cropped images highlight the differences in surface sculpturing of the pronotal sides and in the shape of the propodeal spines.

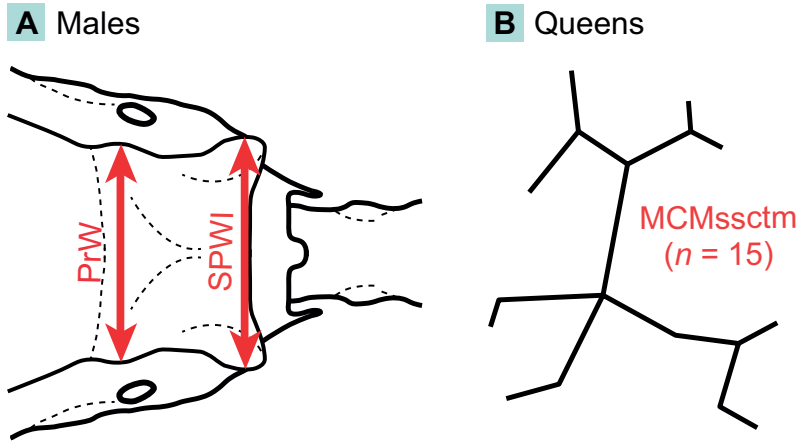


Figure 2. Diagnostic quantitative morphological characters recorded on males (A) and queens (B) of *Aphaenogaster ichnusa* and *A. subterranea*.

All characters are given in μm as mean \pm sd (min, max). A complete list of the investigated material and of the morphological data is provided in the Suppl. material 1.

Results

Male diagnosis (Figs 3, 4)

Compared to *A. subterranea*, *A. ichnusa* is characterized by a different propodeal shape with relatively well-developed dentiform spines, as opposed to slight edges. This difference can be appreciated both in lateral view (as the spines protrude backwards from the propodeal profile and are often preceded by a gibbous form in the distalmost part of the propodeal dorsum) and in dorsal view (as the spines are wider than the remaining propodeum). Consequently, the SPWI/PrW ratio was found to be very different between the two species, with no overlap: 1.36 ± 0.14 (1.12, 1.58) in *A. ichnusa*, 0.911 ± 0.06 (0.80, 0.99) in *A. subterranea* (Fig. 4). Furthermore, *A. ichnusa* males are normally substantially darker than those of *A. subterranea*.

Compared to other sympatric species of the same genus, *A. ichnusa* and *A. subterranea* can be distinguished based on the following combination of characters: shiny integument, mesosoma lacking a pronounced contrast between the anterior gibbosity of the mesosoma and the flat propodeum, the dorsal profile of the propodeum in lateral view relatively short and horizontal, forming approximately a 90° angle with the posterior profile, the rather elongated head shape, the body pigmentation pale to dark brownish.

The following traits are shared by the two species: the head, including mandibles, forms a subtriangular shape; its edges are rounded, and the head capsule is clearly



Figure 3. Males of *Aphaenogaster ichnusa* (on the left, sample from Monte Petroso, Sicily) and of *A. subterranea* (on the right, sample from Parma, Italian peninsula). Cropped images highlight the differences in the shape of the propodeum.

longer than wide. Very large ovoidal compound eyes ($\sim \frac{1}{2}$ length of the head capsule) that significantly protrude out of the head capsule, well-distanced from three large ocelli. Mandibles dentate, $\sim \frac{1}{2}$ length of the head capsule, their external side mostly straight for more than $\frac{3}{4}$. Clypeus medially slightly emarginated. Mesosoma clearly wider than the head, characterized by a well-developed anterior gibbosity. Propodeum much shorter than the remainder of the mesosoma. The horizontal section of the propodeal profile is shorter than its two vertical sections (anterior and posterior), which both form angles of $\sim 90^\circ$ with it. A ventral cuticular process protrudes from the metasternum. Long pedunculate petiole, globose postpetiole, the petiole and postpetiole have a similar height, while the postpetiole is wider than the petiole. The legs are long, with hind femurs approximately the same length as the entire mesosoma. The antennae comprise of 11 flagellomeres, the scapi are short, measuring ca. twice the pedicel, and approximately extending slightly beyond the eyes if aligned perpendicularly to the head length axis. Body color pale to dark brown, appendages whitish. Surface sculpturing mostly weak, most of the ant is smooth and shiny, with at most isolated stickman-like units, very feeble rugae or reticulate microsculpture near the sutures, and feeble reticulate microsculpture on the head. Sparse erect and suberect setae mostly occur dorsally over the head, mesosoma and nodes, and both dorsally and ventrally on the first gastral segment and on the distalmost margins of the remaining segments, while shorter suberect or appressed setae cover the appendages.

The following key is meant to facilitate this distinction in the examined region. However, the intraspecific morphological variation of several species is still little known, so we recommend a careful approach in its use.

- 1 Notably pronounced contrast between the anterior gibbosity of the mesosoma and a long and relatively flat propodeum, as better observed in lateral view; head less elongated.....*A. italica* Bondroit, 1918, *A. sardoa* (Mayr) (only Sardinia and Sicily), *A. splendida* (Roger, 1859), *A. gibbosa* (Latreille, 1798) or ***crocea* group** (only Sicily and southern Italian peninsula), i.e., *A. fiorii* Emery, 1915, *A. sicula* Emery, 1908, *A. strioloides* Forel, 1890, or *A. trinacriae* Alicata & Schifani, 2019 (see Emery 1908; 1916; Santschi 1932; Gómez et al. 2018; Alicata and Schifani 2019)
 - Propodeum much shorter and not as flat 2
- 2 Body color blackish; integument either most extensively matt, or mostly smooth and shiny and paired with a wide subrectangular head, or with reticulate microsculpture on the head and visible striae on the mesosoma and petiole..... **remaining *A. sardoa* group species** (see Boer 2013), the Iberian endemic *A. ulibeli* (Gómez et al., 2018), or *A. epirotes* (in the study area only near the Italian border with Slovenia, see Müller 1923)
 - Body color ferruginous to dark brownish, integument largely smooth and shiny, without strongly developed surface sculpturing..... 3
- 3 Iberia only, very large size (approximate body length 6–6.8 mm) *A. cardenai* Espadaler, 1981 (see Tinaut 1986)
 - Combination not as above 4
- 4 Propodeal dorsum in profile view longer and inclined at ~ 45° before reaching the propodeal spiracle, lacking a clearly horizontal component *A. dulcineae* Emery, 1924, *A. finzii* Müller, 1921, *A. ovaticeps* (Emery, 1898), or *A. pallida* (Nylander, 1849) (Emery 1898; 1916; Müller 1923; Santschi 1932)
 - Propodeal dorsum shorter and more vertical, with a clear horizontal component *A. ichnusa* or *A. subterranea* (discrimination possible based on propodeal shape, see characters illustrated in the second paragraph of this section and Figs 3, 4)

Queen diagnosis (Figs 4, 5)

Queens of *A. ichnusa* and *A. subterranea* are much more difficult to tell apart based on their general shape as compared to workers and males. However, a subtle but very reliable character was found in the surface microsculpture of the dorsal mesosoma: in *A. ichnusa*, stickman-like reticulations occur sparsely and are modestly developed, while in *A. subterranea* they are visibly more developed and sometimes single stickman-like complexes may connect to each other covering very large areas. MCMsctm ranges do not overlap between the two species, while *A. subterranea* shows a high variation in the upper range: 4.33 ± 0.78 (3.00, 5.33) in *A. ichnusa*, 24.68 ± 22.97 (8.67, 87.67) in *A. subterranea* (Fig. 4).

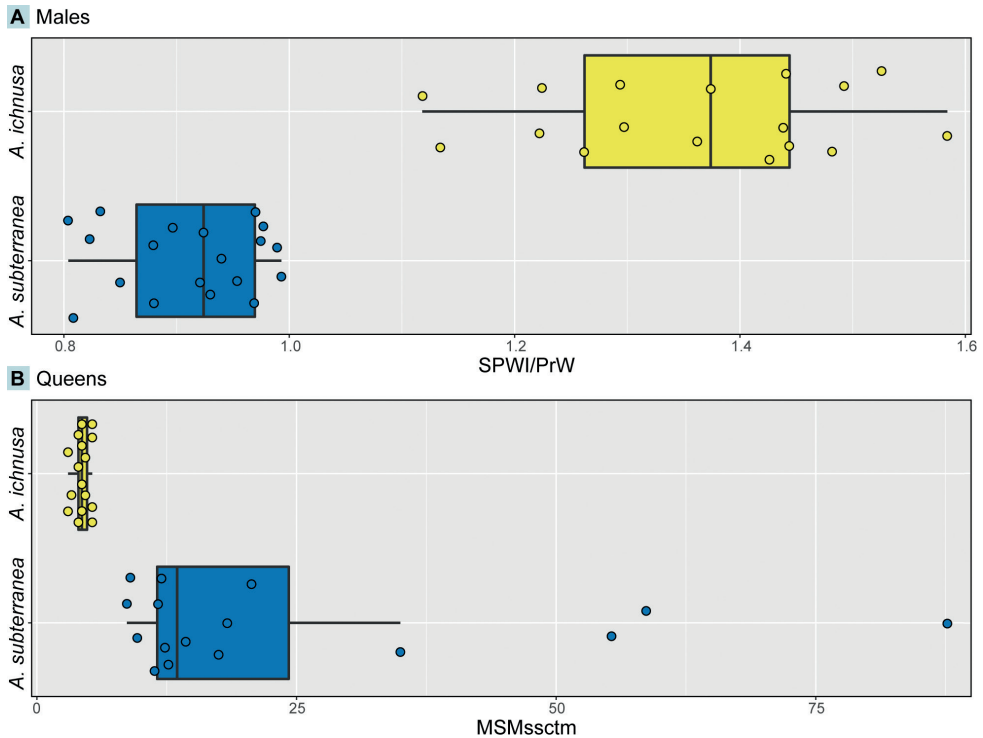


Figure 4. Quantitative morphological differences distinguishing *A. ichnusa* and *A. subterranea* males (A) and queens (B).

Compared to other sympatric species of the same genus, *A. ichnusa* and *A. subterranea* can be distinguished based on the following combination of characters: large mesosoma with wide smooth and shining patches, dark brown to ferruginous pigmentation with blackish areas, body setae relatively sparse, thick propodeal spines and mostly vertical propodeum lateral profile.

The following traits are shared by the two species: The head capsule forms a subrectangular shape, with rounded edges, and is as approximately as long as wide or slightly longer than wide. Large compound eyes (their length $\sim 1/3$ – $1/4$ of the head length) slightly protruding out of the head capsule. The distance between the central among the three ocelli and the level of the compound eyes is ca. the length of the ocellus itself. Mandibles dentate, $\sim 1/2$ length of the head capsule, their external side mostly straight for over $3/4$. Clypeus medially slightly emarginated. Massive mesosoma, slightly wider than the head. Propodeal spines well developed and straight, in profile view the of the propodeum is steep, with the section above the spines slightly inclined and the section below entirely vertical. Long pedunculate petiole, globose postpetiole, the petiole and postpetiole have a similar height, while the postpetiole is wider than the petiole. The antennae comprise ten flagellomeres, the scapi are moderately long, surpassing the posterior margin of the head if aligned parallel to the head length axis,

while the antennal club consists of four flagellomeres and the flagellomeres 3–8 are only slightly longer than wide. Body color normally not uniform, ferruginous to very dark brown, with blackish patches usually occurring on the frons and paler orangish areas near the sutures of the mesosoma. Appendages pale orange to ferruginous. Rugose sculpture on most of the head, partly on the sides of the mesosoma including the entire propodeum, and on the nodes. The remainder of the body is smooth and shiny, except for stickman-like microsculpture. Abundant erect or suberect setae cover the head, the dorsum of the mesosoma and nodes, the first gastral segment, and the distalmost margins of the remaining segments, while shorter suberect or appressed setae cover the appendages.

The following key is meant to facilitate this distinction in the examined region. However, the intraspecific morphological variation of several species is still little known, so we recommend a careful approach in its use.

- 1 Mesosoma matt and smaller, not hosting properly developed flight muscles, all species suspected to be incapable of normal flight dispersal **sardoa group** (see Boer 2013; Schifani et al. 2022a)
- Mesosoma with wide smooth and shining patches and larger..... **2**
- 2 Propodeum longer, its dorsal profile inclined at ~ 45°, propodeal spines thinner, body color uniformly ferruginous..... ***A. ovaticeps*** (see Salata et al. 2021)
- Character combination deviating..... **3**
- 3 Body color blackish, striate sculpture on the posterior part of the mesoscutellum and on the metanotum, only near the Italian border with Slovenia.....
..... ***A. epirotes* (Müller, 1923)**
- Color paler, mesoscutellum without striae..... **4**
- 4 Body color uniformly very dark brown to blackish, flagellomeres more elongated, head with more parallel sides giving the impression of a more rectangular shape.....
..... ***A. italica*, *A. gibbosa*, *A. ulibeli*** (see Santschi 1932; Gómez et al. 2018)
- Body color paler, head sides not as parallel and more convergent frontad..... **5**
- 5 Very hairy, comparatively dense setae at least on the gaster and postpetiole..... ***A. pallida* group** (*A. dulcineae*, *A. finzii*, or *A. pallida*, see Schifani et al. 2022a)
- Setae sparser..... **6**
- 6 Body pigmentation yellowish or uniform ferruginous with at most a darkened area on the frons..... **either *crocea* group** (only Sicily and southern Italian peninsula), i.e., ***A. fiorii*, *A. sicula*, and *A. trinacriae*, or *A. splendida*** which is normally also characterized by a black transversal band on the first gastral tergite (Alicata and Schifani 2019; Salata et al. 2021)
- Body pigmentation overall darker and more irregular, blackish patches on the mesosoma and frons ***A. ichnusa* or *A. subterranea*** (discrimination possible based on microsculpture, see characters illustrated in the second paragraph of this section and Figs 4, 5)



Figure 5. Queens of *Aphaenogaster ichnusa* (on the left, sample from Monte Petroso, Sicily) and of *A. subterranea* (on the right, sample from Parma, Italian peninsula). Cropped images highlight the differences in the microsculpture of the mesoscutellum.

Note: The queens of *A. cardenai* and *A. strioloides* are currently unknown and, therefore, they are not included in this key. The first only occurs in Iberia and, considering that its workers are unique among West Palearctic *Aphaenogaster* and that queens usually retain a number of characters of workers, they are highly unlikely to be confusable with species of the *subterranea* group (Schifani et al. 2022a). In West Europe, *A. strioloides* only occurs on the island of Pantelleria, where neither *A. ichnusa* nor *A. subterranea* exist (Schifani et al. 2021a).

We recovered a total of 274 new records of *A. ichnusa*, and 154 of *A. subterranea* from the study area. We increased the known number of cells of 0.2 decimal degrees (ca. 22 km) occupied by *A. ichnusa* by 145% (103 new compared to 71 from literature) and of those occupied by *A. subterranea* by 64% (130/202). The two species showed a parapatric distribution, with only 4.5% of the cells (22/484) occupied by both species (Fig. 6). The westernmost record of *A. ichnusa* occurs at 0.74 longitude (Catalonia, Spain), the easternmost at 18.46 longitude (Apulia, Italy), the southernmost at 36.94

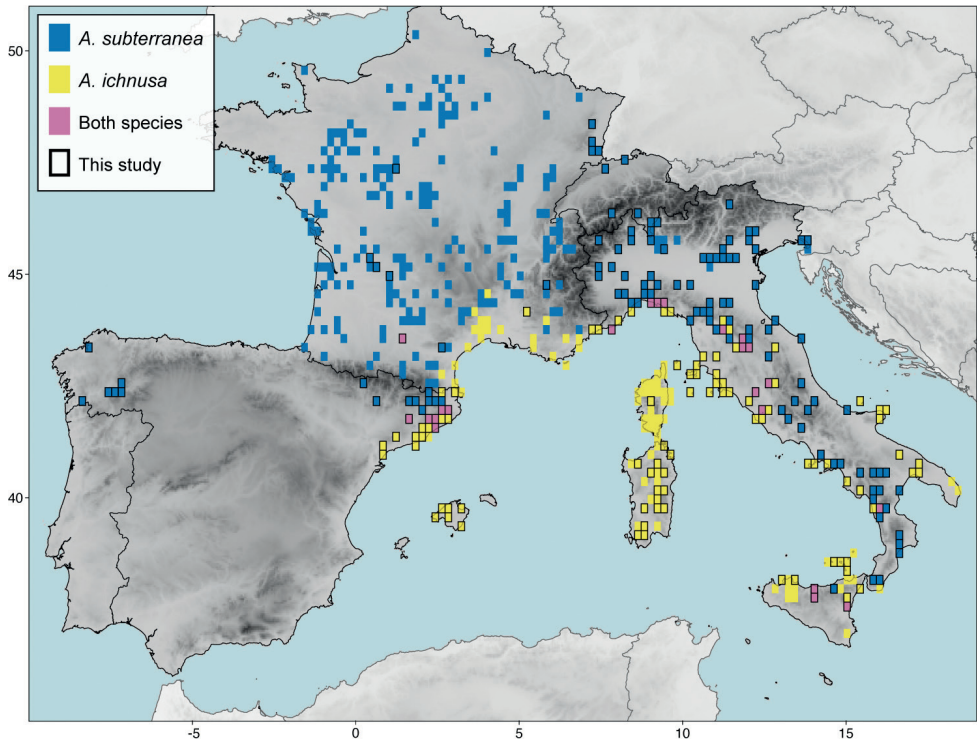


Figure 6. Distribution map showing the locations of the records here newly reported (black border) and retrieved from literature (no border) in a cell grid of 0.2 decimal degrees. Cells are blue for *A. subterranea*, yellow for *A. ichnusa*, and pink if the two species co-occur.

latitude (Sicily, Italy) and the northernmost at 44.48 latitude (mainland France). For *A. subterranea*, the westernmost record is at -8.46 longitude (Galicia, Spain) and the southernmost at 37.64 latitude (Sicily, Italy).

We report *A. ichnusa* for the first time for several islands and archipelagos: some of the Aeolian Islands (Lipari, Vulcano, Salina, Filicudi, Panarea), the Balearic Islands (Mallorca), the Maddalena Archipelago (Caprera), the Phlegrean Islands (Ischia, Procida), Tavolara island, the Tremiti islands (San Domino), and the Tuscan Archipelago (Capraia, Elba, Giglio, Montecristo).

Discussion

The morphological distinction of the *subterranea* group species in the region is relatively easy (Schifani et al. 2022a), and male-based separation of *A. ichnusa* from *A. subterranea* is normally straight-forward as demonstrated by our data. While distinction of queens and workers can be more difficult at first sight, queens are safely separable at adequate magnification and workers are normally easy for a trained eye. Colony samples of *A. ichnusa* with longer spines and colony samples of *A. subterranea* with shorter ones

may occur, always requiring a certain attention to other characters such as spine shape, pronotal sculpture and pigmentation. The different ecological requirements of the two species are often helpful but the two may occur sympatrically. While Galkowski et al. (2019) reported a possible introgression event, we did not encounter colony samples with intermediate morphological characters based on subjective evaluation.

While *A. ichnusa* inhabits areas with a Mediterranean climate, *A. subterranea* in the same region occurs only at higher elevations or in specific microclimates. However, *A. subterranea* is frequent at the sea level in continental climatic zones where *A. ichnusa* is absent (e.g., most of mainland France, the Po Plain). We show that *A. ichnusa* is frequent across a vast region of the western Mediterranean (Wang et al. 2023, including Italy's Tyrrhenian and Ionian coasts, and part of the Adriatic one. Moreover, it is the sole species found on all investigated islands with the only exception of Sicily, where *A. subterranea* is found at higher elevations in the Etna and the Sicilian Apennines alongside other continental species (Schifani et al. 2021b, 2022b).

Notably, both *A. ichnusa* and *A. subterranea* seem to have a more limited distribution in Iberia, where they seem to be restricted to northern Spain. The reliability of few old records from southern Spain appears doubtful in the absence of more recent findings (e.g., Santschi 1919). No historic records exist from Portugal (Arcos et al. 2022), yet our data suggest that targeted investigations may discover *A. subterranea* near the northern border with Spain. The wide distribution of *A. ichnusa* is apparently reflected in the fact that in some old keys, descriptions and drawings attributed to *A. subterranea* were found to depict *A. ichnusa* instead (e.g., Emery 1916 key to the Italian fauna with a drawing of an *A. ichnusa* male). *Aphaenogaster subterranea* may have been temporarily introduced to Madagascar (Csösz et al. 2021).

Colonies of *A. ichnusa* and *A. subterranea* are often found nesting under rocks, and both species may be especially abundant in shady forest habitats with sufficient humidity and leaf litter (Castracani et al. 2010, referring at least part of the records to *A. ichnusa* based on voucher checked; Seifert 2018, assuming Central-European records to represent *A. subterranea*; Zara et al. 2021; Bazzato et al. 2022). Albeit rarely, at least *A. ichnusa* may adapt significantly to urban environments: in summer days, we observed workers foraging in a shady courtyard entirely made of concrete within a historic palace of Florence.

However, despite their ecological success and wide distribution, still relatively little is known ca. the habits of these species besides anecdotal reports. They are probably mostly predators and scavengers, but at least *A. ichnusa* was also observed by the authors to tend root aphids, suggesting that trophobiosis may also play an important role in the diet of both. In addition, we observed isopods (*Platyarthrus* sp.), oribatid mites, silverfish, leaf beetle larvae (Chrysomelidae: Clytrinae), and planthoppers nymphs (Cixiidae) in *A. ichnusa* nests, and isopods (*Platyarthridae* in *A. subterranea* nests, in which also Cixiidae were reported by Lörinczi (2012). In shady habitats, we observed minimal daytime foraging by both species. However, on other occasions, workers of *A. ichnusa* mostly started to forage outside the nest at dusk. Perhaps the foraging activity is often conducted within the leaf litter or in endogean microspaces, but none of these species is truly subterranean (Ortuño et al. 2014).

Some of us also observed cooperative food transport in *A. subterranea* at least. Furthermore, *A. subterranea* workers are known to use tools: they drop small debris into liquid food and transport food-soaked tools back into their nest (Lőrinczi et al. 2018; Módra et al. 2022). This behavior is deemed to be a complex strategy developed to compensate for the inability to ingest and carry into the body large quantities of liquid food (Lőrinczi et al. 2018; Módra et al. 2022). Notably, we found multiple times numerous dealate queens (up to five) in some colonies of *A. ichnusa* and *A. subterranea*, suggesting at least occasional polygyny in both species.

An integrative approach is needed to clarify whether hybridization or introgression between the two species have a significant role as observed in other ants (Seifert 2018). Nuptial flights of *A. subterranea* and *A. ichnusa* seemingly overlap in late summer/early autumn. However, the relatively large size of the contact zone compared to the distribution range of *A. ichnusa*, and the consistent morphological differentiation from *A. subterranea*, suggest some adaptation to counter hybridization. At the same time, the data we are providing could facilitate future studies focused on the ecology and niche partitioning of these species.

Acknowledgements

We are grateful to Rumsais Blatrix for sharing with us the raw species distribution data used by Galkowski et al. (2019), as well as to all the collectors who contributed to gather specimens relevant to this paper (see the list in the Suppl. material 1). We also thank the referees Alexander Wild and Sebastian Salata as well as the editor Brendon Boudinot for their comments on an earlier version of this manuscript.

Support for this research was provided by “la Caixa” Foundation (ID 100010434) to Mattia Menchetti (grant LCF/BQ/ DR20/11790020).

References

- Alicata A, Schifani E (2019) Three endemic *Aphaenogaster* from the Siculo-Maltese archipelago and the Italian Peninsula: part of a hitherto unrecognized species group from the Maghreb? (Hymenoptera: Formicidae: Myrmicinae). *Acta Entomologica Musei Nationalis Pragae* 59(1): 1–16. <https://doi.org/10.2478/aemnp-2019-0001>
- Arcos J, Chaves D, Alarcón P, Rosado A (2022) First record of *Temnothorax convexus* (Forel, 1894) in Portugal (Hymenoptera: Formicidae) with an updated checklist of the ants from the country. *Sociobiology* 69(2): e7623. <https://doi.org/10.13102/sociobiology.v69i2.7623>
- Bazzato E, Lallai E, Caria M, Schifani E, Cillo D, Ancona C, Pantini P, Maccherini S, Bacaro S, Marignani M (2022) Land-use intensification reduces multi-taxa diversity patterns of Small Woodlots Outside Forests in a Mediterranean area. *Agriculture, Ecosystems & Environment* 340: e108149. <https://doi.org/10.1016/j.agee.2022.108149>
- Bernard F (1967) Faune de l'Europe et du Bassin Méditerranéen. 3. Les fourmis (Hymenoptera Formicidae) d'Europe occidentale et septentrionale. Paris: Masson, 411 pp.

- Boer P (2013) Revision of the European ants of the *Aphaenogaster testaceopilosa*-group (Hymenoptera: Formicidae). Tijdschrift voor Entomologie 156(1): 57–93. <https://doi.org/10.1163/22119434-00002022>
- Bolton B (2023) An online catalog of the ants of the world. <https://antcat.org>
- Borowiec L, Salata S (2017) Ants of the Peloponnese, Greece (Hymenoptera: Formicidae). Polish Journal of Entomology 86(3): 193–236. <https://doi.org/10.1515/pjen-2017-0013>
- Branstetter MG, Longino JT, Reyes-López JL, Brady SG, Schultz TR (2022) Out of the temperate zone: A phylogenomic test of the biogeographical conservatism hypothesis in a contrarian clade of ants. Journal of Biogeography 49(9): 1640–1653. <https://doi.org/10.1111/jbi.14462>
- Cagniant H (1970) Deuxième liste de fourmis d'Algérie récoltées principalement en forêt. (1^{re} partie). Bulletin de la Société d'Histoire Naturelle de Toulouse 105: 405–430.
- Castracani C, Grasso DA, Fanfani A, Mori A (2010) The ant fauna of Castelporziano Presidential Reserve (Rome, Italy) as a model for the analysis of ant community structure in relation to environmental variation in Mediterranean ecosystems. Journal of Insect Conservation 14(6): 585–594. <https://doi.org/10.1007/s10841-010-9285-3>
- Csőszy S, Loss AC, Fisher BL (2021) Taxonomic revision of the Malagasy *Aphaenogaster swammerdami* group (Hymenoptera: Formicidae). PeerJ 9: e10900. <https://doi.org/10.7717/peerj.10900>
- Emery C (1898) Beiträge zur Kenntniss der palaearktischen Ameisen. Öfversigt af Finska Vetenskaps-Societetens Förhandlingar 20: 124–151.
- Emery C (1908) Beiträge zur Monographie der Formiciden des paläarktischen Faunengebietes. (Hym.) (Fortsetzung.) III. Die mit *Aphaenogaster* verwandte Gattungengruppe. Deutsche Entomologische Zeitschrift 1908: 305–338. <https://doi.org/10.1002/mmnd.48019080302>
- Emery C (1916) Fauna entomologica italiana. I. Hymenoptera. – Formicidae. Bollettino della Società Entomologica Italiana 47: 79–275.
- Forel A (1890) Fourmis de Tunisie et de l'Algérie orientale. Annales de la Société Entomologique de Belgique 34: 61–76.
- Galkowski C, Aubert C, Blatrix R (2019) *Aphaenogaster ichnusa* Santschi, 1925, bona species, and redescription of *Aphaenogaster subterranea* (Latreille, 1798) (Hymenoptera, Formicidae). Sociobiology 66(3): 420–425. <https://doi.org/10.13102/sociobiology.v66i3.3660>
- García F, Espadaler X, Roig X, Serrano S, Cuesta-Segura AD (2020) Nuptial flights in ants: a study of the drowned sexuals in four Iberian water surfaces (Hymenoptera: Formicidae). Boletín de la Sociedad Entomológica Aragonesa (S.E.A.) 10: 255–268.
- Gómez K, Martínez D, Espadaler X (2018) Phylogeny of the ant genus *Aphaenogaster* (Hymenoptera: Formicidae) in the Iberian Peninsula, with the description of a new species. Sociobiology 65(2): 215–224. <https://doi.org/10.13102/sociobiology.v65i2.2099>
- Henine-Maouche A, Guergouz W, Moudache T (2022) Ant community diversity in two agrosystems in Bejaia wilaya (Northern Algeria). Sociobiology 69(3): e7667. <https://doi.org/10.13102/sociobiology.v69i3.7667>
- Latreille PA (1798) Essai sur l'histoire des Fourmis de la France. F. Bourdeaux, Brive, 50 pp.
- Latreille PA (1802) Histoire Naturelle des Fourmis, et Recueil de Mémoires et D'observations sur les Abeilles, les Araignées, les Faucheurs, et Autres Insectes. Impr. Crapelet (chez T. Barrois), Paris, 445 pp. <https://doi.org/10.5962/bhl.title.11138>

- Lőrinczi G (2012) A novel association between *Aphaenogaster subterranea* (Hymenoptera: Formicidae) and the nymphs of *Reptalus panzeri* (Hemiptera: Cixiidae). *European Journal of Entomology* 109(4): 509–515. <https://doi.org/10.14411/eje.2012.064>
- Lőrinczi G, Módra G, Juhász O, Maák I (2018) Which tools to use? Choice optimization in the tool-using ant, *Aphaenogaster subterranea*. *Behavioral Ecology* 29: 1444–1452. <https://doi.org/10.1093/beheco/ary110>
- Módra G, Maák I, Lőrincz Á, Lőrinczi G (2022) Comparison of foraging tool use in two species of myrmicine ants (Hymenoptera: Formicidae). *Insectes Sociaux* 69(1): 5–12. <https://doi.org/10.1007/s00040-021-00838-0>
- Müller G (1923) Le formiche della Venezia Giulia e della Dalmazia. *Bollettino della Società Adriatica di Scienze Naturali in Trieste* 28: 11–180.
- Ortuño VM, Gilgado JD, Tinaut A (2014) Subterranean ants: the case of *Aphaenogaster cardenai* (Hymenoptera: Formicidae). *Journal of Insect Science* 14(1): e212. <https://doi.org/10.1093/jisesa/ieu074>
- Salata S, Karaman C, Kiran K, Borowiec L (2021) Review of the *Aphaenogaster splendida* species-group (Hymenoptera: Formicidae). *Annales Zoologici* 71(2): 297–343. <https://doi.org/10.3161/00034541ANZ2021.71.2.008>
- Santschi F (1919) Fourmis d'Espagne et des Canaries. *Boletín de la Real Sociedad Española de Historia Natural* 19: 241–248.
- Santschi F (1925) Fourmis d'Espagne et autres espèces paléarctiques (Hymenopt.). *EOS. Revista Española de Entomología* 1: 339–360.
- Santschi F (1932) Études sur quelques *Attomyrma* paléarctiques. *Mitteilungen der Schweizerische Entomologische Gesellschaft* 15: 338–346.
- Schär S, Menchetti M, Schifani E, Hinojosa JC, Platania L, Dapporto L, Vila R (2020) Integrative biodiversity inventory of ants from a Sicilian archipelago reveals high diversity on young volcanic islands (Hymenoptera: Formicidae). *Organisms, Diversity & Evolution* 20(3): 405–416. <https://doi.org/10.1007/s13127-020-00442-3>
- Schifani E, Alicata A (2018) Exploring the myrmecofauna of Sicily: Thirty-two new ant species recorded, including six new to Italy and many new aliens (Hymenoptera, Formicidae). *Polish Journal of Entomology* 87(4): 323–348. <https://doi.org/10.2478/pjen-2018-0023>
- Schifani E, Costa S, Mei M, Alicata A (2021a) A new species for the Italian fauna: *Aphaenogaster strioloides*, not *A. crocea*, inhabits Pantelleria Island (Hymenoptera: Formicidae). *Fragmenta Entomologica* 53: 21–24. <https://doi.org/10.13133/2284-4880/482>
- Schifani E, Csősz S, Viviano R, Alicata A (2021b) Ant diversity on the largest Mediterranean islands: On the presence or absence of 28 species in Sicily (Hymenoptera, Formicidae). *Natural History Sciences : Atti della Società Italiana di Scienze Naturali e del Museo Civico di Storia Naturale in Milano* 8(1): 55–70. <https://doi.org/10.4081/nhs.2021.532>
- Schifani E, Alicata A, Menchetti M, Borowiec L, Fisher BL, Karaman C, Kiran K, Oueslati W, Salata S, Blatrix R (2022a) Revisiting the morphological species groups of West-Paleartic *Aphaenogaster* ants (Hymenoptera: Formicidae) from a phylogenetic perspective: toward an evolutionary classification. *Arthropod Systematics & Phylogeny* 80: 627–648. <https://doi.org/10.3897/asp.80.e84428>

- Schifani E, Alicata A, Menchetti M (2022b) Following the Apennines: Updating the distribution of *Formica clara* and *Formica rufibarbis* in Italy (Hymenoptera, Formicidae). *Biogeographia* 37(1): a014. <https://doi.org/10.21426/B637155107>
- Scupola A, Durante A, Giannuzzi F (2022) The ant fauna (Hymenoptera, Formicidae) of Salento (Apulia, South East Italy): First reports, new occurrences, and an updated species list. *Thalassia Salentina* 44: 107–146. <https://doi.org/10.1285/i15910725v44p107>
- Seifert B (2018) *Ants of Northern and Central Europe*. Lutra Verlags- und Vertriebsgesellschaft, Tauer, Germany.
- Seifert B (2019) A taxonomic revision of the members of the *Camponotus lateralis* species group (Hymenoptera: Formicidae) from Europe, Asia Minor and Caucasia. *Soil Organisms* 91: 7–32. <https://doi.org/10.25674/so-91-1-02>
- Tinaut A (1986) Descripción del macho de *Aphaenogaster cardenai* Espadaler, 1981 (Hymenoptera, Formicidae). *Miscel·lània. Zoològica* 9: 245–249.
- Wagner HC, Arthofer W, Seifert B, Muster C, Steiner FM, Schlick-Steiner BC (2017) Light at the end of the tunnel: Integrative taxonomy delimits cryptic species in the *Tetramorium caespitum* complex (Hymenoptera: Formicidae). *Myrmecological News* 25: 95–129. https://doi.org/10.25849/myrmecol.news_025:095
- Wang R, Kass JM, Galkowski C, Garcia F, Hamer MT, Radchenko A, Salata S, Schifani E, Yusupov ZM, Economo EP, Guénard B (2023) Geographic and climatic constraints on bioregionalization of European ants. *Journal of Biogeography* 50(3): 503–514. <https://doi.org/10.1111/jbi.14546>
- Ward PS, Brady SG, Fisher BL, Schultz TR (2015) The evolution of myrmicine ants: phylogeny and biogeography of a hyperdiverse ant clade (Hymenoptera: Formicidae). *Systematic Entomology* 40(1): 61–81. <https://doi.org/10.1111/syen.12090>
- Zara L, Tordoni E, Castro-Delgado S, Colla A, Maccherini S, Marignani M, Panepinto F, Trittoni M, Bacaro G (2021) Cross-taxon relationships in Mediterranean urban ecosystem: A case study from the city of Trieste. *Ecological Indicators* 125: e107538. <https://doi.org/10.1016/j.ecolind.2021.107538>

Supplementary material I

Distribution data of *Aphaenogaster ichnusa* and *A. subterranea*

Authors: Enrico Schifani, Antonio Alicata, Lech Borowiec, Fede García, Vincenzo Gentile, Kiko Gómez, Elia Nalini, Fabrizio Rigato, Sämi Schär, Antonio Scupola, Roger Vila, Mattia Menchetti

Data type: table (excel document)

Copyright notice: This dataset is made available under the Open Database License (<http://opendatacommons.org/licenses/odbl/1.0/>). The Open Database License (ODbL) is a license agreement intended to allow users to freely share, modify, and use this Dataset while maintaining this same freedom for others, provided that the original source and author(s) are credited.

Link: <https://doi.org/10.3897/zookeys.1153.98297.suppl1>